Chapter 4. Thermal-Hydraulic Analysis of Potential Overcooling Transients Occurring at Calvert Cliffs Unit 1 Nuclear Power Plant

of

A PRESSURIZED THERMAL SHOCK EVALUATION OF THE CALVERT CLIFFS UNIT 1 NUCLEAR POWER PLANT

written by

The PTS Study Group
of
Engineering Physics and Mathematics
Oak Ridge National Laboratory,
Los Alamos National Laboratory,
Purdue University

and

Science Applications, Inc.

Date of Draft: May 31, 1984

NOTICE: This document contains information of a preliminary nature. It is subject to revision or correction and therefore does not represent a final report.

*Research sponsored by U.S. Nuclear Regulatory Commission under Contract No. DE-AC05-840R21400 with the Martin Marietta Energy Systems, Inc.

8407100360 840618
PDR ADOCK 05000317
P PDR

A PRESSURIZED THERMAL SHOCK EVALUATION OF THE CALVERT CLIFFS UNIT 1 NUCLEAR POWER PLANT

List of Chapters

4.0. THERMAL-HYDRAULIC ANALYSIS OF POTENTIAL OVERCOOLING TRANSIENTS OCCURRING AT CALVERT CLIFFS UNIT 1 NUCLEAR POWER PLANT

4.3.3. Runaway Feedwater Events

4.3.3.1. Transient 8: Runaway Main Feedwater to Both Steam Generators from Full Power
4.3.3.2. Transient 9: Runaway Main Feedwater to One Steam Generator from Full Power
4.3.3.3. Transient 10: Runaway Auxiliary Feedwater to Two Steam Generators from Full Power

4.3.4. Small-Break LOCA Events

4.3.4.1. Transient 11: 0.002-m^2 Hot-Leg Break from Full Power
4.3.4.2. Transient 12: Stuck-Open Pressurizer PORV with Stuck-Open Secondary ADV from Full Power

4.4. Downcomer Fluid Mixing Behavior

4.4.1. Stratification Analysis of Twelve LANL Transients
4.4.2. SOLA-PTS Mixing Analysis of Selected Transients
4.4.3. Total Loop Flow Stagnation

4.5. Heat-Transfer Coefficient Evaluation

4.6. Estimations of Pressure, Temperature and Heat-Transfer Coefficient Profiles

4.6.1. Methodology

4.6.1.1. General Approach
4.6.1.2. Sequence Grouping
4.6.1.3. Temperature Evaluation by Cooldown Model
4.6.1.4. Pressure Evaluation by Coolant Swell Model

4.6.2. Results of Simple Model Evaluations

4.6.2.1. Large Main Steam-line Breaks at HZP
4.6.2.2. Small Main Steam-line Break at HZP
4.6.2.3. Large Main Steam-line Break at Full Power
4.6.2.4. Small Main Steam-line Break at Full Power
4.6.2.5. Reactor Trip Sequences
4.6.2.6. Small-Break LOCA ($\leq$0.016 ft^2)
4.6.2.7. Small-Break LOCA ($\sim$0.02 ft^2)

Chapter 4 Appendices

F.* TRAC-PF1 Analysis of Potential Pressurized-Thermal-Shock Transients at a Combustion-Engineering PWR

G.* Brookhaven National Laboratory Review of the TRAC Analysis

H.* Buoyancy Effects in Overcooling Transients Calculated for the Calvert Cliffs Unit 1 Nuclear Power Station

I.* Three-Dimensional Calculations of Transient Fluid-Thermal Mixing in the Downcomer of the Calvert Cliffs-1 Plant Using SOLA-PTS

J. Estimation of Pressure, Temperature, and Heat Transfer Coefficient

*To be published as a separate report.

LIST OF FIGURES

4.36. Extrapolated downcomer pressures for large main steam-line break at HZP

4.37. Extrapolated downcomer heat-transfer coefficients for large main steam-line break at HZP

4.38. Extrapolated downcomer temperatures for small main steam-line break at HZP

4.39. Extrapolated downcomer pressures for small main steam-line break at HZP

4.40. Extrapolated downcomer heat-transfer coefficients for small main steam-line break at HZP

4.41. Extrapolated downcomer temperatures for large main steam-line break at full power

4.42. Extrapolated downcomer pressures for large main steam-line break at full power

4.43. Extrapolated downcomer heat-transfer coefficients for large main steam-line break at full power

4.44. Extrapolated downcomer temperatures for small main steam-line break at full power

4.45. Extrapolated downcomer pressures for small main steam-line break at full power

4.46. Extrapolated downcomer heat-transfer coefficients for small main steam-line break at full power

4.47. Extrapolated downcomer temperatures for reactor trip (Sequences 5.18, 5.19, 5.22, 5.35, 5.36, 5.21 A and B)

4.48. Extrapolated downcomer temperatures for reactor trip (Sequences 5.25 A and B, 5.26 A and B, 5.27 A and B)

4.49. Extrapolated downcomer pressures for reactor trip (Sequences 5.18, 5.19, 5.22, 5.35, 5.36, 5.21 A and B)

4.50. Extrapolated downcomer pressures for reactor trip (Sequences 5.25 A and B, 5.26 A and B, 5.27 A and B)

4.51. Extrapolated downcomer heat-transfer coefficients for reactor trip (Sequences 5.18, 5.19, 5.22, 5.35, 5.36, 5.21 A and B)

4.52. Extrapolated downcomer heat-transfer coefficients for reactor trip (Sequences 5.25 A and B, 5.26 A and B, 5.27 A and B)

4.53. Extrapolated downcomer temperatures for small-break LOCA (<0.016 ft^2)

LIST OF TABLES

4.0. THERMAL-HYDRAULIC ANALYSIS OF POTENTIAL OVERCOOLING TRANSIENTS OCCURRING AT CALVERT CLIFFS UNIT 1 NUCLEAR POWER PLANT

4.1. Introduction

In Chapter 3, 115 sequences were identified for potential thermal-hydraulic analysis. Even though many of these sequences have relatively slow cooldown rates (less than 100°F per hour), some thermal-hydraulic data must be generated for each sequence or at least for each class of event.* Clearly, an extensive thermal-hydraulic analysis of each sequence would be unnecessary. Therefore, the approach used was to analyze 12 selected sequences to provide data that could be used either directly or to estimate the thermal-hydraulic characteristics of each of the 115 sequences.

The selection of the 12 sequences is described in Section 4.2. For each one, an analysis of the system response over a two-hour period was performed by Los Alamos National Laboratory (LANL) as described in Section 4.3. Two topics were identified as requiring special attention: (1) mixing in the downcomer region, and (2) the heat-transfer coefficient at the surface of the reactor vessel wall in the downcomer region. These two characteristics were examined by T. G. Theofanous of Purdue University, and the results are presented in Sections 4.4 and 4.5, respectively. Finally, the results of the analyses discussed in Sections 4.3, 4.4, and 4.5 were used to estimate the thermal-hydraulic characteristics of those sequences for which a specific calculation was not performed. The process applied and the results obtained are presented in Section 4.6.

---

*This is necessary since many of the events with slow cooldown rates have relatively high frequencies of occurrence. Although it is anticipated that high-frequency events with slow cooldown are less important than those low-frequency events with rapid cooldown, the relative risk of a through-wall crack must be determined.

4.2. Selection of Twelve Sequences

The primary objective of the selection process was to identify sequences that would provide information on the impact of the initiating events, potential equipment failures, and operator actions on the primary system cooldown rate and pressure. As a result, many of the sequences chosen are low-frequency probability sequences.

4.2.1. Sequences Initiated by Large Steam-line Break at HZP

Three sequences [sequences 1.4 and 1.7 plus a sequence to represent the residual* (1.8)] were chosen to provide information for sequences initiated by a large steam-line break at HZP. Two large break sizes are covered by the three sequences: 0.1 m^2 and a full double-ended main steam-line break. The two different break sizes will be used to examine the effects of the range of sizes in the large-break category. The 0.1-m^2 break size was used for sequence 1.4, and the full-break size was used for sequence 1.7 and the residual sequence. These three sequences can be used to provide the following information for analysis of the large steam-line break sequences:

(1) The effect of a variance of break size,

(2) The effect of continued feeding to the steam generator on the broken line,

(3) The effect of the blowdown of both steam generators.

In Chapter 2 it was stated that Baltimore Gas and Electric is considering a procedures change at Calvert Cliffs-1 which would leave two reactor coolant

*The residual was represented by the sequence involving the failure of both MSIVs and a full system repressurization.

pumps running during a cooldown caused by a secondary system initiating event. Although this sequence has not been identified as part of the sequence tables, it was felt that a full calculation of this effect was necessary to evaluate the potential effect of this procedures change. Thus sequence 1.4 was analyzed with two reactor coolant pumps left running.

4.2.2. Sequences Initiated by Small Steam-line Break at HZP

At the time the 12 sequences were chosen, it was felt that data from the large-break cases at both HZP and full power, along with data from small-break cases at full power, could be used to estimate the small-break sequences at HZP. Thus no elaborate calculations were performed for small steam-line break sequences at the HZP condition. In retrospect, even though we were able to estimate the temperature and pressures associated with these transients, the evaluation would have been greatly simplified with at least one elaborate evaluation of a small steam-line break at HZP.

4.2.3. Sequences Initiated by Large Steam-line Break at Full Power

One elaborate evaluation was performed for this initiator. This sequence involved the 0.1-m^2 break with failure to control repressurization and failure to throttle auxiliary feedwater.

4.2.4. Sequences Initiated by Small Steam-line Break at Full Power

Small steam-line breaks at full power are dominated from a frequency standpoint by failures of ADVs and/or TBVs. As stated in Section 3.3.3.3,

failures of these valves at full power are treated as failures following a reactor trip initiator. Thus, the data used to estimate sequences in this category will come from calculations performed for the reactor trip initiator as described in Section 4.2.5.

4.2.5. Sequences Initiated by a Reactor Trip

Elaborate calculations were performed for four sequences associated with the reactor trip initiator. Two of these sequences deal with steam-line valve failure, while the remaining two are steam generator main feedwater overfeed sequences.

Both of the steam-line valve failure sequences involve the failure of a TBV. In the first sequence, the MSIVs close as required. This provides information on small steam-line breaks which are downstream of the MSIVs and involve isolation of the broken valve by closure of the MSIV. The second TBV failure sequence includes the failure of a MSIV to close. This not only provides information on small breaks downstream of the MSIVs when a MSIV fails to close, but also represents small breaks upstream of the MSIVs.

The two overfeed sequences involve: (1) the overfeed of one line, and (2) the overfeed of both lines. The overfeed on both lines represents the maximum main feedwater overfeed. The single line overfeed was examined to evaluate the potential for loop stagnation due to the asymmetric cooldown.

In all four sequences, operator actions to control repressurization and AFW

were not considered. This was done since it was determined to be much easier to extrapolate from the case where these operator actions are not performed to the case where they are performed than it would be to extrapolate from the case where these operator actions are performed to the case where they are not performed.

4.2.6. Sequence Initiated by a Small-Break LOCA ($\lesssim$0.016 ft^2)

The sequence chosen to provide information for this category was a PORV-sized break with a failure of one ADV to close. The PORV size was used to ensure that the pressure remains reasonably high during the transient. The additional failure of an ADV to close provides information on the coupling of a small-break LOCA and a small steam-line break. As in previous cases, the operator action to control AFW flow to the intact steam line was not considered for the initial calculation.

4.2.7. Sequence Initiated by a Small-Break LOCA ($\simeq$0.02 ft^2)

The most probable break size in this category is a 2-in. break because of the many 2-in. lines that come off of the main primary piping. A 2-in. break represents a flow area of ~0.02 ft^2 (0.002 m^2). Thus the calculation performed to provide information on this class of event was a 0.02-ft^2 break.

4.2.8. Sequences Initiated by LOCAs with Potential Loop Flow Stagnation

In Section 3.4.5, several sequences were defined which could potentially lead to loop flow stagnation. As stated in that section, it was determined that loop flow stagnation would be assumed for these cases as a screening mechanism. Since loop flow stagnation is assumed, the downcomer temperature becomes a mixing analysis. Thus these sequences were analyzed as part of the mixing analysis discussed in Section 4.4.

4.2.9. Sequence Initiated by Loss of Main Feedwater with Subsequent AFW Overfeed

In Section 3.4.6, a bounding case was identified to represent this category of event. Thus a transient analysis was performed for this sequence. In addition to the sequence description as given in Section 3.4.6, it was assumed that the repressurization was not controlled by the operator.

4.2.10. Summary

The 12 sequences identified can be grouped under three categories: (1) a steam-line break, (2) runaway feedwater, or (3) small-break LOCAs. A summary of these transients is presented in Table 4.1. It should be noted that except as specified in Section 4.3, several operator actions/inactions were assumed to be common to all LANL transient calculations.* These assumptions were:

---

*The probabilities associated with the operator failures were discussed in Chapter 3.

Table 4.1. Summary of twelve postulated overcooling transients

Steam-line Breaks

1-m^2 main steam-line break upstream of MSIVs

(1) From HZP
(2) From full power
(3) From HZP with two operating reactor coolant pumps

Double-ended main steam-line break upstream of MSIVs

(4) From HZP with continued AFW flow to broken steam line
(5) From HZP with two stuck-open MSIVs

Small steam-line break downstream of MSIVs

(6) From full power
(7) From full power with one stuck-open MSIV

Runaway Feedwater

(8) Runaway main feedwater to two steam generators from full power
(9) Runaway main feedwater to one steam generator from full power
(10) Runaway auxiliary feedwater to two steam generators from full power

Small-Break Loss-of-Coolant Accidents

(11) 0.002-m^2 hot-leg break from full power
(12) Stuck-open pressurizer PORV with stuck-open secondary system ADV from full power

(1) Operator turns off all RCPs 30 seconds after SIAS based on low pressurizer pressure.

(2) Operator fails to turn off charging pumps prior to full repressurization.

(3) Operator fails to control repressurization.

(4) Operator fails to maintain level in intact SG.

(5) Operator fails to respond to high SG alarm at 30 inches.

(6) Operator fails to respond to high SG alarm at 50 inches.

4.3. LANL TRAC Analysis

Los Alamos National Laboratory (LANL) participated in the PTS program by using the TRAC-PF1 computer code to provide best-estimate thermal-hydraulic analyses of the 12 postulated overcooling transients identified in Table 4.1. Each of the 12 transients was to be analyzed by LANL for a 2-hour transient period.* A summary of the TRAC model used and the results obtained for each transient analysis are presented in Sections 4.3.1-4.3.13. A separate report, "TRAC-PF1 Analysis of Potential Pressurized-Thermal-Shock Transients at a Combustion-Engineering PWR," has been published by LANL which describes in great detail both the model and the transient analysis performed. This report has been included here as Appendix F.

Since the thermal-hydraulic characteristics of the transients are in some instances a result of complex intra-system cooling mechanisms and since in many instances small differences in temperature can have significant effects on the fracture-mechanics analysis, a separate review of the TRAC analysis was performed by Brookhaven National Laboratory. The report summarizing the BNL work is included in this report as Appendix G.

---

*The 2-hour transient period was chosen for several reasons. First, the calculations are very expensive and the analysis of a 10-hour transient would incur substantial costs. From this standpoint, the 2-hour analysis could be considered an initial calculation where transients requiring further analysis are identified. The second reason is that many people feel that any overcooling event would be recognized and terminated given a 2-hour diagnosis period. Although the authors would not totally agree with this statement, we would concur that for the great majority of transients there are several means of recovery in a 2-hour period. Thus there is some legitimacy associated with limiting the analysis to 2 hours. However, one must be aware of potential transients for which recovery may be beyond the 2-hour period. Finally, beyond the 2-hour time frame the failure mechanism is clearly cold-over-pressurization rather than pressurized thermal shock.

4.3.1. TRAC-PF1 Model of Calvert Cliffs Unit 1

The TRAC model used for the Calvert Cliffs-1 analysis (TRAC-PF1) resulted from a evolutionary process involving several interactions with the plant owner, Baltimore Gas and Electric, and the plant vendor, Combustion Engineering. The TRAC noding diagrams for the primary system, feedwater train, and steam lines are presented in Figures 4.1, 4.2, and 4.3, respectively. The development of the noding and control signals for each system is described in detail in Appendix F.

Two initial condition models, hot-zero power and full power, were required to analyze the 12 transients. For each initial condition model, a steady-state calculation was performed and compared with plant data.

The TRAC-PF1 HZP steady-state calculation for Calvert Cliffs-1 yielded very stable primary-side conditions but oscillatory secondary-side conditions. The fundamental difficulty in determining the secondary-side conditions during HZP occurred because the vapor-generation rate was very small and appeared to destabilize the steady-state solution for the SG model.

Table 4.2 compares the actual plant conditions with the conditions generated by TRAC after 15 minutes (reactor time) of the steady-state HZP calculation. The comparison is reasonable with the exception of secondary steam flow. A simple energy balance dictates that, in the steady state, the tabulated plant value for the steam flow is correct. The over-prediction by TRAC suggests that the liquid temperature entering the SG riser was too high because the temperature profile in the downcomer was not

Table 4.2. Comparison between TRAC and measured plant data at hot zero power conditions

Parameter	Measured Plant Data	TRAC Predictions
	Primary Side	
1. Pressure	15.5 MPa (2250 psia)	15.5 MPa (2250 psia)
2. Fluid temperature	550.9 K (532°F)	551.8 K (534°F)
3. Power	100 hr after shutdown + pump power	9.38 MW decay heat + 17.38 MW from the pump
4. Mass flow	19,300 kg/s (153 x 10^6 lb/h)	19,700 kg/s (156 x 10^6 lb/h)
5. Pressurizer	3.66 m (144 in.)	3.66 m (144 in.)
	Secondary Side	
1. Pressure	6.20 MPa (900 psia)	6.17 MPa (896 psia)
2. MFW temperature	300 K (80°F)	300 K (80°F)
3. Steam flow	10.1 kg/s (22.2 lb/s)	11.8 kg/s (26.0 lb/s)
4. SG inventory	95,000 kg (210,000 lb)	102,000 kg (225,000 lb)
5. TBV flow area	?% open	5% open

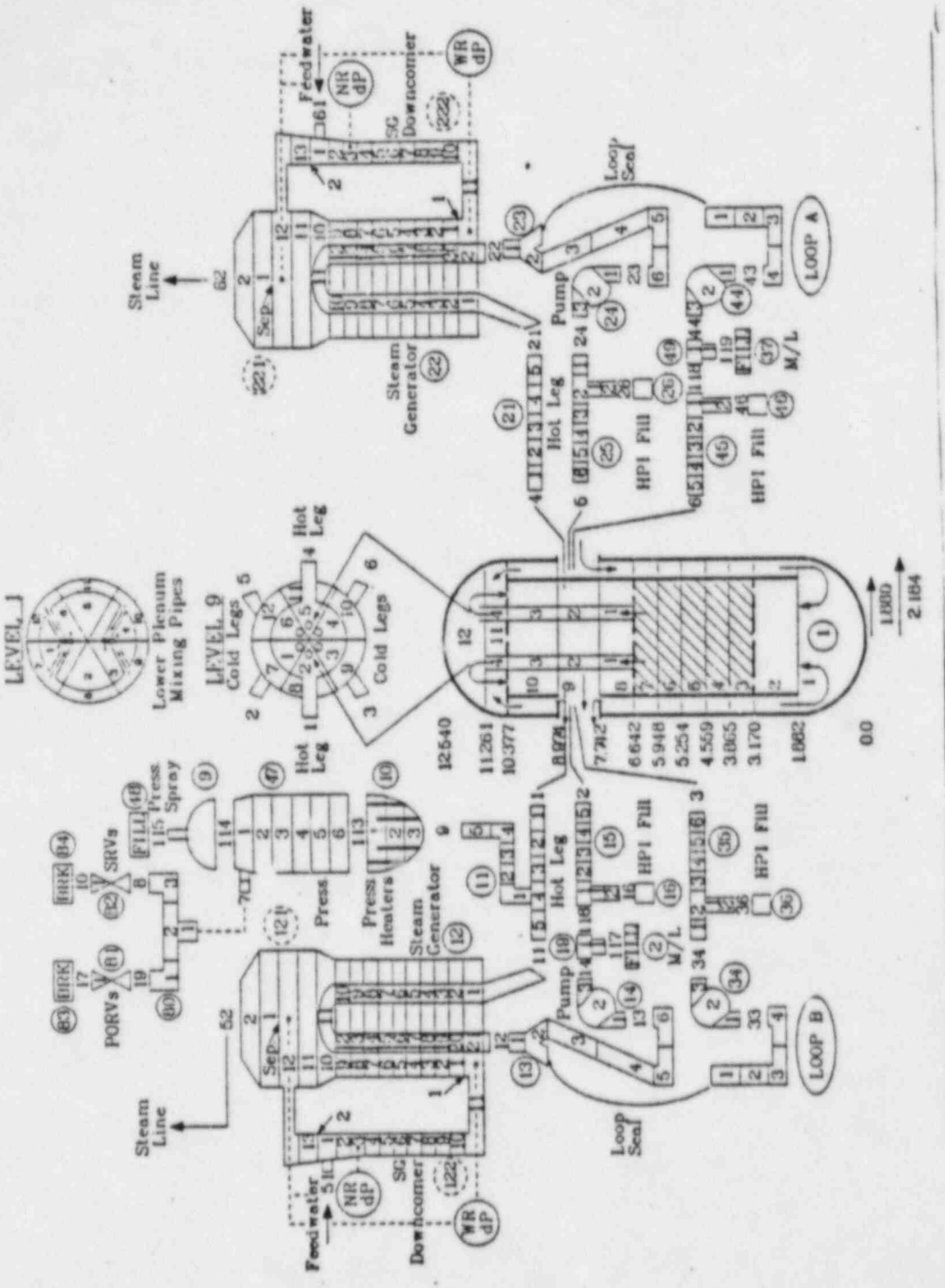

Figure 4.1. TRAC noding diagram for the primary side at Calvert Cliffs-1 (from Ref. 37).

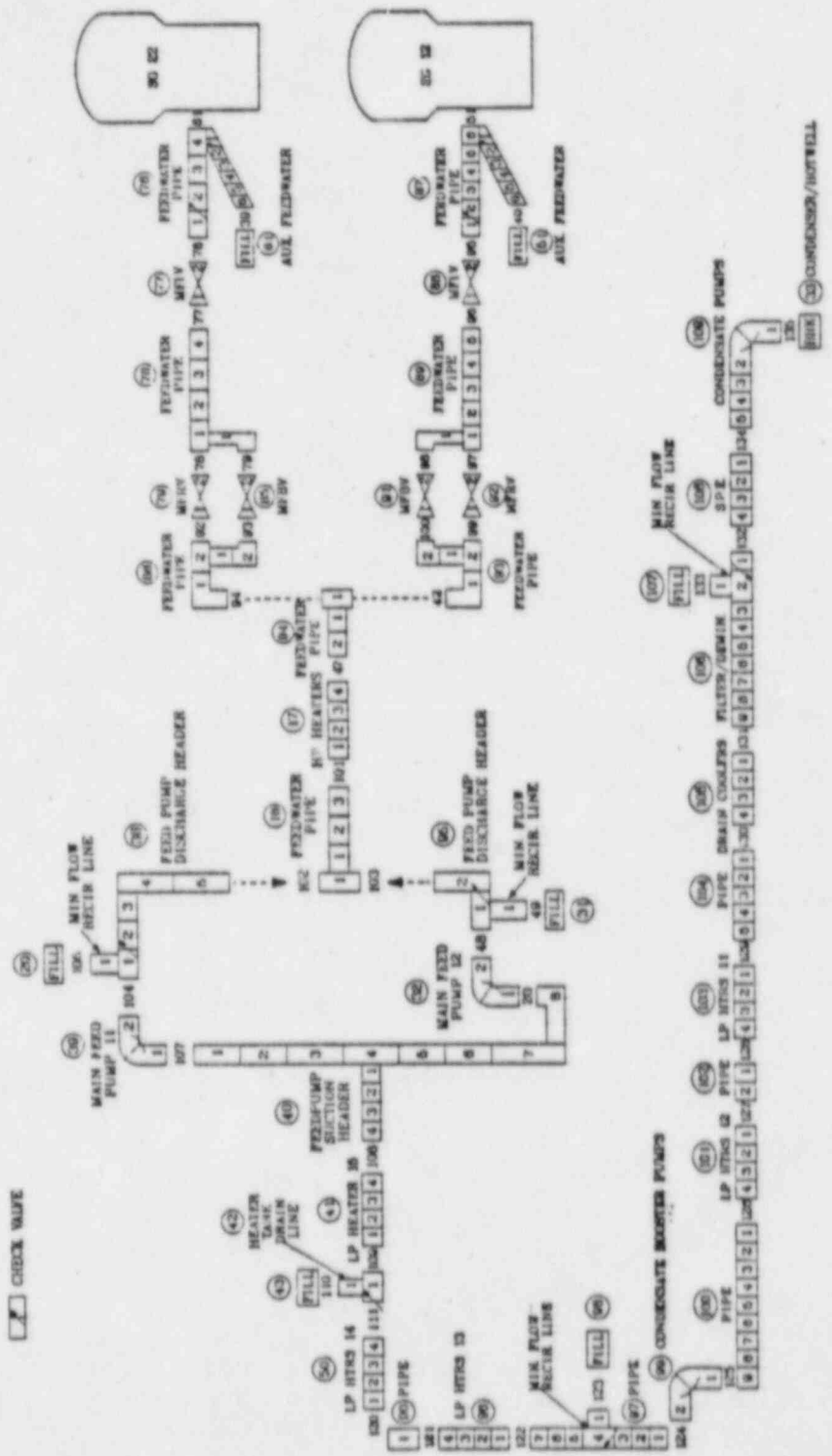

Figure 4.2. TRAC nodding diagram for the feedwater train at Calvert Cliffs-1 (from Ref. 37).

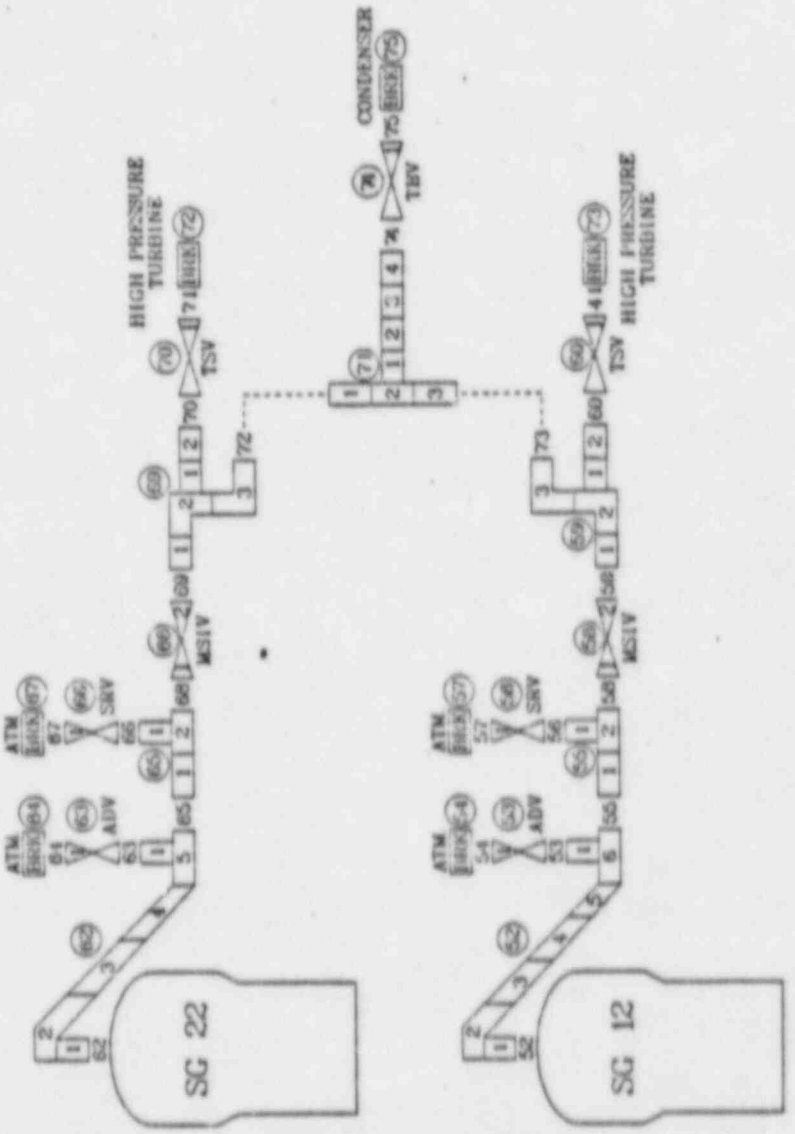

Figure 4.3. TRAC noding diagram for the steam lines at Calvert Cliffs-1 (from Ref. 37).

fully established.

The HZP temperature profiles appear reasonable and reveal a situation in which the cold feedwater heated to saturation by the time it entered the riser section. In the riser, the small vapor-generation rate yielded a very small void fraction until the liquid surface was reached.

Even with the exaggerated steam flow, the LANL analysts believe that the TRAC HZP steady-state solution was close to the actual plant conditions. This belief is supported by the correspondence of the TRAC solution to the conditions intuitively expected when the power was nearly zero, that is, a primary temperature that was essentially uniform and a secondary temperature that resembled a slowly simmering pot of boiling water.

Of the 12 transients, eight were initiated from full-power steady-state conditions. During full power the reactor operated at 2700 MW with an additional energy input of 17.38 MW from the RCPs. The calculated temperature increase across the vessel was 26.4 K (47.6°F) with an inlet temperature of 559.3 K (547.0°F). The pressure drop through the loop was 0.54 MPa (78.7 psid). Makeup/letdown flow regulated the pressurizer level to 5.46 m (215 in.).

Heat was transferred through two SGs to the secondary loop. The feedwater flow was regulated to maintain a specified liquid level by the MFRV using a three-mode controller. The valve area was determined from the SG level and feedwater flow/steam flow mismatch as described in Appendix F. The MFW-pump speed was adjusted to maintain a constant pressure drop of 0.71 MPa

(105 psid) across the MFRVs. The feedwater was heated to 495 K (431°F) by two high-pressure feedwater heaters and four low-pressure feedwater heaters. The liquid mass in each SG was ~62300 kg (136400 lb).

The full-power transients were initiated from different full-power steady-state calculations. As the Calvert Cliffs-1 model evolved during the calculation of the transients, it was necessary to rerun a steady-state calculation whenever a model was modified. Table 4.3 gives a comparison between the TRAC calculation and the measured plant conditions for the last steady-state calculation. The results are in good agreement, as were those from the previous calculations.

4.3.2. Steam-line Break Calculations

The steam-line breaks considered in this analysis ranged from a double-ended guillotine break to a single stuck-open TBV. The general events following a steam-line break were as follows. After a break or stuck-open valve occurred in the steam line, secondary depressurization resulted. If the plant was at full power, the reactor and turbine tripped (probably on liquid level in the SG) and the MFW flow ran back. Because the secondary liquid temperature decreased with the saturation temperature, the primary temperature was governed by the ΔT across the tubes in the SGs.

The decrease in secondary pressure caused an SGIS, initiating closure of the MSIVs and MFIVs. If these valves operated correctly and isolated one SG from the break, asymmetric conditions were induced on the primary side. As described in the TRAC-Analysis-Methodology section of the LANL report,

Table 4.3. Comparison between TRAC and measured plant data at full-power conditions

Parameter	Measured Plant Data	TRAC Predictions
	Primary Side	
1. Core power	2694 MW	2700 MW
2. Vessel flow	25.27 m^3/s (401,100 gpm)	24.9 m^3/s (395,250 gpm)
3. ΔP_{vessel}	—	0.23 MPa (33.5 psid)
4. ΔP_{SG}	0.19 MPa (28.15 psid)	0.19 MPa (28.15 psid)
5. ΔP_{loop}	0.54 MPa (78.73 psid)	0.55 MPa (80.5 psid)
6. T_{cold}	559.3 K (547.0°F)	559.5 K (547.7°F)
7. ΔT_{vessel}	26.4 K (47.6°F)	26.0 K (47.0°F)
	Secondary Side	
1. Feedwater flow per SG	749 kg/s (5.95 x 10^6 lb/h)	737 kg/s (5.85 x 10^6 lb/h)
2. SG dome pressure		
Loop-A SG	5.90 MPa (856 psig)	5.9 MPa (852 psig)
Loop-B SG	5.86 MPa (850 psig)	5.9 MPa (852 psig)
3. MFW pump discharge pressure		
Loop-A SG	7.8 MPa (1130.7 psia)	7.66 MPa (1125.7 psia)
Loop-B SG	7.63 MPa (1106.7 psia)	7.56 M (1111.0 psia)
4. MFW temperature	494.8 K (431.0°F)	496.2 K (433.5°F)
5. MFRV flow area (% open)	~90	93
6. SG liquid mass	62,350 kg (137,458 lb)	63,000 kg (138,600 lb)

Appendix F, this asymmetry could result in temporary flow stagnation in the "intact" SG so that it eventually boiled dry. AFW filled the intact SG and because of assumed operator inaction, the intact SG overfilled. If neither or both SGs were isolated, symmetric conditions would exist on the primary side and AFW would be delivered to both SGs if a low liquid level in the SGs was reached.

4.3.2.1. Transient 1: 0.1-m^2 Main Steam-line Break from HZP

The downcomer temperature and pressure profiles for Transient 1 are presented in Figures 4.4 and 4.5, respectively.

The temperature profile was divided into three phases. Phase 1 (0 - 1300 seconds) was dominated by the blowdown of SG A. The blowdown was limited by choked flow through the 0.1-m^2 (1.0-ft^2) break. Data from Combustion Engineering indicated that the moisture separators would continue to be effective at the predicted steam flows and thus the fluid exiting the break was 100% steam. As SG A depressurized, the saturated liquid flashed and the secondary temperature decreased according to the saturation curve. Power extraction slowed as the liquid inventory depleted because the tubes began uncovering, which steadily decreased the heat-transfer area. Because AFW was valved out to SG A based on an asymmetric-SG-pressure signal, its secondary eventually voided completely. This event marked the end of Phase 1 (at 1300 seconds).

Phase 2 (1300 - 4200 seconds) of the downcomer liquid temperature was the period after SG A dryout and before natural circulation was established in

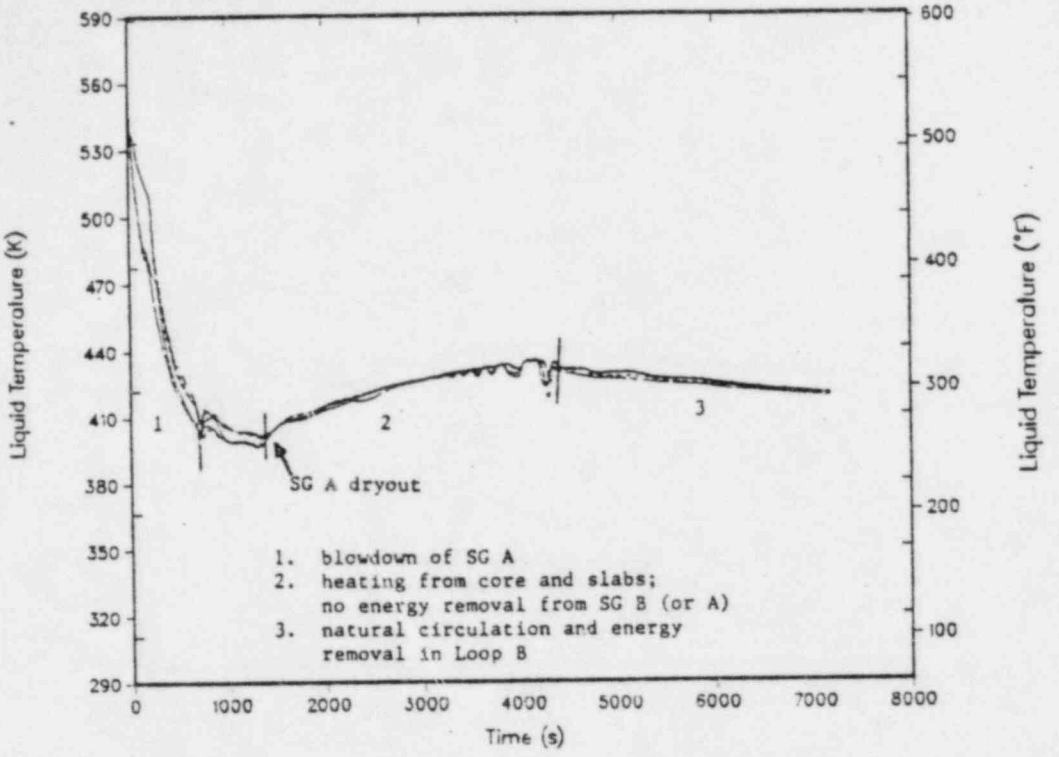

Figure 4.4. Transient 1: Downcomer liquid temperature during 0.1-m² main steam-line break from HZP. (Note: This transient assumes *MULTIPLE* operator/equipment failures; see Section 4.1.10 for failure assumptions.)

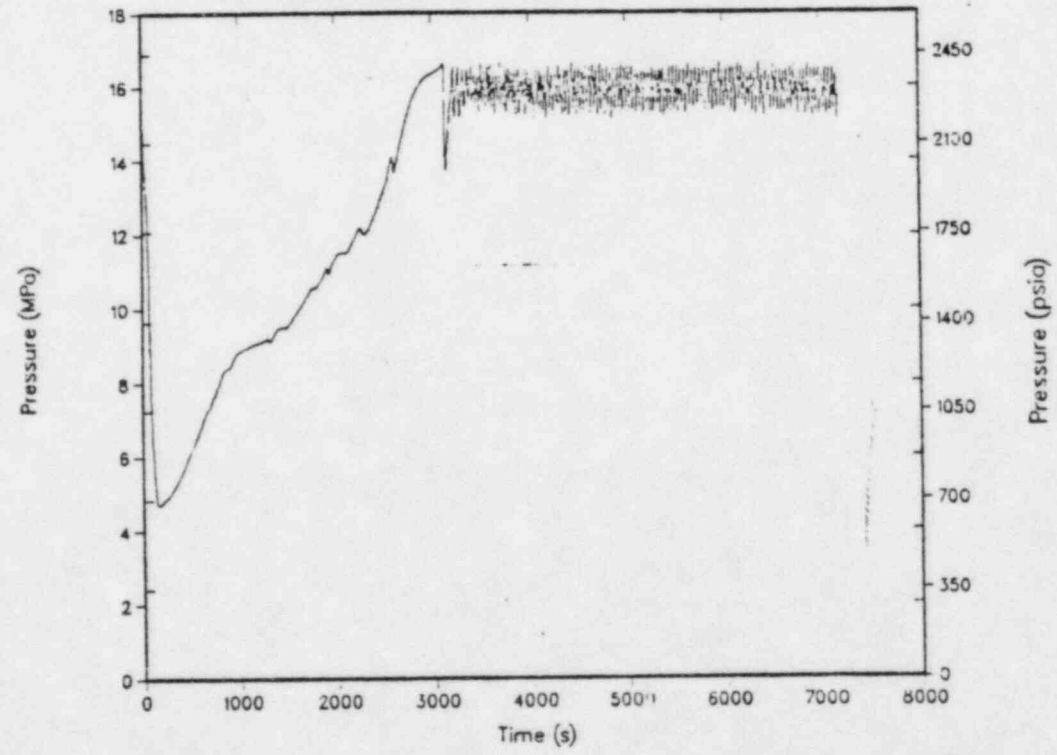

Figure 4.5. Transient 1: Primary system pressure during 0.1-m² main steam-line break from HZP. (Note: This transient assumes *MULTIPLE* operator/equipment failures; see Section 4.1.10 for failure assumptions.)

Loop B. The downcomer temperature went through a maximum of 435 K at 4200 seconds. Energy was added via the core and heat slabs. The RCPs and SG A had no input during this time period. SG B added energy only to the tubes because Loop B was stagnant throughout Phase 2. The deadhead of the HPI pumps was reached at 100 seconds so HPI flow was zero in Phase 2. Charging flow continued throughout the transient. The PORVs opened at 3120 seconds,* relieving the fluid input from the charging system but at a much higher temperature.

Phase 3 (4200 - 7200 seconds) began with the onset of natural circulation in Loop B. Because it was assumed the operator failed to throttle AFW, the liquid level in SG B rose above the moisture separator deck and natural circulation was established on the secondary. AFW mixed with the warmer liquid in the riser, making SG B an effective heat sink. Energy removal by SG B induced natural circulation on the primary side. It is interesting that as the primary fluid mixed in the system, the downcomer temperature approached the bulk temperature circulated at 4200 seconds. The circulation was ended at 7200 seconds with the primary temperature decreasing slightly. SG B was slowly becoming a colder heat sink with continued injection of AFW. The primary temperature was also decreasing as charging flow replaced the hotter fluid leaving through the PORVs.†

4.3.2.2. Transient 2: 0.1-m^2 Main Steam-line Break from Full Power

With the exception of the initial power condition (full power vs HZP), Transient 2 is identical to Transient 1. The temperature and pressure

---

*It is assumed for this calculation that no attempt is made by the operator to control the repressurization. This allows the pressure to reach the point at which the PORV will open.

†This assumes that the PORV is allowed to continually cycle open and shut for the duration of Phase 3.

profiles are presented as Figures 4.6 and 4.7, respectively.

Again Phase 1 of the downcomer liquid temperature profile was the period during SG-A blowdown. Because the system energy was higher and the SG mass lower, SG A dryout occurred much earlier (at 300 seconds) than for the same transient from HZP. MFW [~5000 kg (11000 lb)] was added to each SG for 15 seconds after the reactor/turbine trip, but this was balanced by steam flow through the TBVs. Because loop flows were very low in Loop B from ~250 to 750 seconds, the downcomer liquid temperature varied as much as 30 K (54°F) in the azimuthal direction. The total energy-removal capability of SG A was 98.1 GW-s. SG B removed 30.9 GW-s before SGIS at 44 seconds. After this, SG A cooled the primary below SG B, and the resulting energy addition, though small, severely slowed the flow in Loop B.

Phase 2 (~300 - 800 seconds) was a period of relatively rapid heating following SG-A dryout. Because Loop B was close to stagnation, less primary fluid was available to receive the energy deposition from the core, and so the specific energy of the flowing fluid increased rapidly. As the primary temperature increased, SG B became an effective heat sink. In Phase 3 (800 - 2500 seconds), the average core power was ~46 MW. SG B removed ~24 MW and the PORVs removed some energy after they opened at 1975 seconds,* but the primary fluid continued to heat.

Phase 4 (2500 - 7200 seconds) was extrapolated from a previous calculation of the same transient. As the core power decreased, a balance was achieved with the energy removal by SG B and flow through the PORVs.† A quasi-equilibrium state existed in Phase 4 with the downcomer temperature at

---

*It is assumed for this calculation that no attempt is made by the operator to control the repressurization. This allows the pressure to reach the point at which the PORV will open.

†This assumes that the PORV is allowed to continually cycle open and shut for the duration of Phase 4.

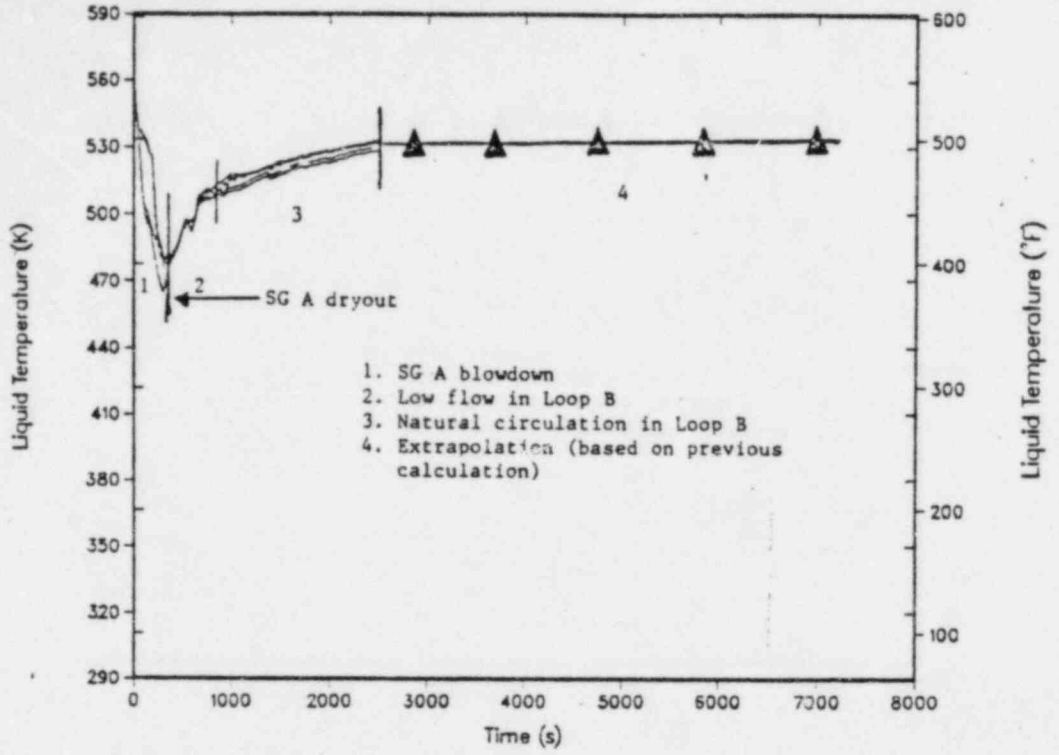

Figure 4.6. Transient 2: Downcomer liquid temperature during 0.1-m² main steam-line break from full power. (Note: This transient assumes *MULTIPLE* operator/equipment failures; see Section 4.1.10 for failure assumptions.)

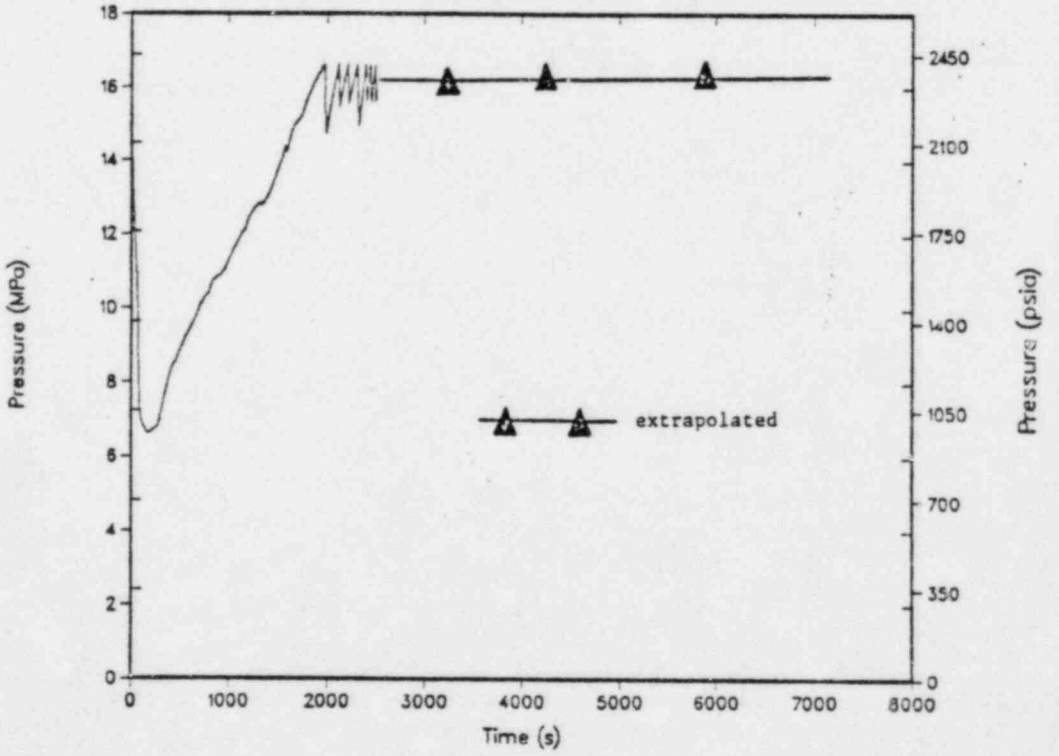

Figure 4.7. Transient 2: Primary system pressure during 0.1-m² main steam-line break from full power. (Note: This transient assumes *MULTIPLE* operator/equipment failures; see Section 4.1.10 for failure assumptions.)

530 K (495°F). The primary temperature would decrease slightly with time because:

(1) The decay heat was decreasing;

(2) SG B was becoming slightly colder with continued AFW; and

(3) charging flow at 300 K (80°F) was replacing hotter fluid that left through the PORVs.

4.3.2.3. Transient 3: 0.1-m^2 Main Steam-line Break from HZP with Two Operating Reactor Coolant Pumps

This transient was identical to Transient 1 except that two diametrically opposite RCPs remained in operation throughout the transient. The principal effect of leaving two RCPs in operation was that loop-flow stagnation did not occur in Loop B and SG B became a considerable heat source during the initial part of the transient (0 - 500 seconds).

Figures 4.8 and 4.9 show the downcomer liquid temperature and the downcomer pressure for this transient. Again the time for the downcomer temperature was divided into three phases. Phase 1 (0 - 500 seconds) corresponded to SG A blowdown and ended at the time of minimum downcomer temperature. Because two RCPs were still operating, energy-transfer rates were much higher than when all four RCPs were tripped and SG A dried out at 500 seconds. The forced circulation in Loop B allowed SG B to deposit considerable energy into the primary while it was being cooled by SG A.

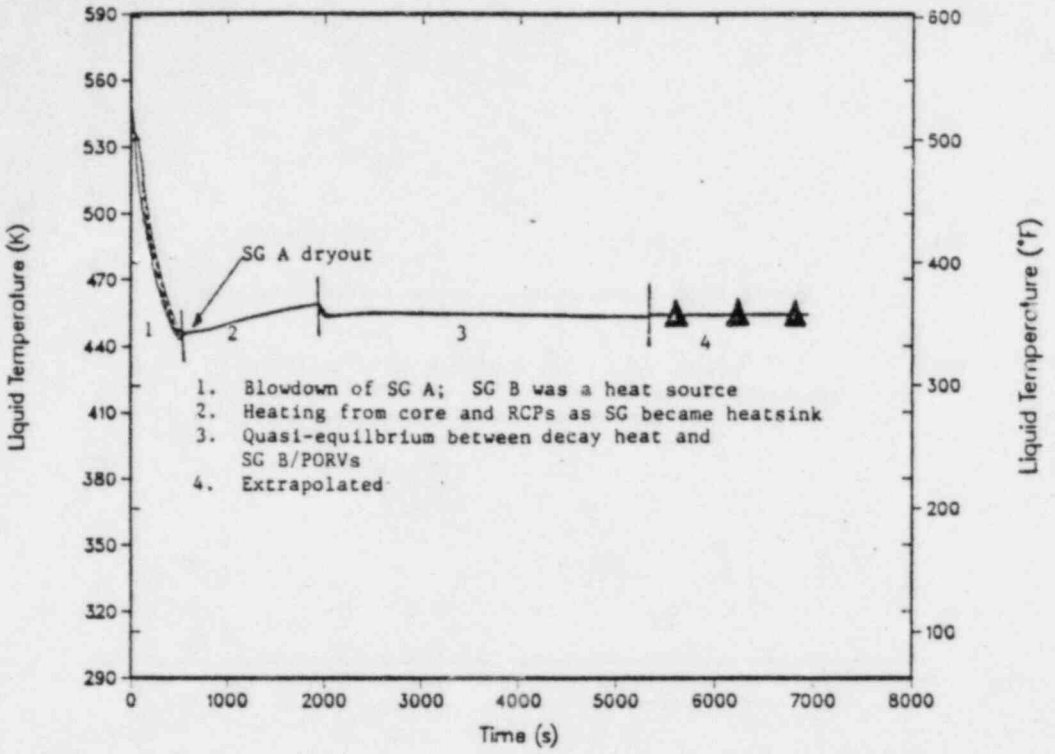

Figure 4.8. Transient 3: Downcomer liquid temperature during 0.1-m^2 main steam-line break from HZP with two operating RCPs. (Note: This transient assumes *MULTIPLE* operator/equipment failures; see Section 4.1.10 for failure assumptions.)

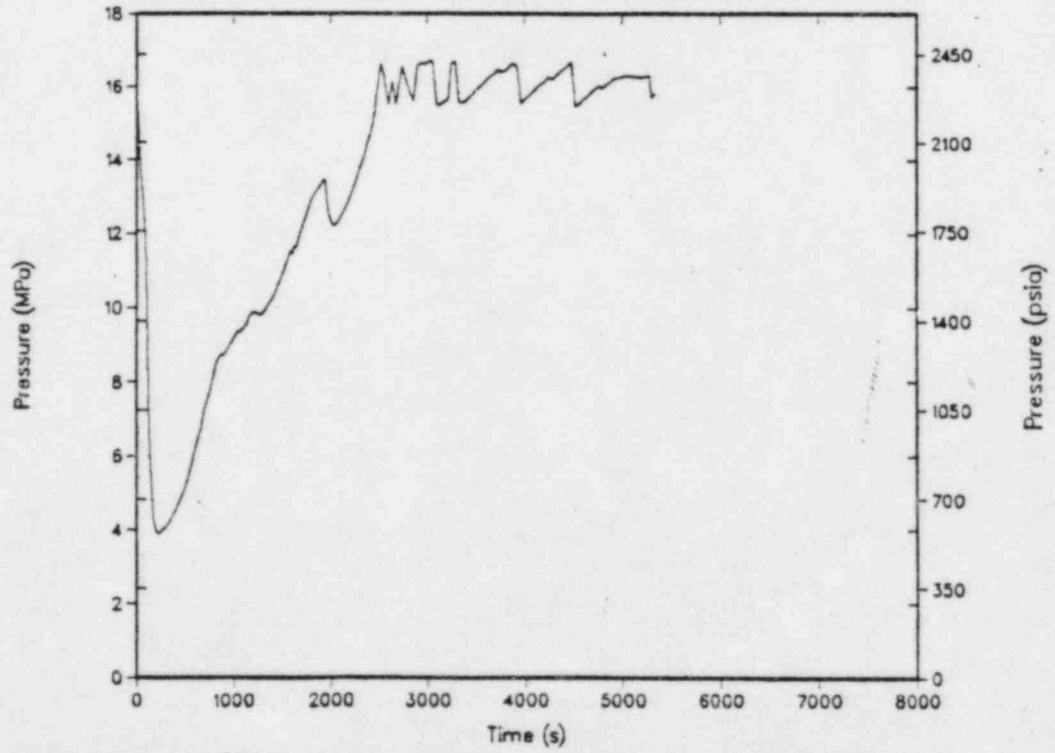

Figure 4.9. Transient 3: Primary system pressure during 0.1-m^2 main steam-line break from HZP with two operating RCPs. (Note: This transient assumes *MULTIPLE* operator/equipment failures; see Section 4.1.10 for failure assumptions.)

Phase 2 (500 - 1900 seconds) was a period of primary fluid heating (from the core, the two operating RCPs, and the primary side heat slabs) before SG B became a significant heat sink. Not much cooling was provided by HPI and charging flow. Phase 3 (1900 - 5300 seconds) began with a significant increase in the heat-transfer rate across the tubes in SG B. This abrupt increase was a result of an inadequacy in the TRAC code but perhaps was physical to some extent. As the secondary side of SG B filled with AFW above the moisture separator deck, the liquid began to spill over into the steam space in the SG downcomer above the feedwater ring. As seen from the rapid depressurization, TRAC overpredicted the condensation rate that would result from this spillover. The resulting depressurization caused the cold AFW that had accumulated in the SG downcomer to flow into the riser region. The colder liquid came into contact with the tubes and the energy-removal rate from the primary increased.

After 2500 seconds, a quasi-equilibrium state was reached. The PORV opened,* removing approximately 8 MW. SG B removed the remainder of the energy input from the core, the heat slabs, and the RCPs, which amounted to ~15 MW. The calculation was terminated at 5300 seconds with the system in this quasi-equilibrium state. The system was cooling slightly with time because SG B was becoming a cooler heat sink with continued AFW and charging flow was replacing the hotter fluid leaving the PORVs.†

4.3.2.4. Transient 4: Double-Ended Main Steam-line Break from HZP with Failure to Isolate‡ AFW Flow to Broken Steam Line

The downcomer temperature and pressure profiles for Transient 4 are

*It is assumed for this calculation that no attempt is made by the operator to control the repressurization. This allows the pressure to reach the point at which the PORV will open.

†This assumes that the PORV is allowed to continually cycle open and shut for the duration of Phase 3.

‡Includes both failure of automatic system and failure of operator to respond.

presented as Figures 4.10 and 4.11. As shown in Figure 4.10, the downcomer temperature was again divided into three phases. The first phase (0 - ~800 seconds) is characterized by severe overcooling of the primary caused by the rapid blowdown of SG A to atmospheric pressure. Although the blowdown rate was limited by the flow restrictors downstream of the SGs, the mass flow out of the SGs increased by more than three orders of magnitude over the HZP steady-state value. Furthermore, the assumed failure of the asymmetric-SG-pressure signal to effect isolation of AFW to SG A ensured that the atmospheric heat sink would not be lost because of SG dryout. During this period, the flow in Loop B stagnated following the RCPs being tripped because of reverse heat transfer in SG B following SGIS. Also, during this period the upper heat of the vessel voided briefly (90 - 350 seconds) because the primary fluid contraction initially exceeded the HPI/charging refilling capacity. A model input error caused closure of the MFIVs on AFAS at 2 seconds instead of on SGIS at 9 seconds, but this error has no significant effect on the results.

The second phase (~800 - 3275 seconds) is characterized by repressurization of the primary caused by unrestricted operation of the charging pumps. During this phase of the transient there is an approximate balance between decay heat, heat transfer from the structure to the fluid and heat rejection to SG A. However, because the HPI and charging flow added substantial mass to the primary [~46000 kg (101000 lb) during 0 - 800 seconds and ~30000 kg (66000 lb) during 800 - 3275 seconds to an initial mass of 224000 kg (493000 lb)] but very little enthalpy, the average specific internal energy decreased slightly. By 3200 seconds the downcomer temperature had leveled off at 380 K.

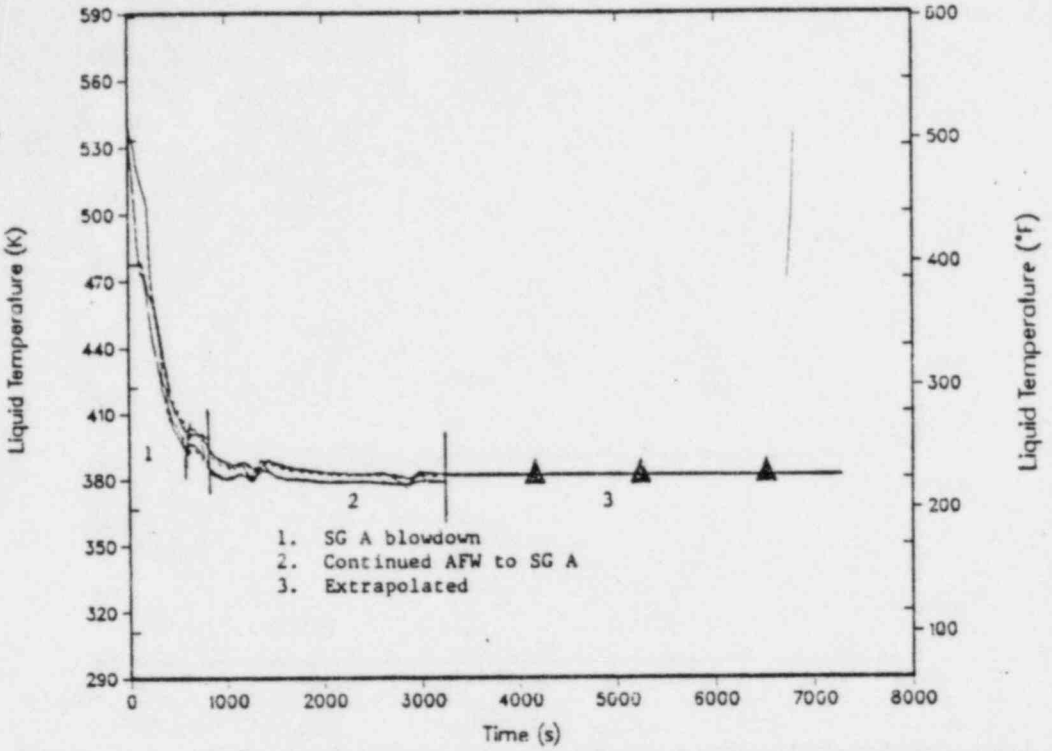

Figure 4.10. Transient 4: Downcomer liquid temperature during double-ended main steam-line break from HZP with failure to isolate AFW flow to broken steam line. (Note: This transient assumes *MULTIPLE* operator/equipment failures; see Section 4.1.10 for failure assumptions.)

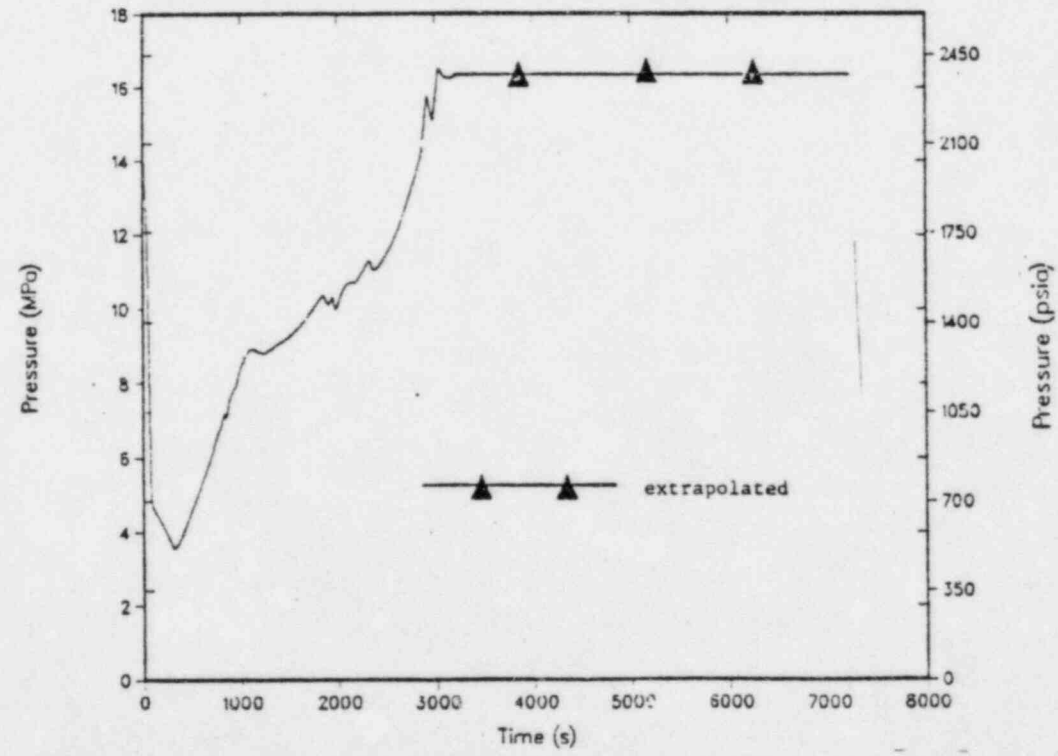

Figure 4.11. Transient 4: Primary system pressure during double-ended main steam-line break from HZP with failure to isolate AFW flow to broken steam line. (Note: This transient assumes *MULTIPLE* operator/equipment failures; see Section 4.1.10 for failure assumptions.)

The problem was terminated at 3275 seconds because the transient had stabilized with respect to downcomer temperature and pressure. PORV cycling between 15.7 MPa and 16.5 MPa would limit the pressure because PORV capacity was more than adequate to relieve the charging flow. Furthermore, the decay power was sufficient to heat the AFW to SG A to the atmospheric boiling temperature; therefore, the liquid temperature in the downcomer of the vessel would not fall below 373 K (121°F) within 7200 seconds (Phase 3).

4.3.2.5. Transient 5: Double-Ended Main Steam-line Break Upstream of MSIVs from HZP with Two Stuck-Open MSIVs

Transient 5 is the same as Transient 4 except that the MSIVs failed to close upon receipt of SGIS and blowdown of both SGs continued. Also, the operator terminated AFW flow at 480 seconds (8 minutes).

The transient may be divided into three phases as shown on a plot of the downcomer liquid temperature in Figure 4.12. In Phase 1 (0 - 1000 seconds), a minimum temperature of 376 K was reached, which was a few degrees above the temperature of the liquid remaining in each SG-secondary after the blowdown to 0.1 MPa (14.7 psia). Each SG removed ~97 GW-s of energy from the primary, which included AFW flow for 390 seconds. The heat slabs added 33.1 GW-s to the primary fluid.

After the AFW ended at 480 seconds, the primary temperature leveled off a few degrees above the secondary temperature (Phase 2). The downcomer temperature increased slightly after the termination of HPI flow at 1000 seconds. In extrapolated Phase 3 (3300 - 7200 seconds) the power from the

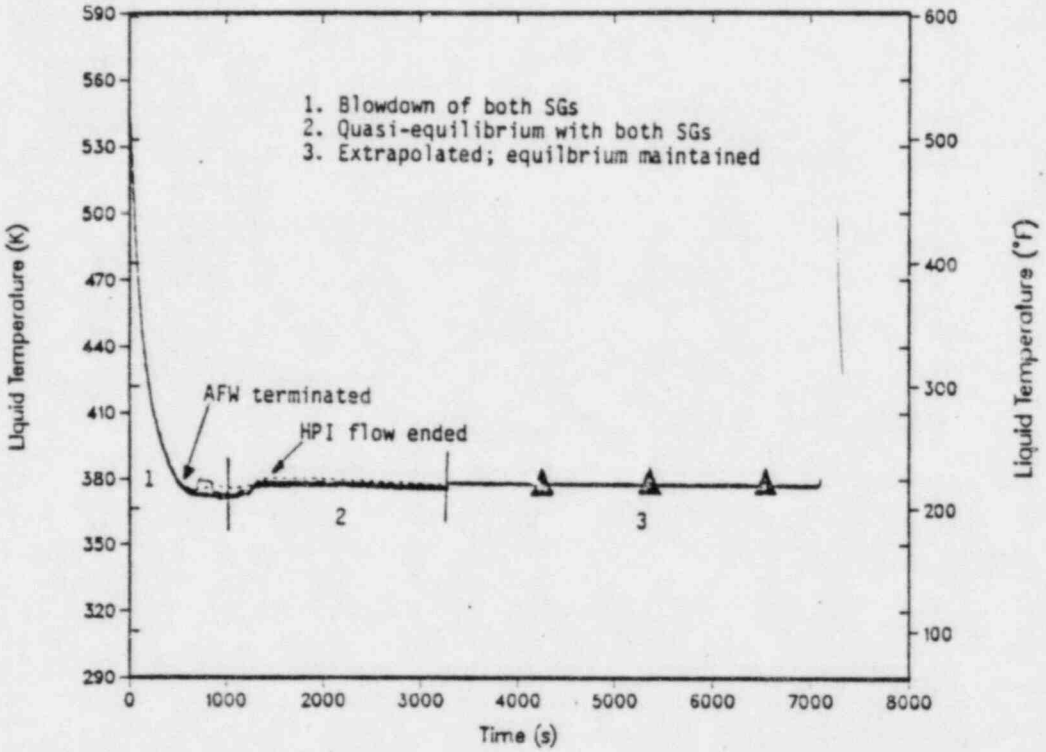

Figure 4.12. Transient 5: Downcomer liquid temperature during double-ended main steam-line break from HZP with two stuck-open MSIVs. (Note: This transient assumes *MULTIPLE* operator/equipment failures; see Section 4.1.10 for failure assumptions.)

primary is expected to slowly boil the remaining liquid in each SG [~18000 kg (~40000 lb)]. At 3300 seconds, the power from the heat slabs was ~7.5 MW. Together with 9 MW from the core, a steaming rate of ~4 kg/s would be produced in each SG. With this rate as a maximum (heat input from the slabs would decrease in time), the SGs would dry out in another 4650 seconds (t = 7950 seconds), which is past the end of this transient. Thus, the temperature is expected to remain at ~378 K (221°F) for the remainder of the transient.

Figure 4.13 gives the system pressure. The blowdown of both SGs caused the system to depressurize to 4.1 MPa. HPI flow reached a maximum of 60 kg/s to make up for the primary liquid contraction. The upper head voided during the 50- to 900-second time frame. Charging flow eventually repressurized the primary system to the PORV setpoint* where it was assumed to remain for the rest of the transient.†

4.3.2.6. Transient 6: Small Steam-line Break Downstream of MSIVs from Full Power

The failure of one TBV to reseat after opening on a turbine trip is postulated in this transient. One full-open TBV is about half the size of the 0.1-m^2 (1.0-ft^2) break described previously (0.05 m^2/0.51 ft^2). Because the TBVs are downstream of the MSIVs, a stuck-open TBV is isolatable, whereas the 0.1-m^2 MSLB described previously was not. The "break" communicated with each SG identically and so the thermal-hydraulic events on both the secondary and the primary side are symmetric.

---

*It is assumed for this calculation that no attempt is made by the operator to control the repressurization. This allows the pressure to reach the point at which the PORV will open.

†This assumes that the PORV is allowed to continually cycle open and shut for the duration of Phase 3.

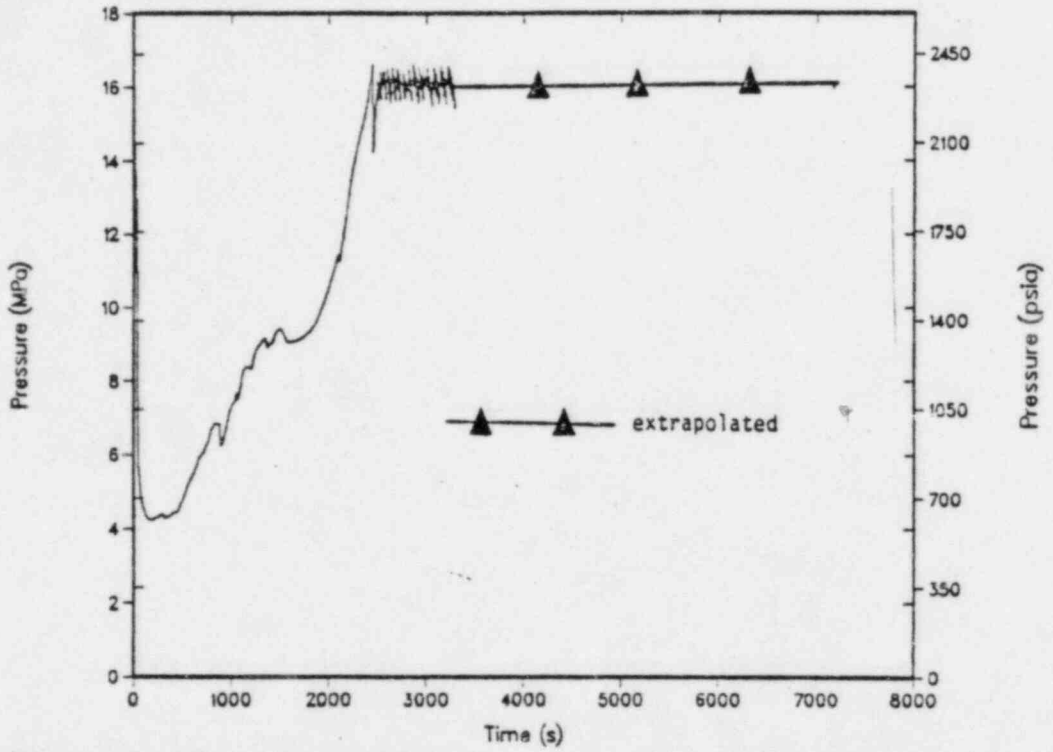

Figure 4.13. Transient 5: Primary system pressure during double-ended main steamline break from HZP with two stuck-open MSIVs. (Note: This transient assumes *MULTIPLE* operator/equipment failures; see Section 4.1.10 for failure assumptions.)

The temperature history in the downcomer (Figure 4.14) was divided into five phases. Phase 1 (0 - 510 seconds) was the time before the stuck-open TBV was isolated from the SGs as a result of the closure of the MSIVs following SGIS. The initial ~50 seconds of the transient should have been identical to a loss-of-load.* The TBVs reseated as the primary temperature decreased. When one failed, a relatively slow depressurization began in both SGs. The secondary pressure decreased until the setpoint for SGIS was reached. This marked the end of the cooldown caused by the stuck-open TBV.

Phase 2 (510 - 1050 seconds) was a time of primary fluid heating ending with opening of the ADVs on high primary temperature. Boiling on the SG secondary continued to remove energy but at a slower rate as the secondary repressurized. The ADVs were open in Phase 3 (1050 - 4200 seconds), modulating to maintain the average primary temperature at 552 K. The TBVs also opened, but they had no effect because the MSIVs were closed.

Boiling in the SGs continued and mass was depleted through the ADVs. AFAS was received at 4200 seconds based on low level in both SGs.† Phase 4 (4200 - 5800 seconds) began with AFW flow to both SGs. A cooldown ensued as the AFW mixed with the boiling liquid in the riser phase. AFW flow affected the primary temperature in this transient more than in others because it was initiated to both SGs (no asymmetric-SG-pressure signal) and both SGs were low in inventory. Also, both loops were in natural circulation on the primary; this allowed rapid feedback to the primary side. The cooldown is expected to continue at the same rate until 7200 seconds, reaching a minimum of ~510 K. Phase 5 (5800 - 7200 seconds) is the extrapolated temperature history.

*Because of an error in the initial liquid temperatures in the pressurizer, the primary side depressurized much too rapidly. This calculation was to be redone, but because it was already predicted not to be of PTS concern, an additional failure of one MSIV was specified. The recalculation is reported in the next section. The period (0 - 570 seconds) before SGIS was identical to the specifications of this transient. This transient is included to give details of a 7200-second transient with the failure of one TBV only.

†AFAS was based on a ΔP measurement of -4.3 m (-170 in.). This corresponded to a liquid inventory of ~17000 kg. Based on a collapsed liquid measurement, AFAS would occur with 45,000 kg remaining in the SGs. It is unknown which method is more correct, but AFAS probably was sent later than it should have been.

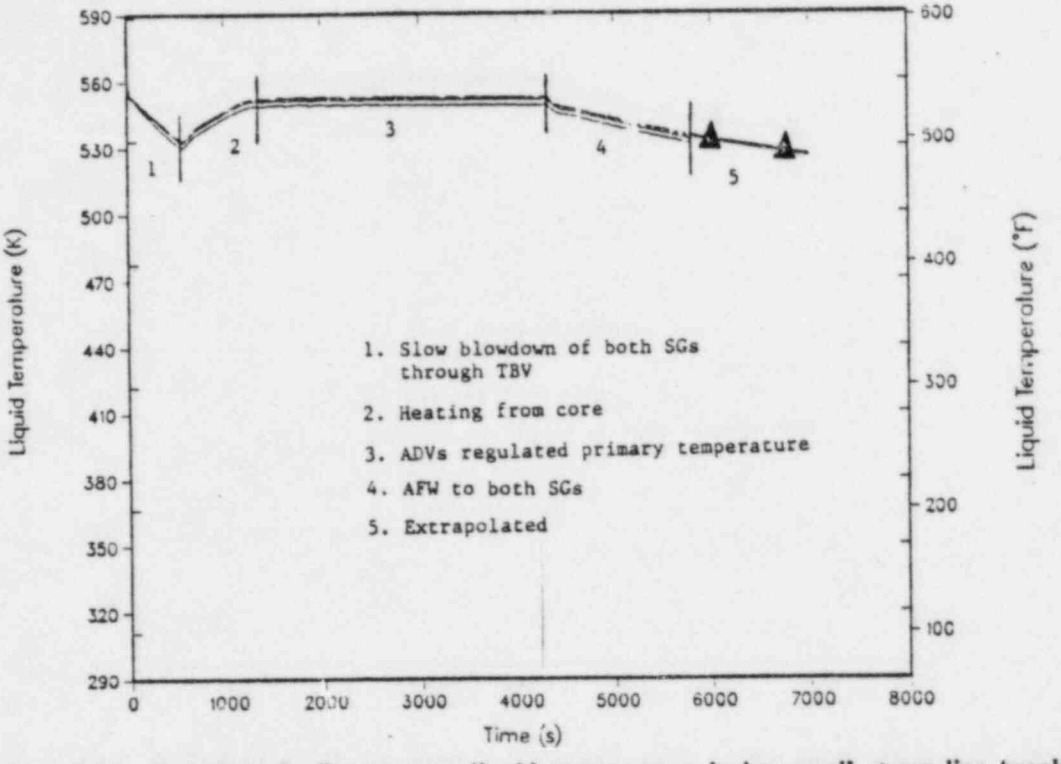

Figure 4.14. Transient 6: Downcomer liquid temperature during small steam-line break from full power with stuck-open TBV. (Note: This transient assumes *MULTIPLE* operator/equipment failures; see Section 4.1.10 for failure assumptions.)

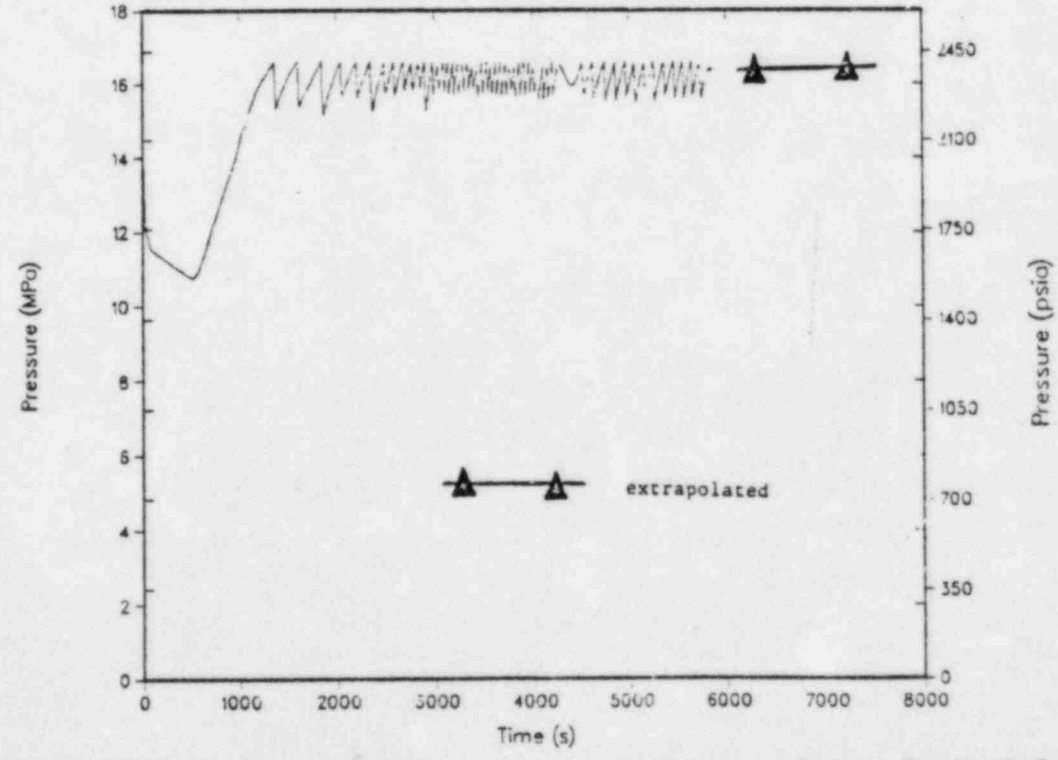

Figure 4.15. Transient 6: Primary system pressure during small steam-line break from full power with stuck-open TBV. (Note: This transient assumes *MULTIPLE* operator/equipment failures; see Section 4.1.10 for failure assumptions.)

The pressure history for this transient is given in Figure 4.15. Energy removal, and consequently depressurization, ended at 510 seconds when the SGs were isolated. As mentioned earlier, the initial depressurization was too rapid because all the initial liquid in the pressurizer was not saturated. SIAS should not have been reached at 28 seconds. After the initial depressurization that was caused by the reactor/turbine trip (which would have brought the system to about 13.2 MPa), a slow depressurization continued because of the slow blowdown of both SGs. Charging flow repressurized the system to the PORV setpoint* after energy removal ceased at 510 seconds. The system pressure was never low enough for HPI flow. The pressure is assumed to remain at the PORV setpoint for the remainder of 7200-second time period.†

4.3.2.7. Transient 7: Small Steam-line Break Downstream of MSIVs with Failure of One MSIV to Close‡ from Full Power

This transient is the same as the previous transient with the additional failure of the MSIV on one loop after SGIS. Thus, one SG blew down completely in this transient.

As shown in Figure 4.16, the downcomer liquid temperature was divided into four phases. Both SGs blew down through the stuck-open TBV during Phase 1 (0 - 570 seconds). The end of this phase was marked by the closure of one MSIV and the failure of the other MSIV after SGIS. The energy-transfer mechanisms were similar to those described for the previous transient. The minimum temperature for Phase 1 would be the minimum reached for the entire transient (as a result of a stuck-open TBV) if only the TBV had failed as

*It is assumed for this calculation that no attempt is made by the operator to control the repressurization. This allows the pressure to reach the point at which the PORV will open.

†This assumes that the PORV is allowed to continually cycle open and shut for the duration of Phase 3.

‡This is the same as a small steam-line break upstream of the MSIVs.

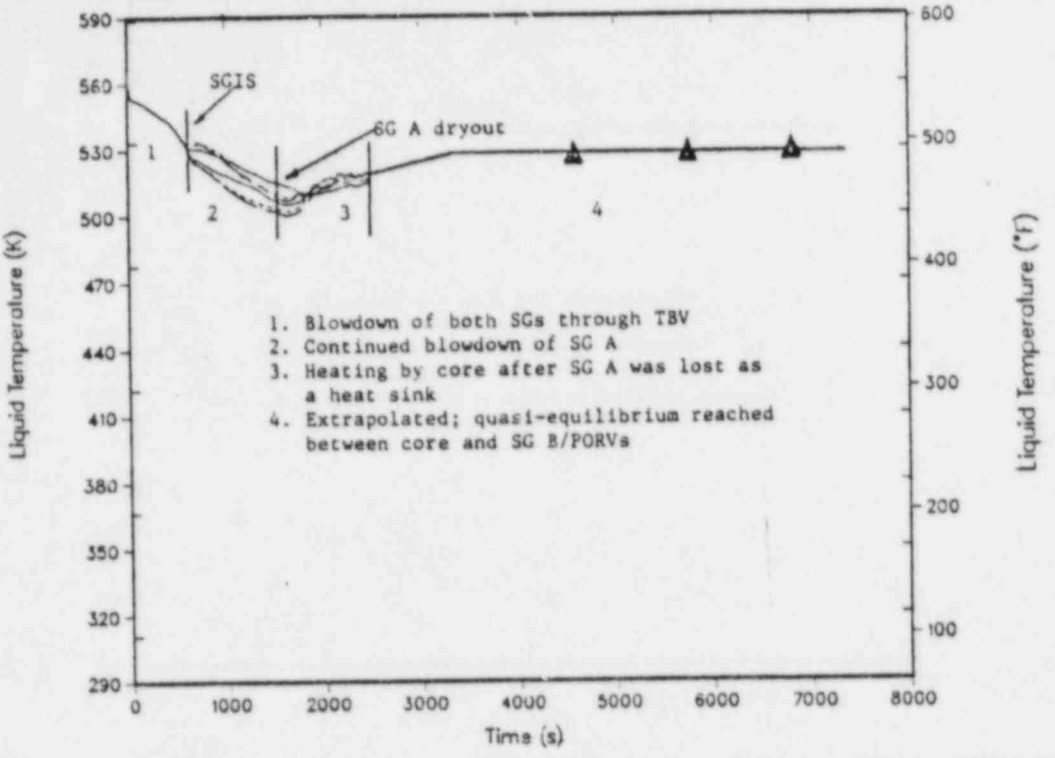

Figure 4.16. Transient 7: Downcomer liquid temperature during small steam-line break from full power with one stuck-open MSIV and a stuck-open TBV. (Note: This transient assumes *MULTIPLE* operator/equipment failures; see Section 4.1.10 for failure assumptions.)

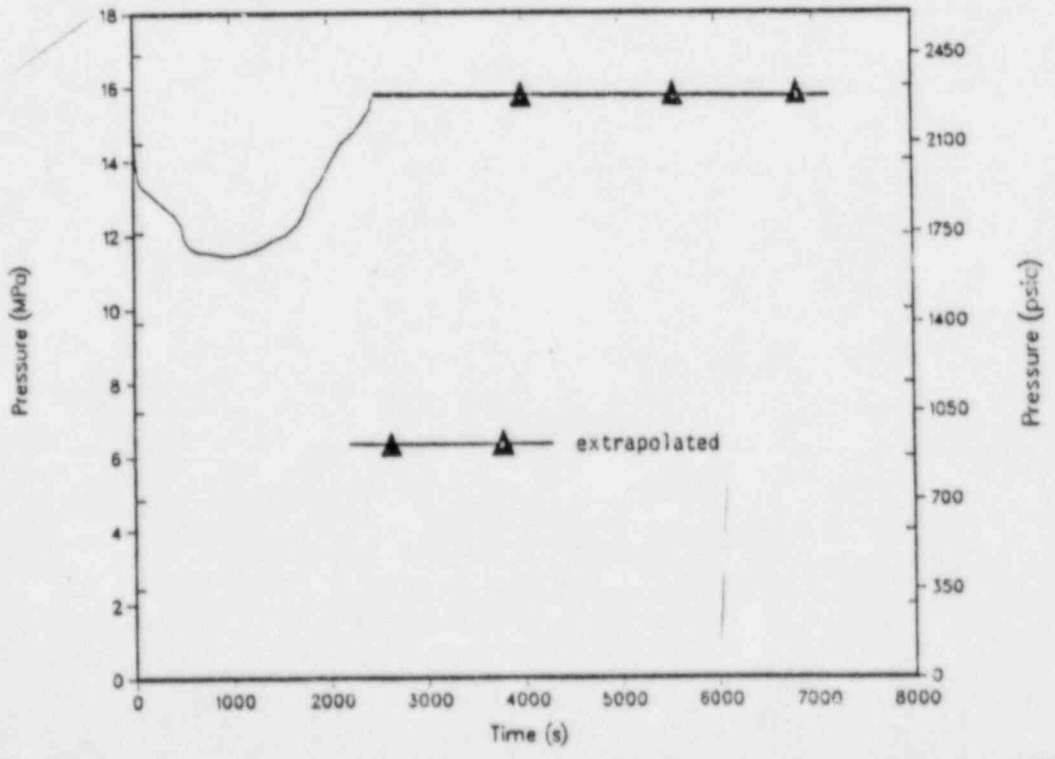

Figure 4.17. Transient 7: Primary system pressure during small steam-line break from full power with one stuck-open MSIV and a stuck-open TBV. (Note: This transient assumes *MULTIPLE* operator/equipment failures; see Section 4.1.10 for failure assumptions.)

specified for the previous transient.

Phase 2 (570 - 1750 seconds) was a period of asymmetric SG conditions. One MSIV closed, isolating SG B from the stuck-open TBV, while SG A continued to blow down. AFW was delivered to both SGs until asymmetric SG pressures were detected at 640 seconds. AFW was then delivered to SG B only. Some azimuthal differences in the downcomer temperature existed because higher heat-transfer rates caused the primary fluid to flow preferentially to Loop A. The dryout of SG A marked the end of Phase 2.

Phase 3 (1750 - 2500 seconds) was a period of primary heating after SG A dryout. The PORVs had not yet opened so SG B was the only heat sink for the energy deposition from the core. Phase 4 (2500 - 7200 seconds) was extrapolated based on the 0.1-m^2 main steam-line break from full power (the original run for 0 - 7200 seconds). The heatup to a quasi-equilibrium state should be similar for both transients, because the energy transfers were similar. In both transients, SG B and the PORVs were removing the decay heat, and the primary side heat slabs, RCPs, and SG A no longer influenced the transient. A quasi-equilibrium state is expected to be reached at ~525 K (486°F).

Figure 4.17 shows the pressure history. The first 50 seconds corresponded to a normal loss of load. When one TBV failed to reseat at 50 seconds, the pressure continued to drop with a sharp decrease after the RCPs were tripped at 500 seconds. The pressure leveled at 11.2 MPa as the cooldown slowed and the primary liquid contraction ended. The PORV setpoint was reached* just as the calculation was terminated. The system pressure is

*It is assumed for this calculation that no attempt is made by the operator to control the repressurization. This allows the pressure to reach the point at which the PORV will open.

assumed to remain at the PORV setpoint during the remainder of the 7200-second time period.* SIAS was received at 470 seconds, but the system pressure was never low enough for HPI.

4.3.3. Runaway Feedwater Events

Three transients were analyzed in the runaway feedwater category. The first two transients involve runaway main feedwater and the third transient involves runaway auxiliary feedwater.

4.3.3.1. Transient 8: Runaway Main Feedwater to Both Steam Generators from Full Power

This transient was initiated by a reactor/turbine trip from full power at t = 0 seconds with an assumed failure of both MFRVs to close. The downcomer temperature and pressure profiles are presented in Figures 4.18 and 4.19, respectively.

As shown in Figure 4.18, for this case the downcomer temperature history was divided into three phases. The first phase (0 - 283 seconds) shows a rapid decrease in downcomer temperature. The initial 10 K (18°F) temperature drop that occurred between 0 and 60 seconds is the normal temperature decrease that occurs when the reactor scrams. The significant decrease in core thermal power caused the ΔT between the primary and secondary sides of the SGs to reduce to a much smaller value that still permitted dissipation of the decay heat. The energy removed from the primary fluid during this interim was ~22 GW-s per SG. At 60 seconds after the scram, the relatively

*This assumes that the PORV is allowed to continually cycle open and shut for the duration of Phase 3.

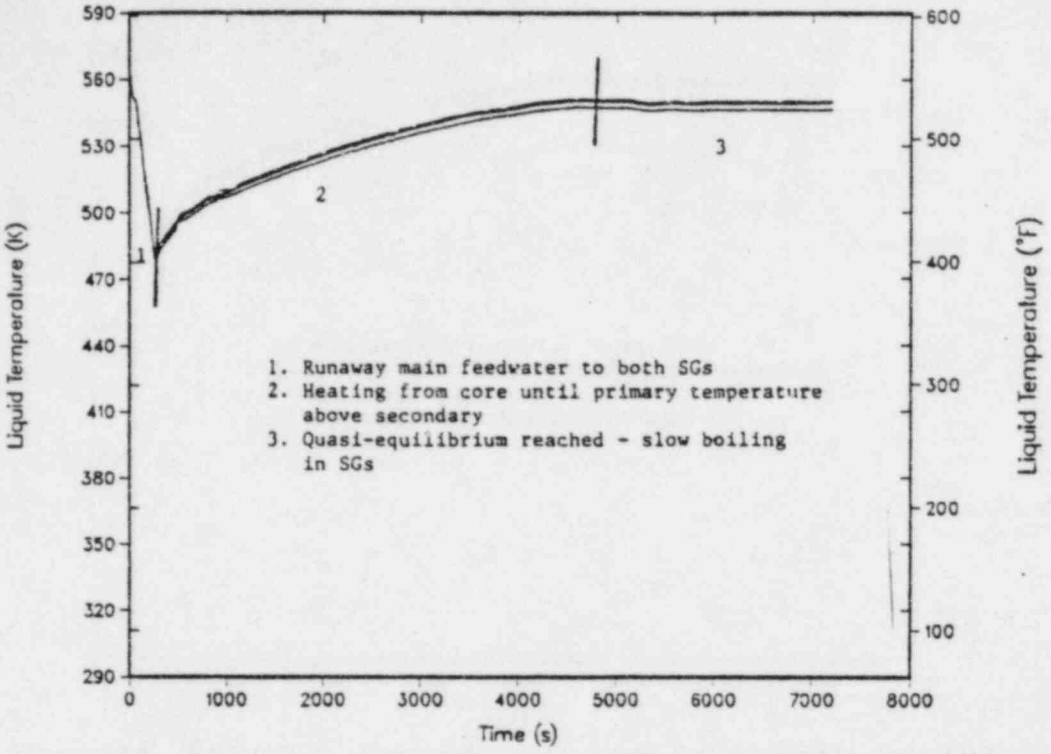

Figure 4.18. Transient 8: Downcomer temperature during runaway main feedwater to two SGs from full power. (Note: This transient assumes *MULTIPLE* operator/equipment failures; see Section 4.1.10 for failure assumptions.)

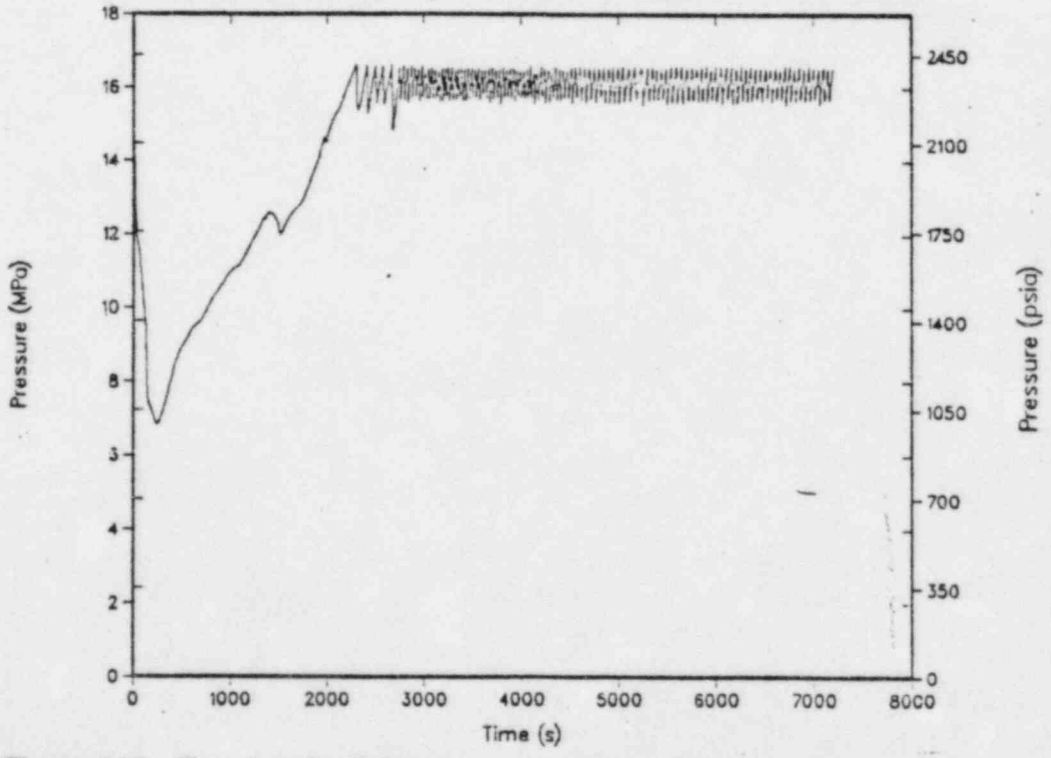

Figure 4.19. Transient 8: Primary system pressure during runaway main feedwater to two SGs from full power. (Note: This transient assumes *MULTIPLE* operator/equipment failures; see Section 4.1.10 for failure assumptions.)

cooler liquid that was in the feedwater pipes downstream of the high-pressure heaters was swept into the riser region of the SGs, pushing the hotter liquid in the riser region into the steam-volume region above the tubes. The effective lower secondary side temperature began to extract energy from the primary side at a rate of ~200 MW per SG. At 218 seconds, the MW pumps tripped on low-suction pressure because of depletion of liquid inventory in the condenser hot wells. At this point, the liquid in the riser could no longer be replenished with cooler liquid. The riser region stagnated and quickly approached thermal equilibrium with the primary liquid temperature. The energy transferred to each SG decreased to ~15 MW. However, the thermal power produced by the decay heat is adding energy to the primary liquid at a rate of ~75 MW. As a result, the primary liquid begins to heat again. The downcomer liquid temperature reaches a minimum temperature of 477.5 K (399.8°F) at 283 seconds.

Phase 2 (283 - 4800 seconds) shows a relatively slow heatup of the primary fluid following the trip of the main feedwater pumps. As the primary temperature increases, energy is continually being transferred from the primary into the secondary. The stagnant liquid in the SGs begins to heat up until it reaches the saturation temperature corresponding to 6.2 MPa (900 psia), the pressure setpoint of the TBV. The primary temperature levels off at a small ΔT above the saturation temperature of the liquid remaining in the SGs. A slow boiling process now begins (Phase 3). The small amount of steam being produced in the secondary side of the SGs is being vented by both the ADVs and the TBVs. [The ADVs and TBVs opened because the primary side temperature exceeded 552.6 K (535°F).]

4.3.3.2. Transient 9: Runaway Main Feedwater to One Steam Generator from Full Power

This transient was initiated by a reactor/turbine trip from full power at t = 0 seconds with an assumed failure of one MFRV to close. The temperature and pressure profiles are presented in Figures 4.20 and 4.21.

Figure 4.20 shows that the downcomer temperature history was divided into five phases. The first phase (0 - 363 seconds) shows a rapid decrease in the downcomer temperature. As with the transient discussed in the previous section, the initial 10 K temperature drop that occurs between 0 and 60 seconds is the normal temperature decrease that occurs when the reactor scrams. The energy removed by each SG during this interim is ~22 GW-s. At 60 seconds after the scram, the relatively cooler liquid that was in the feedwater pipes downstream of the high-pressure heaters feeding SG A has been swept into the riser region of SG A. The effective lower secondary side temperature in SG A begins to extract energy at an average rate of ~260 MW. At 303 seconds, the main feedwater pumps trip on low suction pressure because of depletion of the condenser hot-well liquid inventory. (Unlike the runaway main feedwater to two SGs, failure of one MFRV to close produces a feedwater flow to that SG of ~1000 kg/s. This depletes the condenser hot-well liquid inventory in ~300 seconds.) At this point, the liquid in the riser region of SG A can no longer be replenished with cooler liquid. The riser region stagnated and quickly approached thermal equilibrium with the primary liquid temperature. The energy transfer in SG A decreases to ~28 MW. However, the thermal power produced by the decay heat is adding energy to the primary liquid at a rate of ~75 MW. As a result,

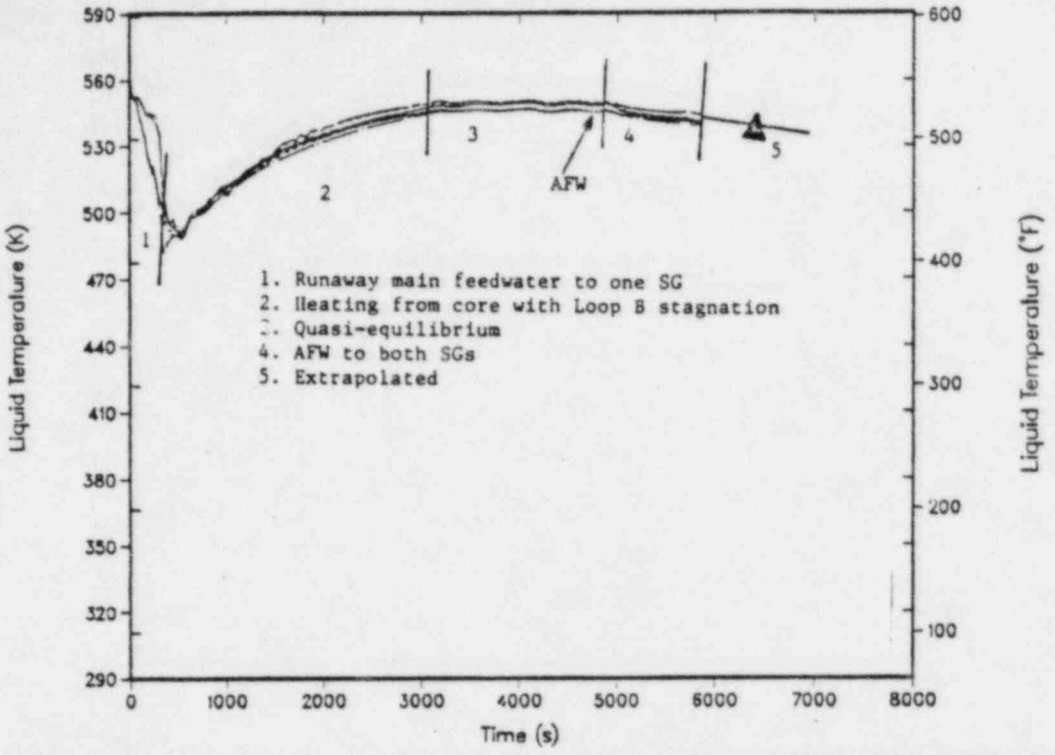

Figure 4.20. Transient 9: Downcomer temperature during runaway main feedwater to one SG from full power. (Note: This transient assumes *MULTIPLE* operator/equipment failures; see Section 4.1.10 for failure assumptions.)

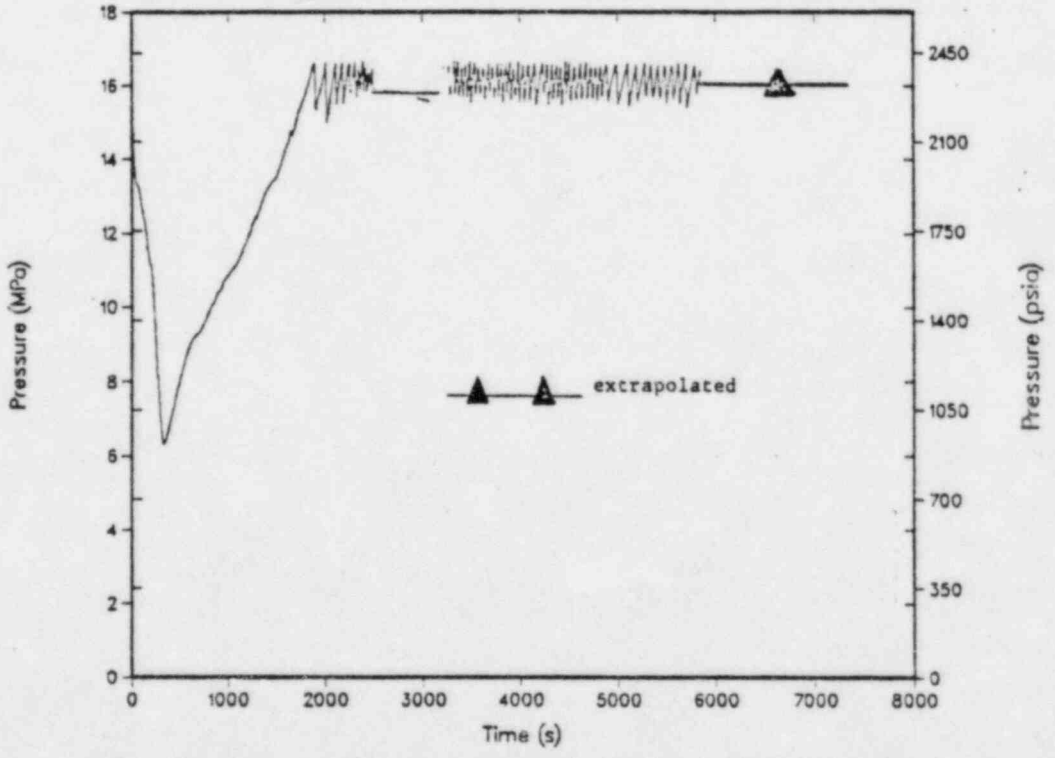

Figure 4.21. Transient 9: Primary system pressure during runaway main feedwater to one SG from full power. (Note: This transient assumes *MULTIPLE* operator/equipment failures; see Section 4.1.10 for failure assumptions.)

the primary liquid begins to heat again. The average downcomer liquid temperature goes through a minimum temperature of 491.0 K at 363 seconds.

Phase 2 (363 - 3200 seconds) shows a relatively slow heatup of the primary fluid following the trip of the main feedwater pumps. This is similar to the heatup observed in the runaway main feedwater to two SGs discussed in the previous section except that the heatup that occurs in this transient has only one heat sink - SG A. The other SG cooled only slightly during the runaway feedwater portion of the transient. As a result, the decay heat added to the primary fluid could be dissipated through only one SG rather than two. Hence, the primary fluid heated up more rapidly for this case. After SG A was heated again to the saturation temperature corresponding to 6.2 MPa (900 psia), both SGs shared the heat load equally. The primary temperature leveled off at a small ΔT above the saturation temperature of the liquid remaining in the two SGs. A slow boiling process began (Phase 3). As in the transient discussed in the previous section, the primary fluid temperature during this period exceeded 552.6 K (535°F). Both the ADVs and the TBVs reopened. This vented the steam being generated by the boiling process. Subsequently, about one-third of the decay heat was removed by each SG. The remaining one-third of the decay heat was removed by convective mass transfer associated with injecting cold charging flow into the primary system at a rate of 8.3 kg/s (6.59×10^4 lb/h) and rejecting, on an average, the same mass flow rate through the PORVs with a much higher temperature.

Because the mass inventory in SG B was initially depleted somewhat at the beginning of the transient and was not replenishing during the runaway

feedwater portion of the transient, the slow boiling process that occurred in Phase 3 continued to boil away the remaining liquid in SG B. At 4800 seconds, the level in SG B was finally low enough to activate AFW to both SGs. The continuous addition of cold 277.6 K (40°F) liquid to each of the SGs resulted in a continuous reduction of the secondary side heat sink temperature. This, in turn, produced a decrease in the primary fluid temperature (Phase 4). Once the primary side temperature decreased below 552.6 K (535°F), both the ADVs and the TBVs reclosed.

The calculation was terminated at 5800 seconds. However, it was anticipated that the primary fluid temperature would continue to decrease at approximately the same rate observed in Phase 4 for the interim from 5800 to 7200 seconds (Phase 5).

4.3.3.3. Transient 10: Runaway Auxiliary Feedwater to Two Steam Generators from Full Power

This transient was initiated by an unanticipated trip of both main feedwater pumps from full power at t = 0 seconds. It was assumed that the AFW system would fail to start following AFAS. At 1200 seconds (20 minutes) into the transient, AFW was recovered to both SGs at its prescribed maximum flow rate of 25 kg/s (400 gpm). Furthermore, it was assumed that the operator would secure AFW to both SGs 3 minutes after the narrow-range level indication in either SG reached the +50-in. high-level alarm. The downcomer temperature and pressure profiles are shown in Figures 4.22 and 4.23.

OAK RIDGE NATIONAL LABORATORY
OPERATED BY MARTIN MARIETTA ENERGY SYSTEMS, INC.

POST OFFICE BOX X
OAK RIDGE, TENNESSEE 37831

May 30, 1984

Review Document Number 5

TO: Distribution

SUBJECT: Review of Calvert Cliffs PTS Report Chapter 4 - Thermal Hydraulic Analysis of Potential Overcooling Sequences

Please find enclosed a copy of Chapter 4 of the Calvert Cliffs Unit 1 PTS report. This material has now been reviewed internally and cleared as draft information for comment. Please note the following items about the appendices:

1. Chapter 4 makes reference to five appendices (F, G, H, I, and J).

2. Appendices F and G are separate reports written by LANL and BNL respectively. These reports have previously been issued (or very soon will be) as draft reports for review. Therefore they are not included in this mailing.

3. Appendices H and I are in preparation and will be sent as soon as possible.

4. Appendix J is enclosed in an early draft format. Some editing requirements have already been identified, but the appendix has been included as-is to allow an initial technical review.

Please review and return comments on Chapter 4 by Friday, June 29. If additional time is needed for review, please let me know.

D. L. Selby
Engr. Phys. & Math. Div.

DLS:nc

Enclosure

Distribution

G. F. Flanagan (w/o encl)
C. E. Johnson, NRC
S. M. Mirsky, BG&E
D. A. Peck, CE
T. G. Theofanous, Purdue U.

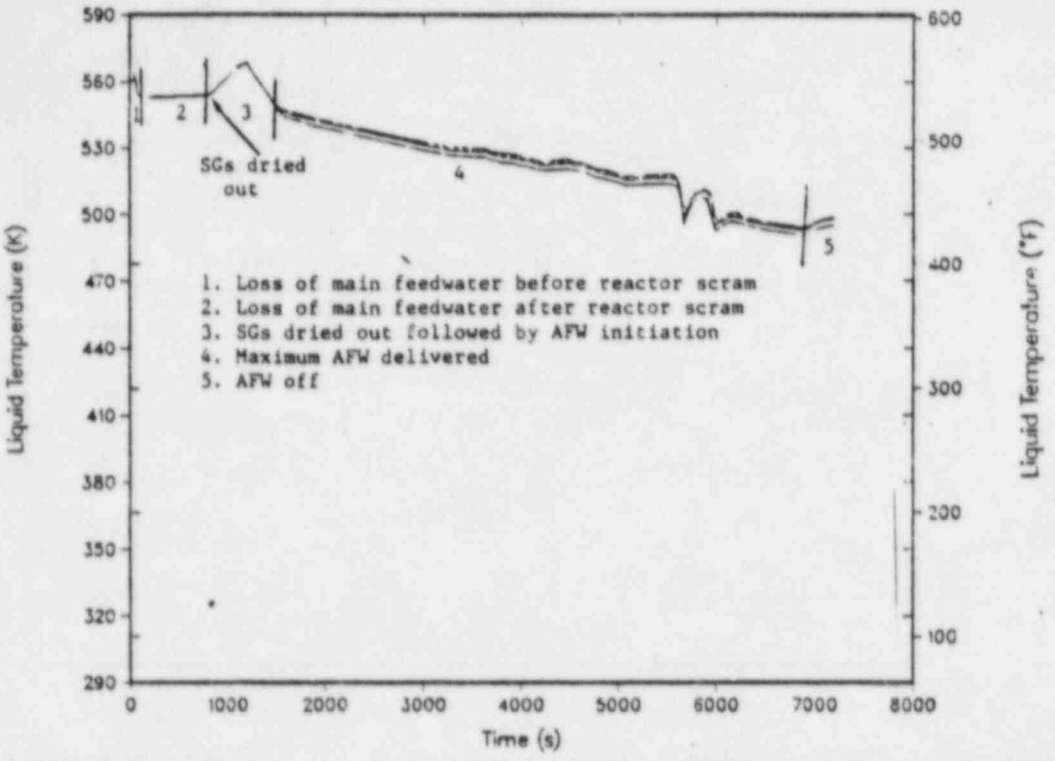

Figure 4.22. Transient 10: Downcomer temperature during runaway auxiliary feedwater to two SGs from full power. (Note: This transient assumes *MULTIPLE* operator/equipment failures; see Section 4.1.10 for failure assumptions.)

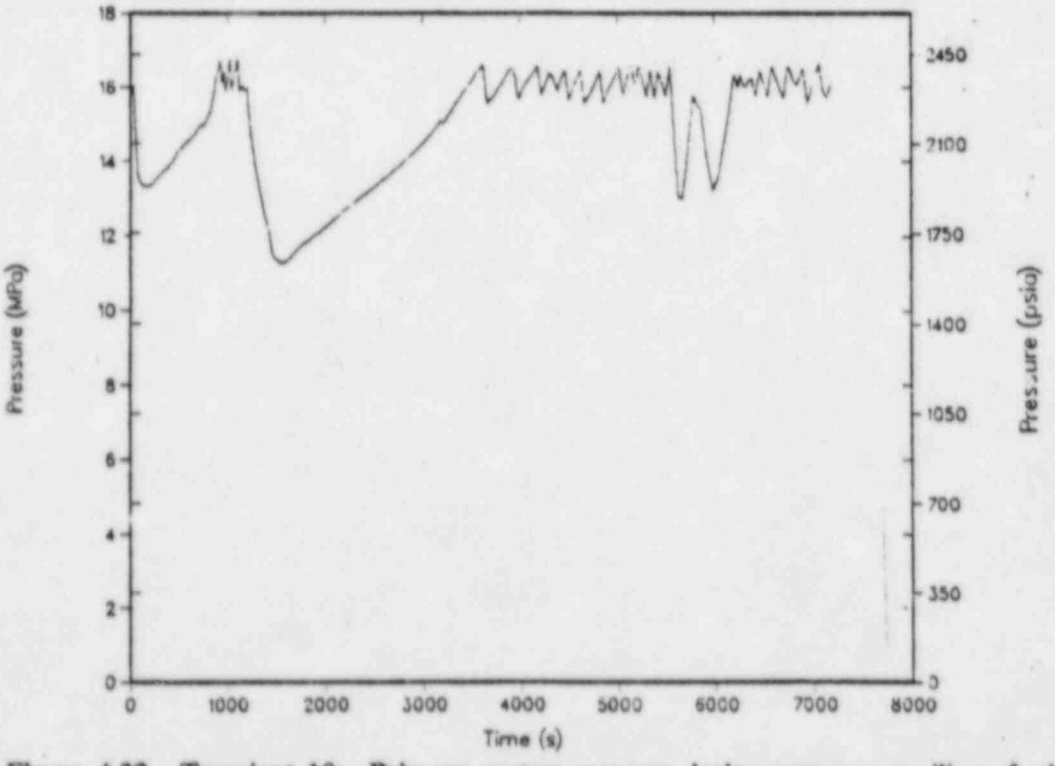

Figure 4.23. Transient 10: Primary system pressure during runaway auxiliary feedwater to two SGs from full power. (Note: This transient assumes *MULTIPLE* operator/equipment failures; see Section 4.1.10 for failure assumptions.)

The first phase (0 - 34.7 seconds) shows a slight temperature increase prior to the reactor/turbine trip at 34.7 seconds. This temperature increase was produced by the degradation of the heat-load capacity of each SG following the loss of main feedwater flow. Because the reactor power was programmed not to change during this interim, a net energy transfer of 0.9 GW-s into the primary fluid resulted, causing the primary temperature to increase a few degrees. The initial SG inventory of ~63,000 kg per SG was reduced by 30% during this period.

As previously mentioned, the reactor/turbine tripped at 34.7 seconds because of low SG narrow-range level indication. The primary liquid temperature quickly dropped to a quasi-static equilibrium temperature a few degrees above the secondary side liquid temperature (Phase 2). The decay heat produced by the reactor during this period was dissipated equally by both SGs at a rate of ~40 MW per SG; this heat continued the boiling process in each SG. This continued to deplete the liquid inventory in each SG and subsequently led to AFAS at 35.5 seconds.

The average primary temperature during Phase 2 was higher than 552.6 K (535°F), which caused both the ADVs and TBVs to be open. Together, they vented all the steam that was being produced. After the SG liquid inventory was depleted, the heat-load capacity of each SG decreased to less than 1 MW. The decay heat produced by the reactor could no longer be dissipated from the primary fluid. The temperature began to rise sharply (Phase 3). This caused the ADVs and the TBVs to open fully, which caused each of the SGs to depressurize. As a result, SGIS occurred at 864 seconds. The MFRVs and MSIVs closed and isolated the SGs from the TBVs.

At 1200 seconds the AFW flow was recovered. The initial surge of cold auxiliary feedwater to enter the SGs vaporized rapidly. This removed 15.4 GW-s of energy from the primary fluid over the next 300 seconds. The injection of cold charging flow over the same period of time resulted in a further decrease in the temperature of the primary fluid. The net result was a rapid temperature decrease of 22.5 K (40.5°F). The average primary temperature dropped below 552.6 K (535°F), causing the control system to close the ADVs. This bottled up both SGs for the remainder of the transient. The continued addition of cold AFW to both SGs resulted in each SG removing energy from the primary fluid at an average rate of ~19 MW. This energy did not boil the auxiliary feedwater. Rather, the energy was added as sensible heat to the liquid, causing its temperature to increase. The increase in the secondary side liquid temperature, however, occurred for only a short period of time. The secondary side liquid temperature peaked at ~540 K (512°F) at ~1600 seconds. The rate at which energy was being added to the secondary side liquid as sensible heat was offset at this time by the continued addition of cold AFW. The net result was an increasing liquid inventory in each SG with a modestly decreasing liquid temperature.

On an average, the primary fluid temperature decreased at a rate of ~32 K/h (58°F/h) over Phase 4 because of convective cooling. Had the operator throttled the charging flow at the time of level recovery in the pressurizer, the primary liquid temperature would have remained constant during Phase 4.

At 6590 seconds, the AFW system had refilled the SGs to the +50-in. level. Per the transient specifications, the operator turned off the AFW system 3

minutes later. The energy that was being dissipated through the SGs began to heat up the liquid in the SGs. As the secondary side temperature increased, the heat-transfer rate to the SGs decreased. The decay heat from the core finally exceeded both the rate at which energy was being removed via the steam generators and the convective energy transfers associated with the charging flow. The primary fluid began to heat again (Phase 5) 100 seconds after the operator turned off the AFW.

4.3.4. Small-Break LOCA Events

In the absence of SIS flow, the depressurization caused by a LOCA will cause the primary system to follow the saturation curve - a condition that is not likely to induce PTS. The break must be large enough to depressurize the system to the SIAS setpoint if it is to generate PTS. However, if the break is too large, the rate of depressurization will be sufficient to maintain a pressure-temperature relationship close to the saturation curve despite the effect of the cold SIS water. Because the HPI flow rate is strictly a function of system pressure, reasoning suggests that the threat of PTS will be increased by any mechanism that localizes and concentrates the effect of the HPI water in the vicinity of the critical vessel welds. One such mechanism is loop stagnation. Loop stagnation not only localizes the HPI effect along the downcomer wall by promoting stratification in the cold legs, it also inhibits reverse heat transfer from the hot SGs that would mitigate the effect of the HPI. Consequently, there is some concern that certain break sizes may generate conditions conducive to loop stagnation yet limit depressurization sufficiently to cause PTS.

To address this concern, two small-break LOCA transients were selected for investigation. The first was a small hot-leg break LOCA with a break size of ~0.002 m^2 (0.02 ft^2) in the range suspected of causing loop stagnation. For that calculation the full-power model was modified to include a break in the hot leg of Loop A with a prescribed pressure boundary condition of 0.1 MPa (1.0 atm). The second transient was a small small-break LOCA having a size of 0.001 m^2 (0.01 ft^2) and caused by the failure of one of the two PORVs to close fully. In addition, it was assumed that the SG A ADV failed to close when it should have. These two transients are described in the following sections.

4.3.4.1. Transient 11: 0.002-m^2 Hot-Leg Break from Full Power

The downcomer temperature and pressure curves for Transient 11 are shown in Figures 4.24 and 4.25. The analysis of these curves can be divided into two phases. The first phase was characterized by a rapid depressurization of the primary that was halted by flashing in the upper head of the vessel at 110 seconds. During this phase of the accident the energetics were dominated by overcooling by the SGs following the reactor trip. Heat rejection to the SGs decreased rapidly with the loss of forced convection following the RCP trip, however, and by the end of this phase of the accident, energy removal by the SGs was almost 90% completed.

The second phase (~110 - 6636 seconds) was characterized by the emergence of an approximate balance between the mass discharge rate from the hot-leg break and the SIS injection rate, a gradual decrease in primary pressure and temperature, and extensive voiding in the upper plenum. At 502

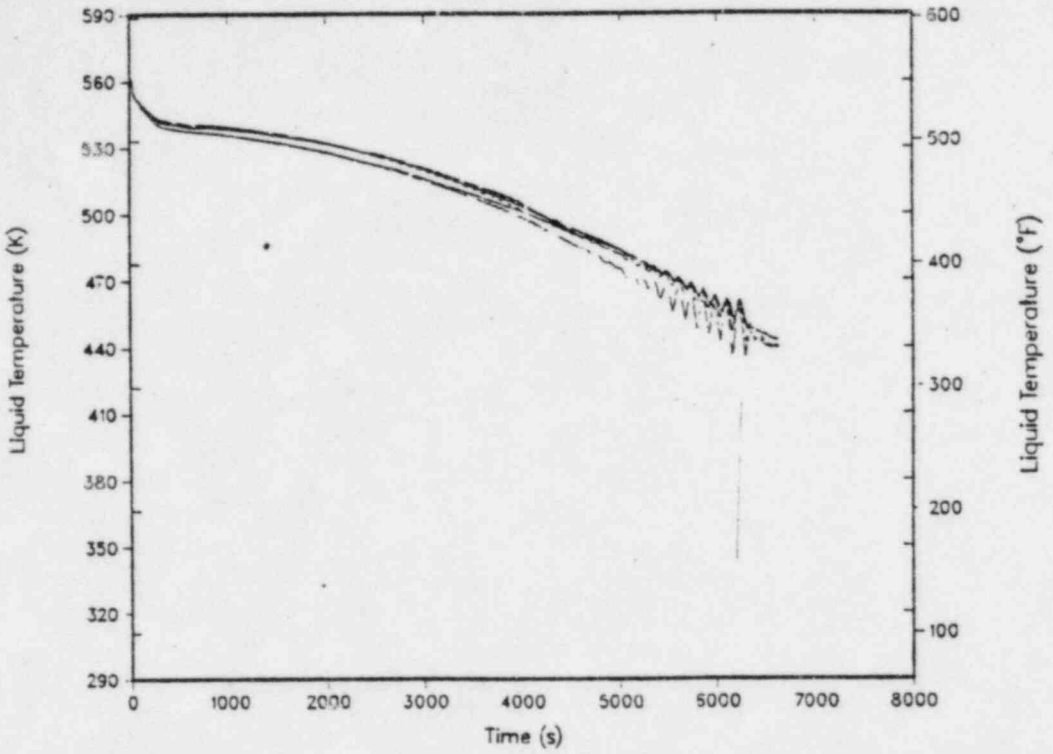

Figure 4.24. Transient 11: Downcomer temperature during 0.002-m² hot-leg break from full power. (Note: This transient assumes *MULTIPLE* operator/equipment failures; see Section 4.1.10 for failure assumptions.)

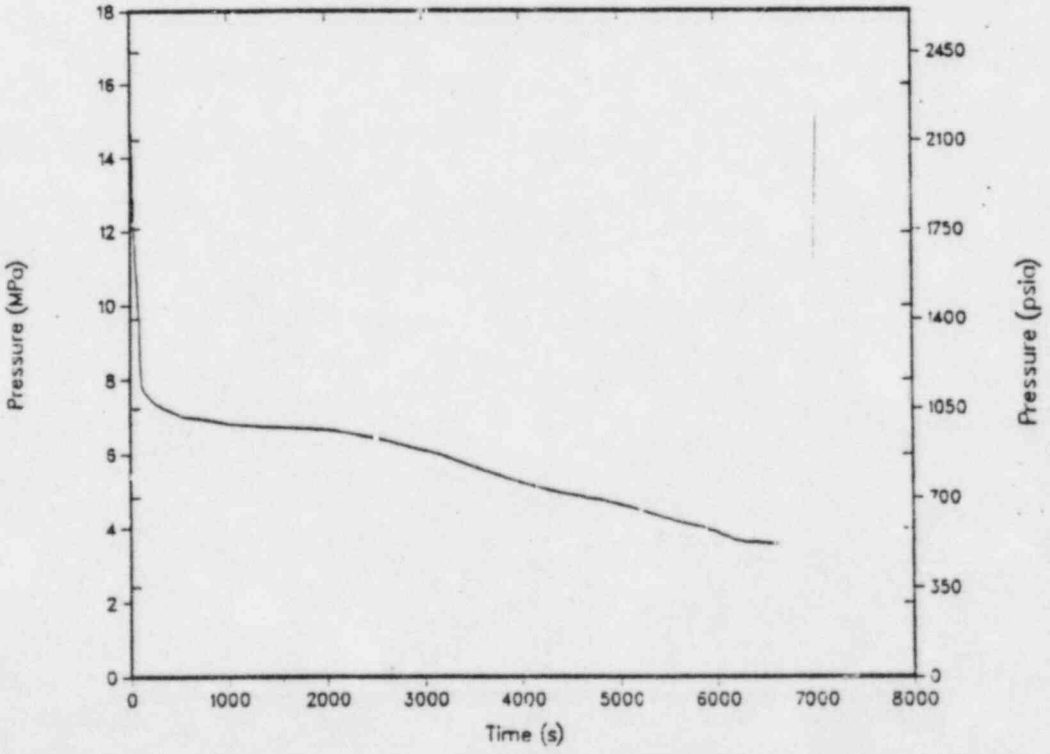

Figure 4.25. Transient 11: Primary system pressure during 0.002-m² hot-leg break from full power. (Note: This transient assumes *MULTIPLE* operator/equipment failures; see Section 4.1.10 for failure assumptions.)

seconds, SGIS was predicted to occur based on an auxiliary calculation presented in Appendix F. This analytical calculation was necessary because the TRAC model did not include the containment. The decrease in pressure and temperature during this phase was attributed to the gradual but persistent decline in primary energy resulting from replacement of the hot fluid issuing from the break with cold SIS water.

An interesting feature of this phase of the calculation was the non-equilibrium between the steam in the upper plenum and the water beneath it. The TRAC non-equilibrium condensation model predicted that conditions at the liquid-vapor interface were not conducive to rapid phase change; hence, condensation could not cool the vapor as quickly as HPI flow cooled the liquid.

Another interesting feature of this phase of the calculation was the reduction in the loop flows that culminated in flow stagnation in Loop A at ~6500 seconds. After the ADVs closed at 968 seconds, the SG could no longer reject heat to the atmosphere; hence, the primary temperature fell below the secondary temperature. The resulting reverse heat transfer cooled the secondary, but it also retarded natural circulation in both loops. The reverse heat transfer and reduced flow downstream of the hot-leg break caused voiding in the top of the U-tubes in the Loop A SG at ~6300 seconds. This voiding caused the stagnation that occurred about 200 seconds later.

4.3.4.2. Transient 12: Stuck-Open Pressurizer PORV with Stuck-Open Secondary ADV from Full Power

The downcomer temperature and pressure profiles for this transient are shown in Figures 4.26 and 4.27. As in the previous case, this transient can be characterized by two phases. The first is distinguished by a rapid depressurization of the primary that was halted by flashing in the upper head of the vessel at ~210 seconds. During this phase of the accident, the energetics were dominated by overcooling by the SGs following the reactor trip. Heat rejection to the SGs decreased rapidly with the loss of forced convection following the RCP trip, however.

The second region (~210 - 7200 seconds) is characterized by a gradual decrease in primary pressure and temperature, stagnation in Loop B resulting from overcooling by the Loop-A SG, and complete refilling of the primary by the SIS. Most of the decrease in primary temperature can be attributed to fluid exchange between the SIS and PORV discharge with the balance of the decrease being caused by continued heat rejection through the stuck-open ADV (Loop A).

Furthermore, the stuck-open ADV was responsible for the stagnation that occurred in Loop B. Following SGIS, SG B could no longer reject heat to the atmosphere, and Loop B lost the density head through the U-tubes that helped to drive natural-circulation flow. Because the ADV near SG A was stuck open, however, SGIS did not isolate SG A and it continued to depressurize. In fact, the steam flow out of SG A essentially doubled following SGIS because the total flow out the ADV did not change but the flow from

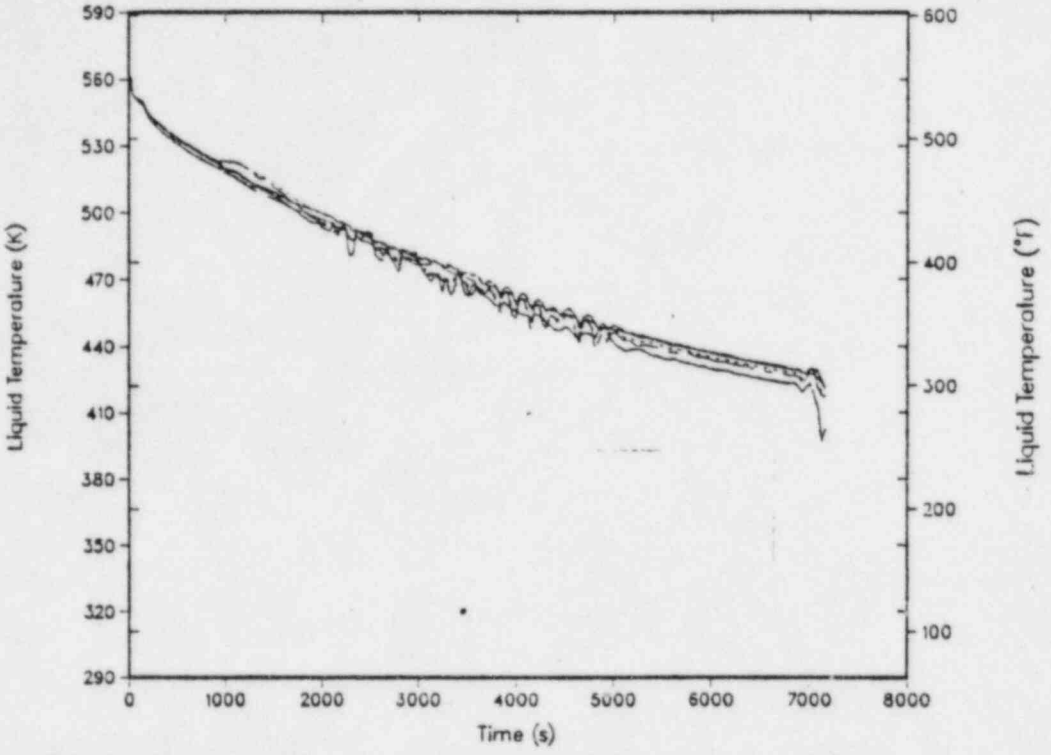

Figure 4.26. Transient 12: Downcomer temperature during break from a stuck-open PORV plus a stuck-open ADV from full power. (Note: This transient assumes *MULTIPLE* operator/equipment failures; see Section 4.1.10 for failure assumptions.)

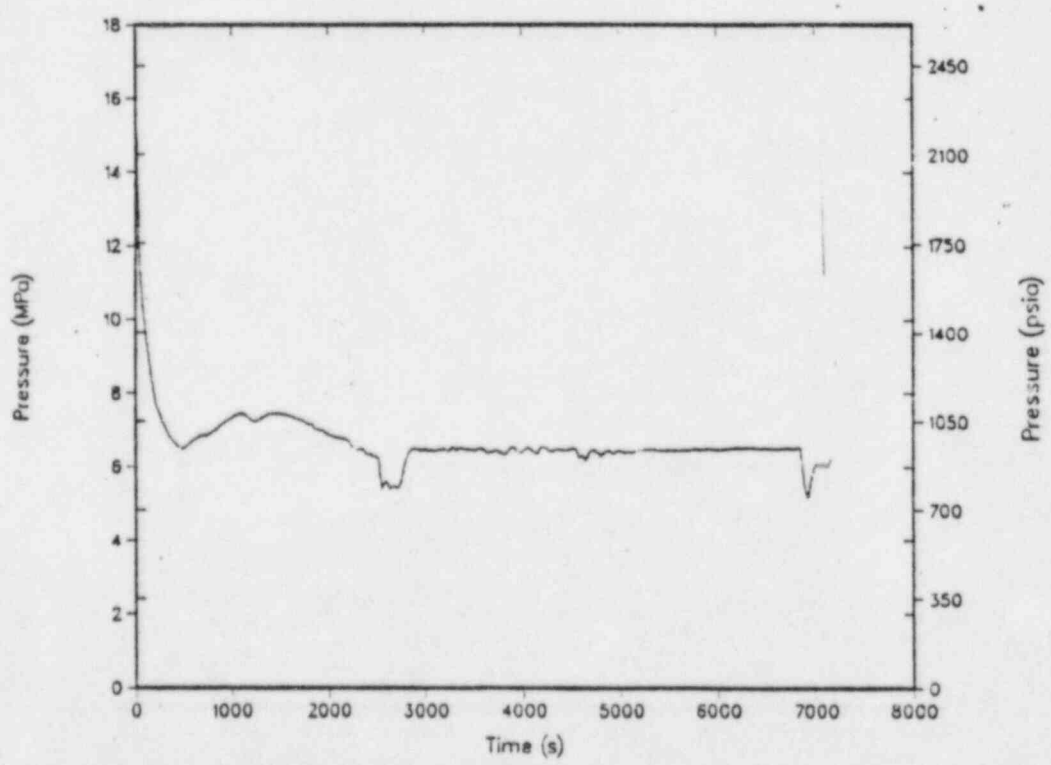

Figure 4.27. Transient 12: Primary system pressure during break from a stuck-open PORV plus a stuck-open ADV from full power. (Note: This transient assumes *MULTIPLE* operator/equipment failures; see Section 4.1.10 for failure assumptions.)

SG B was terminated. Consequently, the heat transfer to SG A practically doubled following SGIS and the increased heat transfer enhanced the density head in Loop-A. The primary temperature decreased throughout the transient and the downcomer temperature had fallen to 425 K (830.6°F) by 7200 seconds.

4.4. Downcomer Fluid Mixing Behavior

A review of many of the transients perceived for Calvert Cliffs Unit 1 revealed several instances in which the flow in one or more cold-leg pipes was very small. This could lead to a stratification phenomenon which would produce localized vessel wall temperatures in the downcomer region that are significantly lower than the bulk fluid temperature as calculated by TRAC. As a result, it was necessary to evaluate this phenomenon and evaluate its potential effect.

Three sets of analysis were performed to quantify the effects of partial or total loop flow stagnation. The first analysis, discussed in Section 4.4.1, was performed at Purdue University by T. G. Theofanous. This analysis involved an evaluation of the 12 LANL calculations to identify the potential for and the effects of stratification phenomena associated with those transients. In addition to the above analysis, an evaluation of the mixing phenomena associated with the LANL transients was performed at LANL by B. J. Daly using the SOLA-PTS mixing code as discussed in Section 4.4.2. Finally, Theofanous was asked to calculate the downcomer temperature profiles associated with total loop flow stagnation. This information was necessary for evaluation of those sequences for which stagnation was assumed. The results of this analysis are presented in Section 4.4.3.

4.4.1. Stratification Analysis of Twelve LANL Transients

This evaluation was performed utilizing a stratification criteria screening process and a regional mixing model (RMM) which had been benchmarked

against experiments carried out in a 1/2-scale facility rigged up to the Calvert Cliffs-1 injection geometry. A summary of the results of this evaluation is presented in this section and the detailed evaluation process and results are presented in Appendix H.

The initial stratification criteria screening identified three transients (Transients 1, 4, and 12) as requiring further analysis. The RMM was then used to evaluate these three transients. The results showed that for Transient 1, high-pressure injection occurs for the first ~1,000 seconds. Loops A1 and A2 run well-mixed at strong natural-circulation rates and cool rapidly in the 400 - 425 K range. Loop B2 goes into momentary stagnation (and stratification) at ~500 seconds and reverses flow for the next 2,500 seconds. Loop B1 exhibits two stratification periods of ~250 seconds each around ~500 and ~1,000 seconds respectively. The possible effect of such short-duration stratification was determined by running the RMM calculation for the cold-leg/pump/loop seal system. The results are shown in Fig. 4.28, along with the TRAC temperature traces for loops A1 and B1. It is apparent that loop A1 (and hence the downcomer and lower plenum) cool much faster than the stagnated loop B1. Note that the "cold stream" in B1 ($B1_{cs}$) is warmer than the A1 outflow for the duration of the stratified condition. In fact, this is the reason for the choice of the mixing control volume as indicated above. It can be concluded that downcomer temperatures will be dominated by loop A1 and A2 flows and their temperatures even for the period of stratification in loops B1 and B2.

The characteristics of Transient 4 are very similar to those of Transient 1, with one addition. Here loops B1 and B2 both exhibit back-flow at ~750

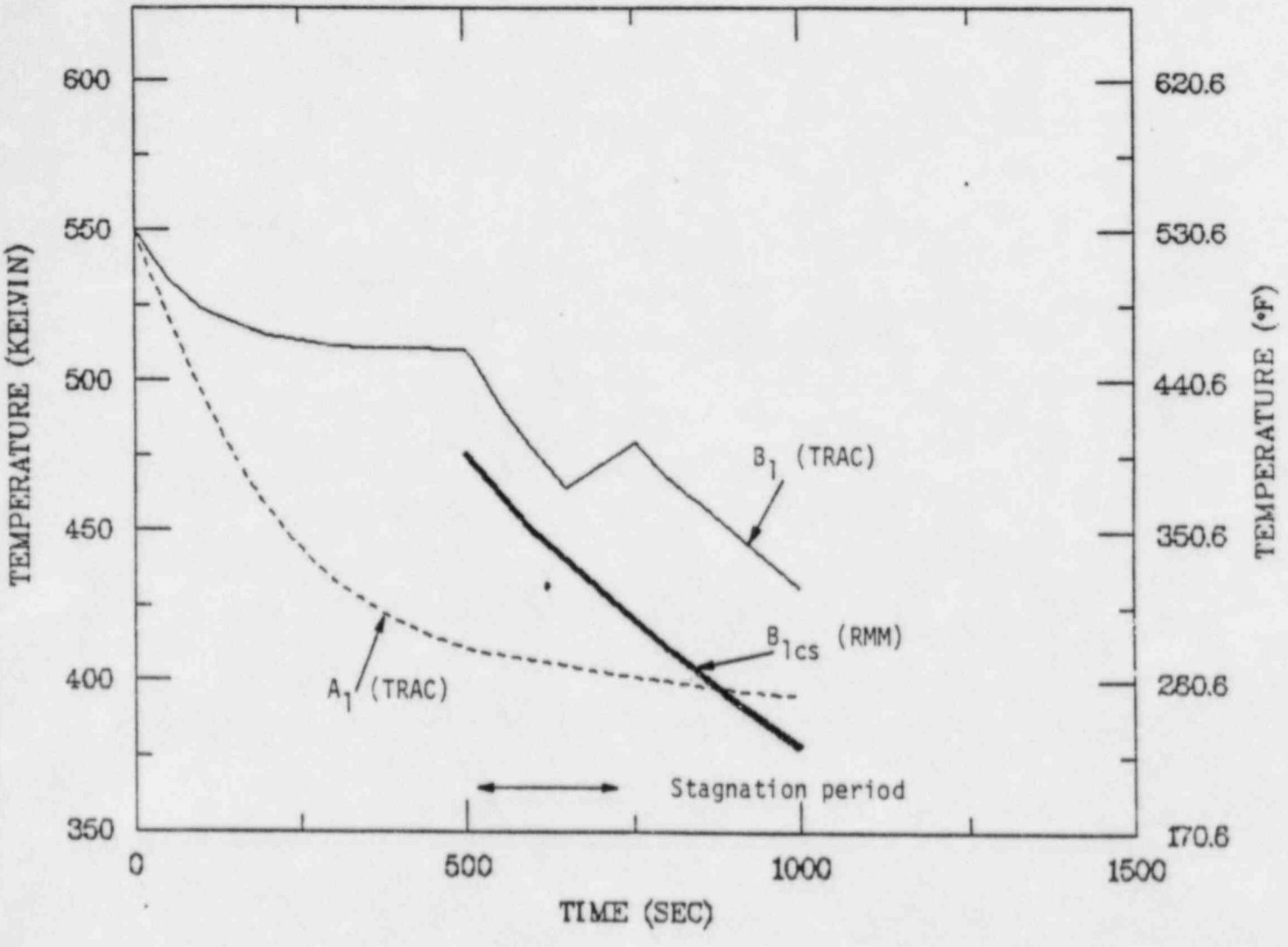

Figure 4.28. Transient 1: Downcomer fluid mixing behavior. B1, stagnated; A1, circulating; therefore, downcomer well-mixed, forced flow.

seconds, which is slow enough to establish a relatively low temperature condition before a stagnation condition for 750 to 1000 seconds is obtained. The possible effects of this stratification, i.e., any additional cooling, was also determined with an RMM calculation with an initial "ambient" temperature of 375 K. The results are shown in Fig. 4.29. Here the cold stream is only ~30 K cooler than the downcomer temperature (A1 outflow). This, plus the strong flows in the downcomer from loops A1 and A2, indicate that any additional cooling effect due to stratification in loop B2 would be negligible.

In Transient 12, loops A1 and A2 again remain at well-mixed conditions, with strong natural circulation. Loops B1 and B2 stagnate for times beyond 2,000 seconds under HPI of ~10 kg/s. The effects of the resulting stratification were scoped by assuming that the strong A1 and A2 loop flows establish the downcomer temperature history. With this taken as the "ambient" in the RMM calculation, a cold stream temperature in the B1 (and B2) cold legs was obtained as shown in Fig. 4.30. The modest degree of stratification seen (~30 K) is the result of the strong mixing within the injection line under the prevailing low injection Froude Numbers (Fr ~0.2). This mixing was determined experimentally in our 1/2-scale facility and found to be considerably higher than that observed at Fr ~0.6, which was examined earlier in connection with Westinghouse reactors. The resulting "plumes" into the downcomer would be <u>extremely weak</u> under these conditions and would mix quickly with the A1 and A2 loop flows, which hence will dominate the downcomer response.

In conclusion, it was determined that, at least for the types of transients

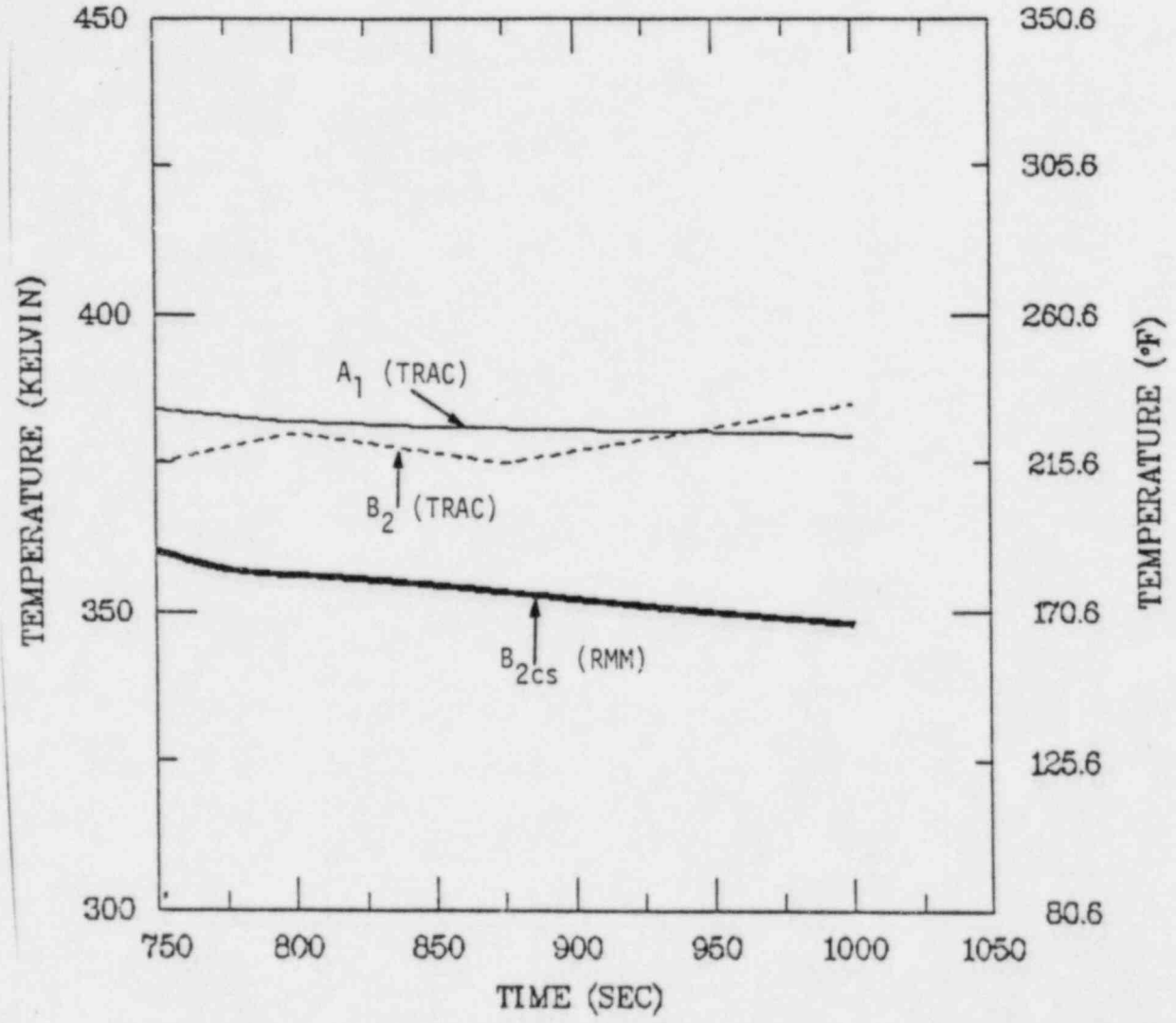

Figure 4.29. Transient 4: Downcomer fluid mixing behavior. A1, A2, circulating; B1, B2, stagnated; therefore, downcomer well-mixed, forced flow.

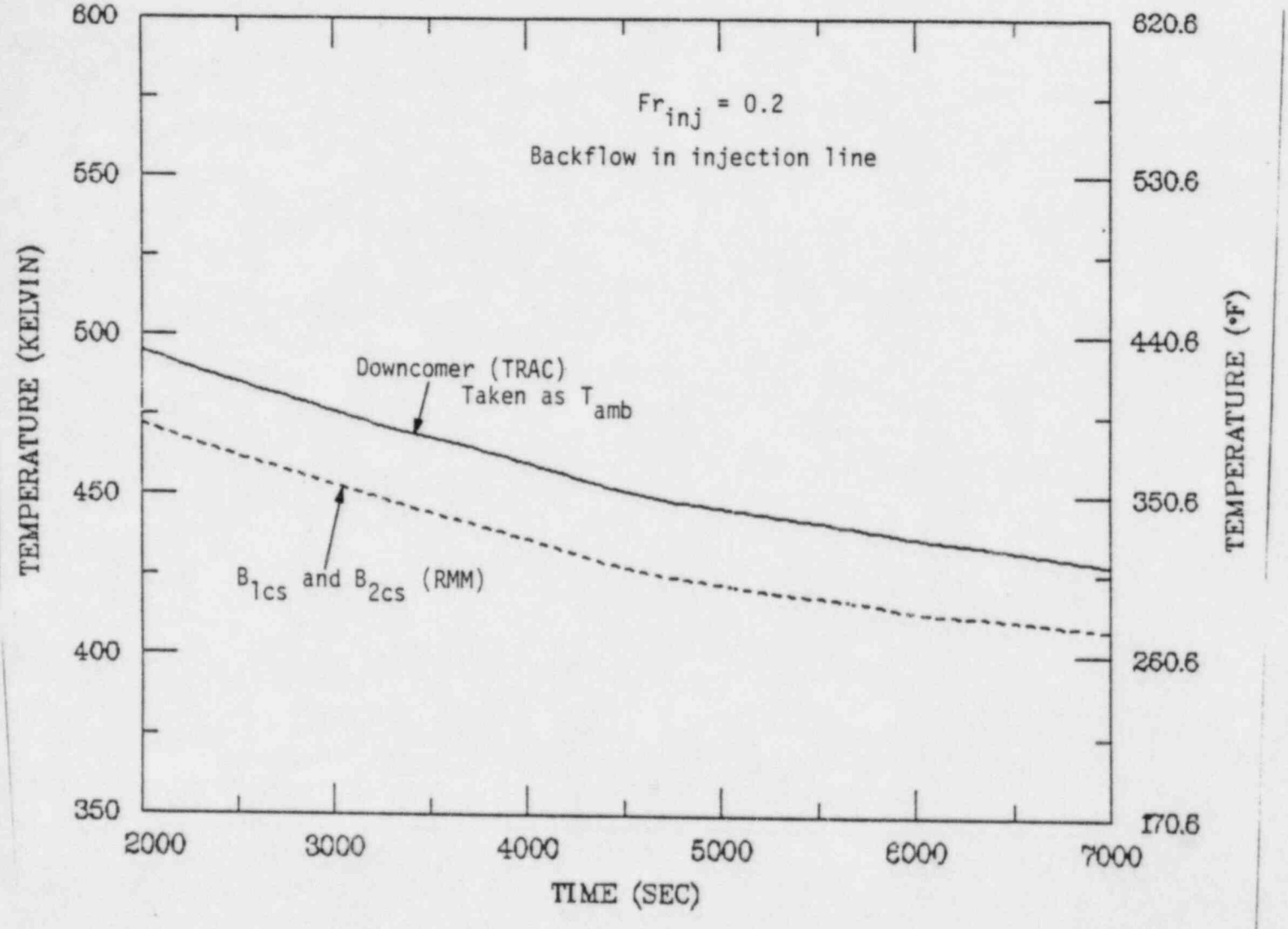

Figure 4.30. Transient 12: Downcomer fluid mixing behavior. A1, A2, circulating; B1, B2, stagnated; therefore, downcomer well-mixed, forced flow.

covered by the 12 LANL transients, stratification phenomena are of no PTS significance for the Calvert Cliffs-1 reactor.

4.4.2. SOLA-PTS Mixing Analysis of Selected Transients

A mixing analysis was performed at LANL for those transients for which mixing was considered to be important. A separate report that documents the results of this analysis is included here as Appendix I.

The conclusions of this analysis were very similar to those obtained by Theofanous. One exception was that for some transients, a very narrow but strong thermal plume was established below the broken loop cold leg. However, as will be discussed in Chapter 5, this narrow plume was not considered to have an impact on the vessel welds of interest. Thus the conclusion of this SOLA-PTS analysis was that the TRAC bulk temperature values were appropriate for use in the fracture mechanics analysis.

4.4.3. Total Loop Flow Stagnation

In performing the thermal-hydraulic analysis for Calvert Cliffs-1, it should be noted that no calculations performed predicted total loop flow stagnation. However, it is also clear that situations exist for which the potential for total loop flow stagnation is greatly increased. As stated earlier in this report, total loop flow stagnation, or at least very low flow, has been assumed for these cases. Theofanous was asked to determine the temperature profiles in the downcomer region under the assumption of total loop flow stagnation.

Two temperature regions were identified. The first region includes the initial planar plume exiting the cold leg. This plume area covered a vertical strip in the downcomer that was two cold-leg diameters wide and about five cold-leg diameters long. The second region includes everything outside the plume region and is called the well-mixed region. The temperatures associated with each region are shown in Fig. 4.31. These are the temperature profiles used to analyze those sequences for which stagnation is assumed.

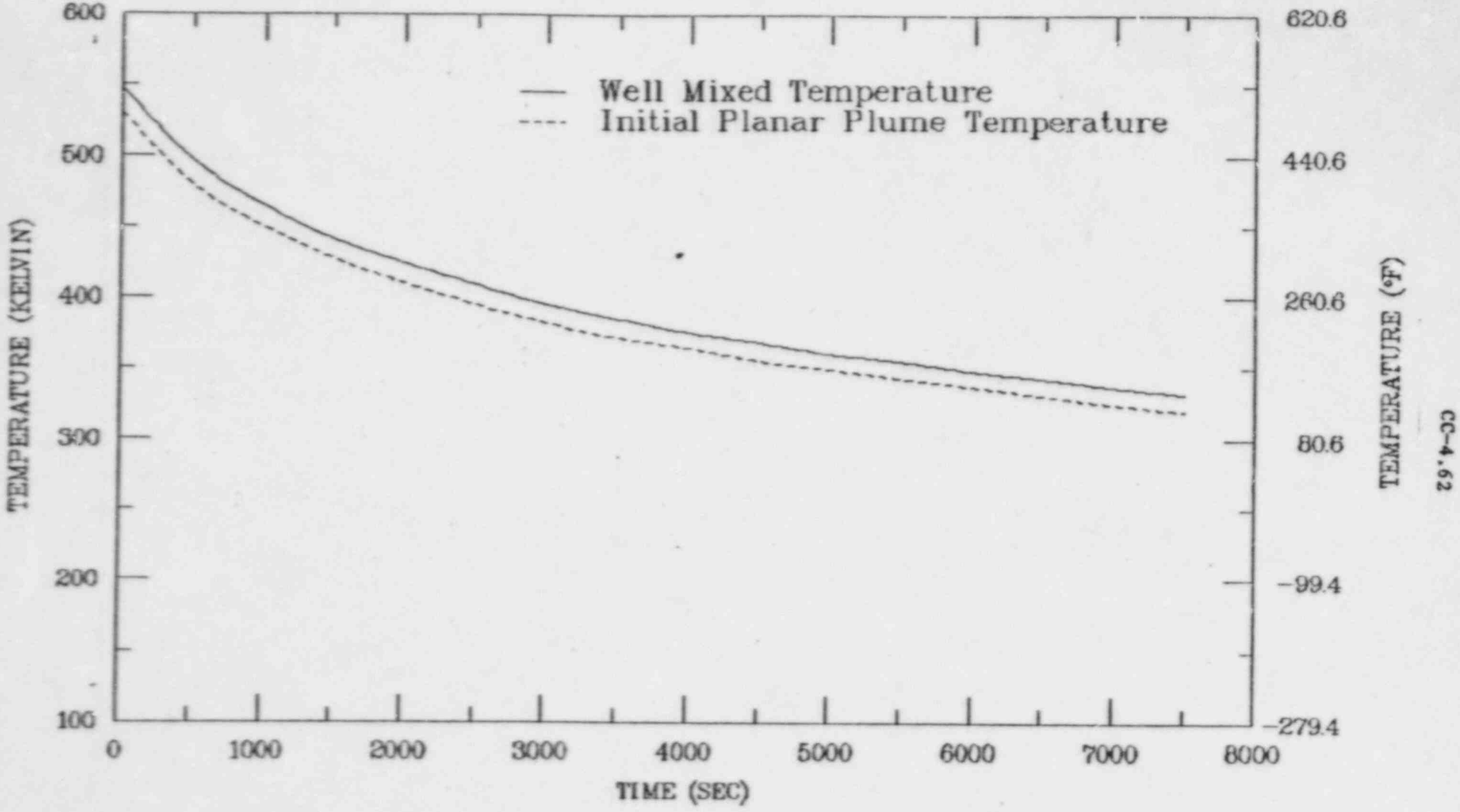

Figure 4.31. Temperatures associated with loop flow stagnation event.

4.5. Heat-Transfer Coefficient Evaluation

A time-dependent heat-transfer coefficient was calculated by TRAC for the fluid film condition associated with each of the transients calculated by LANL.

The fluid film and the vessel wall constitute two thermal resistances in series. Thus the "total" conductivity is

$$h_T \sim \frac{1}{\frac{1}{h_f} + \frac{\Delta r_c}{k_c} + \frac{\Delta r_b}{k_b}} ,$$

where

h_f = thermal conductance of fluid film,

k_c = thermal conductivity of cladding,

k_b = thermal conductivity of base material,

Δr_c = thickness of cladding,

Δr_b = effective thickness of base material (time dependent).

When the resistance of the fluid film ($1/h_f$) is small compared to the resistance of the vessel wall ($\Delta r_c/k_c + \Delta r_b/k_b$), the fluid-film conductivity has little effect on heat removal from the wall. For instance, h_f = 1000 Btu/hr·ft^2·°F (pumps on) is a "large" value, and but even larger values (momentary boiling) have little effect on the severity of the transient.

When the resistance of the fluid film is large (small value of h_f, such as 100 Btu/hr·ft^2·°F), the film resistance is dominant. As h_f approaches zero, the potential for vessel failure disappears.

Plots of the heat-transfer coefficient calculated by TRAC for each transient are presented in the LANL report (Appendix F); however, it was discovered after all the transients had been run that TRAC was not calculating the downcomer heat-transfer coefficient correctly. For the two-dimensional flow field that occurs in the vessel downcomer (azimuthal and vertical flow), the magnitude of the velocity vector should have been used to evaluate the Nusselt number in each of the fluid cells in the downcomer annulus. However, because of an error, only the vertical component of the velocity was considered. In transients in which one loop stagnates and the other loop is flowing, significant azimuthal flows occurred in the downcomer annulus. In cells in which the velocity component in the azimuthal direction is large and the velocity component in the vertical direction is small, the Nusselt number was underestimated and a natural circulation flow regime was predicted. Consequently, the heat-transfer coefficients for those cells were underestimated.

Because of this error, the TRAC-calculated heat-transfer coefficients were modified for use in the fracture mechanics analysis. In the modification the initial drop in the fluid film heat-transfer coefficient was not changed since it was felt that the TRAC calculation for this time frame was quite adequate. For the remainder of the analysis time, it was assumed that the minimum heat-transfer coefficient was 400 Btu/hr·ft^2·°F. This value was chosen for two reasons: (1) After a review of the TRAC

calculations, it appeared that the heat-transfer coefficient would stabilize in the range of ± 100 Btu/hr·ft^2·°F of this value, and (2) the minimum value is large enough so that the total heat transport is not significantly sensitive to the value of the fluid film heat-transfer coefficient (i.e., it is much larger than 100 Btu/hr·ft^2·°F).

As the fracture-mechanics calculations progressed, Theofanous was asked to review this assumption. He used the TRAC velocity histories to calculate fluid film heat-transfer coefficients. A discussion of the complete analysis is included Appendix H. In general, it was determined that typically the forced convection augmentation was overshadowed by the corresponding reduction in the forced convection component (as the velocity decreased) such that the resulting spread in heat-transfer coefficients was much smaller than the variation in the individual "free" or "forced" convection components. The variation in calculated wall temperatures was even smaller.

The calculated fluid film heat-transfer coefficients are shown in Table 4.4 for all 12 LANL transients. As shown, the coefficients are almost all covered by the 400 ± 100 Btu/hr·ft^2·°F range. Thus it was concluded that the original assumption was valid.

Table 4.4. Fluid film heat-transfer coefficients for twelve LANL transients

LANL Transient Number	NU/NU $_{\infty}$ *	h* mixed (BTU/hr-ft^2-°F)	Fraction of h from Forced Convection	Fraction of h From Free Convection
1	1.12	330	0.53	0.47
2	1.00	454	0.98	0.02
3**	—	—	—	—
4	1.00	365	0.55	0.45
5	1.20	345	0.40	0.60
6	1.00	510	0.98	0.02
7	1.00	480	0.91	0.09
8	1.00	460	0.98	0.02
9	1.00	590	1.00	0.00
10	1.00	500	0.59	0.41
11	1.00	515	0.90	0.10
12	1.03	477	0.85	0.15

*Based on maximum velocity in downcomer region at 2000 seconds for each transient.

**With two reactor coolant pumps in operation throughout the transient period, the heat transfer coefficient is assumed to be very large.

4.6. Estimations of Pressure, Temperature and Heat-Transfer Coefficient Profiles

The evaluation of the risks of pressurized thermal shock (PTS) entails the coupling of overcooling incident event trees to fracture-mechanics calculations of the probability of vessel crack propagation. The link between an event tree end state and the fracture-mechanics calculation is the transient behavior of the pressure (P), temperature (T), and heat-transfer coefficient (h) in the reactor vessel downcomer region. That is, the P, T, and h transient profiles from the sequence defined by an event tree end state become inputs for the fracture-mechanics calculation.

There are potentially several million end states produced from overcooling transient event trees and the cost and complexity of thermal-hydraulics and fracture-mechanics calculations preclude the evaluation of every end state separately. Therefore, it becomes necessary to (a) reduce by similarity grouping the number of end states to be evaluated and (b) reduce the number of detailed thermal-hydraulic calculations to be performed through the use of less rigorous estimation techniques. This section summarizes the approach used to group the sequences and estimate P, T, and h profiles for the Calvert Cliffs-1 PTS study. Section 4.6.1 describes the estimation methodology developed for the study and the approach and rationale for sequence grouping, and Section 4.6.2 summarizes the results of evaluations for each of the major initiating events:

1. Large main steam-line break at HZP,

2. Small main steam-line break at HZP,

3. Large main steam-line break at full power,

4. Small main steam-line break at full power,

5. Reactor trip,

6. Small-break LOCA ($\leq$0.016 ft^2),

7. Small-break LOCA (~0.02 ft^2),

8. LOCAs with potential loop flow stagnation, and

9. Loss of main feedwater with subsequent AFW overfeed.

The last two categories involved sequences for which P, T, and h values were determined in earlier sections of this chapter and thus they are not discussed in this section.

The estimated P, T, and h transient profiles presented here are based on the TRAC-PF1 calculations reported by Los Alamos National Laboratory and described in Section 4.2. Computer tapes of TRAC plot output files for these calculated transients were also employed in the development of parameters applied to the temperature and pressure estimation procedures.

The sole and extensive use of these TRAC calculations in estimating the P, T, and h profiles for the various sequences implies that the estimations are subject to the same modeling assumptions and code characteristics driving the uncertainties in the TRAC-calculated results. Additional uncertainties introduced by the estimation procedure have not been fully evaluated. Such uncertainties were minimized by using the estimation procedure to duplicate portions of the transients calculated by TRAC and thereby check the validity of the assumed parameters and extrapolation models.

The estimated P, T, and h profiles presented in this report represent a "single point" estimate of downcomer conditions. That is, the estimated conditions are assumed to hold for the entire downcomer region without any azimuthal or axial variations. Since the detailed TRAC calculations demonstrated both azimuthal and axial variation in fluid temperatures and heat-transfer coefficients, the cooldown model used in the estimation procedure was conservatively set up to yield the expected temperature of the coldest subregion of the downcomer rather than the overall average temperature for the whole downcomer region.

4.6.1. Methodology

4.6.1.1. General Approach

After an initial survey of the data resources and the sequences identified for estimation, the five-step process depicted in Figure 4.32 was employed in estimating the Calvert Cliffs-1 P, T, and h profiles. This approach

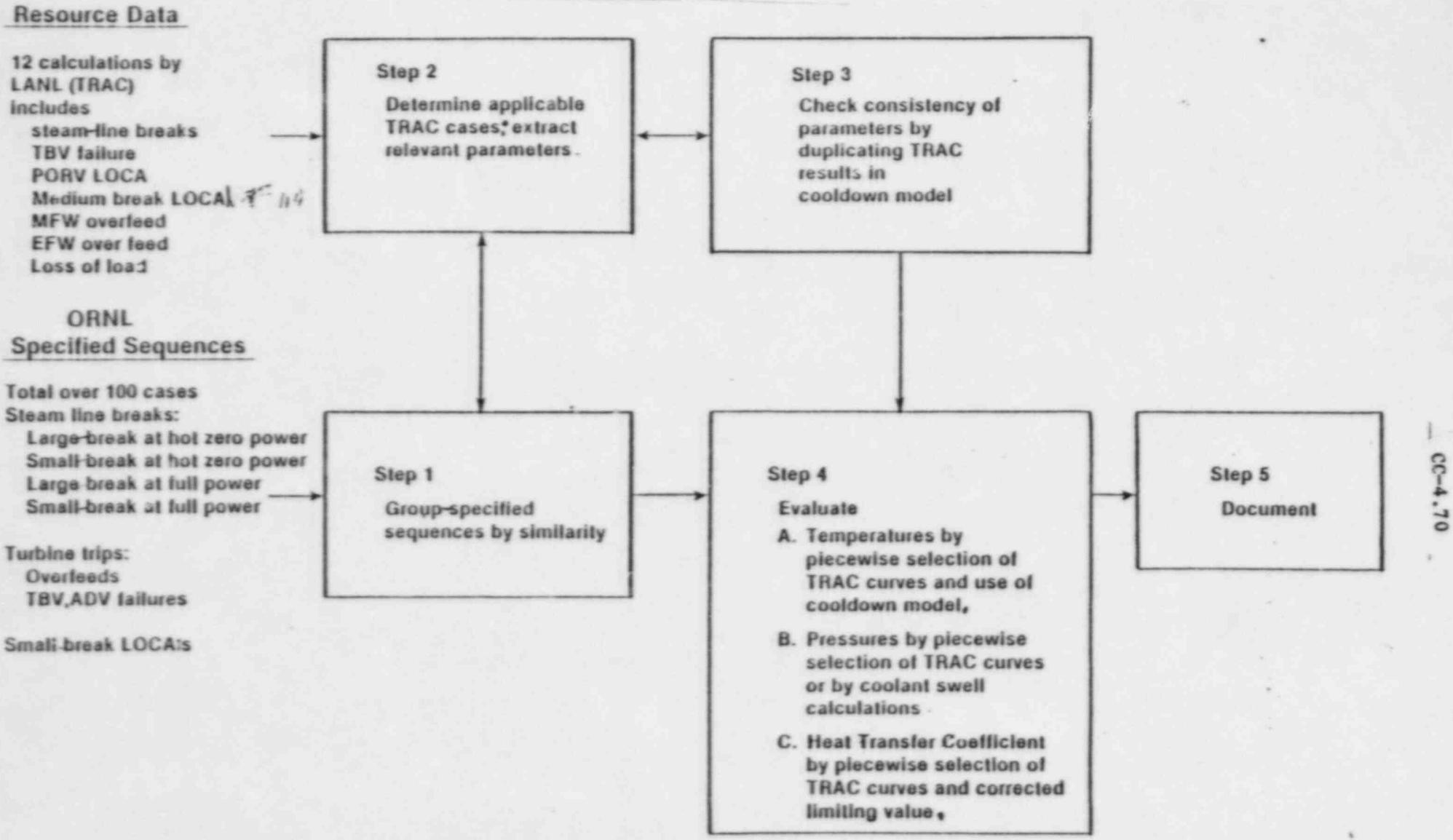

Figure 4.32. P, T, and h estimation approach.

allowed logical reduction of the number of cases to be evaluated and derived the greatest benefit from the information in the TRAC calculations.

The first step involved the grouping of similar sequences within each transient initiator table. An evaluation of the TRAC calculations for the effects of different operating states provided the criteria for assignment of sequences into groups. In step 2 the parameters were developed for the cooldown (temperature) and coolant swell (pressure) models used on occasion for this study. To assure correct interpretation of conditions during sequences, the appropriate parameters were applied to the cooldown model to duplicate portions of sequences calculated by TRAC. These validation efforts took place in step 3 (see Section 4.6.1.3).

In step 4, the pressure, temperature, and heat-transfer coefficients were estimated. Temperature could be estimated by piecewise application of TRAC results and/or by calculation using the cooldown model. The method selection depended on the complexity of the sequence and the availability of applicable data from the TRAC calculations. Early portions of many evaluated sequences had stated configurations identical to those of a particular TRAC calculation, so piecewise use of the TRAC results was applied. The cooldown model was then used to evaluate the remainder of the transient out to 2 hours. Certain mild (i.e., high-temperature) transients were not explicitly evaluated. These mild seqnences were assigned the P, T, and h profiles of a TRAC calculation or the estimated sequence which most closely represented the anticipated response of the sequence.

Pressure estimates were derived from observation of pressure trends in the

TRAC calculations and by a pressure prediction model (the coolant swell model). The Calvert Cliffs-1 plant features a low-head HPSI system which cannot repressurize the primary above the pump shut-off head of 1285 psia. The charging pumps can repressurize the primary up to the PORV setpoint (2400 psia), but does so at a very low rate due to low flow capacity. The charging pumps were not throttled in any of the TRAC calculations. Therefore, there are a number of cases available for evaluation of the contribution of the charging pumps to system repressurization. The coolant swell model accounts for pressure effects due to coolant expansion on reheating. This model is used for evaluation in those cases where charging pump flow is throttled.

Heat-transfer coefficients were based on the piecewise selection of TRAC data and the results of modeling performed by Theofanous at Purdue University (see Section 4.5). In general, the TRAC calculations predicted relatively constant values while the reactor cooling pumps (RCP) are running and a step change to a lower but nearly constant value after RCP trip and establishment of natural circulation. Due to problems in the TRAC heat-transfer regime selection logic, the TRAC values were systematically underpredicted. Theofanous found that the contribution of free convection to the downcomer heat-transfer coefficient offset increases or decreases in forced convection such that a total value of 400 Btu/hr$\cdot$ft$^2\cdot$°F (2270 W/m$^2\cdot$K) was maintained over a wide range of natural-circulation flow conditions. The sequence evaluations presented in this section use a composite of TRAC-calculated heat-transfer coefficients for pre-RCP trip regimes and corrected estimates for natural-circulation regimes.

The completed estimations were documented in step 5. This documentation comprises Sections J.3 - J.8 of Appendix J.

4.6.1.2. Sequence Grouping

When all PTS initiators and failure branches are set up in event trees, several thousand end states result. To obtain a tractable yet representative set of PTS transients requires some method of sequence grouping. Chapter 3 describes the construction of the event trees and the process used to eliminate "non-contribution" states (i.e., component failures made irrelevant by the action of other systems or components). The collapsed event trees from this process still contain a large number of end states. Section 3.5 describes the screening process used to separate end states into a set of discrete sequences for evaluation and a set of residual sequences for which no further evaluation was performed. Sequences representing identical combinations of failures were collapsed to a single group and the corresponding frequencies were summed. Sequences with frequencies between 10^{-7} and 10^{-8} per year, which would normally fall into a residual group, were examined for similarity with the discrete sequences and were collapsed together with specific discrete sequences where appropriate. This approach minimized the cumulative frequency of the residual. The resulting set of discrete sequences are found in tables presented in Section 3.5.

Altogether, 115 sequences emerged from this grouping process, including 11 residual groups. The grouping processes of Chapter 3.0 were based on system configuration and event frequency. Further grouping may occur based on

the thermal-hydraulic impact of the configuration. The impact of a particular component or system can be evaluated from observation and evaluation of the effects of its operation or failure in the TRAC calculations. In this way the importance of failures or actions could be classified as dominant, minor, or inconsequential. Sequences with the same dominant features were grouped together for analysis. In later stages, the influence of minor events was evaluated to check the consistency of the groupings. This checking accounted for the thermal-hydraulic interaction or feedback due to the combination of failures. Some sequences were reassigned to other groups as a result of such checks.

The groupings for each of the initiators are discussed in Appendix J, Sections J.3 - J.9.

4.6.1.3. Temperature Evaluation by Cooldown Model

The temperature response of a transient is a function of the system's configuration during the sequence, including the timing of configuration changes (e.g., RCP trip; MSIV, MFIV closures; AFAS, etc.). The sequences from the LANL TRAC calculations represent only 12 of the thousands of sequences on the overcooling event trees. The cooldown model is a means for applying the information generated by the TRAC calculations to other sequences requiring temperature response estimation. The approach used in the cooldown model was to obtain separate mass-energy balances around the steam generators and the reactor vessel (i.e., balance of the primary cooling system) to predict the rate of temperature change. All pertinent cooling and heating mechanisms were included. In obtaining these mass-energy

balances, it was necessary to make the assumptions listed in Table 4.5 to simplify the system to a two-node model.

The assumption of no steam generator heat-transfer resistance will result in the prediction of slightly lower primary temperatures than are reported by TRAC, the error being proportional to the rate of heat transfer. The error will be less than 10°F for large steam-line breaks (LANL transients 1-5) and less than 5°F for small steam-line breaks (LANL transients 6 and 7) under conditions where natural loop circulation prevails.

The assumption of thermal equilibrium in the steam generator secondary allows the use of simple choke flow models to predict steam flow rate. Conditions close to thermal equilibrium are obtained by TRAC for steam generators during blowdown. Division of the reactor coolant system into only two nodes coupled with the assumption of perfect mixing within a node "smears out" the temperature differences around a loop, thus losing temperature lag information available from a finely noded model such as that used in TRAC. Therefore, the cooldown model will respond faster to input parameter changes than will the TRAC model. Direct comparison of the cooldown model's extrapolated temperature response with TRAC results suggest that this effect is small for cases where natural loop circulation remains large (>500 lb/sec).

A final assumption that allows the use of the cooldown model is the assumption that TRAC-calculated mass flow data from the 12 LANL transients may be applied to the evaluation of other sequences. This assumption is necessary because the mass flow information is required to implement the cooldown

Table 4.5. Cooldown model assumptions

Assumption	Justifications	Limitations	Resulting Model Characteristics
1. No heat-transfer (HT) resistance between primary and secondary	Large HT area; large HT coefficient for boiling, condensation.	Loss of heat flow lags and disequilibrium information.	Simplifies calculation at expense of accounting for SG primary temperature lag of 5-15°F.
2. SG secondaries in thermal equilibrium	Same as for assumption 1 plus good approximation for SG blowdown conditions.	Not a good approximation where overfeed is compressing steam in isolated steam generator.	Allows use of enthalpy transport model based on choked flow pressure, enthalpy conditions.
3. Water inventory is well mixed within a node (energy is uniformly distributed)	Same as for assumption 1 plus natural circulation flow is generally much larger than HPI and secondary flows, allowing equilibration or approach thereto.	Eliminates space-time effects; difficult to quantify flow stagnation effects.	Allows use of two-node mass-energy balance.

model calculated from a simple two-node model. Engineering judgement is used to identify segments of the TRAC calculations relevant to the sequence being evaluated. Pertinent mass flow data are then extracted from the identified TRAC calculations for application to the cooldown model. The required parameters for the model are listed in the derivation of the model as described below.

Model Derivation and Characteristics. The cooldown model consists of two simultaneous nonlinear differential equations describing the mass-energy balance of a primary node (i.e., vessel, loop piping, and RC pumps) and a steam generator node as follows (see Figure 4.33):

$$\frac{d(MU)_{pri}}{dt} = \dot{m}_{HPI} H_{HPI} - \dot{m}_L H_L + Q_{D(t)} + Q_{RCP} + Q_W - Q_{sec} , \tag{4.1}$$

$$\frac{d(MU)_{SG}}{dt} = \dot{m}_{FW} H_{FW} - \dot{m}_{ST} H_{ST} + Q_{sec} , \tag{4.2}$$

where

$\dot{m}_{HPI} H_{HPI}$ = product of HPI mass flow and specific enthalpy at HPI nominal temperature (T_{HPI}) vs. thermodynamic reference temperature (T_{ref})

$= \dot{m}_{HPI} C_p (T_{HPI}-T_{ref})$,

$\dot{m}_L H_L$ = product of primary leak flow (pressurizer surge line or break) and specific enthalpy at hot leg temperature (T_H)

$= \dot{m}_L C_p (T_H-T_{ref})$ (valid for liquid flow only),

$\dot{m}_{FW} H_{FW}$ = product of feedwater mass flow and specific enthalpy at feedwater temperature (T_{FW})

$= \dot{m}_{FW} C_p (T_{FW}-T_{ref})$,

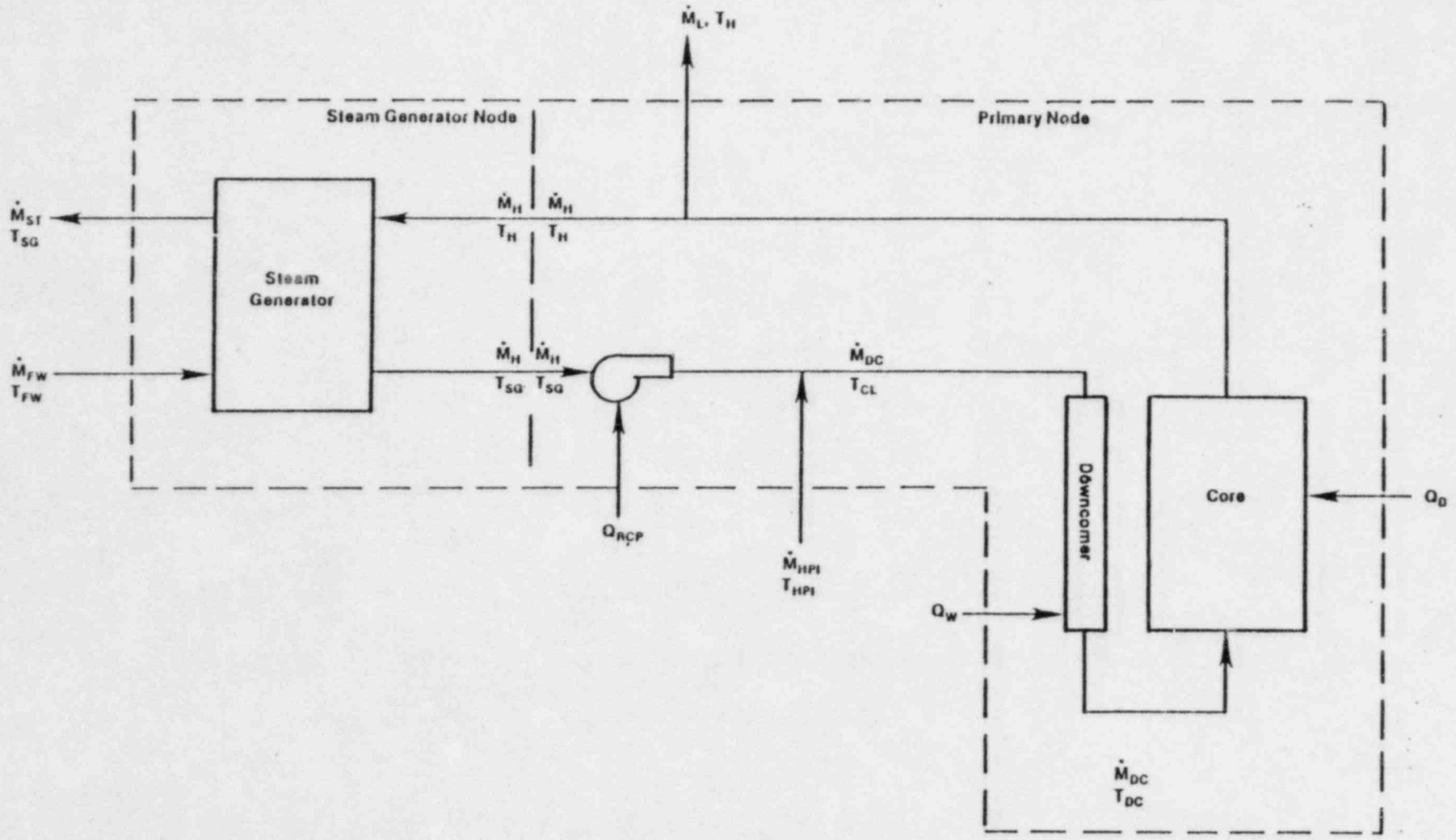

Figure 4.33. Mass and energy flows for two-node cooldown model.

$\dot{m}_{ST} H_{ST}$ = product of secondary steam flow and specific enthalpy for saturated steam at steam generator conditions (T_{SG})

= $\dot{m}_{ST} (\Delta H_{v,T_{SG}}) + C_p (T_{SG}-T_{ref})$,

$Q_D(t)$ = decay heat input as function of time

= ANS Decay Heat Function for transients from full power

= constant value for transients from hot standby,

Q_{RCP} = pump power deposited in coolant

Q_W = heat transferred from vessel wall to coolant

Q_{sec} = heat transferred from primary to secondary.

In the absence of heat-transfer resistance, Q_{sec} is limited only by the transport of energy to the steam generator by the hot leg flow ($\dot{m}_H$):

$$Q_{sec} = \dot{m}_H C_p (T_H - T_{SG}) \quad .$$

The lefthand sides of Equations 4.1 and 4.2 may be expanded by use of the chain rule

$$\frac{d(MU)}{dt} = M \frac{du}{dt} + U \frac{dm}{dt} \quad ,$$

where

M = total mass,

U = specific energy = $C_v (T - T_{ref})$,

$dU/dt = C_v (dT/dt)$,

$dM/dt = \sum \dot{m}$ = mass flow across system boundaries.

Substituting into the lefthand sides of Equations 1 and 2,

$$\frac{d(MU)_{pri}}{dt} = M_{pri} C_v \frac{dT_H}{dt} + C_v (T_H - T_{ref}) (\dot{m}_{HPI} - \dot{m}_L) \quad , \qquad (4.3)$$

$$\frac{d(MU)_{SG}}{dt} = M_{SG}\, C_v \frac{dT_{SG}}{dt} + C_v\, (T_{SG} - T_{ref})\, (\dot{m}_{FW} - \dot{m}_{ST}) \quad , \tag{4.4}$$

and then placing these expressions with their respective righthand sides yields

$$\begin{aligned} M_{pri}\, C_v \frac{dT_H}{dt} &+ C_v\, (T_H - T_{ref})\, (\dot{m}_{HPI} - \dot{m}_L) \\ &= \dot{m}_{HPI}\, C_p\, (T_{HPI} - T_{ref}) - \dot{m}_{LCp}\, (T_H - T_{ref}) \\ &+ Q_D(t) + Q_{RCP} + Q_W - \dot{m}_H\, C_p\, (T_H - T_{SG}) \end{aligned} \tag{4.5}$$

for the primary node and

$$\begin{aligned} M_{SG}\, C_v \frac{dT_{SG}}{dt} &+ C_v\, (T_{SG} - T_{ref})\, (\dot{m}_{FW} - \dot{m}_{ST}) \\ &= \dot{m}_{FW}\, C_p\, (T_{FW} - T_{ref}) - \dot{m}_{ST}\, [\Delta H_{v,T_{SG}} \\ &+ C_p\, (T_{SG} - T_{ref})] + \dot{m}_H\, C_p\, (T_H = T_{SG}) \end{aligned} \tag{4.6}$$

for the steam generator node. For liquids, C_v may be assumed to be equal to C_p. Using this assumption and collecting common terms yields

$$\frac{dT_H}{dt} = \frac{\dot{m}_{HPI} C_p (T_{HPI} - T_H)}{M_{pri} C_p} + \frac{Q_D(t)}{M_{pri} C_p} + \frac{Q_{RCP}}{M_{pri} C_p} + \frac{Q_W}{M_{pri} C_p} - \frac{\dot{m}_H C_p (T_H - T_{SG})}{M_{pri} C_p} \tag{4.7}$$

for the primary node and

$$\frac{dT_{SG}}{dt} = \frac{\dot{m}_{FW} C_p (T_{FW} - T_{SG})}{M_{pri} C_p} - \frac{\dot{m}_{ST} (\Delta H_{v,T_{SG}})}{M_{SG} C_p} + \frac{\dot{m}_H (T_H - T_{SG})}{M_{SG} C_p} \tag{4.8}$$

for the steam generator node. In this form, the thermodynamic reference state (T_{ref}) has been eliminated, leaving only the expressions for heating and cooling mechanisms.

Flow rates for HPI, leak, hot leg and feedwater are independent parameters extracted or estimated from TRAC calculations. Steam flow rate is a function of steam enthalpy and pressure, break (or valve) area, and flow resistance. The estimation of steam flow is based on an isentropic choked model altered to account for these elements. The model is of the form

$$\dot{m}_{ST} = f(P,H)AkP \quad , \tag{4.9}$$

where

$f(P,H)$ = choked isentropic mass flow [lb/hr/in.^{2}-psia (upstream pressure)] as a function of pressure and mixture enthalpy (see ASME steam tables, 4th ed., Figure 14),

A = break (valve) size (in.^{2}),

k = factor by which effective area of break is reduced to compensate for flow resistances in lines and valves,

P = pressure (psia).

By evaluating this expression for saturated steam enthalpy at various temperatures and taking a power curve fit against corresponding saturation temperatures, the expression was converted to

$$\dot{m}_{ST} = Ak \times 1.87045 \times 10^{-4} \, T_{SG}^{4.32991} \text{ (lb/sec)} \quad , \tag{4.10}$$

which has an accuracy better than $\pm 3\%$ between 200°F and 500°F upstream steam temperature. The choked flow condition holds over this range for TBV flows to the condenser, but becomes invalid at low temperatures for breaks to the atmosphere.

With the expression for steam flow substituted into the cooldown equation

for the steam generator, the total model becomes

$$\frac{dT_H}{dt} = \frac{\dot{m}_{HPI}\, C_p(T_{HPI}-T_H) + Q_D(t) + Q_{RCP} + Q_W - \dot{m}_H\, C_p(T_H-T_{SG})}{M_{pri}\, C_p} \qquad (4.11)$$

$$\text{with } M_{pri} = M_{pri0} + \int (\dot{m}_{HPI} - \dot{m}_L)\, dt$$

$$\frac{dT_{SG}}{dt} = \frac{\dot{m}_{FW}C_p(T_{FW}-T_{SG}) - Ak \times 1.87045 \times 10^{-11}\, T_{SG}^{4.32991} + \dot{m}_H C_p(T_H-T_{SG})}{M_{SG}\, C_p} \qquad (4.12)$$

$$\text{with } M_{SG} = M_{SGO} + \int (\dot{m}_{FW} - \dot{m}_{ST})\, dt \quad ,$$

which is a set of simultaneous, nonlinear differential equations which can be solved numerically to obtain the primary hot leg temperature (T_H) and steam generator exit temperature (T_{SG}). The downcomer liquid temperature is obtained from the following equation:

$$T_{DC} = \frac{\dot{m}_H\, H_{SG} + \dot{m}_{HPI}\, H_{HPI} + Q_{RCP} + Q_W}{(\dot{m}_H + \dot{m}_{HPI})\, C_p} \qquad (4.13)$$

with all quantities as defined above. This equation defines the downcomer temperature in terms of the mixing of loop flow and HPI and the heating of the fluid by RCP power input and heat transfer from the vessel wall. This equation does not affect the mass-energy balances (Equations 4.11 and 4.12) described above but is used to define the local fluid temperature in the downcomer.

Application of Cooldown Model. The cooldown model calculates temperatures for the hot leg, steam generator, and vessel downcomer using only a two-node energy balance. The Calvert Cliffs-1 plant is equipped with two separate cooling loops which may be subjected to an asymmetric operating condition (e.g., one steam generator blowing down while the other is isolated). Such situations require application engineering judgement to fit the existing conditions to the model. Judgement is also required to develop the required mass flow data for input to the model.

As described at the beginning of this section, the general approach for evaluating a particular scenario is to first identify which of the TRAC calculations most closely matches the description of the scenario. Often the TRAC calculation and the evaluated scenario are identical out to some specified point in time or particular event (SGIS, RCP trip, etc.), after which the evaluated sequence becomes different from the TRAC calculation. Temperatures and mass inventories of the primary system and the steam generators are extracted from the TRAC calculation at this point to set up the initial conditions for the extrapolation of temperature by the cooldown model. Also, the effective valve area for the model choked flow calculation is selected so that the model will closely follow the steam flow trends observed in the TRAC calculation.

The initial mass inventories in the primary loops and steam generators may be distributed in different ways to account for asymmetric loop operation. For example, when a steam generator is totally isolated from the rest of the primary system (no heat transport possible) due to flow stagnation in that loop, the water mass and its energy content (temperature) are left out

of the model, since they cannot influence temperature trends elsewhere. Should the loop flow be restored later, the water mass and the energy would be put back into the model where they can influence total system heating or cooldown. Another example is when one steam generator is undergoing cooling by blowdown while the other steam generator is losing heat to the primary loop due to continued loop flow. In this case, the inventory of the steam generator would be added to the primary mass since both are working together to retard the cooldown of the system. Should any of these conditions change to a symmetric condition or to another form of asymmetric condition, the extrapolation should be stopped for adjustment of primary and steam generator node masses.

Other system state changes will require interruption of temperature extrapolation to alter input parameters. Some of these system state changes are listed in Table 4.6. Whenever one of these state changes is encountered, the current values of the hot leg and steam generator temperatures as calculated by the cooldown model are applied as input to the next extrapolation segment, together with altered values (as necessary to match the new system state conditions) of the primary and steam generator mass inventories, total loop flow, HPI flow, primary leak (pressurizer surge line) flow, feedwater flow, feedwater temperature, heat input rate from wall heat transfer, decay heat factor, RCP heat, and secondary side break (valve) area. This process continues until the entire 0- to 7200-second period is evaluated.

By estmating the temperature profile of a TRAC-calculated transient, the validity of data interpretation relating to the transient response can be

Table 4.6. System state changes for extrapolation of overcooling sequences by the cooldown model

Trigger Condition	Significance	Action
RCS cools below 535°F.	TBVs and ADVs close.	Adjust valve area.
RCS cools below 537°F.	RCS pressure falls below 1740 psia.	Initiate charging flow.
HPSI time + 30 sec.	-	Trip RCPs and begin 100-sec coastdown.
Extrapolated pressure below 1285 psia.	-	Initiate HPI flow as per heat capacity.
SG cools below 498°F (685 psia).	SGIS	Close MFIVs, MSIVs.
SG inventory below 99,000 lb.	AFAS	Initiate AFW to one or both SGs.
Coexistence of "broken" and isolated steam generators.	-	Isolate AFW to "broken" steam generator.
SG dries out.	-	Set secondary break (valve) area to zero.
Hot-leg temperature drops below SG temperature.	Loop stagnates.	Adjust mass inventories.
SG level reaches +22 in. (250,000 - 300,000 lb).	-	Throttle AFW flow to SG.
Hot-leg temperature becomes greater than stagnant SG temperature.	Natural circulation restored.	Adjust mass inventories.
Commencement of primary system reheat.	Repressurization to HPI shut-off head.	Eliminate HPI flow.
Sequence specified closure of valve.	-	Adjust parameters accordingly.

checked. When the extracted parameters are correct, the extrapolation will closely follow the TRAC calculation. For example, the times to SIAS and SGIS signals for the 0.1-m^2 main steam-line breaks at hot zero power (LANL transient 1) and at full power (LANL transient 2) as estimated by the cooldown model are not significantly different.

An example of a full 7200-second extrapolation is given in Figure 4.34, which compares cooldown model and TRAC results for the case of a PORV LOCA with a stuck-open ADV (LANL transient 12). This case was selected because it features a secondary side break that causes a general system cooldown coupled to a localized cooling due to significant HPI flow. The two TRAC curves represent the downcomer condition under the nozzles of the stagnated (B1) and flowing (A1) loops which represent the expected range of conditions. The cooldown model always assmes that all HPI flow is mixed with the flowing loop, thus yielding a temperature lower than the average for the two loops. In this case the extrapolated temperature stays within 10 to 50°F of the calculated minimum temperature loop values.

4.6.1.4. Pressure Evaluation by Coolant Swell Model

An overcooling event will cause the primary coolant to cool down and contract, drawing water out of the pressurizer via the pressurizer surge line. As the water level drops in the pressurizer, the steam layer expands and the system pressure decreases. As the pressure decreases, SIAS initiates charging pump flow and the safety injection pumps are started. If the pressure then decreases to below 1285 psia, high-pressure injection flow commences. These injection flows help to stabilize system pressure during

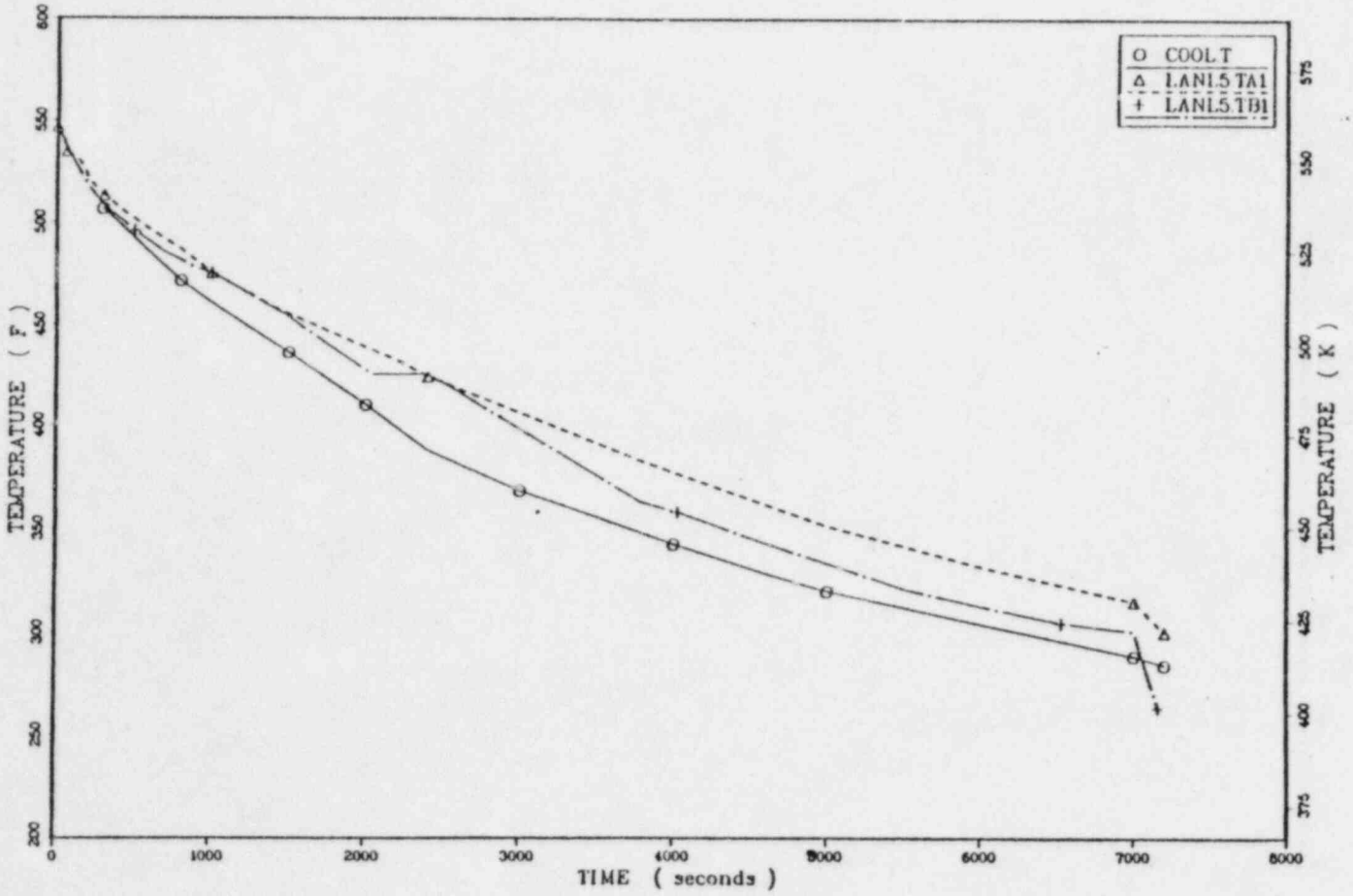

Figure 4.34. Comparison of TRAC and cooldown model temperature profiles for PORV LOCA with stuck-open ADV (LANL transient 12).

the rapid cooldown portion of the event sequence.

If the injection flow volume is greater than the shrinkage rate, or if the system enters a reheating mode, the pressurizer water level will increase, compressing the steam layer and increasing the pressure. The rate at which the pressure recovers is of importance because of the contribution of pressure in the fracture-mechanics calculations.

To determine the best algorithm for estimating pressure recovery rate, the TRAC calculations for Calvert Cliffs-1 were examined in detail. PTS cases calculated by TRAC and also by REALP5 for the Oconee-1 (Ref. and) and H. B. Robinson-2 (Ref.) plants were also examined. It was observed that the codes predict that the system pressure variation with pressurizer water level is essentially linear. Furthermore, the PORV set-point pressure is reached when the pressurizer is on the verge of becoming water solid. A theoretical model of the ideal adiabatic compression of the pressurizer steam layer yields nonlinear pressure vs. pressurizer water level response and predicts an exceedingly fast repressurization to the PORV set-point pressure. Clearly the ideal adiabatic compression model is not representative of repressurization rates predicted by TRAC and REALP5. Therefore, the observed linear relationship between pressurizer level and system pressure was employed for this study.

In most of the Calvert Cliffs-1 sequences that were evaluated, the system pressure dropped below and then recovered to the HPI pump shut-off head of 1285 psia. At this point, system cooldown mechanisms have been isolated or corrected and the system has commenced reheating. Injection flow from the

high-pressure injection system has ceased and injection flow from the charging pumps may or may not be throttled, depending on the specification of the sequence. The reheating of the coolant will cause the coolant volume to swell and (with the charging pump flow) refill the pressurizer. The required increase in temperature to cause total refill of the pressurizer, and therefore repressurization to the PORV set point, may be determined by the following equation:

$$\underline{v}(T_L, \text{ 2400 psia}) = \left(1 + \frac{V_{ST}}{V_{pri}}\right) \underline{v}(T_i, \text{ 1285 psia}) \quad , \tag{4.14}$$

where

$\underline{v}(T,P)$ = specific volume of water at specified temperature and pressure,

T_L = limiting average primary temperature at which coolant swell (and accumulated charging pump flow) volume equals available pressurizer steam volume,

T_i = initial average primary temperature at start of system reheat,

V_{ST} = available steam volume in pressurizer at start of reheat,

V_{pri} = volume of primary system susceptible to reheating

= primary volume without pressurizer or HPI line volume

= 9601 ft^3 - 346 ft^3 = 9255 ft^3.

This empirical relationship ignores the action of the pressurizer heaters. This equation also assumes that there are no primary steam voids outside the pressurizer and that the pressurizer steam volume (V_{ST}) is known at the beginning of repressurization. Table 4.7 contains estimates of effective steam volumes for the repressurization phases of the LANL transients. These volumes represent the amount of volume change which results in attainment of the PORV set-point pressure and do not necessarily represent

Table 4.7. Estimates of initial steam volumes for Calvert Cliffs-1 transients for repressurization from HPI shutoff up to PORV opening[a]

Transient Calculation	Time to repressurize (sec)	Initial/final temperature (°F)	ΔVolume due to coolant reheating (ft^3)	ΔVolume due to charging pump flow (ft^3)	Total Effective Volume (ft^3)
LANL1	2120	258/310	240	670	940
LANL2	800	405/467	486	284	770
LANL3[b]	—	—	—	—	—
LANL4	1980	224/221	0	600	600
LANL5	1200	216/218	0	363	363
LANL6	800	510/540	250	470	720
LANL7[c]	—	—	—	—	—
LANL8	1810	438/497	455	665	1120
LANL9	1250	432/4898	540	460	1000
LANL10[c]	—	—	—	—	—
LANL11[d]	—	—	—	—	—
LANL12[d]	—	—	—	—	—

[a]Repressurization times are calculated assuming no operator actions to control pressure.

[b]Case not analyzed.

[c]Repressurization commences before system reheat; V_{ST} not defined.

[d]LOCA case; system does not repressurize.

the actual steam volume in the pressurizer.

Engineering judgement dictated the selection of V_{ST} for the estimation of repressurization rate. In evaluation of sequences similar to a LANL transient, the corresponding value of V_{ST} would be applied to Equation 4.14. In other cases, generalized values reflecting the trends in Table 4.7 were selected. Hot zero power sequences were evaluated using a V_{ST} of 600 ft^3. A value of 700 ft^3 was applied to severe transients at full power and values between 1000 ft^3, and 1500 ft^3 was applied to milder transients at full power.

For each sequence estimation, the steam volume (V_{ST}) and initial average system temperature (T_i) were applied to obtain the average temperature at which full repressurization is obtained. The sequence temperature extrapolation was then examined to obtain the time at which this temperature is achieved. If charging pump flow continued over this period, the accumulated volume over the interval was subtracted from V_{ST} and the final average temperature was recalculated. This was repeated until convergence was obtained. The resulting sequence time represents the point at which the PORV set-point pressure is reached. Pressure between the beginning of reheat and attainment of full pressure is obtained by linear interpretation.

Due to the assumptions involved in the coolant swell model, the prediction of repressurization rate is imprecise. In most cases the uncertainty in the calculation would be conservatively bounded by the use of the repressurization curves calculated by TRAC. Some mild transients may

repressurize faster than the rates predicted by TRAC, but this is not expected to affect the fracture-mechanics analysis.

4.6.2. Results of Simple Model Evaluations

4.6.2.1. Large Main Steam-line Breaks at HZP

The sequences related to a large break ($\geq$0.1-m^2) in a main steam line with the unit at hot zero power (HZP) are described in Table 3.7 in Chapter 3. The seven sequences in the table reflect a variety of combinations of equipment and operator failures. Section J.3 in Appendix J relates the details of extrapolation development and Figures 4.35 - 4.37 summarize the results of the temperature, pressure, and heat-transfer coefficient extrapolations. Sequences 1.1 - 1.6 are represented in the figures. Sequence 1.7 is very similar to LANL transient 4 (see Figures 4.10 and 4.11 for temperature and pressure profiles respectively), and sequence 1.4 is equivalent to LANL transient 1.

The temperature curves in Figure 4.35 show the influence of the various failure combinations in Table 3.7. The six curves fall into three ranges or families on the figure. Sequences 1.1 - 1.4 are all identical to LANL transient 1 out to 1400 seconds, at which time the affected steam generator dries out. The termination of charging pump flows yields local temperature increases and reduced cooling loads for sequences 1.1 and 1.2, the two warmest sequences for this initiator. These two curves split at about 3500 seconds owing to the failure to throttle AFW to the intact SG in sequence 1.2.

Sequences 1.3 and 1.4 remain cooler than sequences 1.1 and 1.2 because the charging pumps are left running. The separation of these sequences after 4200 seconds is again due to the failure to throttle AFW in sequence 1.4 (LANL transient 1).

Sequences 1.5 and 1.6 (and 1.7) drop lower than the others and do not reheat. In the case of sequence 1.5, the drop is due to the failure to stop flow to the affected steam generator. In the case of sequence 1.6 (and 1.7), it is due to greater blowdown from MSIV failure. These failures provide a cooldown mechanism over the entire period and thus prevent reheating.

The minimum temperature for sequences 1.1 - 1.4, 253°F (396 K), lies in the portion of the profile extracted from LANL transient 4. The minimum temperatures for sequences 1.5 - 1.7 are 212°F (373 K), 211°F (373 K), and 212°F (373 K), respectively.

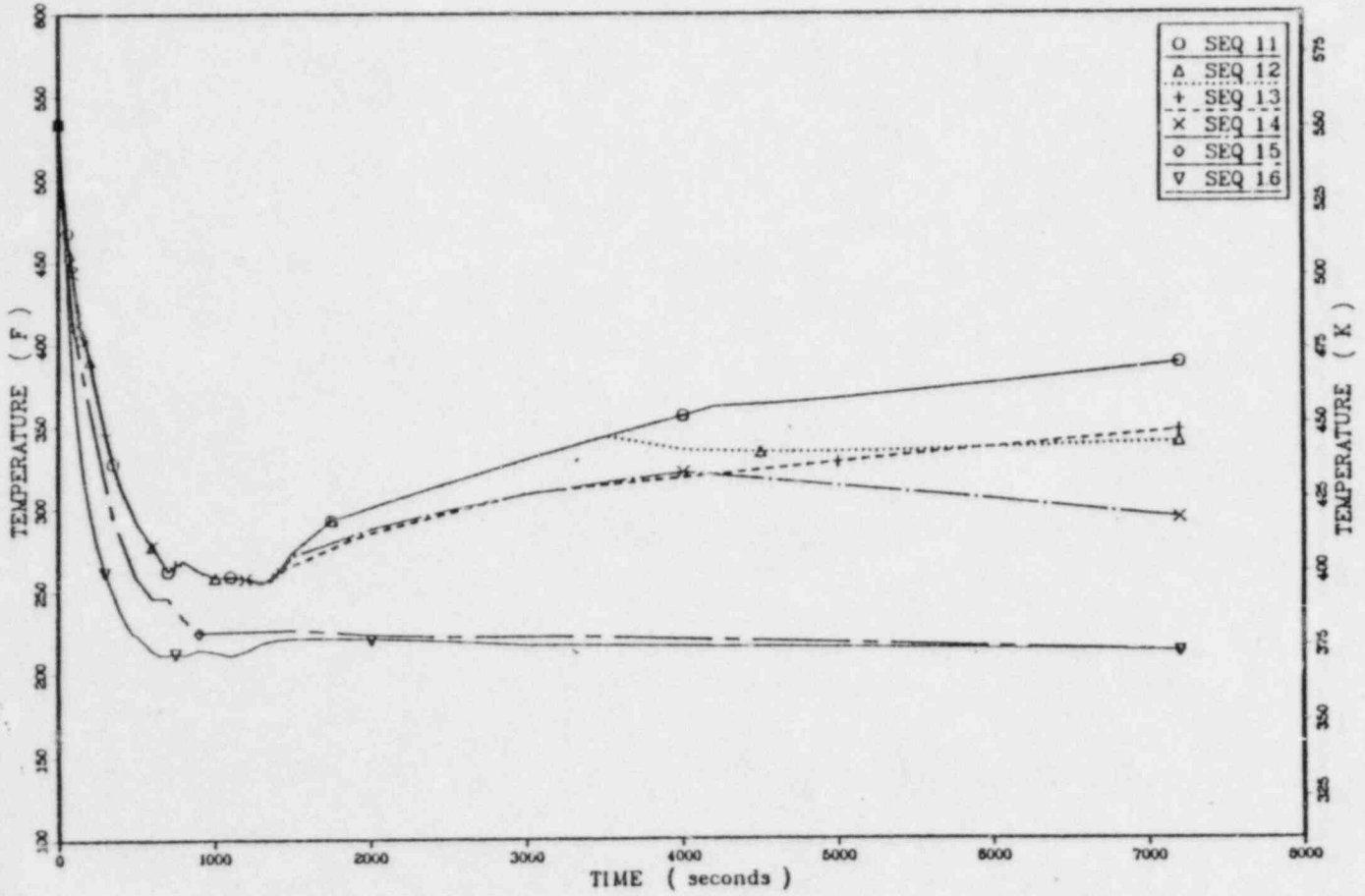

Figure 4.35. Extrapolated downcomer temperatures for large main steam-line break at HZP.

The pressure curves in Figure 4.36 show the influence of charging pump operation and system reheating on repressurization. Sequences 1.3 and 1.4 include charging pump flow and system reheating, which cause total repressurization by 3000 seconds. Sequence 1.7 does not reheat, but also repressurizes by 3000 seconds as predicted in LANL transient 2. The charging pumps are turned off in sequences 1.1, 1.2, 1.5, and 1.6, and sequences 1.5 and 1.6 do not reheat or repressurize. Sequence 1.2 reheats slowly and repressurizes to 2000 psia at 72000 seconds. Greater reheating in sequence 1.1 promotes repressurization to the PORV set point, 2400 psia, by 6000 seconds.

Figure 4.37 shows the heat-transfer coefficient profiles for sequences 1.1 - 1.6. The minimum assumed value, 400 Btu/hr-ft^2-°F, persists throughout the period following RCP trip. The profile for LANL transient 1 (sequence 1.4) is shown for comparison purposes.

4.6.2.2. Small Main Steam-line Break at HZP

The sequences related to a small main steam-line break at HZP are described in Table 3.8 in Chapter 3. The eight sequences in the table reflect combinations of MSIV failure, AFW isolation failure, and failure of the operators to turn off charging pump flow and to throttle AFW. Figures 4.38 - 4.40 present the temperature, pressure, and heat-transfer coefficient profiles for representative sequences 2.1, 2.4, 2.5, 2.7, and 2.8. Due to similarity of conditions, sequence 2.2 was grouped with 2.1, sequence 2.3 was grouped with sequence 2.4, and sequence 2.6 was grouped with sequence 2.7 for the purposes of this summary. Detailed discussion and individual

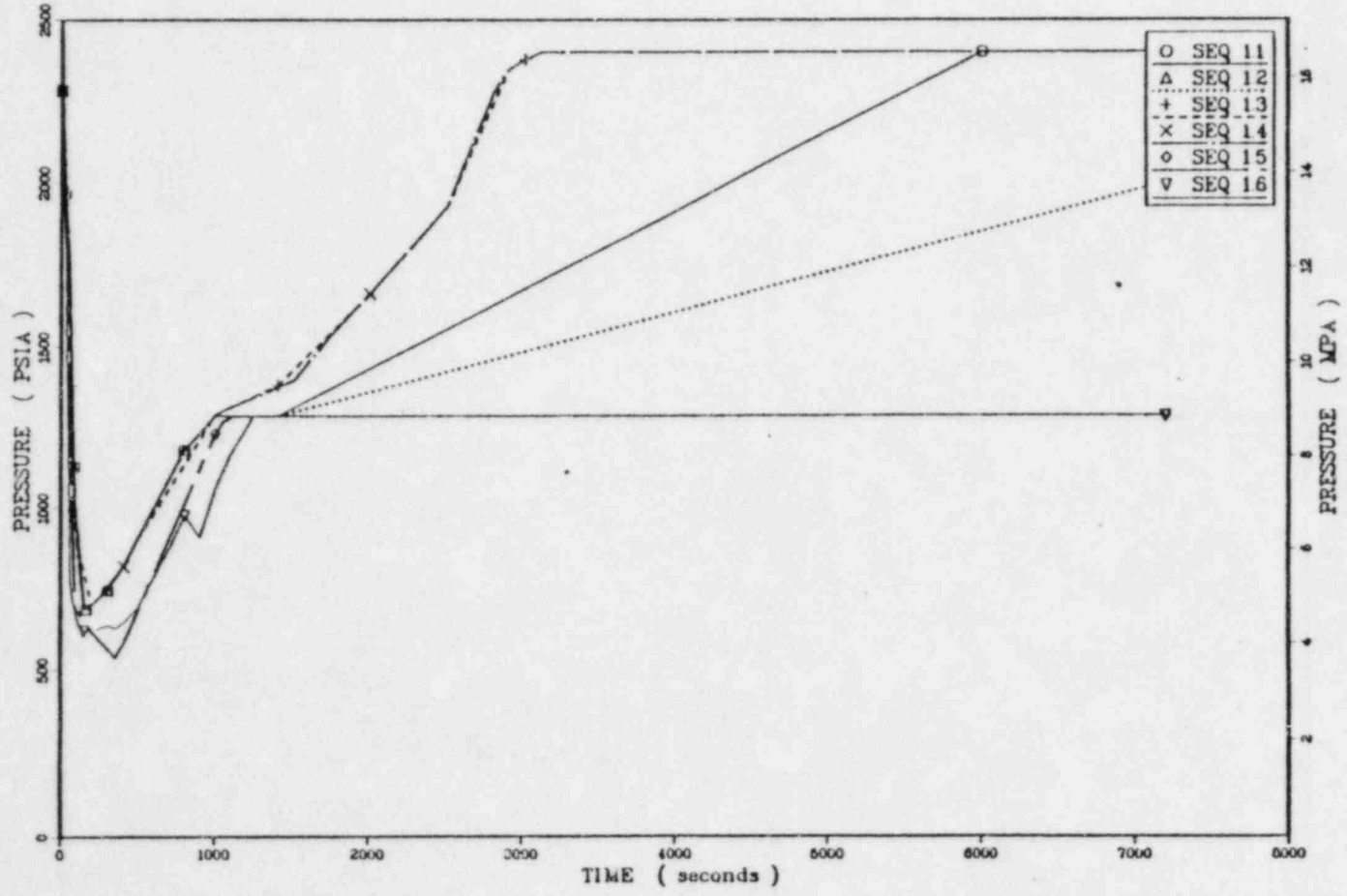

Figure 4.36. Extrapolated downcomer pressures for large main steam-line break at HZP.

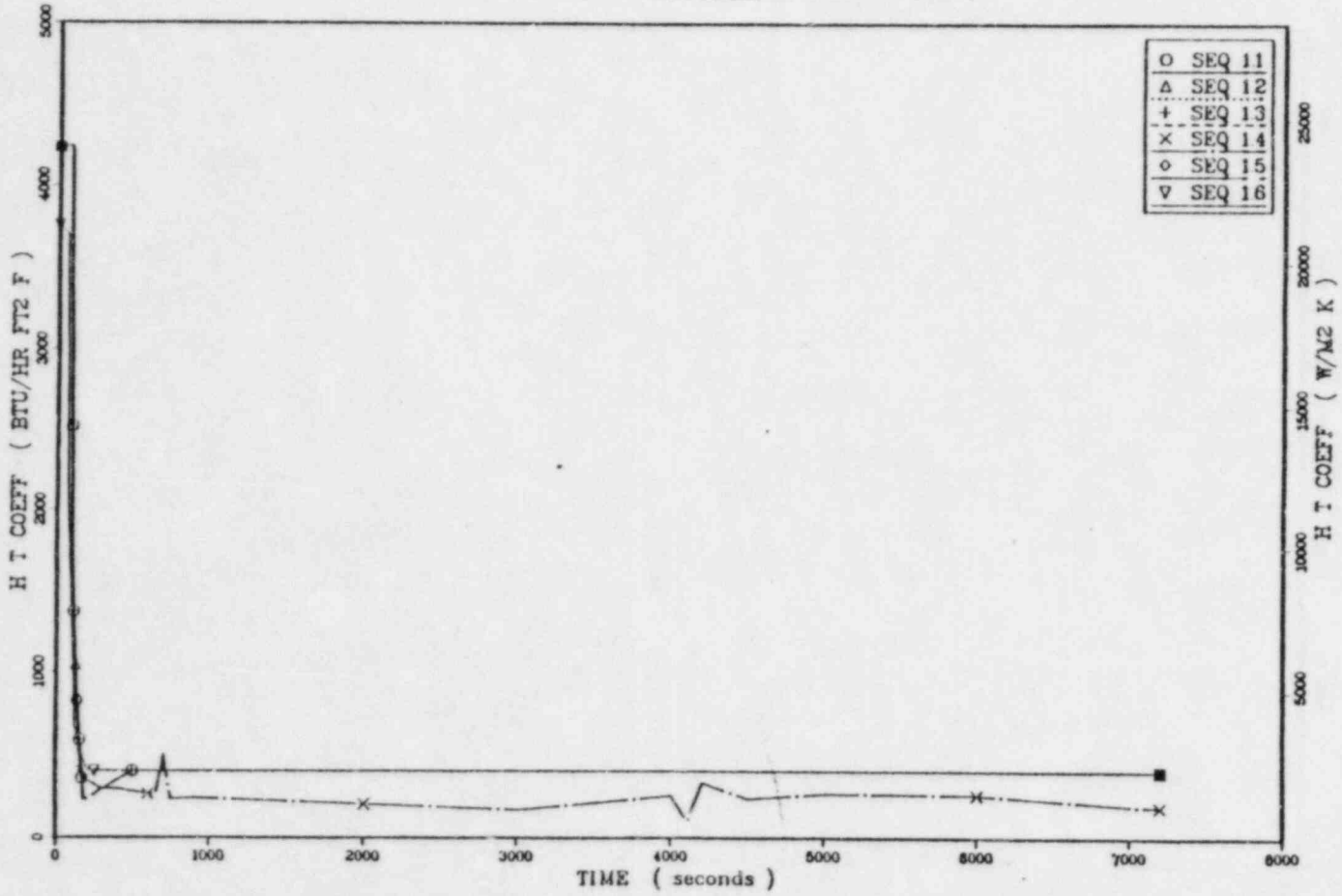

Figure 4.37. Extrapolated downcomer heat-transfer coefficients for large main steam-line break at HZP.

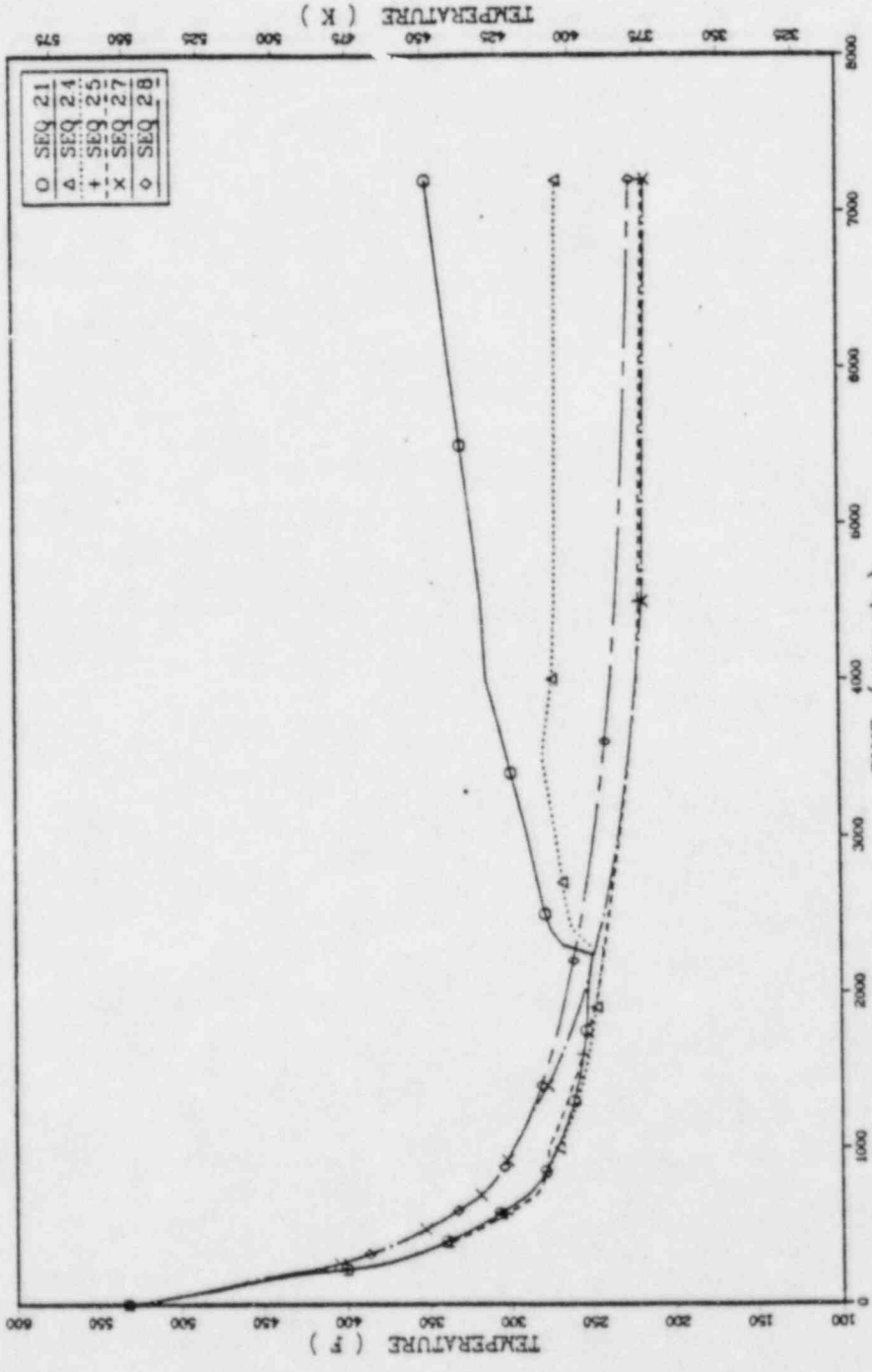

Figure 4.38. Extrapolated downcomer temperatures for small main steam-line break at HZP.

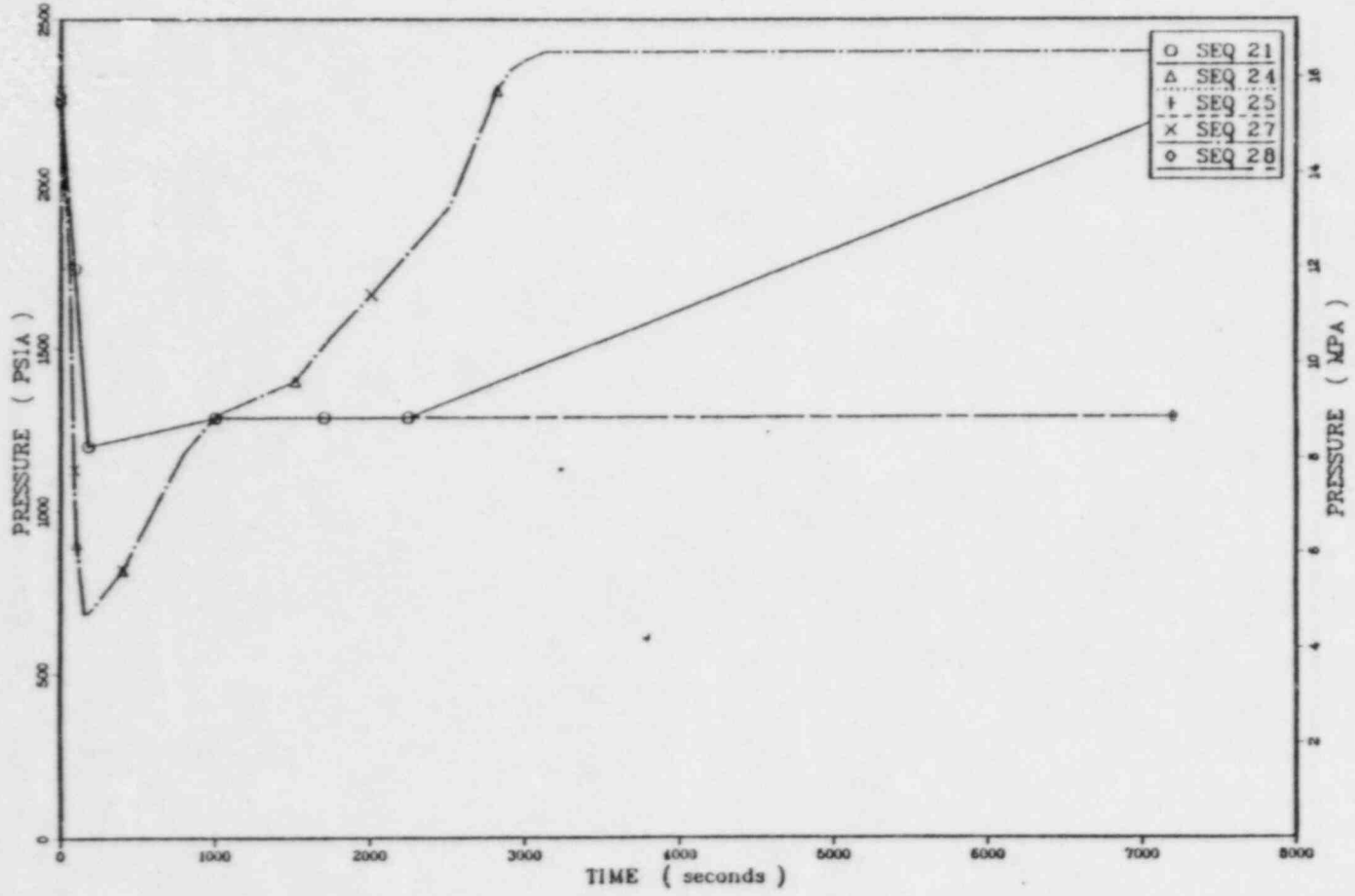

Figure 4.39. Extrapolated downcomer pressures for small main steam-line break at HZP.

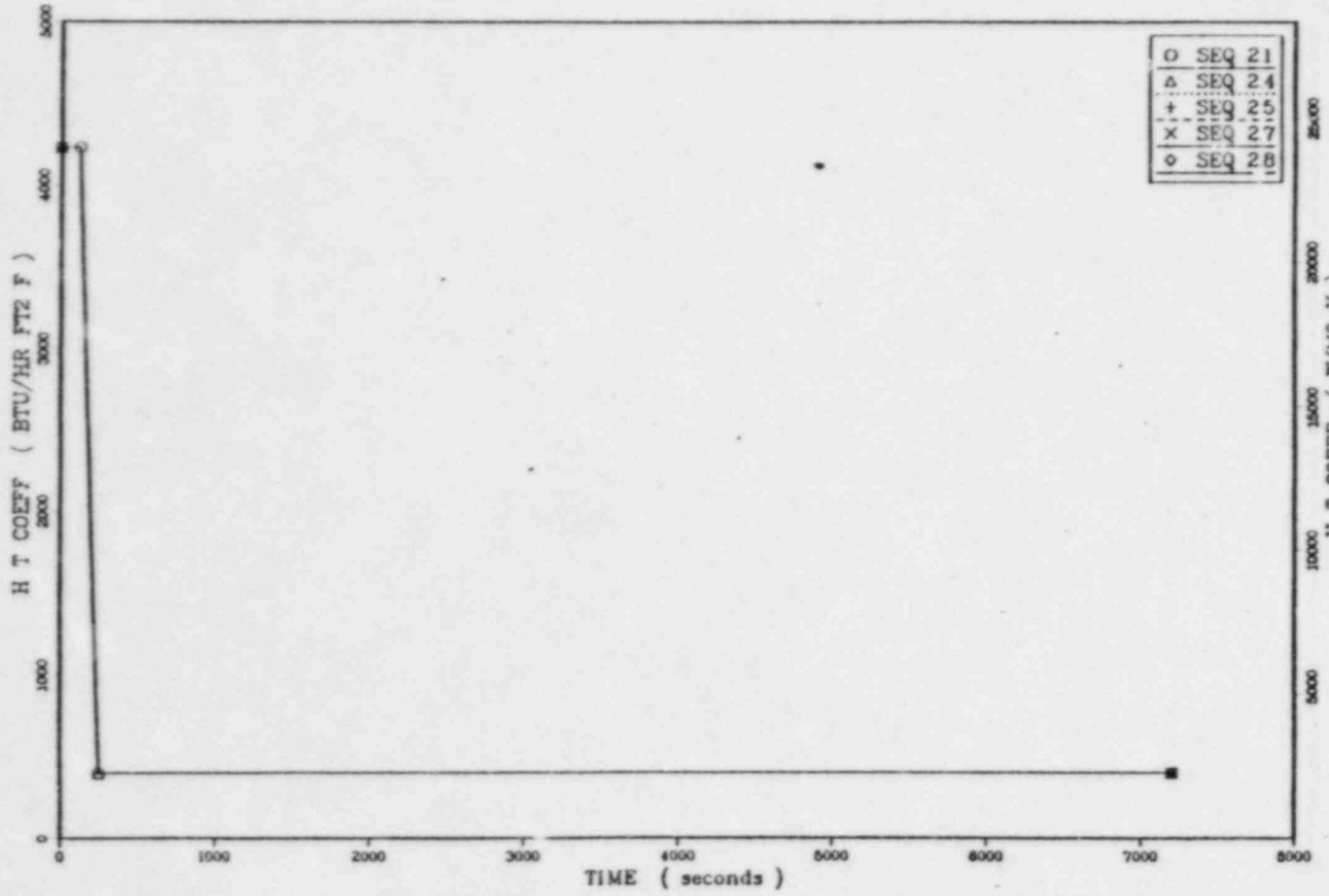

Figure 4.40. Extrapolated downcomer heat-transfer coefficients for small main steam-line break at HZP.

plots of pressure and temperature profiles are provided in Appendix J, Section J.4.

The temperature profiles show two principal regimes: (1) single SG blowdown and dryout with subsequent reheating and (2) extended blowdown from both steam generators without reheating. Sequences 2.1 and 2.4 feature single SG blowdown to dryout with resulting minimum temperatures of 250°F (394 K) and 242°F (390 K), respectively. The failure of the operators to turn off the charging pumps and throttle AFW in sequence 2.4 causes the temperature to remain cooler than in sequence 2.1, where these operator actions are carried out. The effect of these operator action failures is 80°F (44.4°C) at the end of the sequence (7200 seconds), as illustrated by the two upper curves in Figure 4.38. Sequences 2.5, 2.7, and 2.8 do not exhibit reheating because MSIV failures or feed isolation failures augmented the amount of water available for blowdown such that SG dryout does not occur. Sequence 2.8 is 10°F (5.5°C) warmer than sequences 2.5 and 2.7 due to operator actions that terminate feedwater flow to the affected steam generator and terminate charging pump flow.

The pressure profiles for these sequences are shown in Figure 4.39. Sequence 2.1 is assumed to display a mild depressurization which persists until SG dryout, where the ensuing reheat of the system causes repressurization to 2210 psia (15.2 MPa) by 7200 seconds. In sequences 2.4 and 2.7 the charging pumps are not turned off, so early repressurization such as that in LANL transient 1 was projected to occur. Sequences 2.5 and 2.8 have neither charging pump flow nor reheating and thus the pressure is assumed to stay at the HPI flow-limiting pressure.

Figure 4.40 shows that all of the sequences were assigned the same heat-transfer coefficient profile. The initial value of 4230 Btu/hr•ft^2•°F (2400 W/m^2•K) holds until the RCPs are tripped at 120 seconds. By 250 seconds the assumed minimum value of 400 Btu/hr•ft^2•°F (2270 W/m^2•K) is obtained and held for the rest of the sequence.

4.6.2.3. Large Main Steam-line Break at Full Power

The sequences related to a large break at full power are described in Table 3.10 in Chapter 3. The nine sequences include combinations of failures of MSIVs and/or ADVs to close, failure of feedwater isolation, and failures of the operators to control repressurization or throttle AFW. Figures 4.41, 4.42, and 4.43 present the temperature, pressure, and heat-transfer coefficient profiles for sequences 3.4 - 3.8. Sequences 3.1 - 3.3 are grouped with sequence 3.4, which is itself identical to LANL transient 2. Sequence 3.9 is grouped with 3.8 for similarity reasons. Detailed discussion of the individual sequences is provided in Appendix J, Section J.5.

The temperature profiles in Figure 4.41 show a wide range of sequence outcome based on whether or not blowdown is stopped. The higher decay heat levels associated with full-power operation render the operator actions to throttle AFW to the intact SG or to turn off the charging pumps of minor importance to the temperature trends in the sequences. This is significantly different from the HZP cases when the same operator actions greatly impact the trends. In sequence 3.4 (LANL transient 2), SG dryout occurs at about 400 seconds (minimum temperature of 358°F) and then the primary system reheats under the influence of core decay heat. In sequence 3.5, AFW

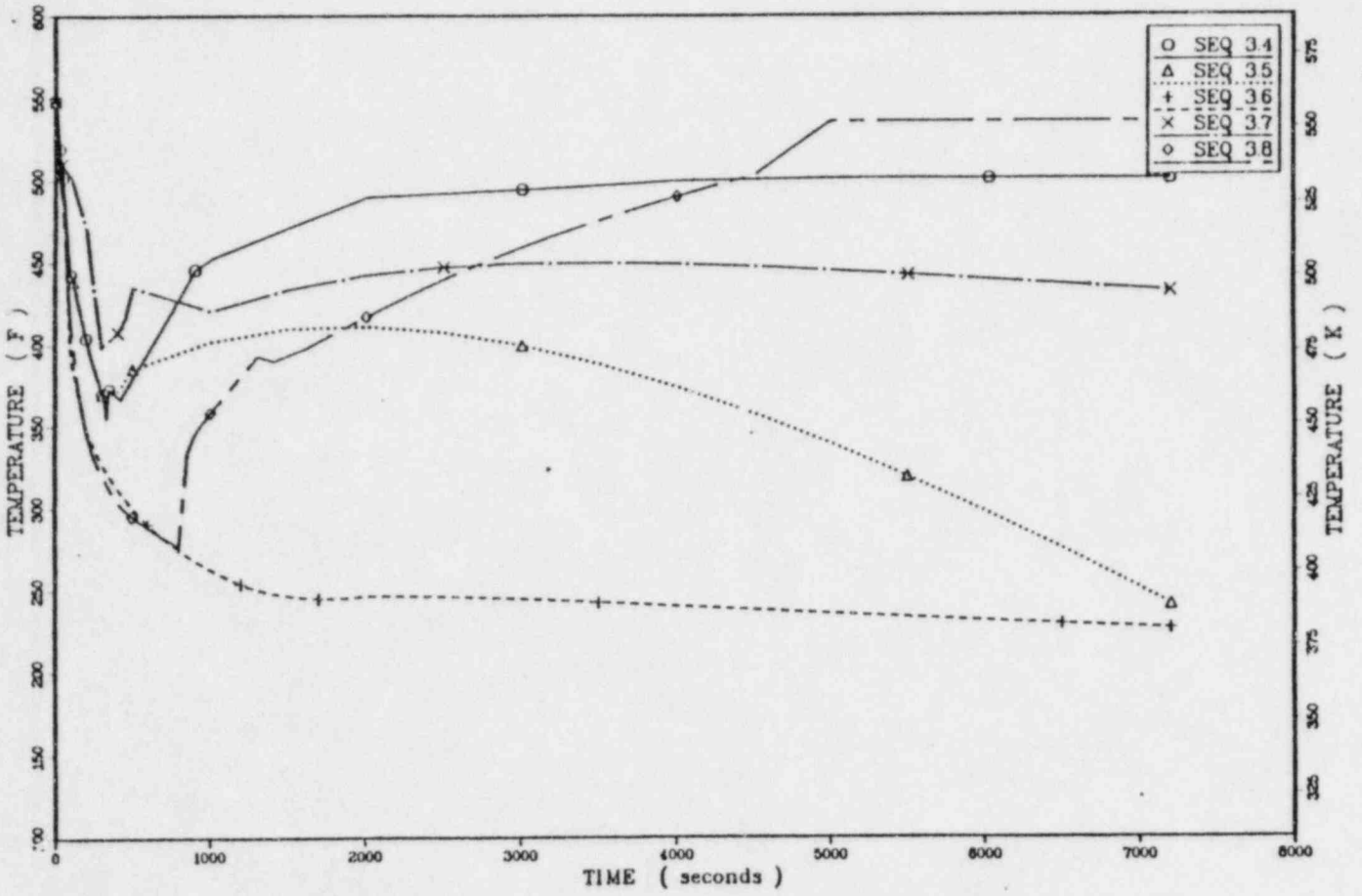

Figure 4.41. Extrapolated downcomer temperatures for large main steam-line break at full power.

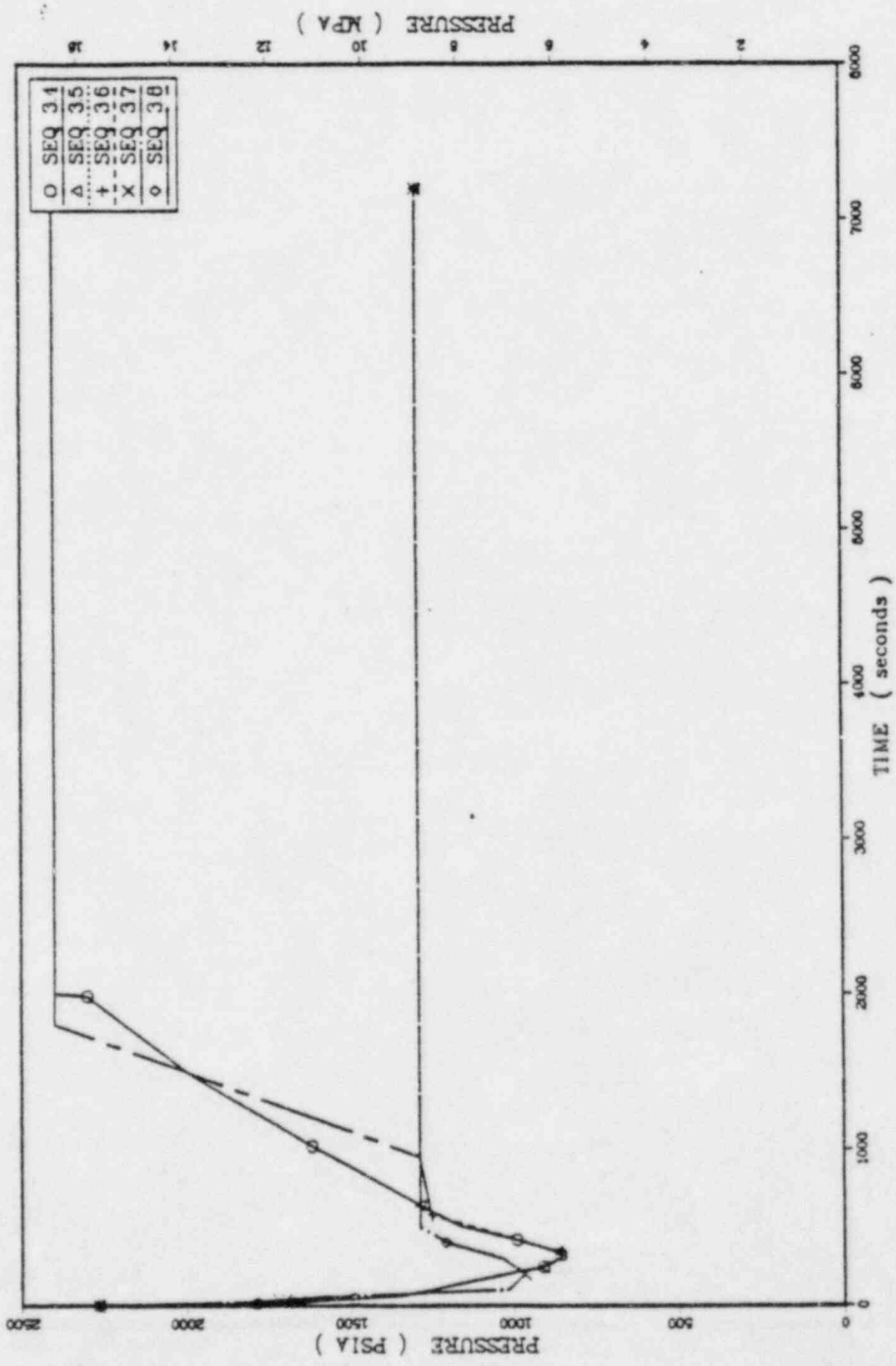

Figure 4.42. Extrapolated downcomer pressures for large main steam-line break at full power.

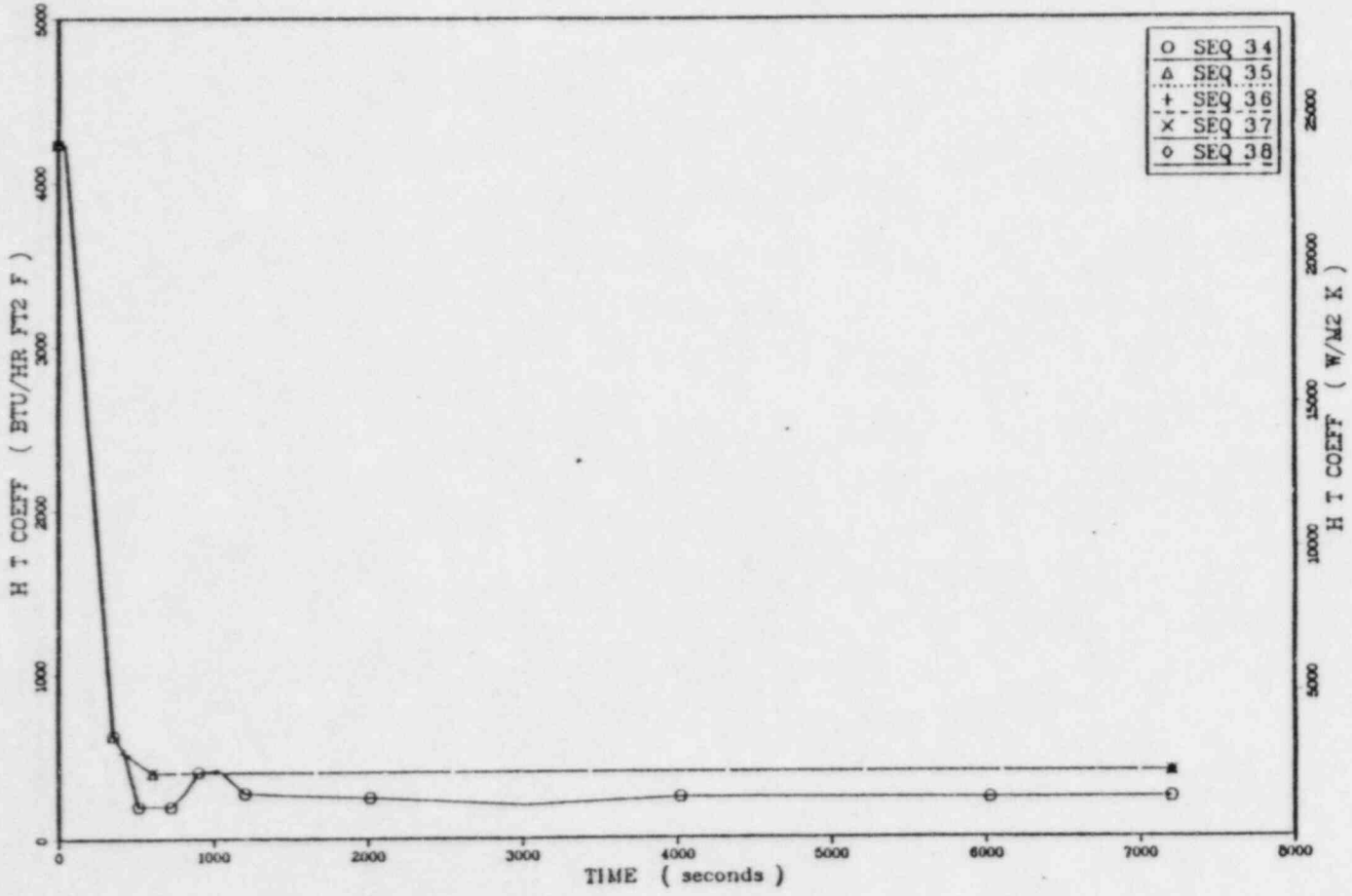

Figure 4.43. Extrapolated downcomer heat-transfer coefficients for large main steam-line break at full power.

isolation failure to the affected steam generator provides 320 gal/min of flow with which to continue blowdown and cooling. However, the cooling provided by this flow did not exceed the decay heat input until 2000 seconds into the sequence. The temperature rises slightly before declining to the minimum of 240°F (388 K) at 7200 seconds. In sequence 3.8, a main feedwater overfeed to the broken steam generator loop prolongs steam generator dryout to about 800 seconds with a minimum downcomer temperature of 276°F (408 K). Decay heat and natural-circulation flow effects cause a rapid recovery in downcomer temperature.

The pressure response as shown for sequence 3.4 (LANL transient 2) in Figure 4.42 predicts full repressurization by 2000 seconds. Sequences 3.5 - 3.7 experience no repressurization beyond recovery to the HPI shut-off head pressure. Sequence 3.8 experiences rapid repressurization on the basis of system reheating.

Figure 4.43 shows the assumed heat-transfer coefficient profile for the sequences. The profile for LANL transient 2 is presented for comparison purposes as sequence 3.4.

4.6.2.4. Small Main Steam-line Break at Full Power

The sequences related to a small main steam-line break at full power are described in Table 3.11 in Chapter 3. The 12 sequences include all of the failure combinations examined in the large-break case: MSIV failure, MFW runback failure, ADV failure, AFW isolation failure and operator failures to control repressurization and to throttle AFW. Figures 4.44 - 4.46

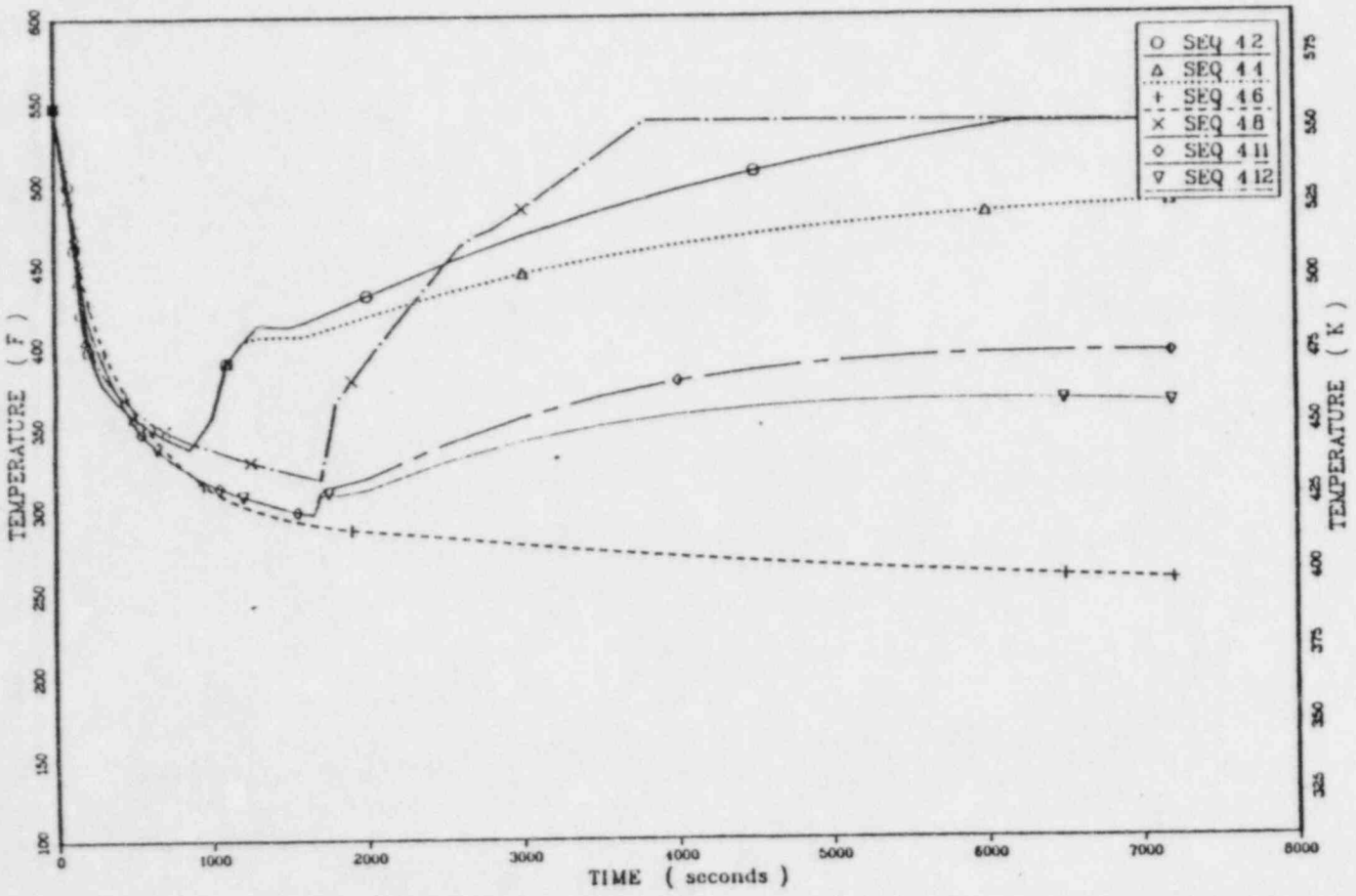

Figure 4.44. Extrapolated downcomer temperatures for small main steam-line break at full power.

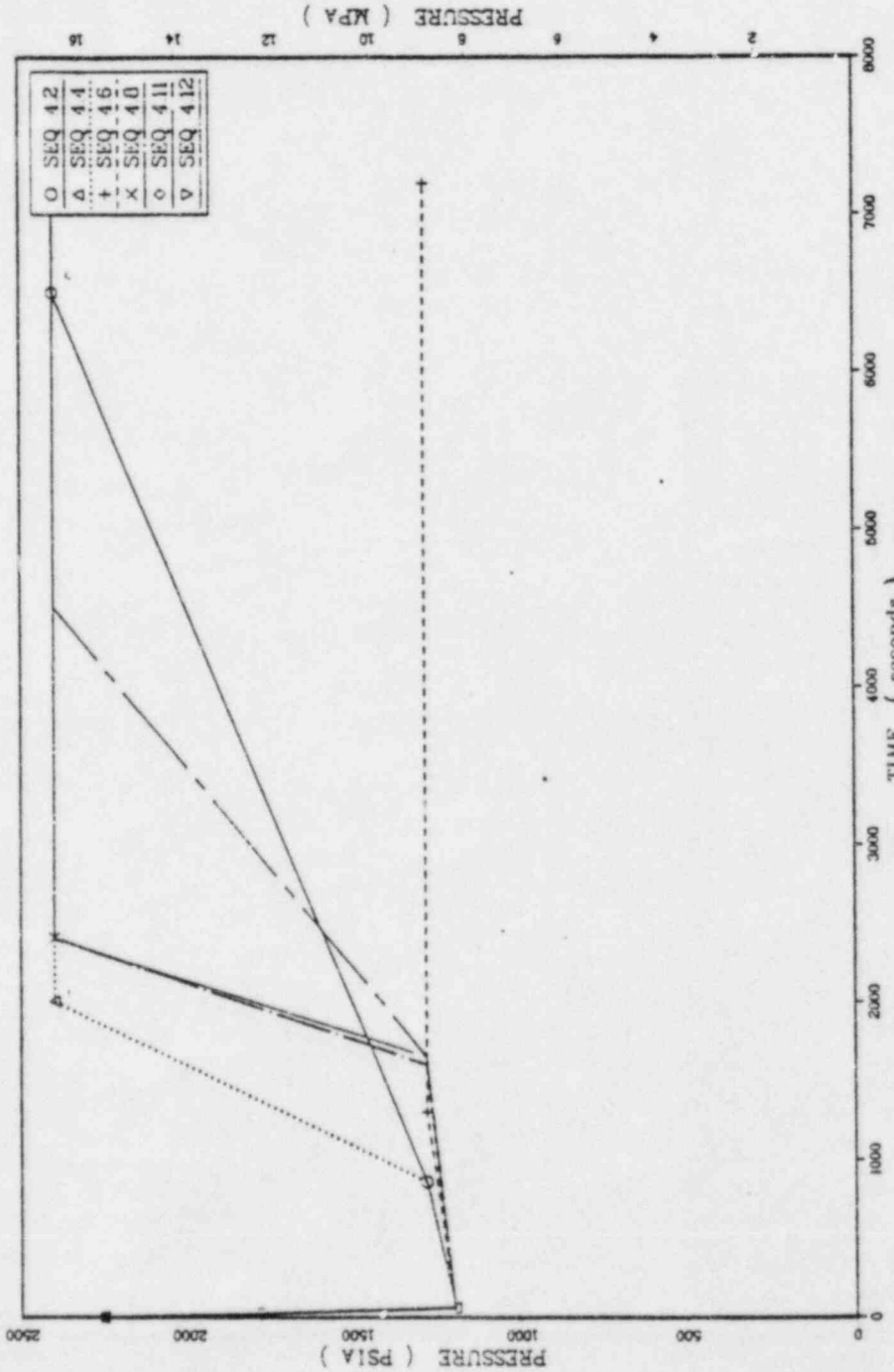

Figure 4.45. Extrapolated downcomer pressures for small main steam-line break at full power.

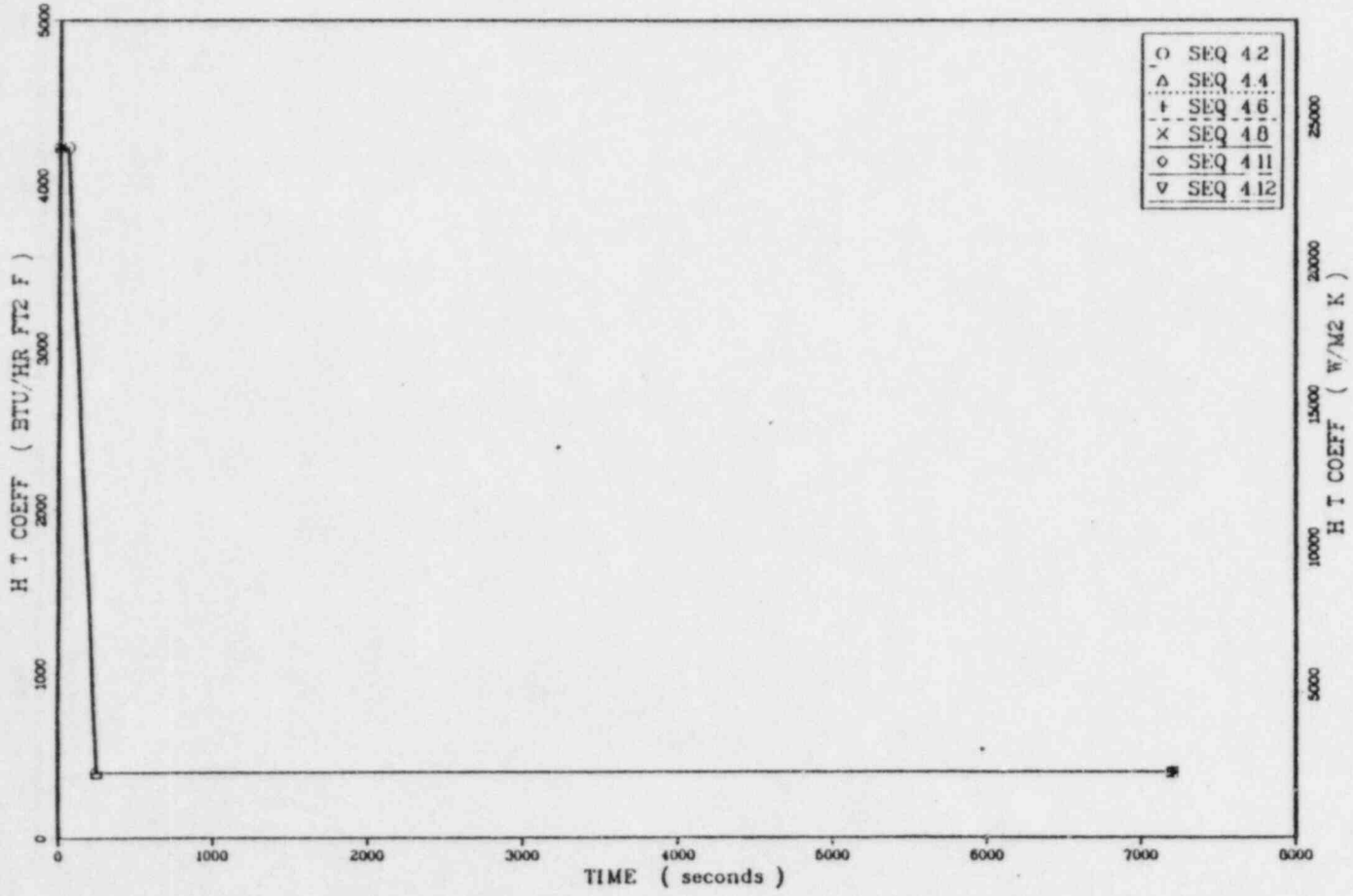

Figure 4.46. Extrapolated downcomer heat-transfer coefficients for small main steam-line break at full power.

contain the temperature, pressure, and heat-transfer coefficient profiles for sequences 4.2, 4.4, 4.6, 4.8, 4.11, and 4.12. For the purposes of this section, sequence 4.1 is grouped with 4.2; 4.3 with 4.4; 4.5 with 4.6; and 4.7, 4.9, and 4.10 with 4.8. Detailed discussion of these sequences is available in Appendix J, Section J.6.

The temperature profiles in Figure 4.44 show a wide range of sequence outcome based mainly on whether or not extended blowdown occurs. The smaller break tends to draw out the period required for SG dryout. This translates into higher minimum temperatures than were obtained for the large-break cases. Also, the delay of reheating to after 2000 seconds reduces the dominance of decay heat and makes the effects of operator actions more noticeable. For example, in sequence 4.2 the operator is to turn off the charging pumps, whereas in sequence 4.4 the operator takes no action. Both sequences behave the same through the affected SG dryout [minimum temperature of 337°F (442 K) at 860 seconds] and begin to diverge thereafter. Sequence 4.8 suffers a MFW overfeed to the affected SG, which extends dryout to 1700 seconds. This case also reheats quickly. Sequences 4.11 and 4.12 feature a stuck-open ADV on line B opposite the break. The additional blowdown extends the time of SG A dryout to 1650 seconds at a minimum temperature of 296°F (397 K).

Figure 4.45 shows that all sequence pressure profiles except that for sequence 4.6 return to the PORV set-point pressure, 2400 psia (16.6 MPa). Sequence 4.4 reaches this pressure first based on mildest cooldown and continued charging pump flow. Next comes sequence 4.8 based on rapid reheating. Finally, sequences 4.11 and 4.2 follow based on their slower reheating rates.

Figure 4.46 shows the heat-transfer coefficient for all sequences. The initial value of 4230 Btu/hr•ft^2•°F (24000 W/m^2•K) holds until the RCP trip. The final value of 400 Btu/hr•ft^2•°F is obtained 55 seconds following the trip.

4.6.2.5. Reactor Trip Sequences

The sequences related to reactor trip from full power are described in Table 3.13 in Chapter 3. These 43 sequences involve various combinations of failures, including failure of the turbine to trip; failures of the ADVs, TBVs, and MSIVs to close; failure of the MFW to run back; failure of the AFW isolation; and failure of the operators to turn off charging pump flow and throttle AFW. The P, T, and h profiles for some selected sequences are presented in Figures 4.47 - 4.52. Table 3.13 summarizes the groupings of sequences for this initiator. Detailed discussions of individual sequences may be found in Appendix J, Section J.7.

Figures 4.47 and 4.48 give the temperature profiles for sequences with failures of one TBV (sequences 5.18, 5.21A,* 5.21B,* and 5.25B*), two TBVs (sequences 5.22, 5.26A,* and 5.26B*), three TBVs (sequences 27A* and 27B*),* one ADV (sequence 5.35), and two ADVs (sequence 5.36) to close.

* For turbine bypass valve failures, there is a potential for manually closing the valve at the valve location. The "A" member of each set represents failures to isolate the valves such that continued cooldown occurs to final temperatures of 348°F (448 K) for sequence 5.25A and 259°F (399 K) for sequence 5.27A. The "B" members of each set represent manual isolation of the stuck valves, yielding minimum temperatures of 433°F (459 K) for sequence 5.25B, 399°F (476 K) for sequence 5.26B, and 339°F (443 K) for sequence 5.27B. The time required for isolation purposes was determined based on conversations with Calvert Cliffs-1 operational staff. A 15-minute period was assumed to be required to isolate one valve, a 20-minute period to isolate two valves, etc. It should be noted that for the actual analysis of risk only the "A" cases were considered. The effects of isolation ("B" cases) were, however, determined for the purpose of consideration in the event that one of the "A" cases was identified as a dominant risk sequence.

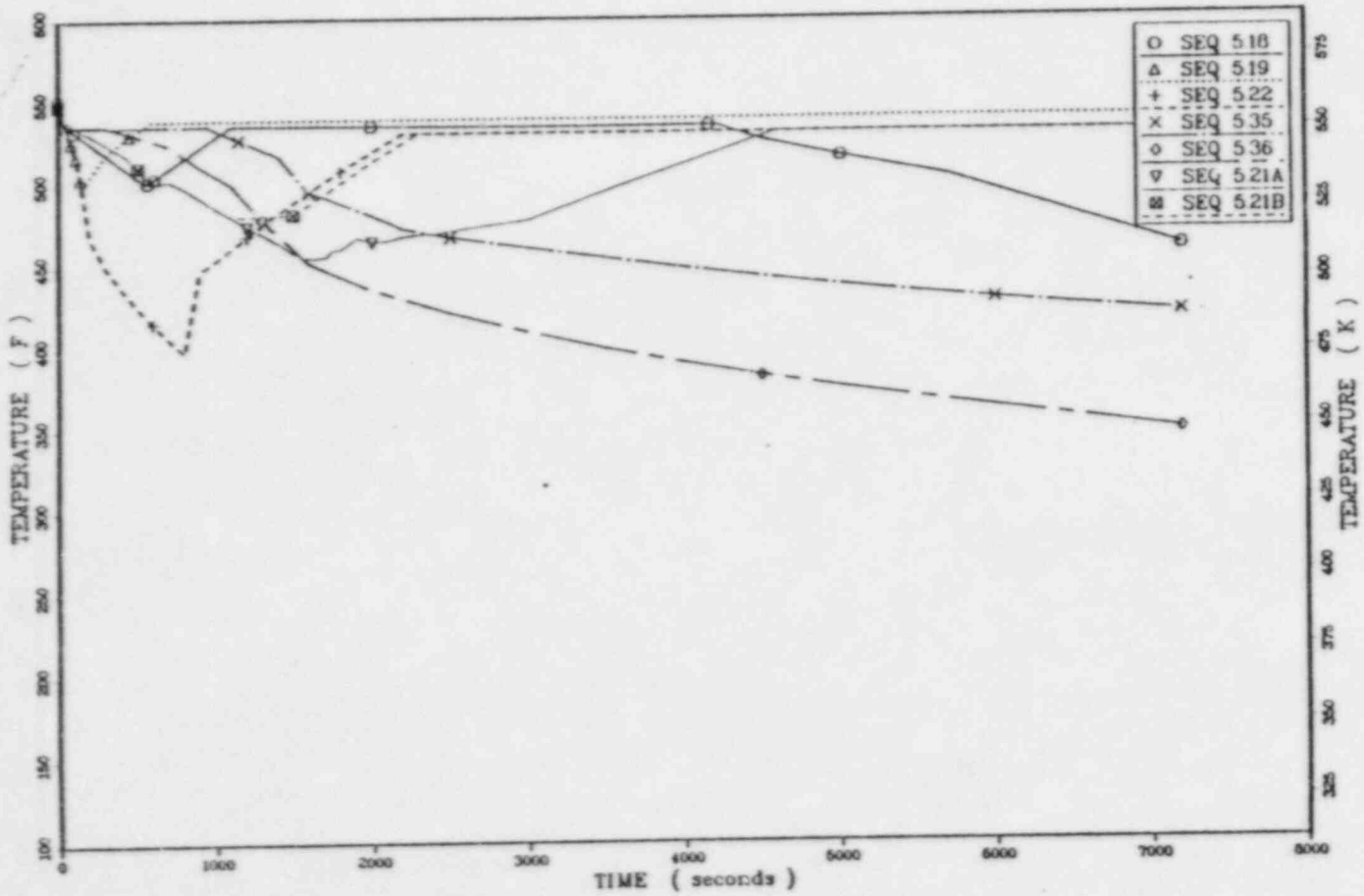

Figure 4.47. Extrapolated downcomer temperatures for reactor trip (Sequences 5.18, 5.19, 5.22, 5.35, 5.36, 5.21 A and B).

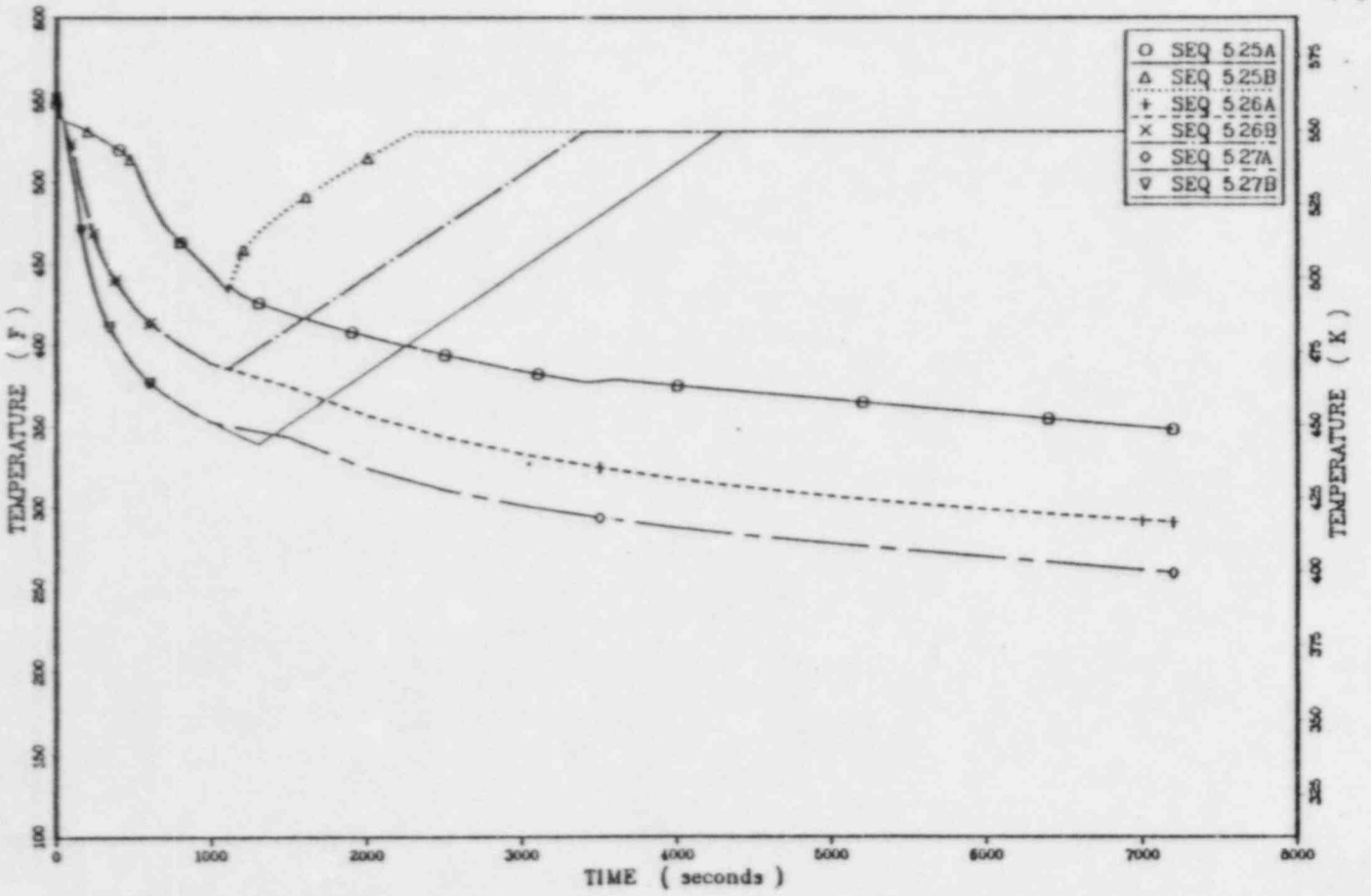

Figure 4.48. Extrapolated downcomer temperatures for reactor trip (Sequences 5.25 A and B, 5.26 A and B, 5.27 A and B).

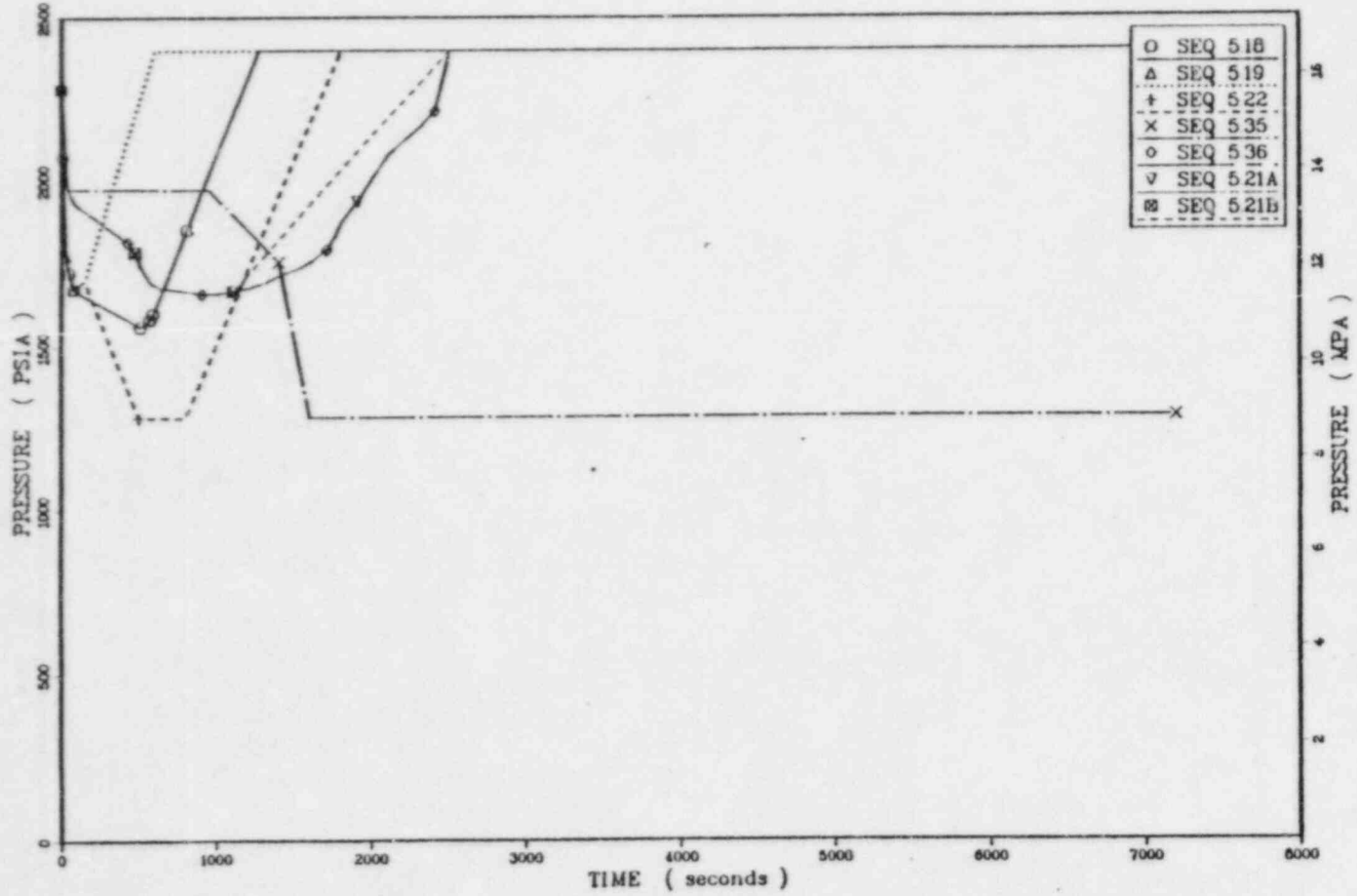

Figure 4.49. Extrapolated downcomer pressures for reactor trip (Sequences 5.18, 5.19, 5.22, 5.35, 5.36, 5.21 A and B).

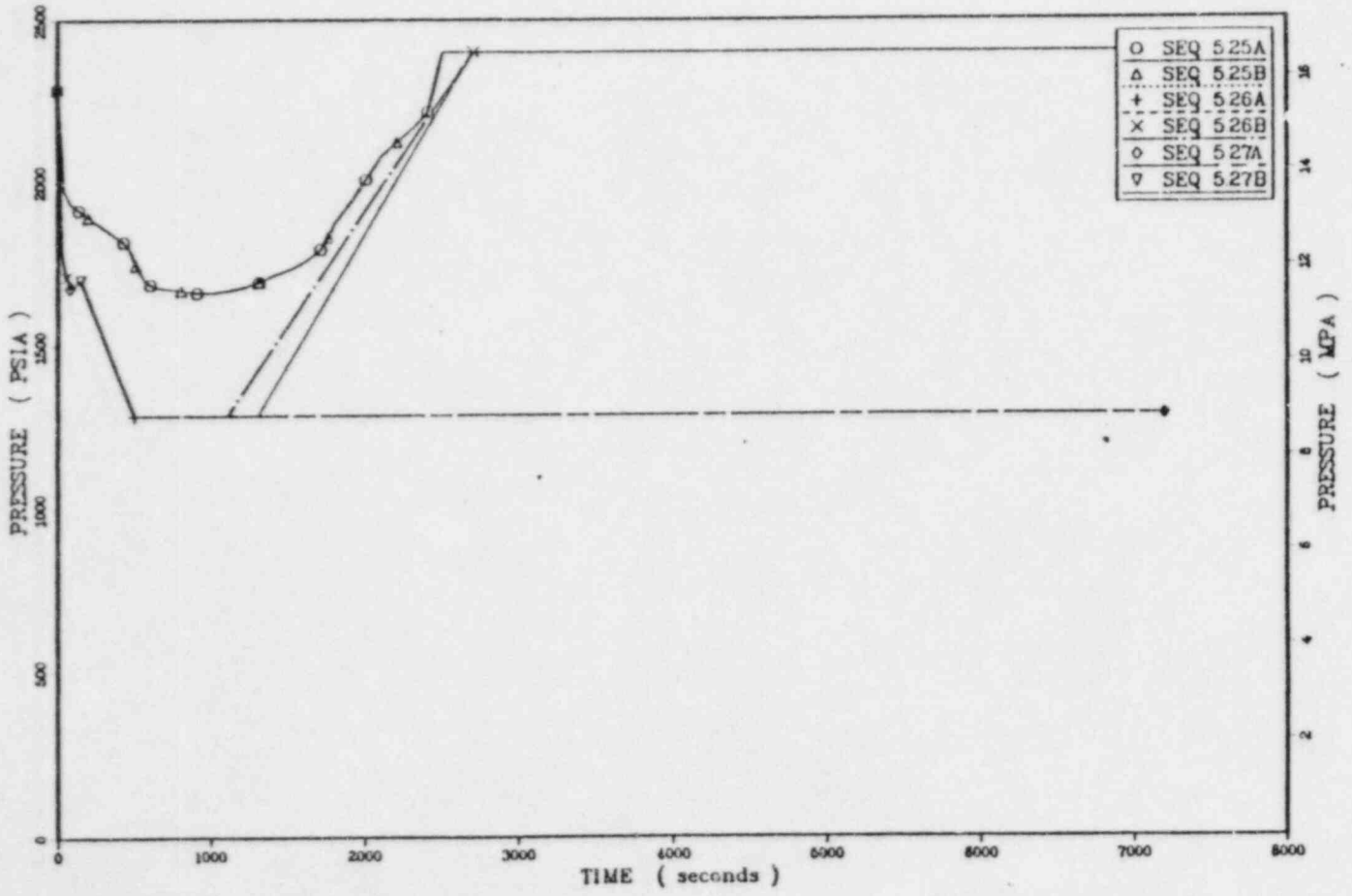

Figure 4.50. Extrapolated downcomer pressures for reactor trip (Sequences 5.25 A and B, 5.26 A and B, 5.27 A and B).

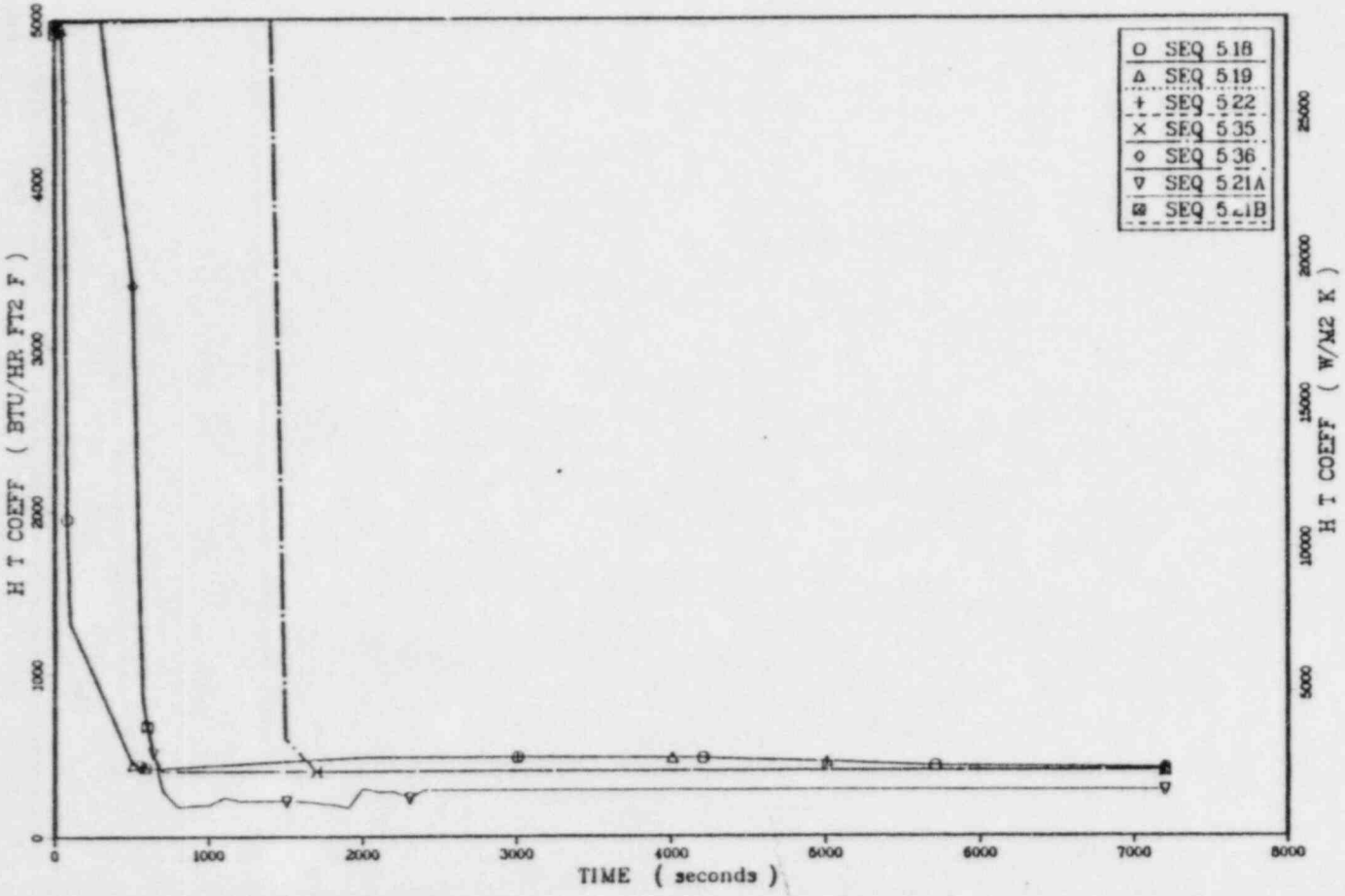

Figure 4.51. Extrapolated downcomer heat-transfer coefficients for reactor trip (Sequences 5.18, 5.19, 5.22, 5.35, 5.36, 5.21 A and B).

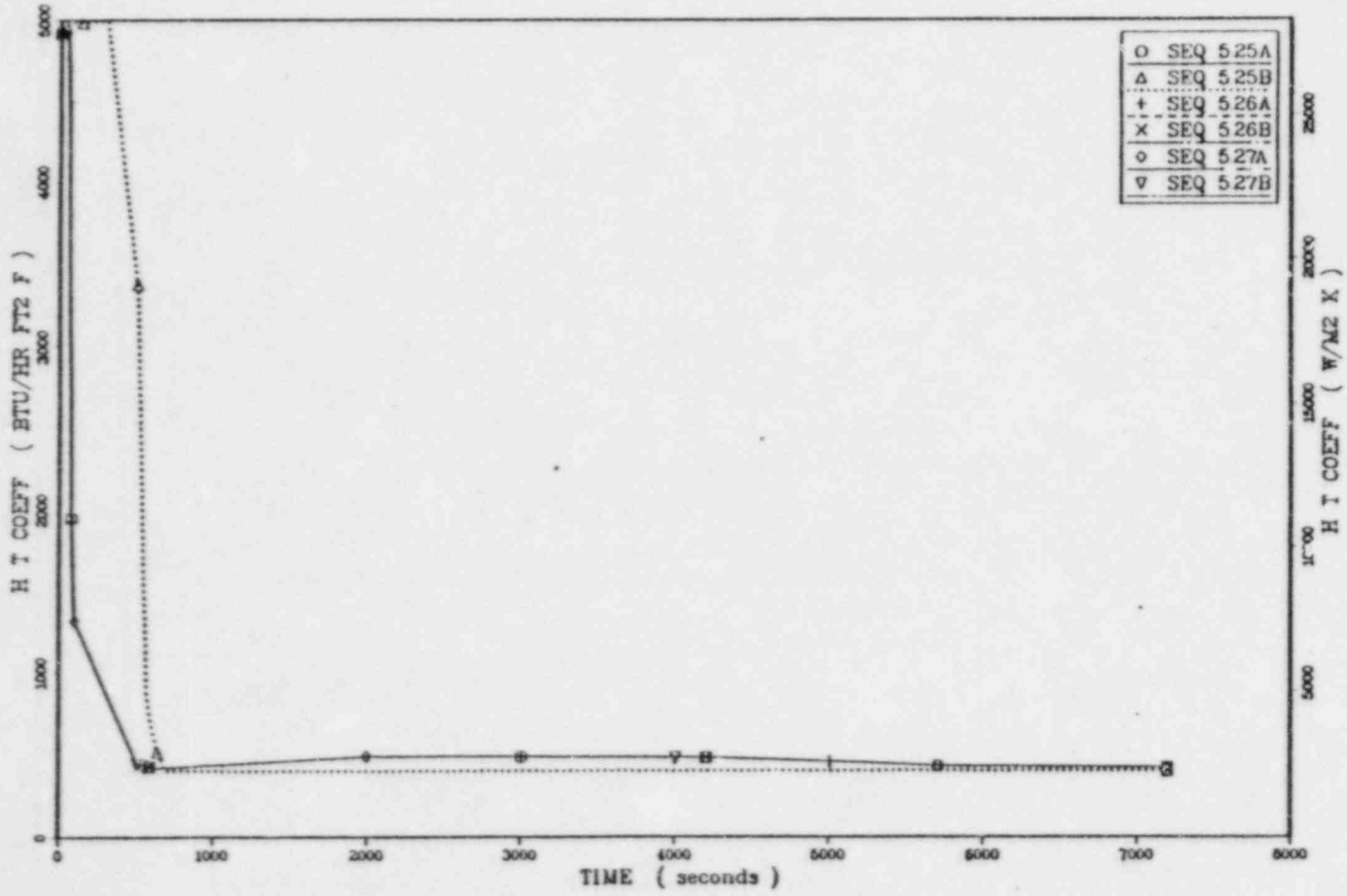

Figure 4.52. Extrapolated downcomer heat-transfer coefficients for reactor trip (Sequences 5.25 A and B, 5.26 A and B, 5.27 A and B).

Parametric cases of zero, one, or two MSIV failures are represented in the above list. The MSIVs have profound influence on the course of TBV failure events. Where the MSIVs are successful, the downcomer temperature does not drop below 500°F (533 K) unless assisted by other cooldown mechanisms as shown in Figure 4.47 for sequences 5.18 and 5.19. One MSIV failure leads to minimum temperatures of 400°F as in sequence 5.22 (two TBVs open) to <50°F as in sequence 5.21A (one TBV open, LANL transient 7). Figure 4.48 shows the response for one TBV (sequences 5.25A and B) failure coupled to the failure of both MSIVs to close.

The pressure profiles for these sequences are presented in Figures 4.49 and 4.50. The combination of system reheating and continued charging pump flow cause full repressurization of most cases.

Figures 4.51 and 4.52 present the heat-transfer coefficient profiles for the above sequences. The main differences are in the timing of the RCP trips, which occur later for the mild ADV and single TBV cases.

4.6.2.6. Small-Break LOCA ($\leq$0.016 ft^2)

The sequences associated with the small-break LOCA ($\leq$0.016 ft^2 in size) are described in Table 3.14 in Chapter 3. The 17 sequences include isolatable and nonisolatable breaks, TBV and ADV failures, MFW runback failure and failure of operators to turn off charging pump flow after break isolation

and to throttle AFW. The temperature, pressure, and heat-transfer coefficient profiles for selected sequences are presented in Figures 4.53 - 4.55. Detailed discussion of the other sequences is provided in Appendix J, Section J.8.

The temperature profiles in Figure 4.53 show diversity in outcome due to combinations of cooldown mechanisms. The warmest sequence, 6.12, experienced early SGIS and loss of MFW flow such that HPI flow and occasional ADV activity were the only sources of cooling. A combination of MFW and HPI flow provided cooldown for sequences 6.1 and 6.3 until SGIS at around 2000 seconds. HPI cooling continues out to 1.5 hours, at which time the break is isolated in sequence 6.1. The next coolest transients are sequences 6.7 (LANL transient 12) and 6.8, in which a stuck-open ADV augments HPI cooldown to yield a final temperature of 300°F (421 K). Sequence 6.10, the coldest sequence among those identified for this initiator, included two stuck-open ADVs augmenting HPI cooldown to yield a minimum temperature of 253°F (396 K).

The pressure profiles in Figure 4.54 basically follow that of LANL transient 12. The isolatable break cases deviate from transient 12 values after break isolation at 1.5 hours. Sequence 6.2 features failure to turn off charging pump flow and so repressurizes to the PORV or safety valve set point.* The other isolation cases, sequences 6.1 and 6.8, repressurize to

* Dependent on whether PORVs are isolated.

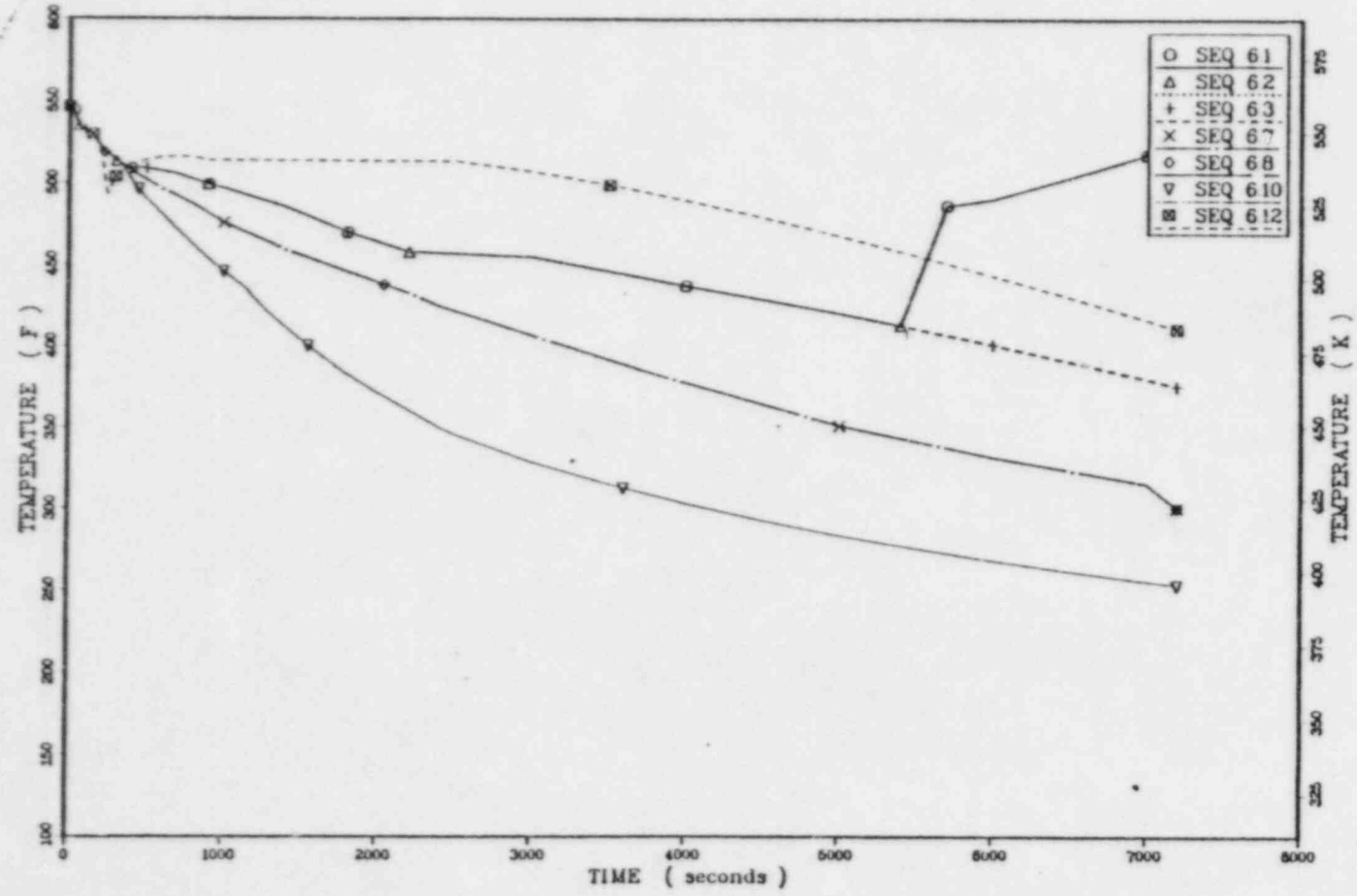

Figure 4.53. Extrapolated downcomer temperatures for small-break LOCA (≤0.016 ft²).

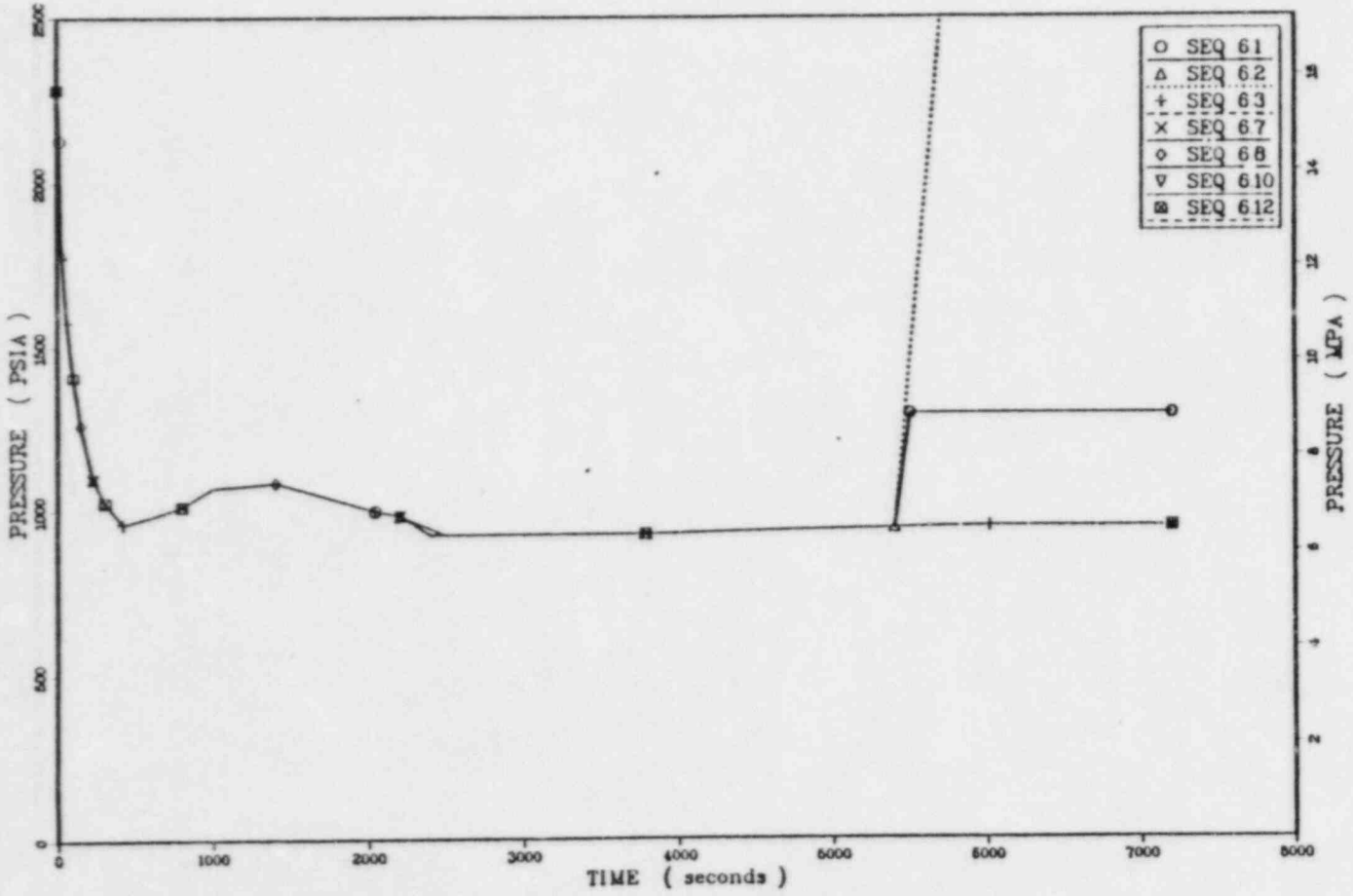

Figure 4.54. Extrapolated downcomer pressures for small-break LOCA ($\leq$0.016 ft^2).

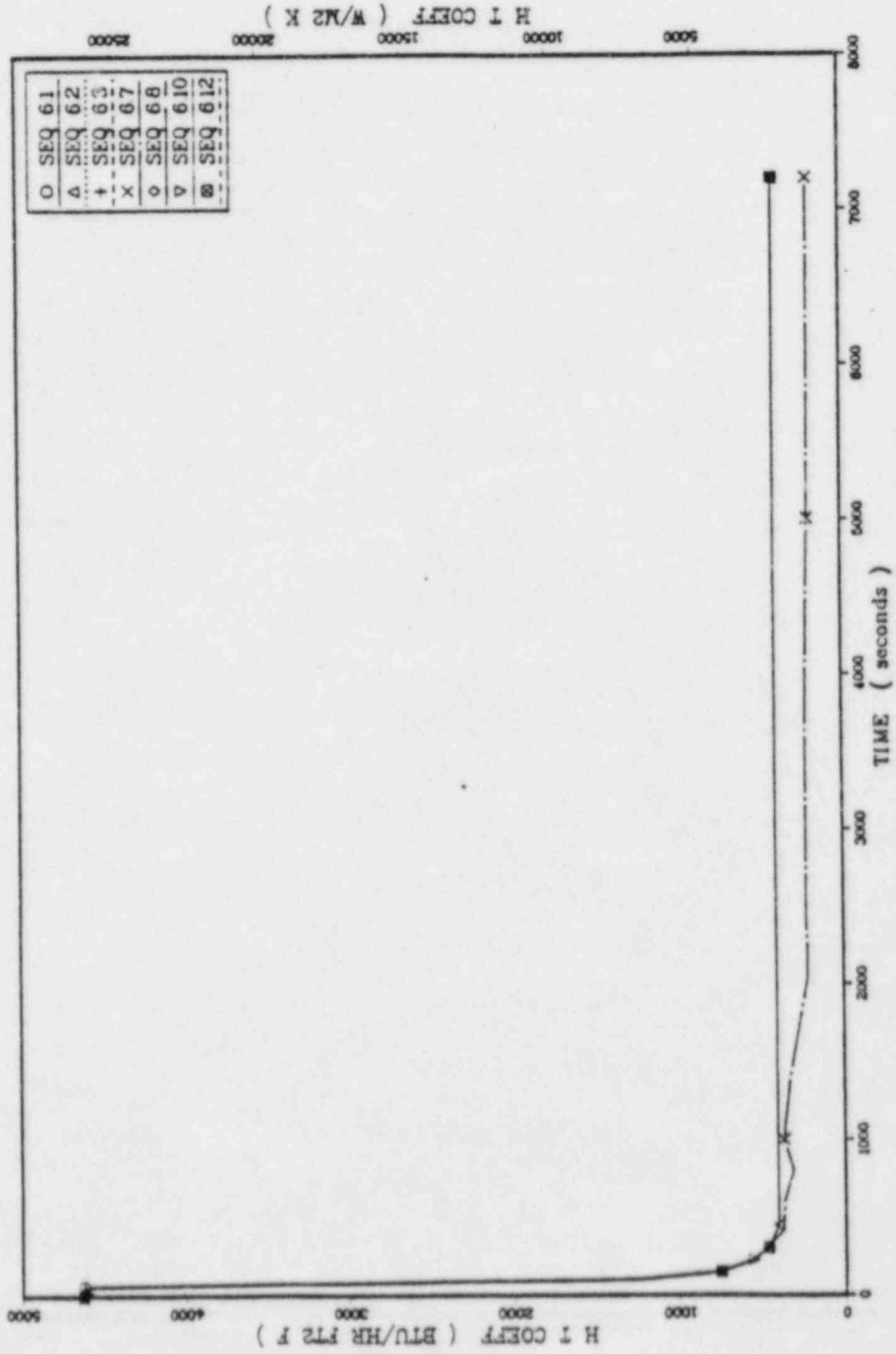

Figure 4.55. Extrapolated downcomer heat-transfer coefficients for small-break LOCA (≤0.016 ft²).

the HPI shut-off head pressure. However, if the system is water solid, i.e., if no steam voids are present, the reheating after break isolation would cause repressurization similar to sequence 6.2.

Figure 4.55 shows the heat-transfer coefficient profiles for these sequences. The behavior for transient 12 (sequence 6.7) is provided for comparison with the assumed minimum value of 400 Btu/hr-ft^2,°F (2270 W/m^2).

4.6.2.7. Small-Break LOCA (~0.02 ft^2)

The sequences dealing with a nonisolatable small primary break (0.02 ft^2) is provided in Table 3.15 in Chapter 3. The eight sequences include various combinations of TBV and ADV failures, MW runback failure, and failure of operators to throttle AFW. Figures 4.56 - 4.58 provide the temperature, pressure, and heat-transfer coefficient profiles for sequences 7.1, 7.4, and 7.6. Sequences 7.2, 7.3, 7.7, and 7.8 correspond to sequence 7.1, which is equivalent to LANL transient 11. Sequence 7.5 is similar to sequence 7.4. Detailed discussion of these sequences is provided in Appendix J, Section J.9.

The temperature profile in Figure 4.56 expresses the influence of HPI cooling alone (sequence 7.1), HPI cooling with one ADV open (sequence 7.4), and HPI cooling with both ADVs open (sequence 7.6). TBV and MFW runback failures only incur an early SGIS, which eliminates such cooldown mechanisms, leaving only the HPI cooling mechanism. Therefore, these other cases

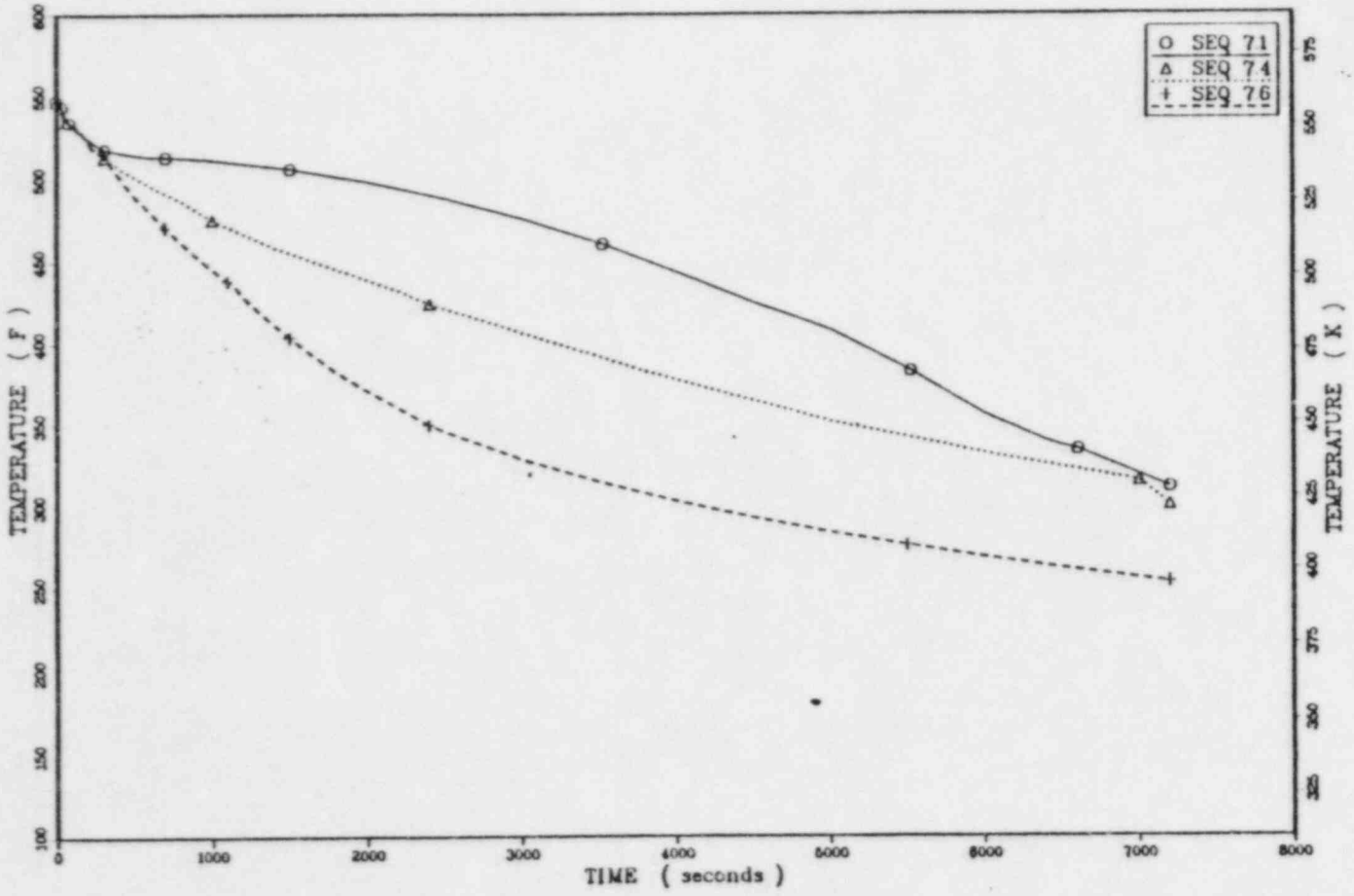

Figure 4.56. Extrapolated downcomer temperatures for small-break LOCA (≈0.02 ft^2).

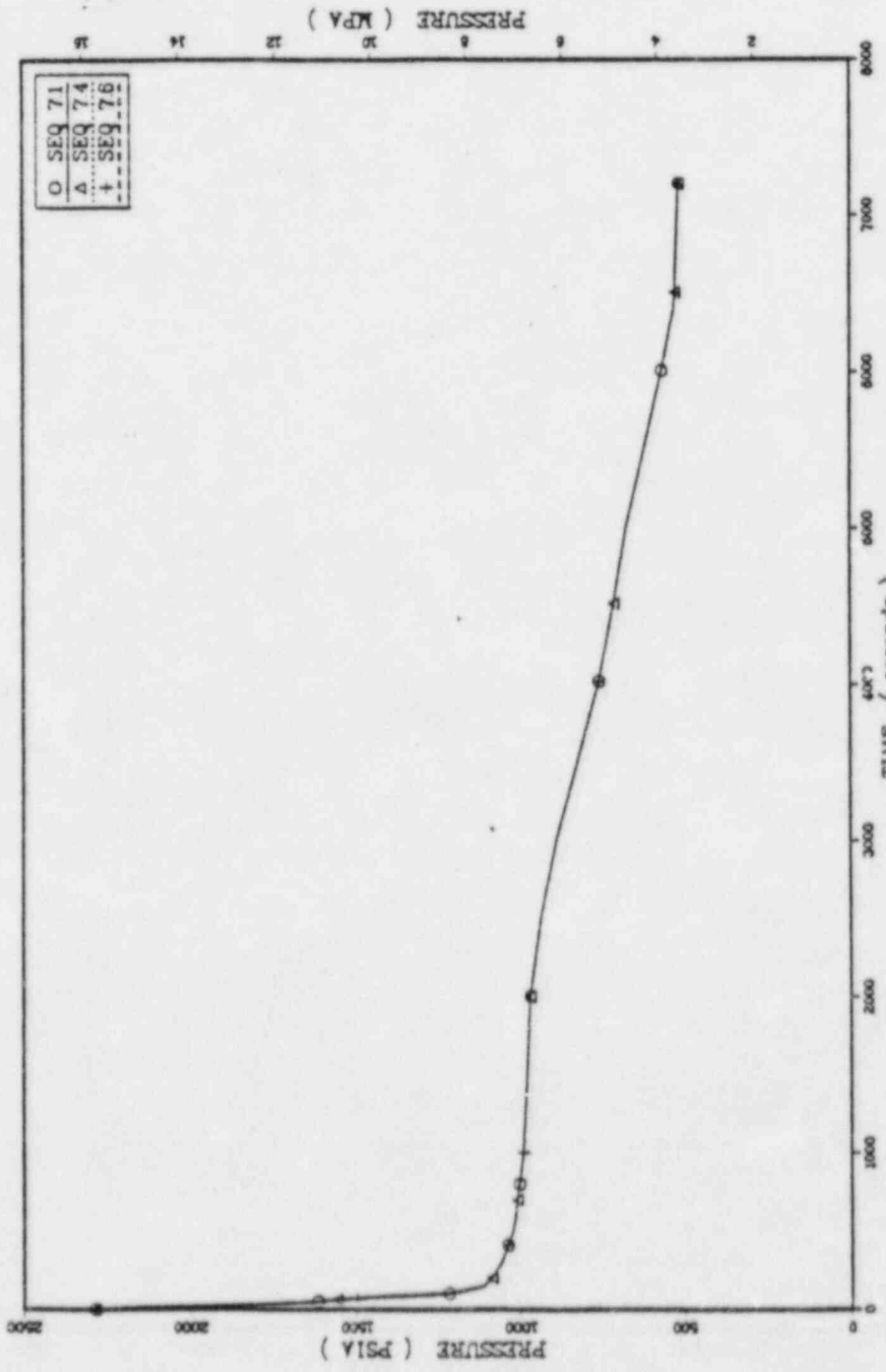

Figure 4.57. Extrapolated downcomer pressures for small-break LOCA (≈0.02 ft²).

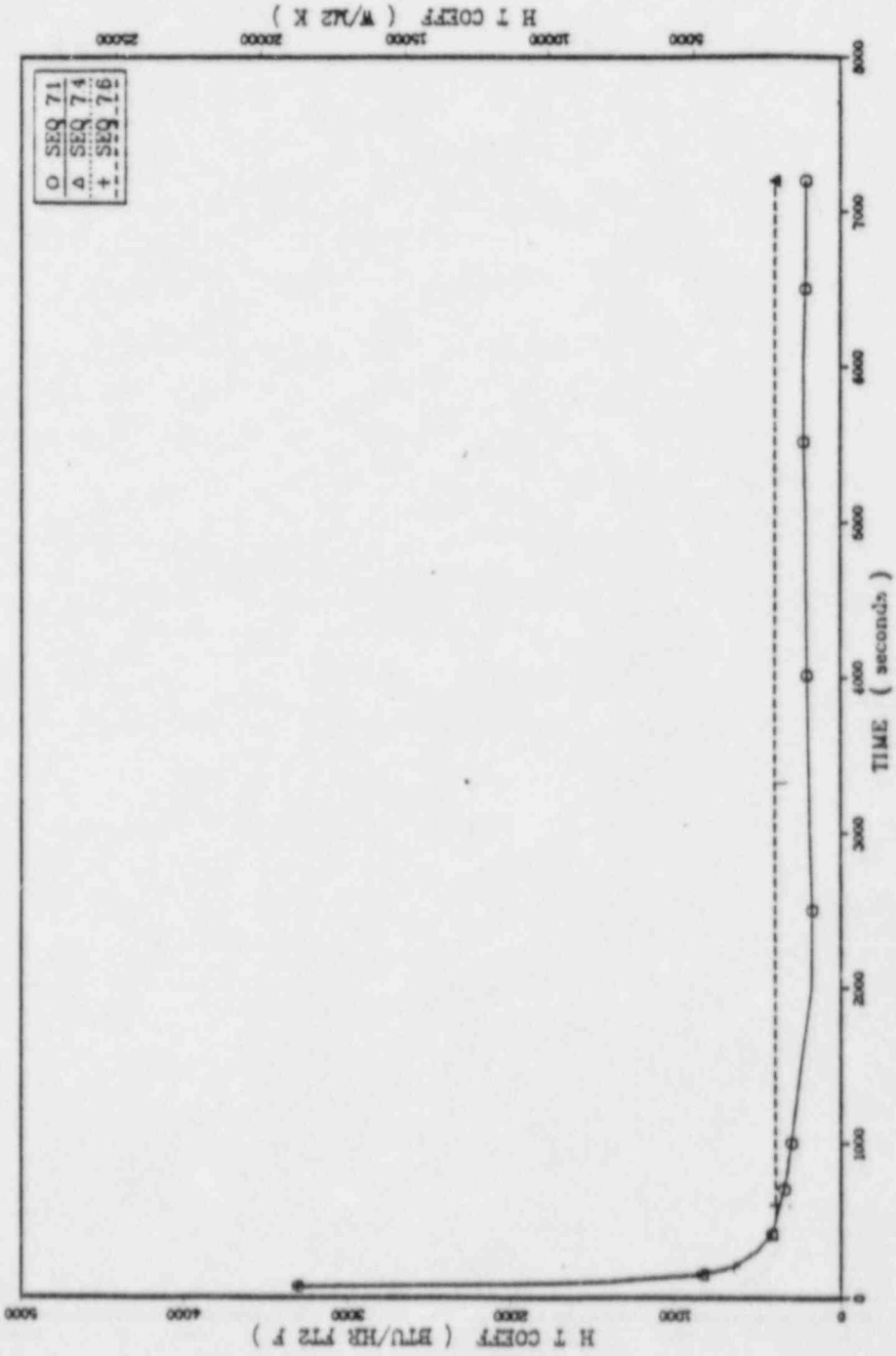

Figure 4.58. Extrapolated downcomer heat-transfer coefficients for small-break LOCA (≈0.02 ft²).

ultimately resemble sequence 7.1. The minimum temperature of sequence 7.6, the coolest sequence is 253°F (396 K).

The pressure profile in Figure 4.57 is that of the LANL transient 11, which is applicable to all of the sequences for this initiator.

The heat-transfer coefficient profiles in Figure 4.58 include the assumed minimum value and also the profile for LANL transient 11 for comparison.

ESTIMATION OF PRESSURE, TEMPERATURE, AND HEAT TRANSFER COEFFICIENT

J.1 Introduction

The evaluation of the risks of pressurized thermal shock (PTS) entails the coupling of overcooling incident event trees to fractured mechanics calculation of the probability of vessel crack propagation. The link between an event tree and state and the fracture mechanics calculation is the transient behavior of pressure (P), temperature (T), and heat transfer coefficient (h), in the reactor vessel downcomer region. That is, the P, T, h transient profiles from the sequence defined by an event tree end state become inputs for the fracture mechanics calculation. There are tens of millions of end states on overcooling transient event trees. Due to the cost and complexity of thermal hydraulics and fracture mechanics calculations, it is not practical to evaluate every end state separately. Therefore it becomes necessary to a) reduce by similarity grouping the number of end states to be evaluated and b) reduce the number of detailed thermal hydraulic calculations through the use of less rigorous estimation techniques.

This appendix summarizes the approach used to group sequences and estimate P, T, h profiles for the Calvert Cliffs PTS study. Section J.2 describes the estimation methodology developed for this study and the approach and rationale for sequence grouping. Sections J.3 through J.9 present the results of evaluations for each of the major initiating events. These initiations include:

1. Large main steam line break at hot zero power,
2. Small main steam line break at hot zero power,
3. Large main steam line break at full power,
4. Small main steam line break at full power,
5. Reactor trip,
6. Small break LOCA at full power, and
7. Medium break LOCA at full power.

Other initiators such as small break LOCA at hot zero power and loss of main feedwater at full power (followed by auxiliary feedwater overfeed) are not addressed in this appendix.

The P, T, h transient profile estimates presented here are based on TRAC-PF1 calculations reported by Los Alamos National Laboratory ( ). The detailed transient calculations are summarized in Chapter 4.0 of this PTS report. Computer tapes of TRAC plot output files for these calculated transients were also employed in the development of parameters applied to the temperature and pressure estimation procedures.

The sole and extensive use of these TRAC calculations in sequence P, T, h profile estimation implies that the estimations reported here will be subject to the same modeling assumptions and code characteristics driving the uncertainties in the TRAC calculated results. Additional uncertainties introduced by the estimation procedure have not been fully evaluated. Such uncertainty was minimized by using the estimation procedure to duplicate portions of the transients calculated by TRAC and thereby check the validity of assumed parameters and extrapolation models.

The estimated P, T, and h profiles presented in this appendix represent a "single point" estimate of downcomer conditions. That is, the estimated conditions are assumed to hold for the entire downcomer region without any azimuthal or axial variations. The detailed TRAC calculations demonstrated both azimuthal and axial variation in fluid temperatures and heat transfer coefficients. To minimize the impact of the fracture mechanics calculations the cooldown model used in the estimation procedure was set up to yield the expected temperature of the coldest sub-region of the downcomer rather than the overall average temperature for the whole downcomer region.

J.2 Methodology

J.2.1 General Approach

After an initial survey of the data resources and the sequences identified for estimation, the five-step process depicted in Figure J.1 was employed in the development of Calvert Cliffs-1 pressure, temperature, and heat transfer coefficient estimates. This approach allowed logical reduction of the number of cases to be evaluated and derived the greatest benefit from the information in the TRAC calculations.

The first step involved the grouping of similar sequences within each transient initiator table. An evaluation of the TRAC calculations for the effects from different operating states provided the criteria for assignment of sequences into groups. Besides providing grouping criteria, step 2 developed the parameters for the cooldown (temperature) and coolant swell (pressure) models used on occasion for this study. To assure correct interpretation of conditions during sequences, the appropriate parameters

were applied to the cooldown model to duplicate portions of sequences calculated by TRAC. These validation efforts took place in step 3. (See Section J.2.3.)

In step 4, the pressure, temperature, and heat transfer coefficients were estimated. Temperature could be estimated either by piecewise application of TRAC results or by calculation using the cooldown model. The method selection depended on the complexity of the sequence and the availability of applicable data from the TRAC calculations. Early portions of many evaluated sequences had stated configurations identical to those of a particular TRAC calculation, so piecewise use of the TRAC results was applied. The cooldown model was then used to extrapolate the remainder of the transient out to 2 h. Certain mild (i.e., high temperature) transients were not explicitly extrapolated, since they were well removed from the threshold temperature E_i; $>10^{-7}$). These mild sequences were assigned the P, T, and h profile of the TRAC calculation or extrapola- at which vessel failure probability can be calculated (P tion most closely representing the anticipated response of the sequence.

Pressure estimates were derived from observation of pressure trends in the TRAC calculations and by a pressure prediction model. The Calvert Cliffs-1 plant features a low-head HPSI system which cannot repressurize the primary above the pump shut-off head of 1285 psia. The charging pumps can repressurize the primary up to the PORV setpoint (2400 psia), but does so at a very low rate due to low flow capacity. The charging pumps were not throttled in any of the TRAC calculations. Therefore, there are ample cases available for evaluation of the contribution of the charging

pumps to system repressurization. The coolant swell model accounts for depressurization due to coolant expansion on reheating. This model is used for extrapolated cases where charging pump flow is throttled.

Heat transfer coefficients were based on piecewise selection of TRAC data and result of modeling performed by Theophanous at Purdue University (see Section 4.4). In general, the TRAC calculations predicted relatively constant values while the reactor cooling pumps (RCP) are running and a step change to a lower but constant value after RCP trip and establishment of natural circulation. The heat transfer coefficients predicted by TRAC did not include correction for free convection effects. Therefore, the TRACS values were underpredicted for natural-circulation flow conditions. Theophanous found that the contribution of free convection to the downcomer heat transfer coefficient off set increases or decreases inforced convection such that a total value of 400 Btu/hr $ft^{2}{}^{o}F$ (2270 $w/m^{2}k$) was maintained over a wide range of natural circulation flow conditions. The extrapolations presented in this appendix are a composite of TRAC calculated heat transfer coefficients for pre-RCP trip regimes and corrected estimates for natural circulation regimes.

The completed estimations were documented in step 5. This documentation comprises Sections J.3 through J.8 of this appendix.

J.2.2 Sequence Grouping

When all PTS initiators and failure branches are set up in event trees, several million end states result. To obtain a tractable yet representative set of PTS transients some method of sequence grouping is necessary.

Chapter 3 describes the construction of the event trees and process used to eliminate "non-contributing" states (i.e., component failures made irrelevant by the action of other systems or components). The collapsed event trees from this process still contain in excess of 100,000 end states. Section 3.5 describes the screening process used to separate end states into a set of discrete sequences for evaluation and a set of residual sequences for which no further evaluation was performed. The discrete sequences include all events with estimated frequencies greater than 10^{-7} per year. Sequences representing identical combinations of failures were collapsed to a single group and the corresponding frequencies were summed. Sequences with frequencies between 10^{-7} and 10^{-8} per year were also examined for similarity with the discrete sequences and were collapsed together with specific discrete sequences and where appropriate. This approach minimized the cumulative frequency of the residual. The resulting set of discrete sequences are found in Tables _____. Altogether, ____ sequences emerged from this grouping process. The grouping process of Chapter 3.0 were based on system configuration and event frequency. Further, grouping may occur based on the thermal hydraulic impact of configuration. The impact of a particular component or system can be evaluated from observation and evaluation of the effects of its operation or failure in the TRAC calculations. In this way the importance of failures or actions could be classified as dominant, minor, or inconsequential. Sequences with the same dominant features were grouped together for analysis. In later stages, the influence of minor events was evaluated to check the consistency of the groupings. This checking accounted for the thermal-hydraulic interaction

or feed-back due to the combination of failures. Some sequences were reassigned to other groups as a result of such checks.

The sequence tables of Chapter 3. (Tables ___) also contain some families of sequences. The members of a family differed from each other only in the timing of certain corrective actions (throttling of charging pump flow, throttling of AFW, etc.). The most severe sequence in the family would be evaluated to determine the extent of the cooldown. Where the "most severe" sequence of a family turned out to be very mild from a fracture mechanics standpoint, no further effort was spent on evaluating other members of the family. Where the most severe sequence did present a significant PTS risk, the other members of the family were evaluated separately or assigned to other groups, as appropriate.

The groupings for each of the initiators are discussed in sections J.3 through J.9.

J.2.3 Cooldown Model

The temperature response of a transient sequence is a function of the system's configuration during the sequence, including the timing of configuration changes (e.g., RCP trip, MSIV, MFIV closure, AFAS, etc). The sequences calculated at Los Alamos National Laboratory using TRAC represent only 12 out of the millions of sequences on the overcooling event trees. The cooldown model is a means to apply the information generated by the TRAC calculations to other sequences requiring temperature response estimation. The approach used in the cooldown model was to obtain separate mass-energy balances around the steam generators and the reactor vessel (i.e., balance

of the primary cooling system) to predict the rate of temperature change. All pertinent cooling and heating mechanisms were included. However, to obtain these mass-energy balances, the assumptions listed in Table J.1 were necessary to simplify the system to a two node model. The assumption of no steam generator heat transfer resistance will result in prediction of slightly lower primary temperatures than are reported by TRAC. The error is proportional to the rate of heat transfer. The error will be less than 10^{oF} for large steam line breaks (LANL Transient 3) and less than 5^{oF} for single turbine bypass valve failures (LANL Transient 4A) under conditions where natural loop circulation prevails. The assumption of thermal equilibrium in the steam generator secondary allows the use of simple choke flow models to predict steam flow rate. Conditions close to thermal equilibrium are obtained by TRAC for steam generators during blowdown. Division of the reactor coolant system into only 2 nodes, "smears out" the type of temperature lag information available from the finely noded model used by TRAC. Therefore, the cooldown model will respond faster to input parameter changes than will the TRAC model. Direct comparison of cooldown model extrapolated temperature response with TRAC calculations suggest that his effect is small for cases where natural loop circulation remains large (>500 lb/sec).

The final assumption involved in the cooldown model is that TRAC calculated mass flow data may be applied to the evaluation of other sequences.

This assumption is necessary because the mass flow information necessary to implement the cooldown model cannot be calculated from a simple 2 node model. Engineering judgement is used to identify segments of the

TRAC calculations relevant to the sequence being evaluated. Pertinent mass flow data are then extracted from the identified TRAC calculations for application to the cooldown model. The required parameters for the model are listed in the derivation of the model as described below.

Model Derivation and Characteristics

The cooldown model consists of 2 simultaneous non-linear differential equations describing the mass-energy balance of a primary node (i.e., vessel, loop piping, and RC pumps) and a steam generator node as follows:

$$\frac{d(MU)_{primary}}{dt} = \dot{m}_{HPI}\ H_{HPI} - \dot{m}_L\ H_L + Q_{D(t)} + Q_{RCP} + Q_W - Q_{sec} \qquad (J.1)$$

$$\frac{d(MU)_{SG}}{dt} = \dot{m}_{FW}\ H_{FW} - \dot{m}_{ST}\ H_{ST} + Q_{sec} \qquad (J.2)$$

where

$\dot{m}_{HPI}\ H_{HPI}$ = product of HPI mass flow and specific enthalpy at HPI nominal temperature (T_{HPI}) vs. thermodynamic reference temperature (T_{ref})

$= \dot{m}_{HPI}\ C_p\ (T_{HPI} - T_{ref})$

$\dot{m}_L\ H_L$ = product of primary leak flow (pressurizer surge line or break) and specific enthalpy at hot leg temperature (T_H).

$= \dot{m}_L\ C_p\ (T_H - T_{ref})$, (valid for liquid flow only)

$\dot{m}_{FW}\ H_{FW}$ = product of feedwater mass flow and specific enthalpy at feedwater temperature (T_{FW})

$= \dot{m}_{FW}\ C_p\ (T_{FW} - T_{ref})$

$\dot{m}_{ST}\ H_{ST}$ = product of secondary steam flow and specific enthalpy for saturated steam at steam generator conditions (T_{SG})

$= \dot{m}_{ST}\ (\Delta H_{vap}(T_{SG}) + C_p\ (T_{SG} - T_{ref}))$

$Q_D(t)$ = decay heat input as function of time
= ANS Decay Heat Function for transients from full power
= constant value for transients from hot standby

Q_{RCP} = Pump power deposited in coolant
Q_W = Heat transferred from vessel wall to coolant
Q_{sec} = Heat transferred from primary to secondary

In the absence of heat transfer resistance, Q_{sec} is limited only by transport of energy to steam generator by the hot leg flow ($\dot{m}_H$) or

$$Q_{sec} = \dot{m}_H C_p (T_H - T_{SG})$$

The left had sides of equations J.1 and J.2 may be expanded by use of the chain rule

$$\frac{d(MU)}{dt} = M \frac{dU}{dt} + U \frac{dM}{dt}$$

where

M = total mass
U = specific energy = $C_v (T - T_{ref})$

$$\frac{du}{dt} = C_v \frac{dT}{dt}$$

$$\frac{dM}{dt} = \sum \dot{m} = \text{mass flow across system boundaries.}$$

Substitution into the left hand sides of equations J.1 and J.2

$$\frac{d(MU)_{primary}}{dt} = M_{pri} C_v \frac{dTh}{dt} + C_v (T_H - T_{ref}) (\dot{m}_{HPI} - \dot{m}_L) \qquad (J.3)$$

$$\frac{d(MU)_{SG}}{dt} = M_{SG} C_v \frac{dT_{SG}}{dt} + C_v (T_{SG} - T_{ref}) (\dot{m}_{FW} - \dot{m}_{ST}) \qquad (J.4)$$

then placing these expressions with their respective right hand sides yields

Primary

$$M_{pri}\, C_v \frac{dT_H}{dt} + C_v\,(T_H - T_{res})\,(\dot{m}_{HPI} - \dot{m}_L) =$$

$$\dot{m}_{HPI} C_p\,(T_{HPI} - T_{ref}) - \dot{m}_L C_p (T_H - T_{ref}) + Q_D(t) + Q_{RCP} + Q_W - \dot{m}_H\, C_p\,(T_H - T_{SG}) \quad \text{(J.5)}$$

Steam Generator

$$M_{SG}\, C_v \frac{dT_{SG}}{dt} + C_v\,(T_{SG} - T_{ref})\,(\dot{m}_{FW} - \dot{m}_{ST}) =$$

$$\dot{m}_{FW}\, C_p\,(T_{FW} - T_{ref}) - \dot{m}_{ST}\,(\Delta H_v(T_{SG}) + C_p\,(T_{SG} - T_{ref})) + \dot{m}_H\, C_p\,(T_H - T_{SG}) \quad \text{(J.6)}$$

For liquids C_v may be assumed to be equal to C_p. Using this assumption and cancelling common terms yields

Primary

$$\frac{dT_H}{dt} = \frac{\dot{m}_{HPI} C_p (T_{HPI} - T_H)}{M_{pri} C_p} + \frac{Q_D(t)}{M_{pri} C_p} + \frac{Q_{RCP}}{M_{pri} C_p} + \frac{Q_W}{M_{pri} C_p} - \frac{\dot{m}_H C_p (T_H - T_{SG})}{M_{pri} C_p} \quad \text{(J.7)}$$

Steam Generator

$$\frac{dT_{SG}}{dt} = \frac{\dot{m}_{FW}\, C_p (T_{FW} - T_{SG})}{M_{SG} C_p} - \frac{\dot{m}_{ST}\, \Delta H_v(TSG)}{M_{SG} C_p} + \frac{\dot{m}_H\,(T_H - T_{SG})}{M_{SG} C_p} \quad \text{(J.8)}$$

In this form, the thermodynamic reference state (T_{ref}) has been eliminated, leaving only the expressions for heating and cooling mechanisms.

Flow rates for HPI, leak, hot leg and feedwater are independent parameters extracted or estimated from TRAC calculations. Steam flow rate is a function of steam enthalpy and pressure, break (or valve) area, and flow

resistance. The estimation of steam flow is based on an isentropic choked flow model altered to account for these elements. The model is of the form

$$\dot{m}_{ST} = f(P,H)AkP \qquad (J.9)$$

where

f(P,H) = choked isentropic mass flow (lb/hr/in^2-psia (upstream pressure)) as a function of pressure and mixture enthalpy. See ASME steam tables, 4th ed., Figure 14.

A = break (valve) size (in^2)

k = factor by which effective area of break is reduced to compensate for flow resistances in lines and valves

P = Pressure (psia)

By evaluating this expression for saturated steam enthalpy at various temperatures and taking a power curve fit against corresponding saturation temperatures the expression was converted to

$$\dot{m}_{ST} = Ak\,(1.87045 \times 10^{-4})\,T_{SG}^{4.32991} \text{ (lb/sec)} \qquad (J.10)$$

which has an accuracy better than $\pm 3\%$ between 200°F and 500°F upstream steam temperature. The choked flow condition holds over this range for TBV flows to the condenser, but becomes invalid at low temperatures for breaks to the atmosphere.

With the expression for steam flow substituted into the cooldown equation for the steam generator, the total model becomes

Vessel

$$\frac{dT_H}{dt} = \frac{\dot{m}_{HPI}\,C_p(T_{HPI} - T_H) + Q_D(t) + Q_{RCP} + Q_W - \dot{m}_H\,C_p(T_H - T_{SG})}{M_{pri}\,C_p} \qquad (J.11)$$

with $M_{pri} = M_{pri0} + (\dot{m}_{HPI} - \dot{m}_L)\,dt$

Steam Generator

$$\frac{dT_{ST}}{dt} = \frac{\dot{m}_{FW}C_p(T_{FW}-T_{SG})-AKx1.87045x10^{-11}\ T_{SG}^{4.32991}+\dot{m}_H C_p(T_H-T_{SG})}{M_{SG}\ C_p} \qquad (J.12)$$

$$\text{with } M_{SG} = M_{SGO} + \int (\dot{m}_{FW} - \dot{m}_{ST})\, dt$$

which is a set of simultaneous, non-linear differential equations which can be solved numerically to obtain the hot leg temperature (T_H) and steam generator exit temperature. Downcomer liquid temperature is obtained from the following equation

$$T_{DC} = \frac{\dot{m}_H\ H_{SG} + \dot{m}_{HPI}\ H_{HPI} + Q_{RCP} + Q_W}{(\dot{m}_H + \dot{m}_{HPI})\ C_P} \qquad (J.13)$$

with all quantities as defined above. This equation defines the downcomer temperature in terms of the mixing of loop flow and HPI and the heating of the fluid by RCP power input and heat transfer from the vessel wall. This equation does not affect the mass-energy balances (equations J.11 and J.12) described above but is used only to define the local fluid temperature in the downcomer.

Application of Cooldown Model

The cooldown model calculates temperatures for the hotleg, steam generator, and vessel downcomer using only a 2 node energy balance. The Calvert Cliffs 1 plant is equipped with 2 separate cooling loops which may be subjected to asymmetric operating condition (e.g., one steam generator blowing down while the other is isolated). Such situations require application engineering judgement to fit the existing conditions to the model. Judgement is also required to develop the required mass flow data for input to the model.

As described in the introduction to this section the general approach for evaluating a particular scenario is to first identify which of the TRAC calculations most closely matches the description of the scenario. Often the TRAC calculation and the evaluated scenario are identical out to some specified point in time or particular event (SGIS, RCP trip, etc.) where the evaluated sequence becomes different from the TRAC calculation. Temperatures and mass inventories of the primary system and the steam generators are extracted from the TRAC calculation at this point to set up the initial conditions for the extrapolation of temperature by the cooldown model. Also, the effective value area for the model choked flow calculations is selected so that the model will closely follow the steam flow rends observed in the TRAC calculation.

The initial mass inventories in the primary and steam generators may be distributed in different ways to account for assymmetric loop operation. For example, where a steam generator totally isolated from the rest of the primary (no heat transport possible) due to flow stagnation in that loop, the water mass and its energy content (temperature) is left out of the model, since it cannot influence temperature trends elsewhere. Should the loop flow be restored later, both the water mass and the energy would be put back into the model where it can influence total system heating or cooldown. Another example is where one steam generator is undergoing cooling by blowdown with the other steam generator loosing heat to the primary due to continued loop flow. In this case, the inventory of steam generator would be added to the primary mass since both are working together to retard the cooldown of the system. Should any of these conditions change to symmetric or another form of assymmetric conditions,

the extrapolation should be stopped for adjustment of primary and steam generator node masses.

Other system state changes will require interruption of temperature extrapolation to alter input parameters. Some of these state changes and required changes in parameters are listed in Table J.2. Whenever one of these state changes are encountered the current values of the hot leg and steam generator temperatures as calculated by the cooldown model are applied as input to the next extrapolation segment. New values of primary and steam generator mass inventories, total loop flow, HPI flow, primary leak (pressurizer surge line) flow, feedwater flow, feedwater temperature, heat input rate from wall heat transfer, decay heat factor, RCP heat, and secondary side break (valve) area are also supplied to match the new system state conditions. This process continues until the entire 0-7200 second period is evaluated.

By estimating the temperature profile of a TRAC calculated transient, the validity of data interpretation relating to transient response can be checked. Where the extracted parameters are correct, the extrapolation will closely follow the TRAC calculation. For example, the times to SIAS and SGIS signals for 1 ft^2 main steam line breaks at Hot Zero Power (LANL Transient 1) and at Full Power (LANL Transient 2) as estimated by the cooldown model were not significantly different. An example of a full 7200 second extrapolation is given in Figure J.3 which compares the cooldown model to the results for LANL Transient 12, PORV LOA with stuck open ADV. This case was selected because it features a secondary side break which causes a general system cooldown coupled to localized cooling

due to significant HPI flow. The two TRAC curves represent downcomer condition under the nozzles of the stagnated (B1) and flowing (A1) loops which represent the expected range of conditions. The cooldown model always assumes that all HPI flow is mixed with the flowing loop, thus yielding a temperature lower than the average for the two loops. In this case the extrapolated temperature stays within 10 to 50°F of the calculated minimum temperature loop values.

J.2.4 Pressure Estimation by Coolant Swell Model

An overcooling event will cause the primary coolant to cooldown and contract, drawing water out of the pressurizer via the pressurizer surge line. As the water level drops in the pressurizer, the steam layer expands and the system pressure decreases. As the pressure decreases SIAS initiates charging pump flow and, if the pressure decreases to below 1285 psia, high pressure injection flow commences. These injection flows stabilize system pressure during the rapid cooldown portion of the event sequence.

If the injection flow volume is greater than the shrinkage rate or if the system enters a reheating mode, the pressurizer water level will increase, compressing the steam layer and increasing the pressure. The rate at which the pressure recovers is of importance because of the contribution of pressure in the fracture mechanics calculations.

To determine the best algorithm for estimation of pressure recovery rate, the TRAC calculations for Calvert Cliffs were examined in detail. TRAC and RELAP5 calculated PTS cases for the Oconee-1 and H.B. Robinson-2 plants

were also examined. It was observed that the codes predict that the system pressure varies linearly with pressurizer water level. Furthermore, the PORV set point pressure is reached when the pressurizer is on the verge of becoming water solid. The alternate theoretical model of the ideal adiabatic compression of the pressurizer steam layer yields non-linear pressure vs. pressurizer water level response and predicts an exceedingly fast repressurization to the PORV set point pressure. Clearly the ideal adiabatic compression model is not representative of repressurization rates predicted by TRAC and RELAP5. Therefore, the observed linear relationship between pressurizer level and system pressure was employed for this study.

In most of the Calvert Cliffs sequences evaluated, the system pressure dropped below and then stabilized at the HPI pump shut off head of 1285 psia. At this point system cooldown mechanisms had been isolated or corrected and the system has commenced reheating. Injection flow from the high pressure injection system had ceased and injection flow from the charging pumps may or may not be throttled depending on the specification of the sequence. The reheating of the coolant will cause the coolant volume to swell and (with the charging pump flow) refill the pressurizer. The required increase in temperature to cause total refill of the pressurizer and therefore repressurization to the PORV set point may be determined by the following equation

$$\underline{V}\,(T_L,\ 2400\text{psia}) = \left(1 + \frac{V_{ST}}{V_{pri}}\right)\underline{V}\,(T_i,\ 1285\text{psia}) \qquad (J.14)$$

where

$\underline{v}$ (T,P) = specific volume of water at specified temperature and pressure

T_L = Limiting average primary temperature at which coolant swell (and charging pump flow) volume equals available pressurizer steam volume

T_i = Initial average primary temperature at start of system reheat

V_{ST} = Available steam volume in pressurizer at start of reheat, and

V_{pri} = Volume of primary system susceptible to reheating
= primary volume without pressurizer or HPI line volume
= 9601 ft^3 - 346 ft^3 = 9255 ft^3

This equation assumes that there are no primary steam voids outside of the pressurizer and that the pressurizer steam volume (V_{ST}) is known at the beginning of repressurization. Table J.3 contains estimates of effective-steam volumes for the repressurization phases of the LANL transients. These volumes represent the effective steam volume (i.e., the amount of volume change which results in attainment of PORV-set point pressure) and do not necessarily represent the actual steam volume in the pressurizer.

Engineering judgement dictated the selection of V_{ST}, for the estimation of repressurization rate. In evaluation of sequences similar to a LANL transient, the corresponding value of V_{ST} would be applied to equation J.14. In other cases generalized values reflecting the trends in Table J.3 were used. Hot zero power sequences were evaluated using a V_{ST} of 600 ft^3. A value of 700 ft^3 was applied to severe transients at full power and values between 1000 ft^3 and 1500 ft^3 was applied to milder transients at full power.

For each sequence estimation, the steam volume (V_{ST}) and initial average system temperature (T_i) were applied to obtain the average temperature at which full repressurization is obtained. The sequence temperature

extrapolation is then examined to obtain the time at which this temperature is achieved. If charging pump flow continued over this period, the accumulated volume over the interval is subtracted from V_{ST} and the final average temperature is recalculated. This is repeated until covergence is obtained. The resulting time represents the moment at which the PORV set point pressure is reached. Pressure between the beginning of reheat and attainment of full pressure is obtained by linear interpolation.

Due to the assumptions involved in the coolant swell model, the prediction of repressurization rate is imprecise. In most cases the uncertainty in the calculation would be conservatively bounded by the use of the repressurization curves calculated by TRAC. Some mild transients may repressurize faster than the rates predicted by TRAC.

J.2.5 Heat Transfer Coefficient Estimation

As discussed in Section 4.4 corrections to downcomer convection heat transfer coefficient have been developed. The trade-offs between forced and free convection effects under natural circulation conditions resulted in a nearly constant heat transfer coefficient of 400 Btu/hr $ft^2{}^0F$. This value was applied as a floor or lower limit for all evaluated cases following coast down of the RCP's. Therefore all evaluated cases had similar heat transfer coefficient profiles.

J.3 Large Steam Line Break at Hot Zero Power

J.3.1 Description of sequences

The sequences for large main steam line break at hot zero power are initiated by a 1 ft^2 (or larger) break in a main steam line down steam of the flow restricter and upstream of the MSIV. The system is initially at steady state conditions and nominal steam generator levels for hot zero power. The decay heat level is 9.38 MW, corresponding to 100 hours after shutdown.

The seven specified sequences for this initiator are listed in Table J.4. The differences in the sequences relate to MSIV operation, isolation of AFW to the affected steam generator, HPI operation, and operator actions to turn off the charging pumps and throttle AFW flow.

J.3.2 Bases for extrapolation

LANL Transients 1, 3, 4, and 5 relate to large steam line breaks at hot zero power. Transient 1 features a 1 ft^2 break in steam line A. The only other assumed failures in this transient are failures to turn off charging pump flow and to throttle AFW at +22 inches in the intact steam generator B. These conditions make Transient 1 equivalent to sequence 1.4 in Table J.4.

Transient 4 features a double-ended break in loop A coupled with system failures to isolate AFW to SGA and operator failures to turning off the charging pumps and throttle AFW to both SGA and SGB.

Transient 5 also assumes a double ended steam line break in loop A and operator failure to turn off the charging pumps upon reaching the HPI flow limiting pressure. For this case, however, the MSIV's fail open and the operator is assumed to throttle AFW to both steam generators after 8 minutes.

Transient 3 duplicates the events of Transient 1 with the exception that only two RCP's tripped 30 s after SIAS. This transient does not correspond to any of the sequences in Table J.4, but it does illustrate the beneficial effects of not tripping all RCP's for a steam line break incident.

For the purposes of extrapolation, Transients 1, 4, and 5 provide temperature and pressure profiles directly applicable to first 1000-1400 s of the specified sequences since there is no deviation of condition between the sequences and corresponding LANL transients over this period. The stable loop flow and vessel wall heat transfer conditions later in Transients 1 and 5 and the condition pertinent to restoration of flow in loop B late in Transient 1 were employed generally in the evaluation of sequences of Table J.4.

J.3.3 Results and Discussion

J.3.3.1 Sequence 1.1

A. Basis - Transient 1

B. Departures from Basis

The departures involve operator actions to turn off charging pumps when primary systems regain pressure to the HPI shut off head 8.9 MPa (1285 psia) and to throttle AFW to intact SGB on reaching + 22 inches level.

C. Temperature extrapolation

The specified departures from Transient 1 will not affect temperatures until after broken SGA dryout. Therefore Transient 1 was used out to 1400 s. By this time the charging pump and HPI flows have ceased. AFW continues to SGB until reaching +22 inches level at 1900 s. However, flow in Loop B will remain stagnant until the primary becomes warmer than SGB (379°F (446K) at AFW cutoff). The lowest temperature, 253°F (396K), occurs at 1308 s. Extrapolation proceeded in two segments. Heat transfer from metal to water increased system temperatures to 379°F (446K) at about 4200 s. There after Loop B flow limited further temperature increases by heat transfer into SGB. Since AFW was throttled, general system cooldown was not experienced for the remainder of the sequence. The temperature reached 388°F (470.7K) at 7200 s. The temperature profile is presented in Figure J.3.

D. Pressure Extrapolation

HPI flow ceases at around 1000 s in Transient 1. However, some additional charging pump flow would be required to maintain pressure until SGA dryout is complete. Primary system pressures from Transient 1 were used out to 1400 after which the coolant swell model was employed to predict

repressurization to the PORV set point, 2400 spia (16.6 MPa) at 6000 s. The pressure profile is presented in Figure J.3.

E. Heat transfer coefficient extrapolation

The heat transfer coefficient data from Transient 1 was used out to 500 s at which time the value had declined to the final corrected value of 400 Btu/hr ft^2 ^oF (2270 W/m^2K).

C.3.3.2 Sequence 1.2

A. Basis - Transient 1 and Sequence 1.1

B. Departures from Basis

This sequence differs from sequence 1.1 only in the failure of the operator to throttle AFW to intact SGB. See Section J.3.3.1 for other details.

C. Temperatures extrapolation

This sequence will follow the temperature profile of sequence 1.1 out to the point at which primary flow in stagnated loop B is restored. The minimum temperature of 253^{o}F (396K) at 1308 s was taken. The effect of unthrottled AFW on the stagnated loop B is to increase the secondary inventory and reduce the average temperature of the loop. Since the loop is isolated from the balance of the primary due to temperature induced flow stagnation, the temperature reduction in the stagnated loop occurs concurrently with the reheating of the flowing loop and the balance of the primary. Based on data from Transient 1, the temperatures of the flowing and stagnant loops becomes equal (340^{o}F) at around 3500 s. Since

the now flowing loop B is still receiving AFW, it cools the primary and causes stagnation of loop B. The downcomer temperature sags to and remains nearly constant at 340°F (444K) for the remainder of the transient. The temperature profile for sequence 1.2 is presented in Figure J.5.

D. Pressure extrapolation

The coolant swell model does not predict water solid primary condition for this sequence, hence the PORV set point pressure is not achieved. The prediction of a final pressure of 2000 psia (13.8 MPa) is based on the fractional rise of primary average temperature relative to the temperature required for full repressurization. This method is imprecise as to timing. The pressure could reach this maximum value as early as 3500 s compared to 7200 s as shown in Figure J.5.

E. Heat transfer coefficient

The downcomer heat transfer coefficient data from Transient 1 was used out to 165 s at which time the value had declined to the final corrective value of 400 Btu/hr ft^2 °F (2269 W/m^2K).

J.3.3.3 Sequence 1.3

A. Basis - Transient 1

B. Departures from Basis

The throttling of AFW to intact SGB in sequence 1.3 is the only departure from Transient 1 conditions.

C. Temperature extrapolation

The throttling of AFW to the intact and stagnated SGB occurs at about 2000 s at which time the average temperature in the steam generator is 379°F (466K). Primary flow in loop B will not be restored until the primary exceeds this temperature. Transient 1 data were used to 3000 s. After which extrapolation proceeded assuming charging pump flow of 18.3 lb/s (8.3Kg/s), loop A flow of 540 lb/s (245 Kg/s) and wall heat transfer varying linearly from 500 Btu/s (0.53 MW) to 300 Btu/s) 0.32 MW) over the period 3000 s to 7200 s. As seen in Figure 4.3 in Section 4.5.2.1, the extrapolation closely follows Transient 1 to 4000 s and then proceeds to a final temperature of 346°F (447K) at 7200 s. The overall cooling effect of charging pump flow limited primary reheating such that loop B flow restoration does not occur. As in Transient 1, the minimum temperature of 253°F (396K) was observed at 1308 s. The temperature profile is presented in Figure J.6.

D. Pressure extrapolation

There are no mechanisms to cause the pressure profile for the sequence to vary from that of Transient 1. Therefore, Transient 1 data were used. See Figure J.6.

E. Heat transfer coefficient

The heat transfer coefficient conditions for sequence 1.1 are equivalent to this sequence. The final value of 400 Btu/hr ft^2 °F (2269 W/m^2K) is obtained by 165 s into the sequence.

J.3.3.4 Sequence 1.4

The specified conditions for sequence 1.4 are identical to the case modeled in Transient 1.

J.3.3.5 Sequence 1.5

A. Basis - Transient 4

B. Departures from Basis

The operator action tc turn of the charging pumps on attainment of HPI shut off pressure is the only departure of sequence 1.5 from Transient 2.

C. Temperature extrapolation

The temperature profile for the sequence is assumed to be identical to Transient 4. See Figure J.7.

D. Pressure extrapolation

The pressure profile for the sequence is identical to that of Transient 4 out to 1125 s where the HPI flow limiting pressure of 1285 psia (8.9 MPa) is achieved and the operator is assumed to shut off the charging pumps. Since there is no significant heating of the system after this time, the pressure remains at this final value as depicted in Figure J.7.

E. Heat transfer coefficient

The heat transfer coefficient profile is identical to that of sequence 1.1 (Section J.3.3.1).

J.3.3.6 Sequence 1.6

A. Basis - Transient 5

B. Departures from Basis

These sequences specify operator action to turn off charging pump flow on achievement of HPI shut off pressure. Transient 5 does not. In Transient 5 the operator kills AFW to both steam generators at 480 s. In sequence 1.6 the operator limits the AFW to 160 gal/min per SG.

C. Temperature extrapolation

There is sufficient SG secondary water inventory present to cool the primary down near to 212°F (373K) given a large break and MSIV failure. Therefore, sequence 1.6 is essentially equivalent to Transient 5. Figure J.8 depicts the temperature data for Transient 5 to the end of the calculation, 3300 s, and the extrapolation to 212°F (373K) at 7200 s.

D. Pressure extrapolation

The pressure profile for Transient 5 was used to 1250 s, at which point the primary reaches the final pressure of 1285 psia (8.6 MPa) as shown in Figure J.8.

E. Heat transfer coefficient

The heat transfer coefficient drops from its initial value of 3700 Btu/hr ft^2 °F (2100 W/m^2K) after RCP trip at 62.2 s to a final value of 400 Btu/hr ft^2 at 250 s.

J.3.3.7 Sequence 1.7

This sequence features a large break in a steam line and failures to isolate feed flow to the broken SG, to limit repressurization by turning off the charging pumps, and to throttle AFW to the intact steam generator. This sequence is as assigned the temperature pressure and heat transfer coefficient profiles of Transient 4 due to the close similarity of the transients.

J.4 Small Steam Line Break at Hot Zero Power

J.4.1 Description of Sequences

The sequences for the small steam line break at hot zero power are initiated by a TBV size break, 0.52 ft^2 (0.048 m^2), located in a steam line down stream of the flow restricter and upstream of the MSIV. The system is initially at steady state condition and nominal steam generator levels for hot zero power. The decay heat level is 9.38 MW, corresponding to 100 hours after shutdown.

The eight specified sequences for this initiator are listed in Table J.5. The differences in the sequence specifications involve MSIV operation, isolation of AFW to the affected steam generator, HPI operation, and operator action to turn off the charging pumps and throttle AFW flow.

J.4.2 Bases for Extrapolation

LANL Transient 1 (1 ft^2 steam line break at HZP) comes closest to matching the conditions for the small (TBV-sized) steam line breaks at hot zero

power. The primary and secondary water inventory data, looped flows prior to RCP trip and after RCP trip, and system average temperatures corresponding to SIAS and SGIS from Transient 1 were used to construct the initial response of the plant to the small break at hot zero power. To check the accuracy of the projection assumptions, duplication of Transient 1 was attempted. SGIS was predicted at 16 to 18 s, within 1 to 2 s of the Transient 1 value, and SIAS was predicted at 56 s versus 54 s for TRAC. Next, the same flow and system temperature relationship were applied to the 0.52 ft^2 small break. The resulting predictions were SGIS at 55 s and SIAS at 90 s. The RCP's were assumed to be tripped at 120 s. Natural circulation flow data from Transient 1 was used for predictions later in the sequences.

J.4.3 Results and discussion

J.4.3.1 Sequences 2.1 and 2.2

A. Basis - Transient 1

B. Departures from Basis

The flow and thermal data in Transient 1 were used in the extrapolation of these small break sequences. Early responses of both of the named sequences are similar. Later responses are determined by associated system failures and operator actions. Neither of the sequences will repressurize completely due to operator action to shut off the charging pumps. Sequence 2.2 lacks operator action to throttle AFW to SGB.

C. Temperature extrapolation

Using Transient 1 data as discussed above, Sequence 2.1 was extrapolated over the period 0 to 7200 s as shown in Figure J.9. Events along the course of the extrapolation include SGIS at 55 s, SIAS at 90 s, RCP trip at 120 s with establishment of natural circulation assumed at 220 s. AFAS occurs at 360 s based on SGA inventory, but prior isolation of AFW to that SG directed all flow to SGB until throttling at 3000 s on level. The minimum temperature of 250°F (394K) occurs at SG dry out (2240 s). Temperature recovers after this point with flow in loop B starting at about 4000 s. The system reheats to a final temperature of 348°F (449K).

D. Pressure extrapolation

Pressure is assumed to drop from 2250 psia (15.5 MPa) to 1740 psia (12.0 MPa) at 90 s (SIAS) and then to 1200 psia (8.3 MPa) at 180 s. Since the system cooldown is less severe than in Transient 1 further depressurization was not assumed. The system is assumed to repressurize to 1285 psia (8.9 MPa) by 1000 s at which point the charging pumps are turned off. HPI flow maintains pressure at this level until SGA dryout. The coolant swell model predicted a final pressure of 2210 psia (15.2 MPa) at 7200 s due to system reheating. (See Figure J.9.)

E. Heat transfer coefficient

The downcomer heat transfer coefficient drops from 4230 Btu/hr ft^2 °F (24000 W/m^{2}K) at the tripping of the RCP's (120 s) to a final value of 400 Btu/hr ft^2 °F (2270 W/m^{2}K) by 250 s.

J.4.3.2 Sequences 2.3 and 2.4

A. Basis - Transient 1 and extrapolations for Sequence 2.1

B. Departures from Basis

The failure to turn off the charging pumps in sequences 2.3 and 2.4 and subsequent early repressurization separates thes two sequences from the group discussed in Section J.3.4.1. Sequence 2.3 includes throttling of AFW to the intact steam generator while sequence 2.4 does not. The failure to throttle will results in colder intact loop temperatures, an earlier restoration of loop flow, and lower final temperatures. Therefore, sequence 2.4 was selected to represent the group.

C. Temperature extrapolation

The events for sequences 2.3 and 2.4 follow basically the same path as for sequence 2.1 except for some minor differences due to continued charging pump flow. The time of SGA dry out shifts 40 s later to 2280 s at which point the minimum temperature of 242°F (390 k) is obtained. Some reheating occurs until loop B flow resumes at 3500 s. The system then cools to its final value of 269°F (405 k) at 7200 s. Figure J.10 gives the temperature profile for the group.

D. Pressure extrapolation

Due to similarities in cooldown rates and related conditions the pressure profile for Transient 1 was assigned to sequence 2.4 (see Figure J.10).

E. Heat transfer coefficient

The heat transfer coefficient profile for sequence 2.4 is identical to that for sequence 2.1.

J.4.3.3 Sequence 2.5

A. Basis - Transient 1 and Sequence 2.1

B. Departures from Basis

The failure to isolate AFW to the broken SGA in sequence 2.5 is the only departure from sequence 2.1.

C. Temperature extrapolation

The initial response of Sequence 2.1 applies for the first 360 s of the transient. Failure of AFW isolation to SGA assures continual cooldown throughout the duration of the sequence. After 1000 s the continued flow of AFW adds to SGA inventory faster than water is lost to blowdown. The minimum temperature of 216^{o}F (375 k) occurs at 7200 s as shown by Figure J.11.

D. Pressure extrapolation

The shut down of the charging pumps prevents any repressurization of the system above 1285 psia (8.9 MPa) since the system does not reheat. The pressure response is in Figure J.11.

E. Heat transfer coefficient

The downcomer heat transfer coefficient response is the same as that for sequence 2.1 (Section J.3.4.1).

J.4.3.4 Sequence 2.6

A. Basis - Transient 1

B. Departures from Basis

The main departures from Transient 1 in this sequence are the failure of both MSIVs to close and the operator action to turn off the charging pumps. Since neither loop will stagnate and both loops will be undergoing significant cooldowns, the data for the flowing loop in Transient 1 was applied to this sequence.

C. Temperature extrapolation

This sequence begins to diverge from sequence 2.1 soon after the MSIV failure to close at 55 s. SIAS and RCP trip do not shift significantly from their respective 90 s and 120 s values in Sequence 2.1. However, feeding this small steamline break with both steam generators delays AFAS to 1250 s. AFW flow exceeds the break stream flow for the remainder of the transient, yielding a net increase in steam generator water inventories. As shown in Figure J.12 the minimum temperature of 215^{o}F (375 k) is obtained at 7200 s.

D. Pressure extrapolation

The pressure profile for sequence 2.6 is assumed to be identical to the profile for sequence 2.5 (see Figure J.12).

E. Heat transfer coefficient

Due to similar timing of the RCP trip the profile for this case is assumed to be identical to that of sequence 2.1.

J.4.3.5 Sequence 2.7

A. Basis - Transient 1, Sequence 2.6

B. Departures from Basis

In sequence 2.7 the charging pumps are not turned off, leading to full repressurization of the primary. This is the only difference between sequence 2.7 and 2.6.

C. Temperature extrapolation

The cooldown due to steam blowdown from the break will dominate the sequence. Therefore, the temperature profile of sequence 2.6 was assigned to this case. The profile is presented in Figure J.13.

D. Pressure extrapolation

Due to the similarities between this sequence and Transient 1, the pressure profiles from Transient 1 was applied to this sequence as shown in Figure J.13.

E. Heat transfer coefficient

The heat transfer coefficient profile for this sequence is assumed to be the same as that of sequence 2.1.

J.4.3.6 Sequence 2.8

A. Basis - Transient 1, Sequence 2.6

B. Departures from Basis

Sequence 2.8 differs from 2.6 only in the operator killing AFW at 300 s, in essence throttling the AFW system before it comes on. Like 2.6, sequence 2.8 differs from Transient 1 by the operator turning off the charging pumps.

C. Temperature extrapolation

This sequence is identical to sequence 2.6 out to 1250 s when AFAS is generated. Since AFW was killed previously by the operator, there is no AFW supplied to either SG. There is still nearly 200,000 lb of water in the secondary system available for blowdown, through the break. The blowdown rate also decreases due to the decreasing temperature and pressures in the secondary system such that SG dryout does not occur prior to 7200 s. As shown in Figure J.14 the minimum temperature of 224^{o}F (380 k) occurs at the end of the period. The temperature difference between sequences 2.6 and 2.8 is due to the influence of AFW addition.

D. Pressure extrapolation

The pressure profile (Figure J.14) for this sequence is assumed to be identical to that of sequence 2.5 due to operator action to turn off the charging pumps coupled with no reheating of the system.

E. Heat transfer coefficient

The heat transfer coefficient profile for this sequence is assumed to be the same as that of sequence 2.1.

J.5 Large Steam Line Break at Full Power

J.5.1 Description of Sequences

The sequences for large steam line break at full power are initiated by a 1 ft^2 (0.0929 m^2) break in a steam line downstream of the flow restricter and upstream of the MSIV. The system is initially at steady state at full power. Both the reactor and the turbines are assumed to trip coincident with the appearance of the break. The system decay heat function is assumed to be 1.0 times the ANS standard.

The nine specified sequences for this initiator are listed in Table J.6. The differences in sequence specification involve MSIV operation, MFW runback after trip, ADV operation, HPI operation, and operator actions to turn off the charging pumps and throttle AFW flow.

J.5.2 Bases for extrapolation

LANL Transient 2 serves as the basis for evaluation of large steam line breaks at full power. Transients 8 and 9 also provide information on SG overfeeds useful for evaluation of sequences 3.8 and 3.9. The similarities between late transient natural circulation flows in the basically different Transients 2, 8, and 9 also lends credence to the applicability of transient data in sequence extrapolation.

J.5.3 Results and Discussions

J.5.3.1 Sequences 3.1, 3.2, 3.3, and 3.4

As seen in Table J.6 sequences 3.1 through 3.4 feature all the combinations of operator success or failure to turnoff the charging pumps upon attainment of HPI shut off pressure and throttling of AFW to the intact SG. With both of these failures, sequence 3.4 is identical to the specifications for Transient 2 and is represented by that calculation.

As noted above, sequences 3.1, 3.2, and 3.3 will differ slightly from Transient 2. Variations will be typically in the direction to reduce PTS risk, i.e., higher temperatures and lower pressures. Since Transient 2 itself does not represent any great risk due to its high temperatures, assignment of Transient 2 P, T, and h profiles to sequences 3.1 through 3.4 does not represent any significant error.

J.5.3.2 Sequence 3.5

A. Basis-Transients 2

B. Departures from Basis

In this sequence the AFW is not isolated to the broken steam generator. The operator is assumed to turn off the charging pumps and to throttle AFW to the intact steam generator on reaching +22 inch level indication.

C. Temperature Extrapolation

The temperature profile for Transient 2 was used out to 400 s where the broken SGA dries out. At SGA dryout the downcomer temperature is 371°F (461K). (Detailed examination of the TRAC data for Transient 2 revealed that AFW was directed to the broken SGA rather than to the intact SGB during this period. This modeling error was corrected in the restarted TRAC calculation after 400 s. However, this modeling error matches the specification of sequence 3.5, thus enhancing the accuracy of the extrapolation.) After 400 s, the extrapolation continues with an AFW flow of 44.5 lb/s (20.2 Kg/s) to the affected steam generator. The boiling and blowdown of this AFW flow is the sole cooldown mechanism for the remainder of the sequence. Decay heat input exceeds the cooling capacity of this AFW flow out to 2000 s, with the system reheating to 411°F (483K). After 2000 s, the cooling exceeds decay heat and wall heat inputs such that the system cools to a minimum of 240°F (388K) at 7200 s as shown in Figure J.15.

D. Pressure extrapolation

The pressure profile for this sequence follows that of Transient 3 rerun (3A) out to SGA dryout at 400 s. The limited cooling after this point allows the primary to repressurize to the HPI flow limiting pressure of 1285 psia (8.9 MPa) by 640 s when the operator is assumed to turn off the charging pumps. HPI pump action will prevent depressurization for the remainder of the sequence as shown in Figure J.15.

E. Heat Transfer Coefficient

The downcomer heat transfer coefficient profile is assumed to be similar to that for Transient 2. The initial value of 4230 Btu/hr $ft^{2o}F$ (24000 w/m^2K) holds out to the tripping of the RCPs at 45 s. The coefficient drops to the assumed minimum value of 400 Btu/hr $ft^{2o}F$ (2270 w/m^2K).

J.5.3.3 Sequence 3.6

A. Basis - Transient 2 - response to large steamline break at full power
Transient 5 - qualitative response to double MSIV failure during large steam line break

B. Departure from Basis

Sequence 3.6 features failure of both MSIV's and throttling of AFW to a rate of 160 gal/min to each steam generator. The charging pumps are also shut off upon attainment of HPI shut off pressure. The differences between Transient 2 and sequence 3.6 are assumed to parallel the differences between Transient 4 and Transient 5 relating magnitude of total loop flows for flowing-stagnated loop conditions versus symmetric loop conditions. In

the case of Transients 4 and 5, roughly the same levels of total loop natural circulation flow are obtained. The same behavior is assumed for evaluation of Sequence 3.6.

C. Temperature extrapolation

Extrapolation commenced after 40 s in Transient 2 with parameters chosen to reflect the failure to isolate SGB, the sustained flow of AFW, and the symmetric nature of primary loop flows. The timing of basic events such as AFAS, SIAS, and SGIS did not change for the sequence. The failure of the MSIV's effectually doubled the secondary water inventory available for blowdown. As shown in Figure J.16 the temperature decreases out to 1700 s and then stabilizes momentarily due to balancing of declining loop flow and temperature with wall heat transfer to yield relatively constant downcomer fluid temperature. This occurs although the cold leg temperature is continuing to decline. About this same time a balance has been struck between the energy flow out the break and the energy input by decay heat and wall heat transfer. The steam generator temperature, which determines the break energy flow, declines slowly after this point in response to declines in wall heat transfer and decay heat input. This steam generator temperature response drives the downcomer temperature for the rest of the transient. The steam generators do not dry out. The AFW flow overwhelms the break flow by 5500 s causing partial refill of both steam generators for the rest of the sequence. The minimum temperature of 226°F (381 k) occurs at 7200 s.

D. Pressure extrapolation

The bulk of the cooldown occurs prior to 600 s and the pressure response for Transient 2 is used to this point. In Transient 2 the HPI shut off pressure of 1285 psia (8.9 MPa) has been reached and the charging pumps are assumed to be shut off at this point. The HPI system will maintain the primary at this final pressure for the remainder of the transient (see Figure J.16).

E. Heat transfer coefficient

The heat transfer coefficient holds its initial value, 4230 Btu/hr ft^2 ^oF (24000 W/m^2K), out to RCP trip at 45 s. RCP coast down and an initially very strong natural circulation flow delay to 600 s the attainment of the final value of 400 Btu/hr ft^2 ^oF (2270 W/m^2K).

J.5.3.4 Sequences 3.7

A. Basis - Transient 2 - response to large steamline break

Transient 12 - response to stuck open ADV

B. Departures from Basis

Sequences 3.7 features operator action to turn off charging pumps and throttle AFW to the intact steam generator (SGB). This sequence also features a stuck open ADV on the "intact" loop (SGB) which is not isolated. Transient 12 data were used to calibrate the cooldown model for ADV flow versus steam generator temperature.

C. Temperature extrapolation

The severe cooldown at the beginning of the transient was expected to overwhelm the cooldown due to the ADV. Therefore, Transient 2 data were used out to 450 s when SGA has dried out. The minimum temperature of 399°F (477 k) occurs at 300 s. Stagnation of loop B allows the ADV to cool SGB so that loop B flow begins at around 500 s. A balance between break energy flow, AFW heating load, and decay heat input is established by 1500 s and persists through to 7200 s yielding a final temperature of 432°F (495 k) as shown in Figure J.17. Through AFW was refilling SGB through the later stages of the transient, the +22 inch limit was not achieved, so AFW was not throttled.

D. Pressure extrapolation

The pressure response for Transient 2 was used for this sequence out to the attainment of HPI shut off pressure at 500 s as shown in Figure J.17.

E. Heat transfer coefficient

The heat transfer coefficient profile is taken to be identical to that of sequence 3.6.

I.5.3.5 Sequences 3.8 and 3.9

A. Basis - Transient 2

Transient 8 - response to 2 loop MFW overfeed

Transient 9 - response to 1 loop MFW overfeed

B. Departures from Basis

Sequences 3.8 and 3.9 include operator actions to turn off charging pumps and to throttle AFW to the intact steam generator. Sequence 3.8 specifies a MFW overfeed to the broken steam generator. Sequence 3.9 specifies overfeeds to both steam generators. The effect of the double overfeed in 3.9 is masked by the stagnation of loop B and the generally minimal PTS impacts of overfeeds as evidenced by Transients 8 and 9. Therefore, sequence 3.9 is grouped together with sequence 3.8 for evaluation.

C. Temperature extrapolation

The overfeed of the broken steam generator (SGA) serves to extend the period for dryout and produce lower minimum temperatures. The closure of the MFIV upon SGIS at 44 s stops the overfeed, leaving SGA with an additional 80,000 lb (36400 kg) of water relative to the inventory for Transient 2 at the same instant. Projection of temperature trends based on Transient 2 loop flow data yielded a minimum temperature of 276°F (408 k) at 800 s, when SGA dries out. With the collapse of the cooldown mechanism, the downcomer is soon reheated to the hot leg temperature as the loop flow sweeps warm liquid into the downcomer. Following this initial rise, a slower rise due to general reheating of the system takes place over the rest of the sequence. By 5000 s the temperature rises to 534°F (552 k) where the ADV system is used to control temperature. The temperature profile is presented in Figure J.18.

D. Pressure extrapolation

The pressure profile from Transient 2 is used out to 450 s due to the similarity of conditions. Repressurization to 1285 psia (8.9 MPa) is assumed to be delayed to 950 s due to the rapid cooldown prior to SGA dryout. The coolant swell model predicts full repressurization to 2400 psia (16.6 MPa) by 1800 s as shown in Figure J.18.

E. Heat transfer coefficient

The downcomer heat transfer coefficient profile for these sequences is assumed to be identical to that of sequence 3.6.

J.6 Small Steam Line Break at Full Power

J.6.1 Description of Sequences

The sequences for small steam line break at full power are initiated by a TBV sized break, 0.52 ft^2 (0.048 m^2), located in a steam line downstream of the flow restricter and upstream of the MSIV. The system is initially at steady state at full power. Both the reactor and the turbines are assumed to trip coincident to the appearance of the break. The system decay heat function is assumed to be 1.0 times the ANS standard.

The 12 specified sequences for this initiator are listed in Table J.7. The differences in sequence specification involve MSIV operation, MFW runback after trip, ADV operation, isolation of AFW to the affected steam generator, HPI operation, and operator action to turn off the charging pumps and throttle AFW flow.

J.6.2 Basis for Extrapolation

LANL Transient 2 serves as the basis for evaluation of sequences involving small (TBV sized) steam line breaks. It is assumed that the loop flow data in this transient is applicable to the smaller break transients although cooldown rates are lower. For a 1 ft^2 break the cooldown model predicted timing for SIAS, SGIS, and AFAS very similar to the timing predicted by TRAC. With the Transient 2 loop flow trends and the TBV sized break, the cooldown model predicts SIAS at 25 s, SGIS at 85s and AFAS at 230 s for 1 loop blowdown or 410 s for blowdown of both SG (i.e. MSIV failure). All of the sequences use the same initial extrapolation but proceed to different end points based on specified conditions and actions.

J.6.3 Results and Discussion

J.6.3.1 Sequences 4.1 and 4.2

A. Basis - Transient 2

B. Departures from Basis

Sequences 4.1 and 4.2 require the operator to shut off the charging pumps when the primary repressurizes to the HPI shut off pressure. Sequence 4.1 also require operator action to throttle AFW to the intact SG while sequence 4.2 does not. Sequence 4.2 represents the most severe overcooling sequence of the two and will be used to characterize the group.

C. Temperature Extrapolation

The initial extrapolation described in Section I.6.2 was extended to SGA dryout at 860 s at which point the minimum temperature of 337°F (442 k) was obtained. Displacement of cold fluid by hot leg flow and reduction in HPI flow caused the downcomer temperature to rebound. The primary becomes hotter than the SGB secondary at about 1300 s causing restoration of natural circulation flow in loop B. Throttling of AFW in sequence 4.1 would occur later and therefore would not affect the course of the transient. Under the influence of decay heat the system reheats to 534°F (552 k) by 600 s. The temperature profile is presented in Figure J.19.

D. Pressure Extrapolation

The pressure during the sequences will drop an initial value of 2250 psia (15.5 MPa) to 1784 psia (12.3 MPa) at SIAS (25 s) and then to an assumed

minimum of 1200 psia (8.3 MPa) at 60 s. The primary is assumed to repressurize to the HPI flow limiting pressure of 1285 psia (8.9 MPa) when SGA dries out (860 s). System reheating and coolant swell causes water solid conditions at 6500 s, at which point the pressure is at the PORV set point pressure 2400 psia (16.6 MPa). The pressure profile is presented in Figure J.19.

E. Heat Transfer Coefficient

The downcomer heat transfer coefficient holds its initial value of 4230 Btu/hr $ft^{2o}F$ (24000 w/m^2 k) until RCP trip at 55 s. By 250 s the coefficient has dropped to its final value of 400 Btu/hr $ft^{2o}F$ (2270 w/m^2 k).

J.6.3.2 Sequences 4.3 and 4.4

A. Basis - Transient 2, Sequence 4.2

B. Departures from Basis

The sequences are similar to sequences 4.1 and 4.2 except that the charging pumps are not shut off, leading to complete repressurization early in the transient. Sequence 4.4 also features failure to throttle AFW to the intact SG and is chosen to represent this group.

C. Temperature Extrapolation

These sequences are virtually identical to sequence 4.2 out to SGA dryout (860 s). The continued addition of charging pump and AFW flow supplies excessive cooling to the system, limiting the final temperature to 486°F

(525 k) as shown in Figure J.20. The minimum temperature of 337°F (442 k) occurs at 860 s, the same as in sequence 4.2.

D. Pressure Extrapolation

This sequence follows the same profile as sequence 4.2 out to 860 s, where the operator is assumed to fail to shut off the charging pumps. The combination of coolant swell and charging pump flow increases the primary pressure to 2400 psia (16.6 MPa) by 2000 s as shown in Figure J.20. This rate of repressurization is consistent with the rate of the more severe transients.

E. Heat Transfer Coefficient

The downcomer heat transfer coefficient profile for sequence 4.4 is assumed to be the same as that for sequence 4.2.

J.6.3.3 Sequence 4.5

A. Basis - Transient 2, Sequence 4.2

B. Departures from Basis

Sequence 4.5 features operator actions to turn off charging pumps and to throttle AFW to the intact SG. However this sequence also specifies failure to isolate AFW to the affected steam generator.

C. Temperature Extrapolation

The initial extrapolation for sequence 4.2 applies out to 230 s. At this point AFAS initiates AFW flow to the broken SGA. The addition of AFW flow

to SGA inventory delays SGA dryout to 1300 s where the temperature is 314°F (430 K). Thereafter, break mass flow and system cooldown are limited by AFW flow to SGA. The arrival of the break flow limitation is signalled by a small temperature increase to 1350 s (see Figure J.21). The collective action of continued AFW flow and declining decay heat cause a cooldown to 281°F (411 k) at 7200 s).

D. Pressure Extrapolation

The primary pressure declines to an assumed minimum of 1200 psia (8.3 MPa) by 60 s and is assumed to recover to the HPI shut off pressure of 1285 psia (8.9 MPa) at 1300 s, where the operator kills the charging pumps. Despite continued but slow cooldown, the pressure is assumed to remain at 1285 psia (8.9 MPa) by occasional flow of HPI. (See Figure J.21).

E. Heat Transfer Coefficient

The downcomer heat transfer coefficient profile is assumed to the same as that of Sequence 4.2.

J.6.3.4 Sequence 4.6

A. Basis - Transient 2

B. Departures from Basis

In sequence 4.6 both MSIV's fail to close, resulting in blowdown from both steam generators. The operator is assumed to limit AFW flow to 160 gal/min per SG and turn off the charging pumps. These changes were extrapolated assuming symmetric loop flows with total flows equivalent to total loop

flows from Transient 2. Under these conditions SIAS, and SGIS occur at 25 s and 85 s, as they do in sequence 4.2. With blowdown from both steam generators, AFAS is delayed to 410 s. SG water inventory declines out to 5000 s where AFW begins to exceed break flow. There is a slight increase in SG water inventory out till the end of the sequence. The cooldown curve shown in Figure J.22 is dominated by the heat balance between decay heat and wall heat transfer inputs and losses due to AFW heating and break flow. The minimum temperature, 225°F (397 k) occurs at 7200 s.

D. Pressure Extrapolation

The pressure declines to the assumed lowest value of 1200 psia (8.3 MPa) by 60 s and is further assumed to rise to HPI shut off pressure, 1285 psia (8.9 MPa) by 1300 s, by which time the bulk of the cooldown and coolant shrinkage has concluded. The action of the HPI system will maintain pressure at this final value as indicated in Figure J.22.

E. Heat Transfer Coefficient

The downcomer heat transfer coefficient profile is assumed to be the same as that for sequence 4.2.

J.6.3.5 Sequences 4.7, 4.9, and 4.10

A. Basis - Transient 2 - System Response to Steam Line Break

B. Departures from Basis

Sequence 4.7 features a MFW overfeed to the affected steam generator and operator actions to throttle AFW to the intact SG and to turn off the

charging pumps. The loop flow data from Transient 2 and the overfeed flows and temperatures from Transient 9 were applied to these cases.

In sequence 4.9 the AFW is not throttled to the intact steam generator. In sequence 4.10 both steam generators are overfed. However, as illustrated in Transients 8 and 9, MFW overfeeds to intact steam generators does not result in significant overcooling events and so, inclusion with sequence 4.7 was assumed to be a valid representation.

C. Temperature Extrapolation

The overfeeding of SGA concurrent with the opening of the small steamline break results in SGIS being generated at 55 s versus 85 s for sequences where MFW overfeed does not occur. Approximately 100,000 lb (45,400 kg) of excess water is fed to SGA. This added inventory extends SGA dryout to 1700 s, at which time the minimum temperature of 318°F (432°F) is obtained. The system reheats to 534°F (552 k) by 3800 s where it is maintained by ADV action on SGB. Figure J.23 presents the temperature profile for this sequence.

D. Pressure Extrapolation

The pressure drops to the assumed lowest value of 1200 psia (8.3 MPa) by 60 s. The charging pumps are shut off as the system reaches HPI flow limiting pressure at 1600 s. The rapid reheating causes coolant swell and water solid conditions by 3500 s as predicted by the coolant swell model. The pressure profile is shown in Figure J.23.

E. Heat Transfer Coefficient

The downcomer heat transfer coefficient profile is assumed to be the same as that for sequence 4.2.

J.6.3.6 Sequence 4.8

Sequence 4.8 differs from Sequence 4.7 only in the failure of the operator to turn off the charging pumps. Because decay heat would overwhelm any cooling due to charging pump flow, this failure was judged to have negligible impact on temperature profile. The pressure profile is the same as that for Sequence 4.7 except that the action of the charging pumps will be to advance the timing of repressurization to the PORV set point, 2400 psia (16.6 MPa), at 2400 s versus 3500 s for Sequence 4.7. This difference is illustrated in Figure J.24. The downcomer heat transfer coefficient profile is assumed to be the same as that for Sequence 4.2.

J.6.3.7 Sequence 4.11

A. Basis - Transient 2 - response to steam line break

Transient 12 - behavior of stuck open ADV

B. Departures from Basis

This sequence features operator action to turn off charging pumps and to throttle AFW to the intact steam generator. This sequence also specifies a stuck open ADV in the line opposite the break. This value is not isolated. Since both steam generators are blowing down, provision was made for throttling AFW to 160 gal/min per line if no SG differential pressure

develops to initiate AFW isolation to the low pressure SG. Due to the disparity of "break" sizes, isolation is expected to occur.

C. Temperature Extrapolation

The open ADV does not perturb the timing of SIAS relative to that of Sequence 4.2. SGIS is advanced to 80 s and AFAS is advanced to 140 s. The signal to isolate AFW to the broken loop is expected before AFAS is generated. Therefore all AFW is directed to the loop with the stuck open ADV. The broken steam generator, SGA, dries out at 1650 s, where the system reaches its minimum temperature of 297°F (420 k). Decay heat input is greater than cooling due to ADV flow and AFW heating in SGB, so the downcomer temperature begins to recover. SGB begins to refill also, but never reaches the level where AFW is throttled. The final temperature is 394°F (474 k). The temperature profile is presented in Figure J.25.

D. Pressure Extrapolation

The primary pressure drops to its assumed minimum of 1200 psia (8.3 MPa) by 60 s and recover to HPI flow cut off pressure of 1285 psia (8.9 MPa) at SGA dryout, 1650 s. The charging pumps are turned off at that point. System reheating and coolant swell lead to water solid conditions and full repressurization to 2400 psia (16.6 MPa) at 4500 s as shown in Figure J.25.

E. Heat Transfer Coefficient

The downcomer heat transfer coefficient profile is assumed to be the same as that of Sequence 4.2.

J.6.3.8 Sequence 4.12

A. Basis Sequence 4.11

B. Departures from Basis

The only difference between Sequence 4.12 and 4.11 is the failure to turn off the charging pumps. All other descriptions of the sequences in Section J.6.3.7 apply here also.

C. Temperature Extrapolation

Sequence 4.11 and 4.12 are identical out to 1650 s where SGA dries out. The minimum temperature, as shown in Figure J.26, is 297°F (420 k). The cooling mechanisms of ADV steam flow, AFW heating in SGB, and charging pump flow combine to limit reheating relative to sequence 4.11. The final temperature is 363°F (457 K). This 31°F (17 C) difference is due to the incremental contribution of charging pump flow to a cooling regime dominated by ADV flow. As noted in Section J.6.3.6, charging pump flow alone will not significantly influence cooldown.

D. Pressure Extrapolation

The primary pressure response for this sequence will be the same as for sequence 4.11 out to 1650 s. Thereafter charging pump flow and coolant swell due to reheating will cause water solid conditions and repressurization to the PORV set point, 2400 psia (16.6 MPa) at 2400 s. This response is shown is Figure J.26.

E. Heat Transfer Coefficient

The downcomer heat transfer coefficient profile for Sequence 4.12 is assumed to be the same as that for Sequence 4.2.

J.7 Reactor Trip at Full Power

J.7.1 Description of Sequences

The sequences for reactor trip at full power are initiated by a reactor trip and simultaneous turbine trip. The cause of these trips is not specified. These sequences are characterized by subsequent failures of components and systems as delineated in Table J.8. The system was at steady state at full power prior to the trip. The decay heat function is assumed to be 1.0 times the ANS standard.

A total of 42 sequences are identified for this initiator on Table J.8. The differences in sequence specification involve MSIV operation, MFW runback after trip, various combinations of TBV and ADV failure, and operator actions to isolate stuck open ADV's and TBV's, turn off charging pumps, and throttle AFW flow.

C.7.2 Basis for Extrapolation

The course of sequences for the reactor trip initiators will be determined by the types of failures accompanying the initiator. The LANL calculations addressing these situations are:

Transient 2 - 1 ft^2 mainsteam line break at full power,

Transient 6 - turbine trip with turbine bypass valve stuck open,

Transient 7 - turbine trip with one TBV and one MSIV stuck open,

Transient 8 - main feedwater overfeed (both SG's), and

Transient 9 - main feedwater overfeed to one SG.

Transient 6 corresponds exactly to Sequence 5.18. Transient 9 corresponds closely to Sequences 5.2 and 5.3. All other sequences were either estimated explicitly or were assigned to a particular transient or extrapolated sequence. The types of cooldown mechanisms, such as multiple TBV failures or ADV-TBV combinations and mitigating factors such as SG isolation or SG dryout serve as the basis for sequence assignment. Of the 42 sequences in Table J.8 only 12 were evaluated explicitly. These are addressed separately.

J.7.3 Results and Discussion

J.7.3.1 Sequence 5.19

A. Basis - Transient 6

B. Departures from Basis

In this sequence two TBV's fail to close. The MSIVs are operable. All other conditions are similar to Transients 6 and 7.

C. Temperature Extrapolation

For two stuck open TBV's the cooldown model using Transient 6 flow parameters predicts SGIS just before 150 s. The minimum downcomer temperature is 498°F (532 k). MSIV closure ends the cooldown and the system reheats above 535°F (552 k) by 600 s. See Figure J.27.

D. Pressure Extrapolation

Due to similarities in conditions, pressure profile for Transient 6 was used to 150 s where the pressure is 1700 psia (11.7 MPa). Full repressurization to 2400 psia (16.6 MPa) is assumed at 600 s as shown in Figure J.27.

E. Heat Transfer Coefficient

The downcomer heat transfer coefficient profile of Transient 6 was used as the heat transfer coefficient from the TRAC calculation remains above 420 Btu/hr $ft^2{}^oF$ (2380 w/m^2 k) throughout the transient.

J.7.3.2 Sequence 5.20

A. Basis - Transient 6

B. Departures from Basis

In this sequence three TBV's fail to close. The MSIVs are operable. All other conditions are similar to Transients 6 and 7.

C. Temperature Extrapolation

For three stuck open TBV's and flow parameters for Transient 6, the cooldown model predicts SGIS by 120 s with a downcomer minimum temperature of 499^oF (532 k). The system reheats to 530^oF (550 k) by 600 s. The temperature profile is presented in Figure J.28.

D. Pressure Extrapolation

The pressure profile from Transient 6 is used for this sequence (see Figure J.28).

E. Heat Transfer Coefficient

The downcomer heat transfer coefficient profile of Transient 6 is used for this sequence.

I.7.3.3 Sequence 5.21B

A. Basis - Transient 7

B. Departure from Basis

In this sequence on TBV fails to close and one MSIV fails to close. 600 s after the MSIV failure, the TBV is isolated. The operator is also assumed to turn off the charging pumps and throttle AFW at + 22 inches level.

C. Temperature Extrapolation

In Transient 7, a MSIV fails to close at 509 s. 600 s later (1109 s) the stuck open TBV is isolated. Transient 7 data are used to this point, where the minimum temperature of 479°F (521K) is obtained. The system reheats above 530°F (550 k) by 2300 s. (See Figure J.29).

D. Pressure Extrapolation

The pressure profile for Transient 7 is used for this transient out to 1106 s where the pressure is 1668 psia (11.5 MPa). The pressure never drops below the HPI flow cut off pressure, so the requirement to turn off the charging pumps is ignored. Between system reheating and charging pump flow, the system repressurizes to the PORV set point pressure of 2400 psia (16.6 MPa) by 2500 s.

E. Heat Transfer Coefficient

This sequence uses the downcomer heat transfer coefficient profile for Transient 4A out to 700 s where the value is held at the assumed minimum value of 400 Btu/hr $ft^2{}^oF$ (2270 w/m^2k).

J.7.3.4 Sequence 5.22

A. Basis - Transients 6 and 7, Sequence 5.19

B. Departures from Basis

In sequence 5.22 two TBV's fail to close and one MSIV fails to close. The TBV's are isolated by operator action 900 s after the MSIV fails. The operator also turns off the charging pumps and throttles AFW to the intact SG. The larger break (two TBV's) suggested early SIAS and SGIS so Transient 6 and Sequence 5.19 data were used for the early pressure extrapolation. Transient 7 was applied to later stages of the event.

C. Temperature Extrapolation

The results of Sequence 5.19 were used out to the initiation of SGIS at 150 s. One MSIV fails to close resulting in assymmetric steam generator pressure which isolates the AFW line to the affected steam generator before AFAS occurs. Therefore there is no AFW flow to the affected steam generator. Due to the size of the break, the affected steam generator dries out at 800 s where the minimum temperature of 397°F (476 k) is obtained. Affected SG dryout occurs 150 s before the TBVs are assumed to be isolated, so this action is too late to have any effect. The primary

reheats to above 530°F (550 k) by 2200 s. The temperature profile is presented in Figure J.30.

D. Pressure Extrapolation

As in Sequence 5.19, the pressure is assumed to follow Transient 6 out to 150 s where the pressure is 1700 psia (11.7 MPa). Continued cooldown due to the stuck MSIV allows the pressure to drop below 1285 psia (8.9 MPa) by 500 s. Further depressurization was not shown in Figure J.30 although it did occur. HPI flow rates for primary pressures as low as 1100 psia (7.6 MPa) were used in temperature extrapolation prior to affected SG dryout. At 800 s, the SG dryout is complete and the system has repressurized to the HPI flow cut off pressure, 1285 psi (8.9 MPa), and the operator turns off the charging pumps. The coolant swell model predicted water solid conditions and full repressurization to the PORV set point, 2400 psia (16.6 MPa) by 1800 s.

E. Heat Transfer Coefficient

The downcomer heat transfer coefficient profile of Transient 6 was used for this sequence.

J.7.3.5 Sequence 5.25A

A. Basis - Transient 7

B. Departures from Basis

The only differences between this sequence and Transient 7 are the failure of both MSIV's to close the requirements that the operator turns off the

charging pumps on repressurization to the HPI flow cut off pressure and reduction of AFW flow to 160 gal/min per steam generator.

C. Temperature Extrapolation

The sequence follows the temperature profile of Transient 7 out to 570 s where SGIS fails to cause closure of both MSIV's. The operator limits AFW to 160 gpm per steam generator, at which flow, neither steam generator goes dry throughout the sequence. Blowdown continues until 7200 s where the final minimum temperature is 348°F (449K). The temperature profile is presented in Figure J.31.

D. Pressure Extrapolation

The transient is sufficiently mild that depressurization below the HPI cut off pressure does not occur. The requirement to shut off charging pumps is ignored here and the system is allowed to fully repressurize. The pressure profile for Transient 7 was applied to this sequence as shown in Figure J.31.

E. Heat Transient Coefficient

The downcomer heat transfer coefficient profile is assumed to be the same as that for Transient 6, which never drops below a value of 420 Btu/hr ft^2 °F (2380 W/m^2 °F).

J.7.3.6 Sequence 5.25B

A. Basis - Transient 7

B. Departures from Basis

In this sequence 1 TBV sticks open and both MSIV's fail to close. The operator isolates the TBV 600 s after SGIS. The operator is assumed to turn off the charging pumps and limit AFW after MSIV failure to 160 gal/min per SG.

C. Temperature Extrapolation

The temperature profile for Transient 7 is used for this sequence out to 570 s where SGIS occurs. The failure of both MSIV's to close requires extrapolation after this point. The total loop flow rates from Transient 7 were assumed to be evenly divided between loops A and B for the extrapolation. No assymmetry effects were assumed. The minimum temperature at TBV isolation, approximately 1100 s, was 433°F (496 k). Thereafter, the system reheats to above 530°F (550 k) by 2300 s as shown in Figure J.32.

D. Pressure Extrapolation

The pressure profile for Transient 7 was assigned to this sequence due to similarity of conditions.

E. Heat Transfer Coefficient

The downcomer heat transfer coefficient for this sequence is assumed to be the same as that for Sequence 5.21B, which assumes Transient 7 response out to 700 s and assignment of the corrected minimum of 400 Btu/hr ft^2°F (2270 w/m^2) thereafter.

J.7.3.7 Sequence 5.26A

A. Basis - Transient 7

B. Departures from Basis

In this sequence, 2 TBV's fail to close and both MSIV's fail to close. The operator is assumed to limit AFW flow to 160 gal/min per SG, throttle AFW upon reaching +22 inch indicator level in the SG's, and turn off the charging pumps on repressurizing the primary to the HPI flow limiting pressure. It is assumed that the TBV's are not isolated over the course of the sequence.

C. Temperature Extrapolation

The temperature profile for Transient 6 or 7 is used out to 50 s where 2 TBV's fail to close. Loop flow data for transient was adapted for extrapolation throughout the sequence. Extrapolation predicts SGIS generation at 150 s with failure of the MSIV's to close. AFAS occurs by 240 s. As shown in Figure J.33, the cooldown continues unchecked throughout the sequence. Steam generator secondary water inventory reaches its minimum at 3500 s. After this point AFW flow exceeds blowdown flow and the steam generators start to refill. However, the +22 inch level is not attained, so AFW is not throttled. The minimum temperature of 290°F (416K) occurs at 7200 s.

D. Pressure Extrapolation

The pressure profile for Transient 6 is used out to 150 s where the failure of the MSIS's to close causes continued depressurization to 1285 psia (8.9 MPa) at 500 s. Some further depressurization would occur but is not included here (see Figure J.33). The charging pumps are assumed to be turned off and the HPI is assumed to stabilize pressure at this final value.

E. Heat Transfer Coefficient

The downcomer heat transfer coefficient profile of Transient 6 is used for this sequence.

J.7.3.8 Sequence 5.26B

A. Basis - Transient 7, Sequence 5.22

B. Departures from Basis

In this sequence, 2 TBV's fail to close and both MSIV's fail to close. The operator is assumed to isolate the TBV's approximately 900 s after the MSIV failures. The operator is also assumed to turn off the charging pumps and limit AFW flow to 160 gal/min per steam generator.

C. Temperature Extrapolation

For this sequence the temperature profile for Sequence 5.22 was followed out to 150 s where SGIS occurs. The failure of both MSIV's allows the blowdown to continue until the stuck open TBV's are isolated (1050 s). The minimum temperature of 386°F (470 k) is obtained at 1100 s. Thereafter,

the system reheats above 530°F (550 k) by 3500 s. The temperature profile is presented in Figure J.34.

D. Pressure Extrapolation

The pressure profile for this sequence is shown in Figure J.34. The data for Transient 7 is used out to 150 s. Thereafter, the pressure is assumed to drop to 1285 psia (8.9 MPa) by 500 s and there remain until TBV isolation at 1050 s. Pressure would actually drop below the stated values for portions for the period prior to 1100 s, but such deviations could not be explicitly determined. As presented, the pressure profile represents an expected upper bound. The system will repressurize to the HPI flow cut off pressure, 1285 psia, and the operator will shut off the charging pumps. The reheating after TBV isolation will cause water solid conditions within the primary by 2700 s as predicted by the coolant swell model. The pressure will achieve its final value, 2400 psia (16.6 MPa) at this point.

E. Heat Transfer Coefficient

The downcomer heat transfer coefficient for Transient 6 was used for this sequence.

J.7.3.9 Sequence 5.27A

A. Basis - Transient 7

B. Departures from Basis

In this sequence 3 TBV's fail to close and both MSIV's fail to close. The operator is assumed to limit AFW flow to 160 gal/min per SG, to throttle

AFW upon reaching +22 inch indicator level in the SG's, and to turn off charging pumps upon repressurization to the HPI flow limiting pressure. It is assumed that the TBV's are not isolated throughout the sequence.

C. Temperature Extrapolation

The temperature profile for Transient 7 is used to 50 s where 3 TBV's fail to close. Extrapolation predicts SGIS at 120 s at which point both MSIV's fail to close. AFAS occurs at 140 s. The steam generators do not dry out, but do experience a minimum in secondary water inventor between 3000 s and 3500 s. AFW flow exceeds blowdown flow for the remainder of the sequence but the level does not rise enough to require AFW throttling. As shown in Figure J.35, the system obtains a minimum downcomer temperature of 259°F (399K).

D. Pressure Extrapolation

The pressure profile for this sequence is shown in Figure J.35. The profile from Transient 6 is used out to 150 s followed by an assumed drop to the final pressure of 1285 psia (8.9 MPa) by 500 s. Early in the sequence, lower pressures than the predicted values are expected.

E. Heat Transfer Coefficient

The downcomer heat transfer coefficient profile for Transient 6 is used for this sequence.

J.7.3.10 Sequence 5.27B

A. Basis - Transient 7, Sequence 5.20

B. Departures from Basis

In this sequence 3 TBV's are assumed to stick open following reactor trip and both MSIV's fail to close. The operator is assumed to isolate the TBV's 1200 s after SGIS, to throttle AFW flow to 160 gal/min per steam generator, and to turn off charging pump flow as the system repressurizes to the HPI flow cut off pressure.

C. Temperature Extrapolation

For this sequence the temperature profile for Sequence 5.20 was used out to 120 s where SGIS occurs. The MSIV failures allow blowdown to continue until 1300 s when the operator is assumed to isolate the TBV's. A minimum temperature of 339°F (443 k) is obtained at isolation. The system then reheats above 530°F (550 k) by 4300 s. The temperature profiles for the sequence is presented in Figure J.36.

D. Pressure Extrapolation

The pressure profile for the sequence is presented in Figure J.36. Transient 7 data were used out to 150 s where a pressure of 1700 psia (11.7 MPa) is obtained. Thereafter the pressure is assumed to drop to 1285 psia (8.9 MPa) by 500 s and remain at this level until 1300 s, just after isolation of the TBV's. Actual pressures will be lower than the assumed values over most of this period. Following TBV isolation the system reheats and eventually goes water solid. The coolant swell model

predicts repressurization to the PORV set point, 2400 psia (16.6 MPa), by 2700 s.

E. Heat Transfer Coefficient

The downcomer heat transfer coefficient profile of Transient 6 was selected for this sequence.

J.7.3.10 Sequence 5.35

A. Basis - Transients, 6, 7 - initial conditions, Transient 12-ADV flow behavior

B. Departures from Basis

In this sequence one ADV fails to close and both MSIV's fail to close. The operator is assumed to turn off the charging pumps upon repressurization to the HPI flow cut off pressure and to reduce AFW flow to 160 gal/min per steam generator. The loop flow data from Transient 6 was adapted to this sequence. Transient 12 ADV flow data were used to calibrate the choked flow function in the cooldown model.

C. Temperature Extrapolation

The sequence follows the first 50 s of Transient 6. At this point the TBV's and 1 ADV close. The remaining stuck open ADV does not cause any significant cooldown or primary depressurization due to its small flow. By 950 s, AFAS is obtained and AFW flow commences. Together, the open ADV and the AFW flow provide sufficient cooling to cause SIAS at 1400 s and RCP trip by 1430 s. SGIS occurs at about 1550 s but both MSIV's fail to

close. The operator reduces AFW flows and turns off the charging pumps as required. The SG blowdown and AFW flow reduce downcomer temperature to 419°F (488K) at 7200 s as shown in Figure J.37.

D. Pressure Extrapolation

The pressure profile follows Transient 6 out to 50 s where all of the TBV's and 1 ADV close. The pressure drops from an initial value of 2283 psia (15.7 MPa) to 1970 psia (13.6 MPa) at 50 s. The pressure stays at this level until cooldown commences upon initiation of AFW at 950 s. SIAS at 1755 psia (12.1 MPa) occurs by 1400 s and the system is assumed to depressurize to a final pressure of 1285 psia (8.9 MPa) by 1600 s. This behavior is shown in Figure J.37. The mildness of the transient suggests the depressurization to this level might not occur.

E. Heat Transfer Coefficient

The downcomer heat transfer coefficient remains constant at about 5000 Btu/hr ft^2 °F (28,360 W/m^2K) (Transient 6 data) out to he trip of thc RCP pumps after 1400 s. By 1500 s the heat transfer coefficient drops to its assumed minimum value of 400 Btu/hr ft^2 °F (2270 W/m^2K).

J.7.3.12 Sequence 5.36

A. Basis - Transients 6, 7 - initial conditions, Transient 12-ADV flow behavior

B. Departures from Basis

In this sequence both ADV's fail open, thus prolonging steam generator blowdown throughout the sequence period. The operator is assumed to turn off the charging pumps upon repressurization to the HPI flow cut off pressure and to throttle AFW at +22 inches indicated steam generator level. Automatic isolation of AFW is not generated since SG blowdown is symmetric.

C. Temperature Extrapolation

The temperature profile follows Transient 6 out to 50 s where all TBV's close. AFAS initiates AFW at 700 s. SGIS at 1100 s cuts off the MFW systems. As shown in Figure J.38, steam generator blowdown leads to a minimum temperature of 347°F (448K) at 7200 s.

D. Pressure Extrapolation

This sequence is initially milder than Transient 6 or 7. It is expected that the charging pumps flow can maintain primary pressure above the HPI flow cut off pressure. Although such selection is conservative, the pressure profile of Transient 7 was applied to this sequence (see Figure J.38).

E. Heat Transfer Coefficient

For this sequence, the downcomer heat transfer coefficient profile of Transient 7 was used out to 700 s where the assumed minimum value of 400 Btu/hr ft^2 °F is reached.

J.7.3.13 Remaining Sequences

Reactor trip sequences not explicitly evaluated in this section were assigned to the TRAC calculated transients or extrapolated sequences most closely aligned to the particular non-extrapolated sequences. The sorting procedure emphasized similarities in temperature profiles, sometimes at the expense of significant deviation in pressure profiles.

Table J.9 summarizes the assignments of the reactor trip and supporting rationale.

Sequences 5.1, 5.6, 5.9, 5.10, 5.13, 5.14, 5.17, 5.18, 5.21A, and 5.28 either do not suffer any overcooling at all or are mild events mitigated by the MSIV and MFIV systems. These are all grouped with Transient 6, a very mild transient, even though the temperature and pressure responses will be different. Sequences 5.2 and 5.3 are most like the mild Transient 9. Sequences 5.4 and 5.5 are likewise similar to Transient 8. All of these transients are so mild that the fracture mechanics calculation would likely not distinguish between them.

Sequences 5.7, 5.11, 5.15, 5.19 and 5.29 all feature failure of 2 TBV's with successful operation of the MSIV's and MFIV's. These sequences are represented by Sequence 5.19 (Section J.7.3.1), the most conservative of the group, which is still very mild (T_{min}=500°F) by FM standards. Sequences 5.8, 5.12, 5.16, 5.20, and 5.30 featuring 3 stuck open TBV's are all likewise mitigated by SGIs and are represented by Sequence 5.20.

Sequence 5.21A features one stuck open TBV and failure of 1 MSIV to close makes this sequence very similar to LANL Transient 7. Sequences 5.23 and

Table J.9 Reactor Trip Sequence Assignments

Sequence	P,T,h Profile Source	Comments
5.1	T-6	Normal trip sequence
5.2	T-9	Lower P
5.3	T-9	Exact match
5.4	T-8	Lower P
5.5	T-8	Exact match
5.6	T-6	Lower P
5.7	Seq. 5.19	SGIs ends cooldown, lower P
5.8	Seq. 5.20	SGIs ends cooldown, lower P
5.9	T-6	SGIs ends cooldown, lower P
5.10	T-6	SGIs ends cooldown
5.11	Seq. 5.19	SGIs ends cooldown
5.12	Seq. 5.20	SGIs ends cooldown
5.13	T-6	SGIs ends cooldown
5.14	T-6	SGIs ends cooldown, lower P
5.15	Seq. 5.19	SGIs ends cooldown, lower P
5.16	Seq. 5.20	SGIs ends cooldown, lower P
5.17	T-6	SGIs ends cooldown, lower P
5.18	T-6	Exact match
5.19	Sec. J.7.3.1	Extrapolated sequence
5.20	Sec. J.7.3.2	Extrapolated sequence
5.21A	T-7	lower p
5.21B	Sec. J.7.3.3	Extrapolated sequence
5.22	Sec. J.7.3.4	Extrapolated sequence
5.23	T-2	Higher T, lower P
5.24	T-2	Higher T, lower P
5.25A	Sec. J.7.3.5	Extrapolated Sequence
5.25B	Sec. J.7.3.6	Extrapolated Sequence
5.26A	Sec. J.7.3.7	Extrapolated Sequence
5.26B	Sec. J.7.3.8	Extrapolated Sequence

Table J.9 Reactor Trip Sequence Assignments (Continued)

Sequence	P,T,h Profile Source	Comments
5.27A	Sec. J.7.3.9	Extrapolated Sequence
5.27B	Sec. J.7.3.10	Extrapolated Sequence
5.28	T-6	SGIS ends Cooldown, lower P
5.29	Seq. 5.19	SGIS ends Cooldown, lower P
5.30	Seq. 5.20	SGIS ends Cooldown, lower P
5.31	Seq. 5.35	Higher T
5.32	Seq. 5.35	Higher T
5.33	Seq. 5.35	Higher T
5.34	Seq. 5.35	Higher T
5.35	Sec. J.7.3.11	Extrapolated sequence
5.36	Sec. J.7.3.12	Extrapolated sequence
5.37	T-2	Expected severity between T-2 and T-6
5.38	Seq. 3.6	Extected severity between Seq. 3.6 and T-6

5.24 which feature 3 and 4 TBV failures with failure of a single MSIV resemble Transient 2.

Sequences 5.31, 5.32, 5.33, and 5.34 feature a stuck open ADV but all are milder than Sequence 5.35, to which they are assigned.

Sequences 5.37 and 5.38 feature a failure to trip the turbine following a reactor trip. In addition, 1 MSIV fails to close in 5.37 and both MSIV's fail in 5.38. If turbine overspeed or underspeed protection systems promptly detect and correct the situation, these events will not have significant PTS consequence. As a conservative bounding case, such events could be considered equivalent to main steam line break cases Transient 2 and Sequence 3.6, respectively.

J.8 Small Break LOCA

J.8.1 Description of Sequences

The sequences for small break LOCA at full power are initiated by a PORV-sized break, 0.016 ft^2 (0.0015 m^3) opening at the top of the pressurizer with the system operating at full power. The break may be either non-isclatable or isolatable as required by the sequence specifications. Prior to the appearance of the break the system was at steady state at full power. The decay heat function following the trip was assumed to be 1.0 times the ANS standard.

The 17 specified sequences for this initiator are listed in Table J.10. The differences is sequence specification involve ADV operation, TBV operation,

and operator action to isolate the break, turn off the charging pumps where applicable, and throttle AFW flows.

J.8.2 Basis for Extrapolation

The basic course of the sequences will be directed by LANL Transient 12 which features 1 PORV and 1 ADV stuck open. Other LANL transients which address phenomena relevant to the required sequences are:

Transient 6 - 1 stuck open TBV,

Transient 7 - 1 stuck open TBV and 1 stuck open MSIV,

Transient 11 - medium break LOCA with intact SG's,

Transient 8 - main feedwater overfeed (both SG), and

Transient 9 - main feedwater overfeed to one SG.

Transient 12 corresponds almost exactly with Sequence 6.7. All other sequences require explicit estimation or selective assignment of profiles.

J.8.3 Results and Discussion

J.8.3.1 Sequences 6.1, 6.5, 6.17

A. Basis - Transient 12

B. Departures from basis

In sequence 6.1 a PORV fails open and all TBV's and ADV's operate properly. The operator is assumed to isolate the break at 1.5 h (5400 s) to turn off the charging pumps upn repressurization to the HPI flow limiting pressure, and to throttle AFW on SG level. The loop flow data from Transient 12

were applied to this sequence (total Transient 12 loop flow was divided equally among both loops) although the stuck open ADV in Transient 12 would tend to augment loop flow relative to these sequences.

Sequence 6.5 features and overfeed to one steam generator. Sequence 6.17 features a stuck open TBV. Both of these situations are corrected by SGIS such that the initial perturbation is lost by 2000 s such that these sequences are very similar to Sequence 6.1 late in the event.

C. Temperature Extrapolation

The temperature profile for Transient 12 was used out to 227 s where the ADV's are assumed to close. Afterwards cooldown continues on the basis of HPI, charging pump and MFW flows absorbing heat from the system. SGIS occurs at 2200 s and eliminates the MFW flow. AFW is never initiated. Decay heat has declined to the extent that HPI and charging pump flows alone can continue cooldown at a rate which accelerates with time (i.e. as decay heat decreases) out to isolation of the break (PORV) at 5400 s (1.5 h). The system is water solid, so isolation of the break causes immediate repressurization which eliminates HPI flow and causes the operator to turn off the charging pumps. The minimum temperature of 412°F (484 K) occurs at this point. The downcomer temperature jumps to the SG temperature due to the loss of the localized cooling effects from HPI flow. General reheating of the system results in a final temperature of 523°F (546 K). The temperature profile is presented in Figure J.39.

D. Pressure Extrapolation

The pressure profile for Transient 12 is used out to 5400 s (1.5 h) as shown in Figure J.39. After isolation, the system is assumed to quickly repressurize to the HPI flow limiting pressure, 1285 psia (8.9 MPa) where the operator turns off the charging pumps. The system is essentially water solid and will experience repressurization to the primiary safety valve setpoint pressure due to the swelling of coolant from system reheating (see Section J.8.3.2, Sequence 6.3). Here it is assumed that the operator can manipulate coolant inventory to prevent such repressurization.

E. Heat Transfer Coefficient

The downcomer heat transfer coefficient profile of Transient 12 is used out to 450 s where the coefficient reaches the assumed minimum level of 400 Btu/hr $ft^2{}^oF$ (2270 W/m^2K).

J.8.3.2 Sequence 6.2

This sequence is similar to Sequence 6.1 in every particular except for the failure of the operator to turn off the charging pumps following isolation of the break. As shown in Figure J.40, the effect of this failure is to allow prompt repressurization to the primary safety valve set point pressure, 2500 psia (17.2 MPa). The temperature and heat transfer coefficient profiles are essentially unchanged.

J.8.3.3 Sequences 6.3, 6.4, and 6.6

A. Basis - Transient 12

B. Departures from Basis

These sequences feature a non-isolatable PORV sized break. Sequence 6.3 features normal runback of MFW while sequences 6.4 and 6.6 feature overfeeds of one and both steam generators respectively. The overfeeds will have little impact upon the system response late in the sequences and so may be grouped with Sequence 6.3. Transient 12 loop flows and wall heat flows are used in extrapolation of the sequences.

C. Temperature J.41 gives the temperature profile for the sequence. Transient 12 data is used out to 227 s after which the failure of 1 ADV to close causes Transient 12 to become colder than this sequence. The combined effects of MFW flow to the system generators and increasing HPI flow provides enough cooling to cause continued decline in the downcomer temperature. By 2200 s the steam generators have cooled to below 500°F (533 K) where SGIS terminates MFW flow. Decay heating has declined to the extent that cooling from HPI flow alone can continue the cooling, but at a slower pace. There are no demands on the AFW systems in this sequence. The final downcomer temperature is 375°F (464 K).

D. Pressure Extrapolation

The pressure profile for Transient 12 was applied to this sequence in its entirety, 0 to 7200 s. This profile is presented in Figure J.41.

E. Heat Transfer Coefficient

The downcomer heat transfer coefficient profile of Transient 12 is used out to 450 s where the coefficient reaches the assumed minimum of 400 Btu/hr $ft^2{}^oF$ (2270 W/m^2K).

J.8.3.4 Sequences 6.7, 6.9, and 6.13

A. Basis - Transient 12

B. Departures from Basis

These sequences feature a non-isolatable PORV-sized break and 1 stuck open ADV. The operator is assumed to throttle AFW to the intact steam generator, an action not assumed for Transient 12. Sequence 6.9 features MFW runback failure to one steam generator and throttling of AFW and SG level. Sequence 6.13 includes failure of a single TBV to close and throttling of AFW to level.

C. Temperature Extrapolation

These sequences were treated as being equivalent even though Sequences 5.9 and 5.13 experience relatively strong cooldowns early on due to a MFW overfeed and a stuck open TBV respectively. SGIS will terminate cooldown from these mechanisms such that temperatures will still be above 500^oF (533 K). Some mild reheating of the system will occur until the Transient 12 cooldown mechanisms (i.e., 1 open ADV and HPI flow) can resume the system cooldown. This type of behavior is also demonstrated in Sequence 6.12 as discussed in Section J.8.3.7. Since the early cooldown mechanisms tend to resemble Transient 5 in the later stages they are grouped together with

Sequence 6.7. Sequence 6.7 itself is deemed equivalent to Transient 12. The only difference in specifications of Sequence 6.7 and Transient 12 is the throttling of AFW to the intact steam generator. Since, the intact loop is essentially stagnant for most of the sequence, there would be no discernable effect from the throttling of AFW. Therefore, the Transient 12 temperature profile was applied throughtout the event. The minimum temperature of 300°F (422 K) was obtained at 7200 s. (See Figure J.42).

C. Pressure Extrapolation

Due to similarities of case specification, the pressure profile of Transient 12 was used throughout the event. The pressure at 7200 s, the time of the minimum temperature, was 944 psia (6.5 MPa). (See Figure J.42).

D. Heat Transfer Coefficient

The downcomer heat transfer coefficient profile of Transient 12 was applied to this sequence out to 450 s where the coefficient reaches the assumed minimum level of 400 Btu/hr ft^2°F (2270 W/m^2 K).

J.8.3.5 Sequence 6.8

Sequence 6.8 varies from 6.7 in that the primary break is isolated at 5400 s (1.5 h) with the charging pumps being turned off as the system repressurizes to the HPI flow limiting pressure. The temperature response is taken to be the same as that of Transient 12. Some localized increase in downcomer temperature would be expected upon loss of HPI and charging pump flow. However, the open ADV is driving the cooldown at this point and

will prevent the type of large temperature increases reported for Sequences 6.1 and 6.2.

The pressure response follows that of Transient 12 out to 5400 s. Since the primary system is essentially water solid at the time the break (PORV) is isolated, the pressure rapidly rises to the HPI flow limiting pressure of 1285 psia (8.9 MPa) and the operator turns off the charging pumps. The temperature and pressure profiles are given in Figure J.43. The downcomer heat transfer coefficient profile is assumed to the same as that of Sequence 6.7.

J.8.3.6 Sequence 6.10

A. Basis - Transient 12

B. Departures from Basis

In Sequence 6.10 both ADV's fail to close after reactor trip. The operator is assumed to throttle AFW on SG level. With both ADV's open there will be sufficient cooling so that neither steam generator will stagnate. The affected loop flow from Transient 12 was applied to both loops in the sequence. This assumed symmetry will not yield differential pressures in the steam generators and the associated isolation of AFW to the low pressure steam generator.

C. Temperature Extrapolation

The sequence follows the trends for Transient 227 s where both ADV's are now assumed to fail open. SGIS occurs by 500 s, cutting off MFW flows. The closing of the MSIV's, of course, does not influence blowdown from the

open ADV's. AFAS occurs at 1150 s with the operator limiting AFW to 160 gal/min per steam generator. Blowdown and shrinkage of the SG secondary inventory coupled with this reduced AFW flow prevent attainment of the +22 in indicator level in the SG's by 7200 s. Higher AFW flow rates would result in AFW throttling within 7200 s but would not cause significantly lower temperatures. As shown in Figure J.44, the temperature declines to 252°F (395 K) by 7200 s.

D. Pressure Extrapolation

The pressure profile for Transient 12 was applied fully to this sequence as shown in Figure J.44.

E. Heat Transfer Coefficient

The downcomer heat transfer coefficient profile for Transient 12 was used out to 450 s where it decreases to the assumed minimum value of 400 Btu/hr ft^2°F (2270 W/m^2 K).

J.8.3.7 Sequences 6.11, 6.12, 6.14, 6.15, 6.16

A. Basis - Transients 11, 12

B. Departures from Basis

These sequences feature failures from 1 to 4 TBV's to close after reactor trip following initiation of the transient. MSIV and MFIV closure at SGIS will terminate this cooldown mechanism early, leaving HPI and charging pump flows as the only cooldown mechanism. Sequence 6.12 also features

a MFW runback failure to one SG and as a conservative case, was selected to represent the group.

C. Temperature Extrapolation

The combination of MFW overfeed and a stuck open TBV cause SGIS by 250 s. The closure of the MSIV's and MFIV's terminate cooldown from the SG's. Decay heat overwhelms the cooling due to HPI flow and the system reheats until the ADV's open at 600 s to limit temperature. The ADV's will cycle until 2500 s, when decay heat declines to the extent that HPI flow alone can continue the cooldown of the system. This early behavior is different than for sequences 6.1, 6.2, and 6.3 where continued MFW flow with HPI flow prevented reheating during the first 2500 s. AFAS is not induced in this sequence and hence AFW does not enter the picture. HPI induced cooling yields a final temperature of 410°F (483 K) at 7200 s as shown in Figure J.45. Stagnation of both SG loops was not assumed to occur based on the trends of Transient 11.

D. Pressure Extrapolation

The pressure profile for Transient 12 was used for this group of sequences. The profile is shown in Figure J.45.

E. Heat Transfer Coefficient

The downcomer heat transfer coefficient profile for Transient 12 was used out to 450 s where it drops to the assumed minimum value of 400 Btu/hr ft^2°F (2270 W/m^2K).

J.9 Medium Break LOCA

J.9.1 Description of Sequences

The sequences for medium break LOCA are initiated by a 2 inch diameter or 0.0218 ft^2 (0.002 m^2) break in the hot leg. The intent for choosing a break of this size is to obtain loop stagnation without total depressurization of the primary. The system is assumed to be at steady state at full power prior to the break. The decay heat function following reactor trip is assumed to be 1.0 times the ANS standard.

The seven specified sequences for this initiator are listed in Table J.11. The differences in sequence specification involve ADV operation, TBV operation, MFW runback and operator action throttle AFW when applicable.

J.9.2 Basis for Extrapolation

The basic course of the sequences will be directed by LANL Transient 11. Other LANL transients reflecting expected sequence phenomena include

Transient 6 - 1 stuck open TBV,

Transient 12 - small break LOCA with one stuck open ADV,

Transient 8 - main feedwater overfeed (both SG's), and

Transient 9 - main feedwater overfeed to one SG.

Transient 11 corresponds exactly to Sequence 7.1. All other sequences require explicit estimation or assignment of profiles.

J.9.3.1 Transients 7.1, 7.2, 7.3, 7.7, and 7.8

A. Basis - Transient 11

B. Departures from Basis

Sequence 7.1 corresponds exactly with Transient 11. Sequences 7.2 and 7.3 include overfeeds to one and both SG's respectively. Sequences 7.7 and 7.8 feature one and two stuck open TBV's respectively.

C. Temperature Extrapolations

The early cooldown mechanisms (TBV, overfeed) of Sequences 7.2, 7.3, 7.7, and 7.8 are terminated by SGIS. The temperature profiles for these case will recover somewhat and will closely resemble Transient 11 in the later stages. The potential for these deviations to bring on stagnated conditions could not be assessed. The temperature profile of Transient 11 was assigned to this group of sequences. The profile is shown in Figure J.46. The minimum temperature

D. Pressure Extrapolation

The pressure profile of Transient 11 is applicable to this group. The profile is given in Figure J.46.

E. Heat Transfer Coefficient

The downcomer heat transfer coefficient profile for this group follows the basic trends in Transient 11. The coefficient holds its initial value of 5040 Btu/hr $ft^2{}^oF$ (28530 W/m^2K) out to 64 s where the RCP's are tripped. By 250 s the value has dropped to about 650 Btu/hr $ft^2{}^oF$ (3690 W/m^2 K)

and the coefficient drops to its assumed minimum value of 400 Btu/hr $ft^2{}^oF$ (2270 w/m^2K) by 600 s.

J.9.3.2 Sequences 7.4 and 7.5

A. Basis - Transients 11, 12

B. Departures from Basis

These sequences feature a non-isolatable medium size primary break and a stuck open ADV. In Sequence 7.4 the operator is assumed to throttle AFW to the intact SG on level, in Sequence 7.5 the AFW is not throttled.

C. Temperature Extrapolation

Due to the similarity of conditions, the temperature profile of Transient 5 was applied to these sequences. The profile is shown in Figure J.47. The open ADV will ensure cooling induced loop flow in one loop so that the total stagnation predicted late in Transient 11 will not occur. The final temperature for the sequence is 300°F (422 K).

D. Pressure Extrapolation

The pressure profile for the sequences was assumed to be that of Transient 11. The profile is shown in Figure J.47. The final pressure is 512 psia (3.5 MPa).

E. Heat Transfer Coefficient

The downcomer heat transfer coefficient profile for these sequences is assumed to be the same as that for Sequence 7.1 (Section J.9.3.1). The

assumed minimum value of 400 Btu/hr $ft^2{}^oF$ (2270 W/m^2K) is obtained by 600 s in the sequence.

J.9.3.3 Sequence 7.6

A. Basis - Transient 11, Sequence 6.10

B. Departures from Basis

In Sequence 7.6, the non-isolatable primary break is accompanied by the failure of both ADV's to close after reactor trip. The operator is assumed to throttle the AFW on SG level reaching +22 inches.

C. Temperature Extrapolation

The failure of the ADV's to close will keep with SG's cool relative to the core exit and will promote natural circulation in both loops. Flow stagnation of the type in Transient 11 is not expected. The conditions in Sequences 7.6 and 6.10 are very similar so the temperature profile for Sequence 6.10 was applied to Sequence 7.6 (see Figure J.48). The minimum temperature of 252°F (395 K) is obtained at 7200 s.

D. Pressure Extrapolation

The pressure profile for Transient 11 was assigned to Sequence 7.6 due to similarity of conditions. The profile is presented in Figure J.48.

E. Heat Transfer Coefficient

The downcomer heat transfer coefficient profile for this sequence is assumed to be the same as that for Sequence 7.1 (Section J.9.3.1). The

assumed minimum value of 400 Btu/hr $ft^{2o}F$ (2270 W/m^2K) is obtained by 600 s in the sequence.

Figure C.1. P, T, h Estimation Approach

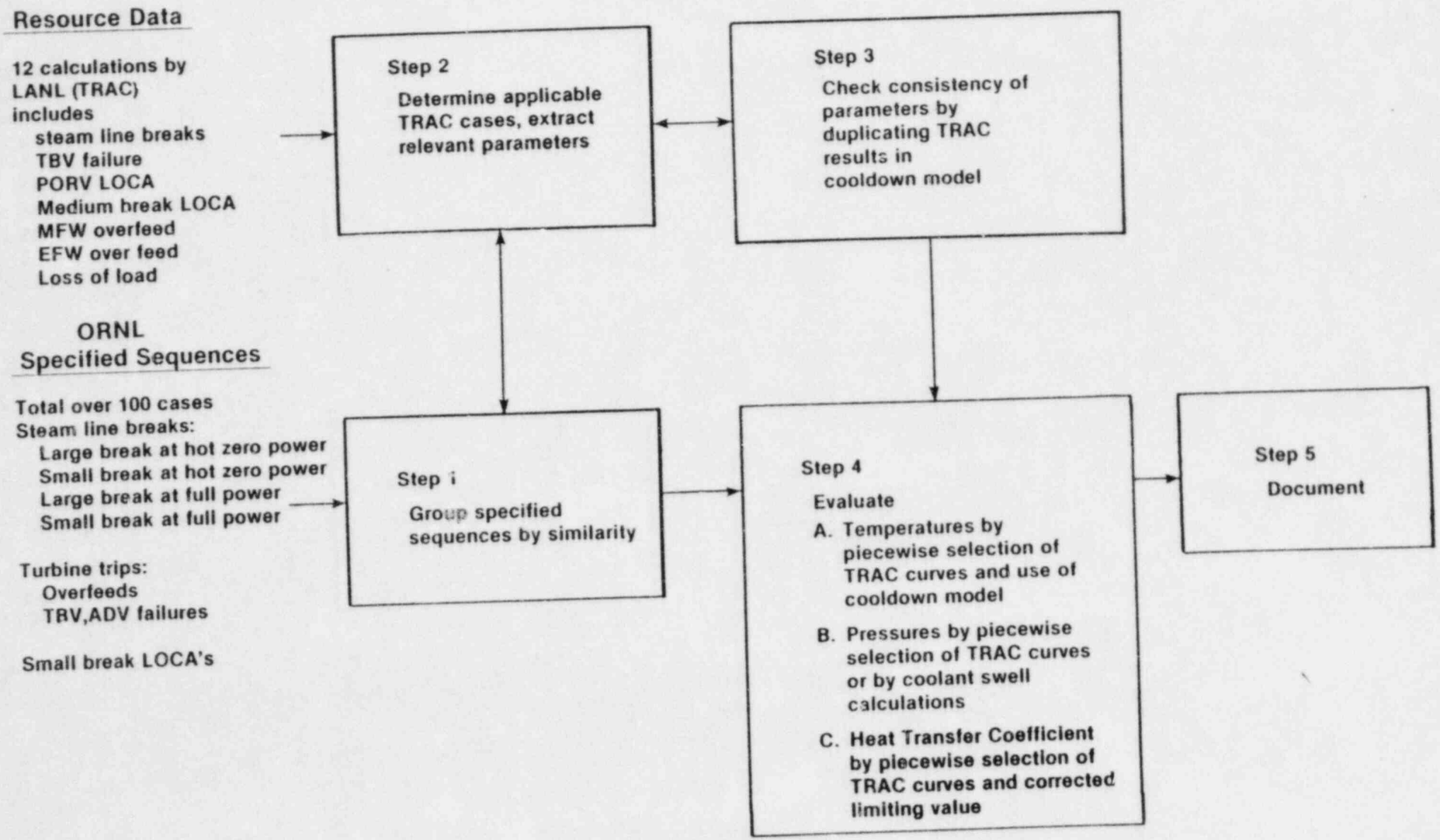

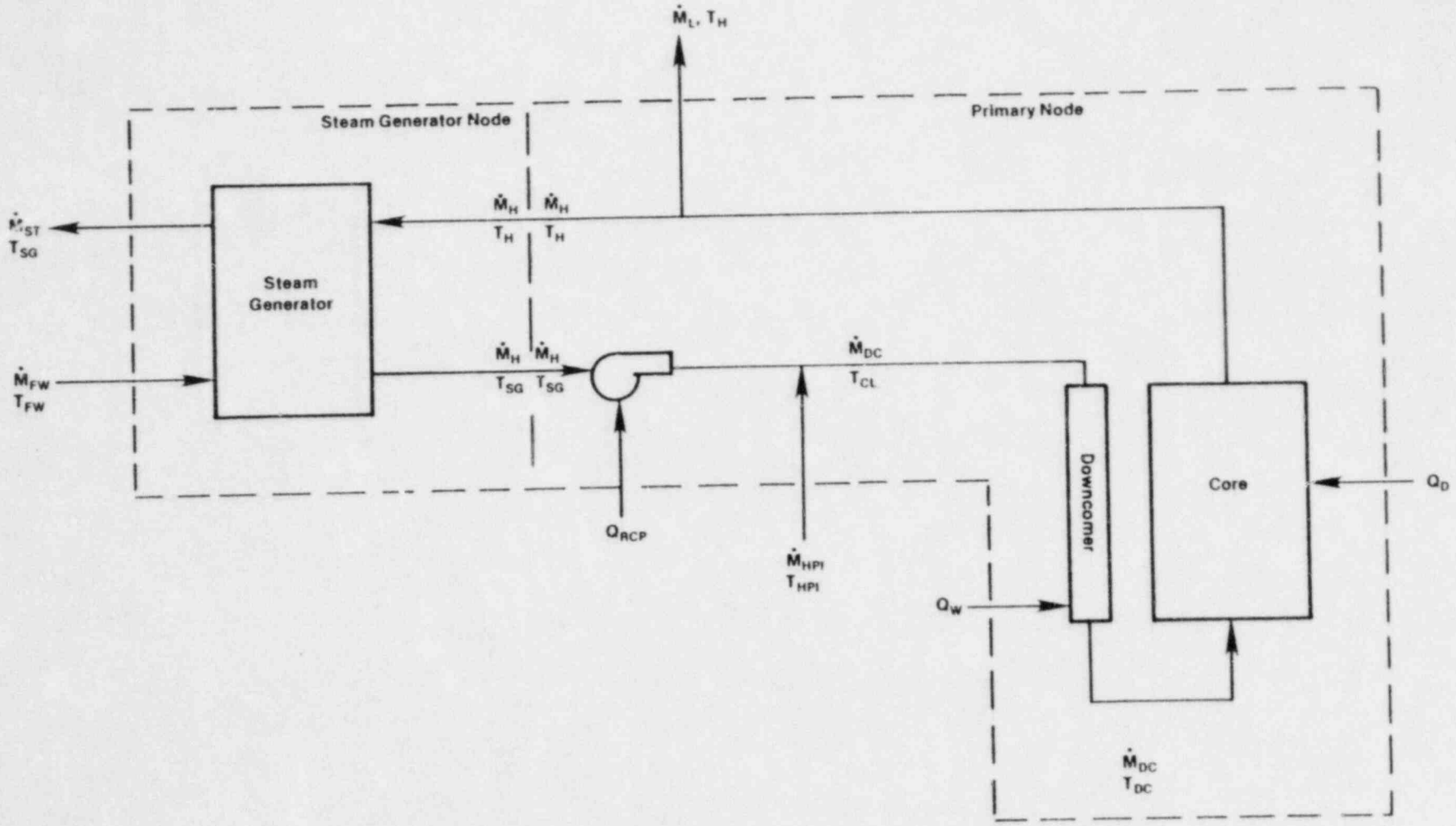

FIGURE C.2 MASS AND ENERGY FLOWS FOR 2 NODE COOLDOWN MODEL

TEMPERATURES AND PRESSURES FOR SEQUENCE 11

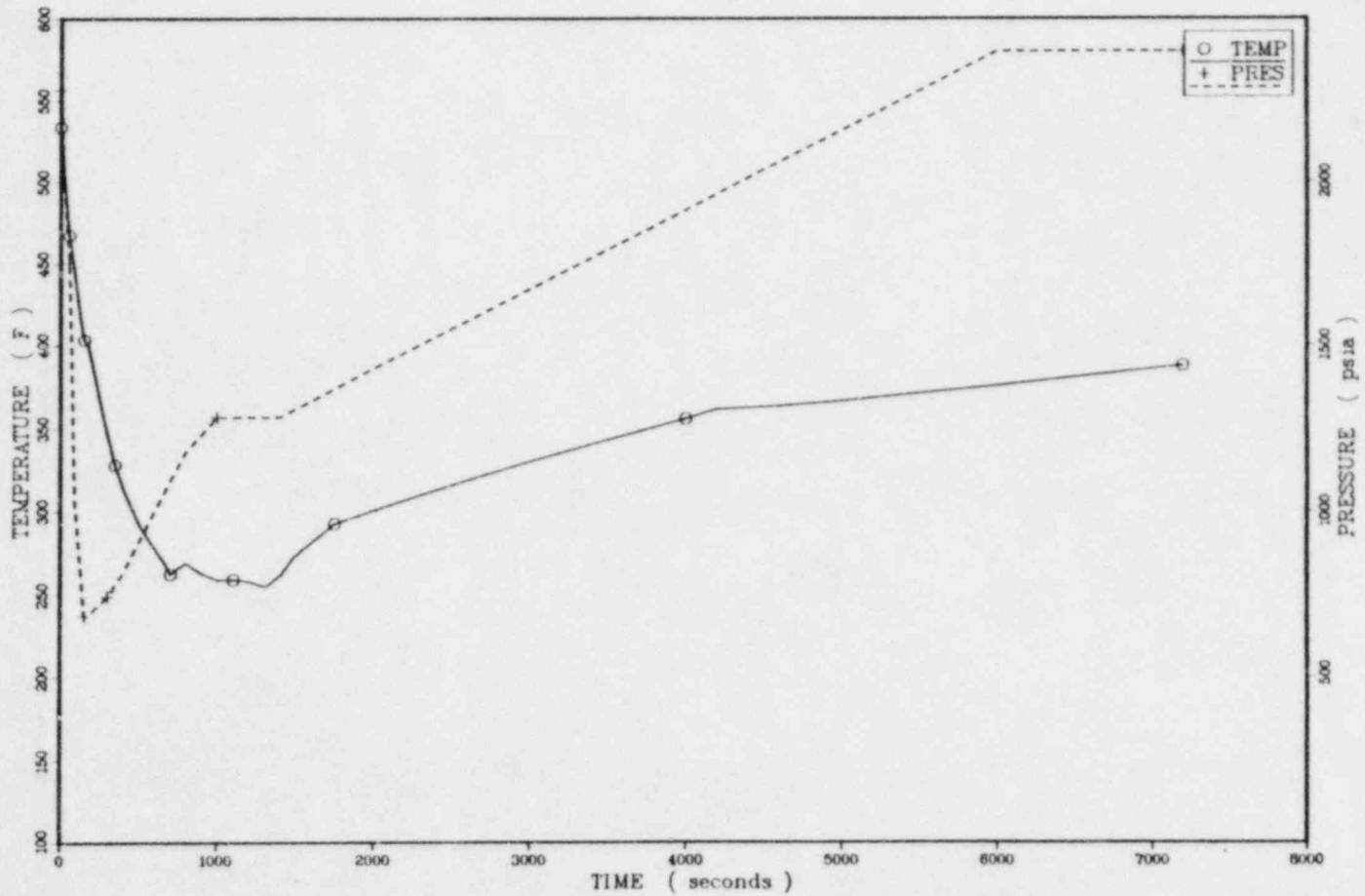

TEMPERATURES AND PRESSURES FOR SEQUENCE 12

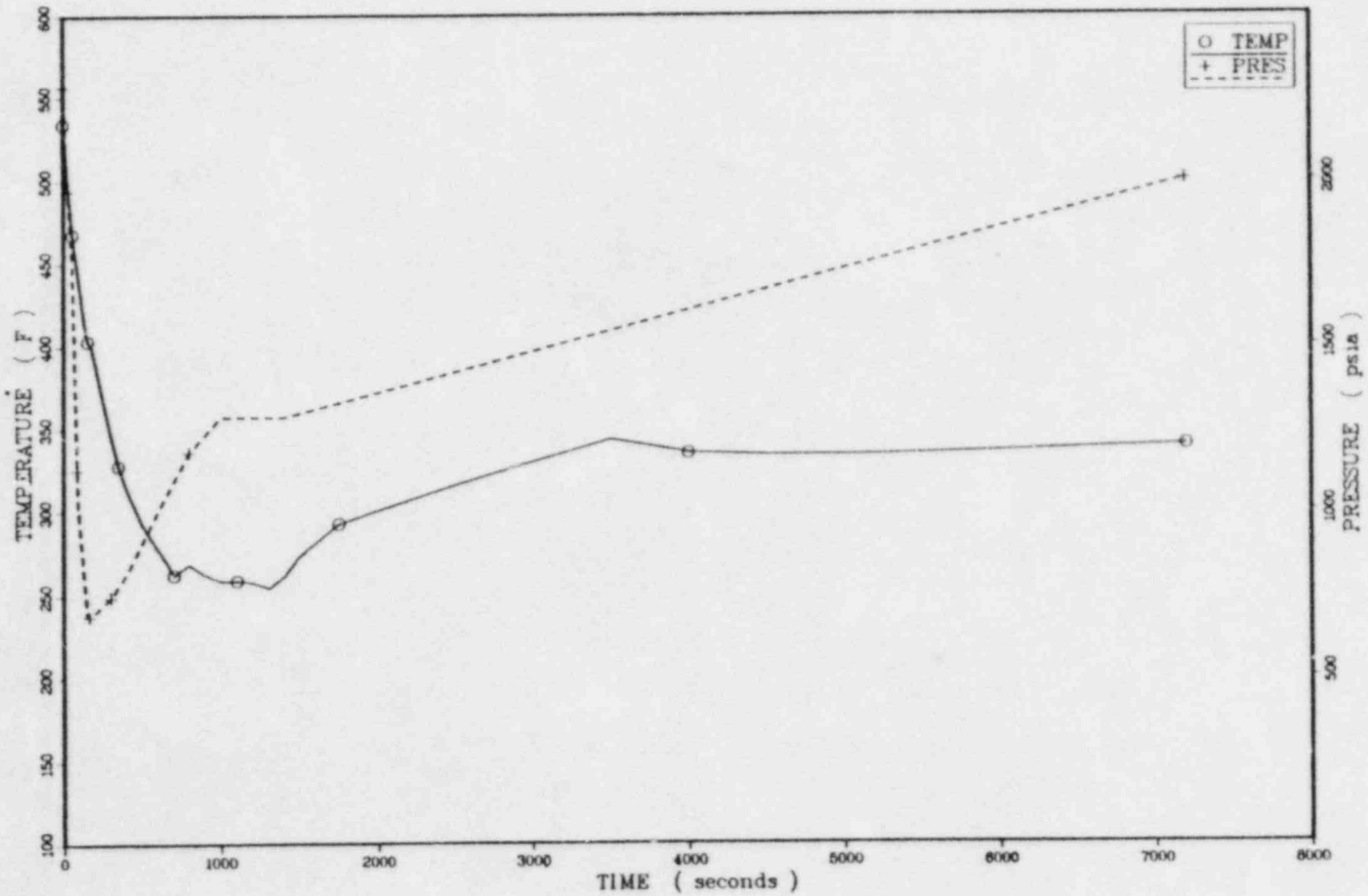

TEMPERATURES AND PRESSURES FOR SEQUENCE 1.3

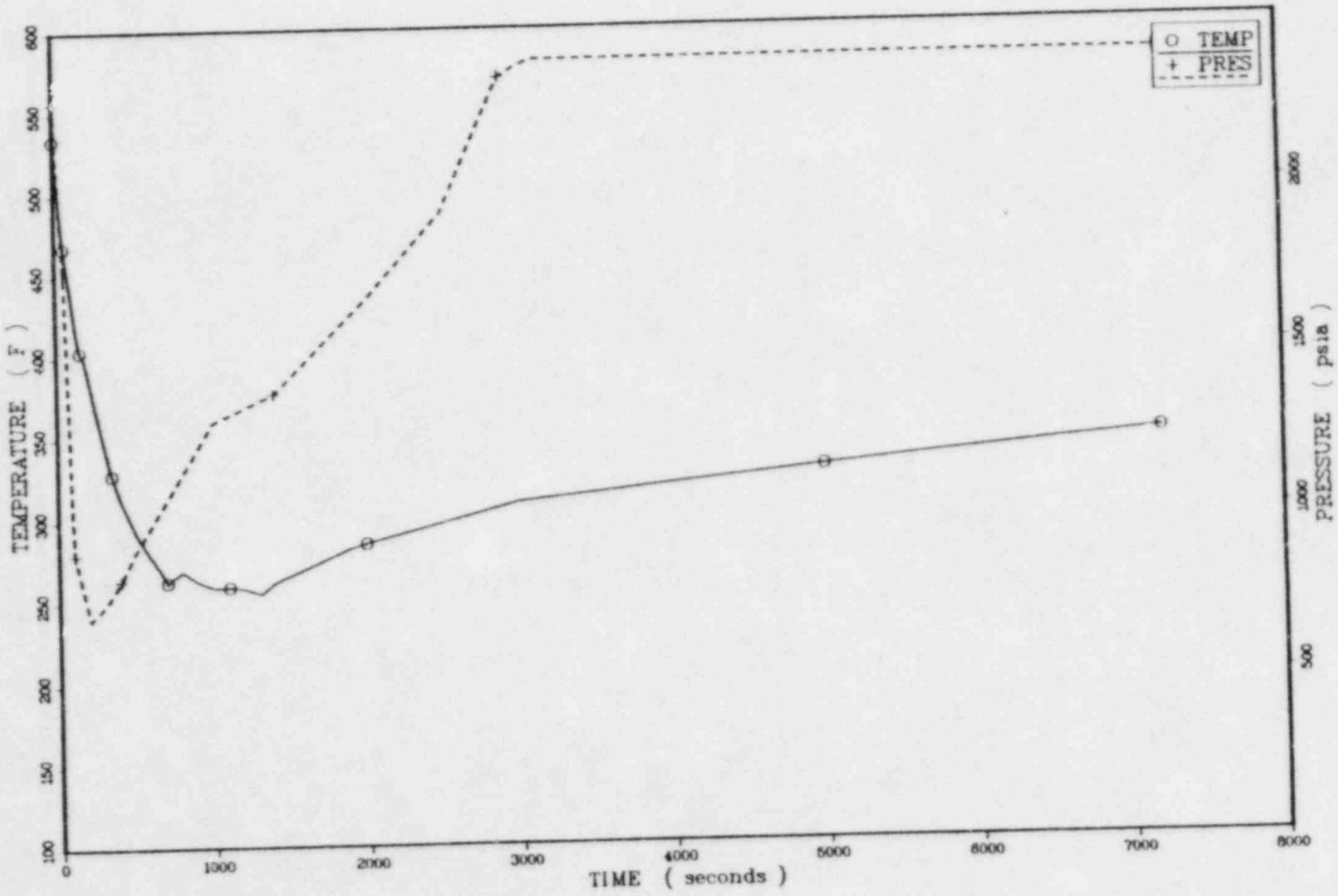

TEMPERATURES AND PRESSURES FOR SEQUENCE 1.5

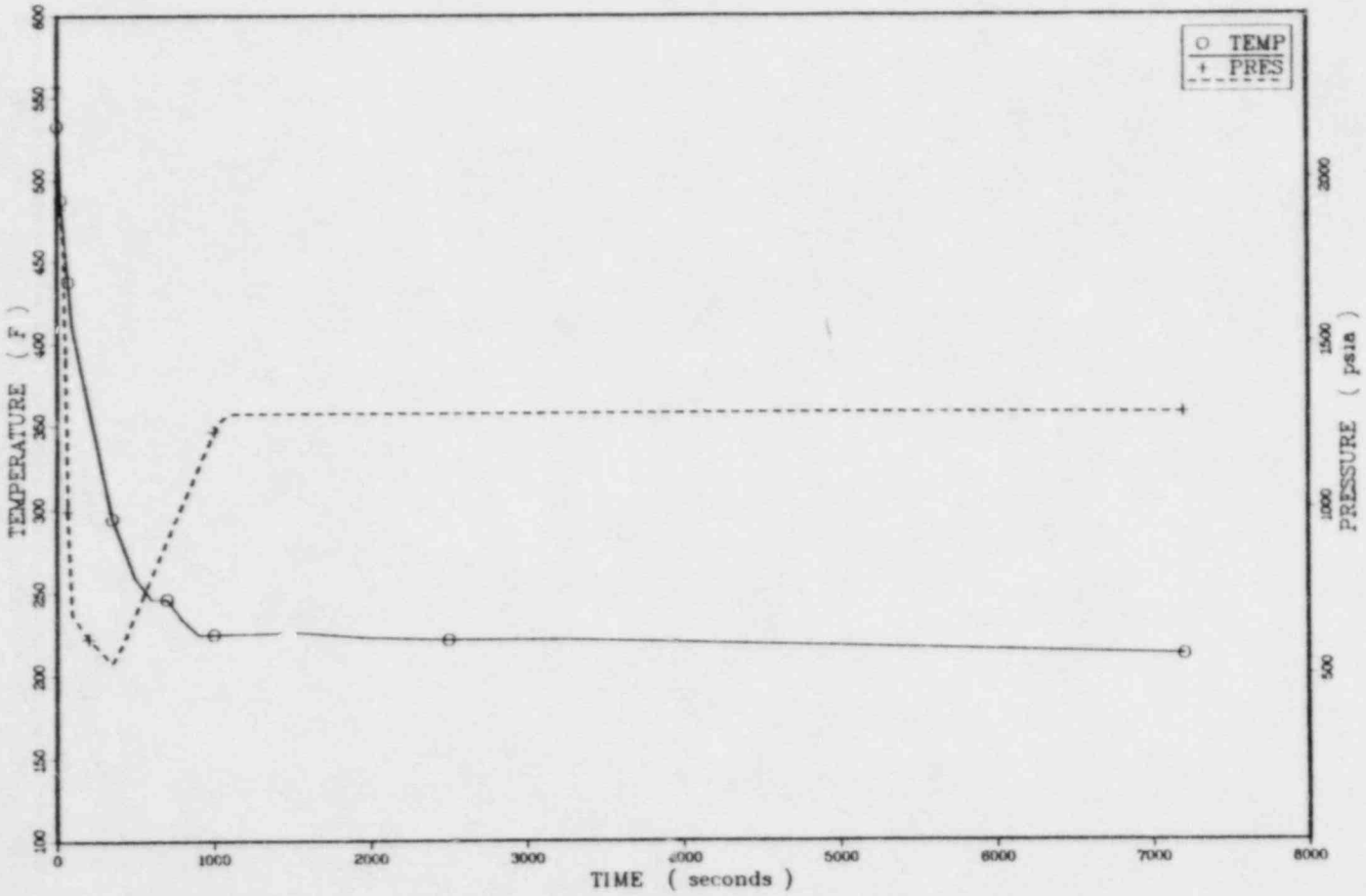

PLOT 1 08.26.52 WED 9 MAY, 1984 JOB-KTNOOS , ISSCO DISSPLA VER 8.2

TEMPERATURES AND PRESSURES FOR SEQUENCE 16

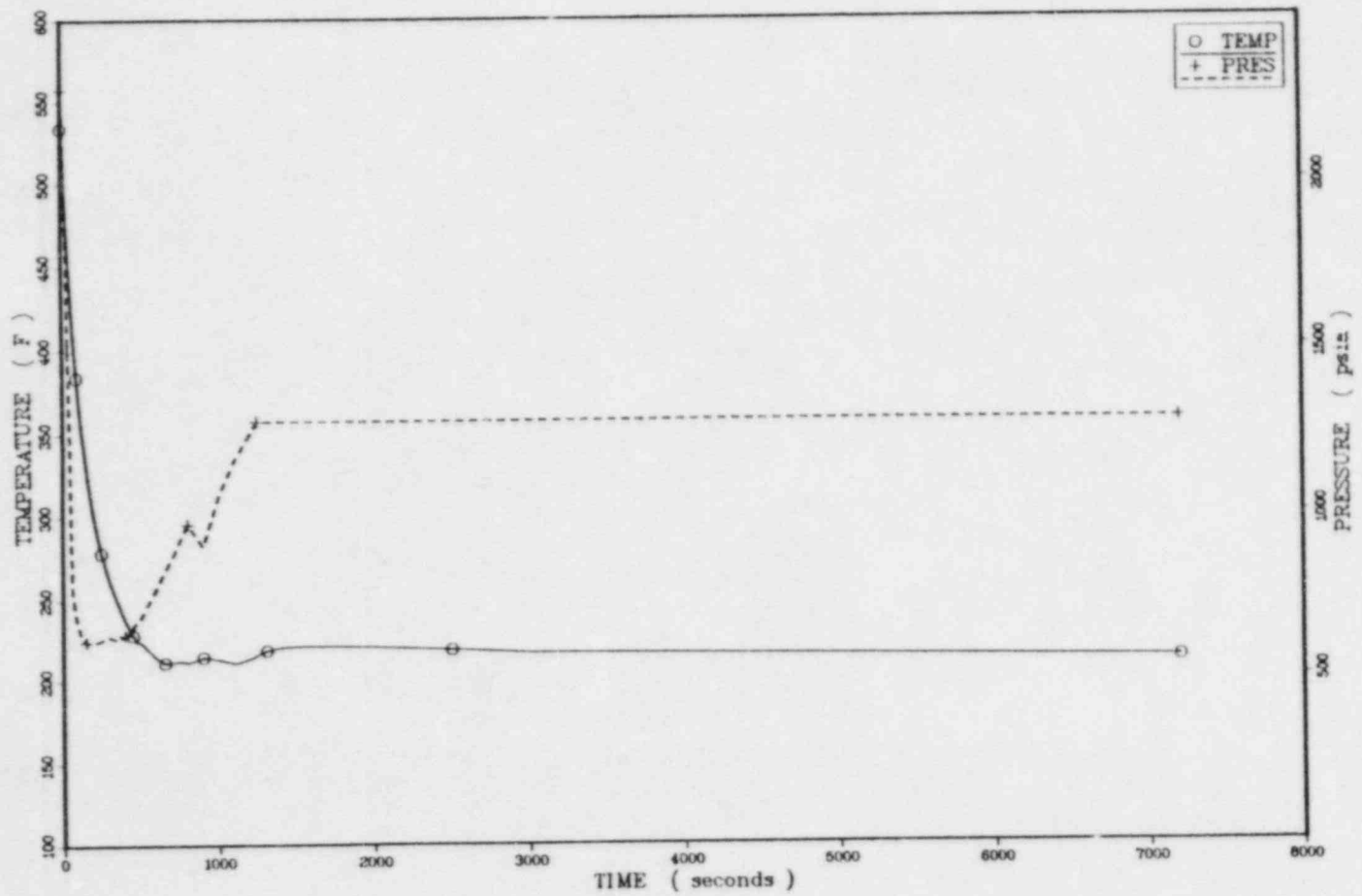

TEMPERATURES AND PRESSURES FOR SEQUENCE 21

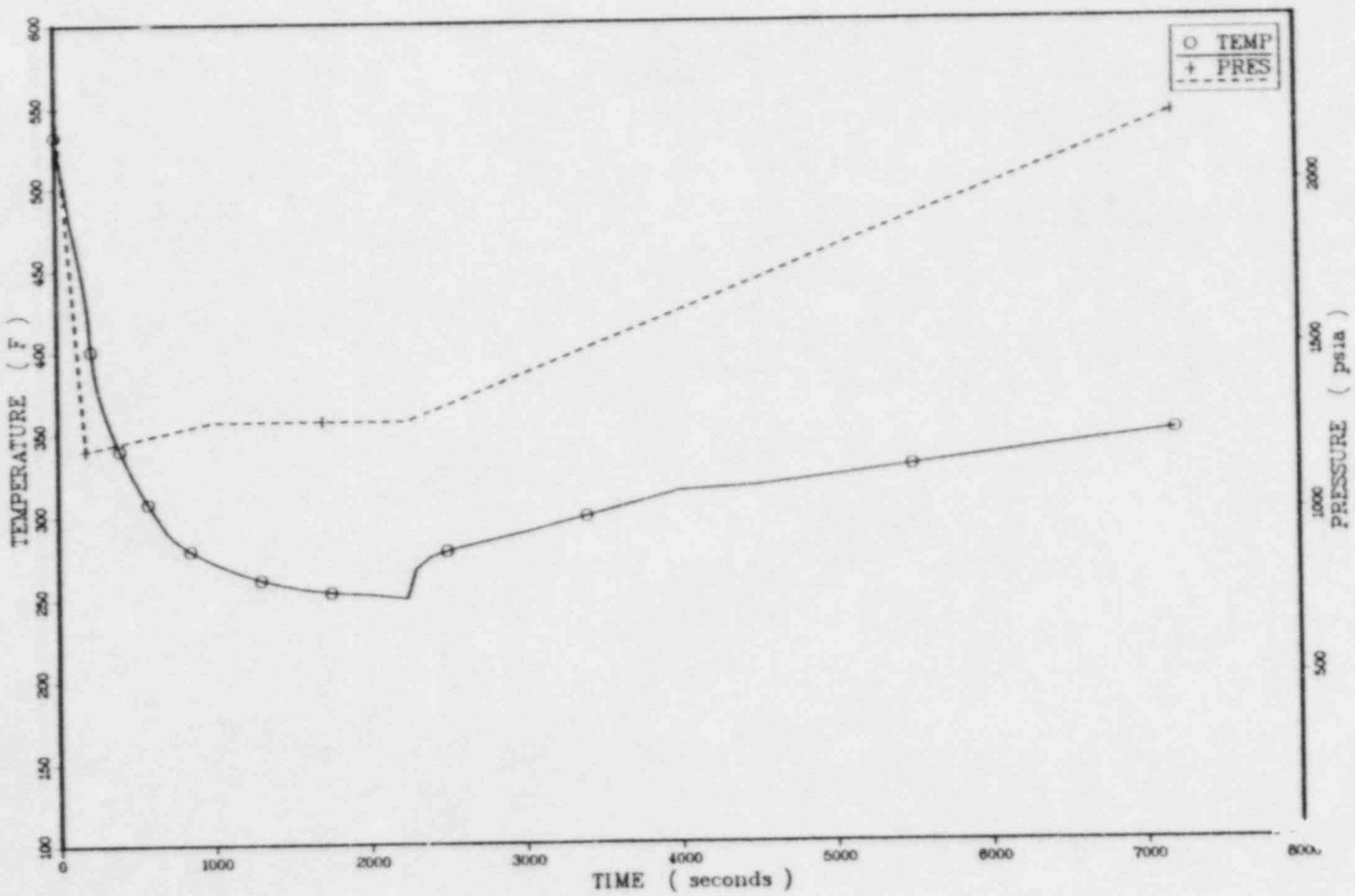

LGI 1 08.31.47 WED 9 MAY, 1984 JOB-KIM029 , ISSCO DISSPLA VER 8.2

TEMPERATURES AND PRESSURES FOR SEQUENCE 24

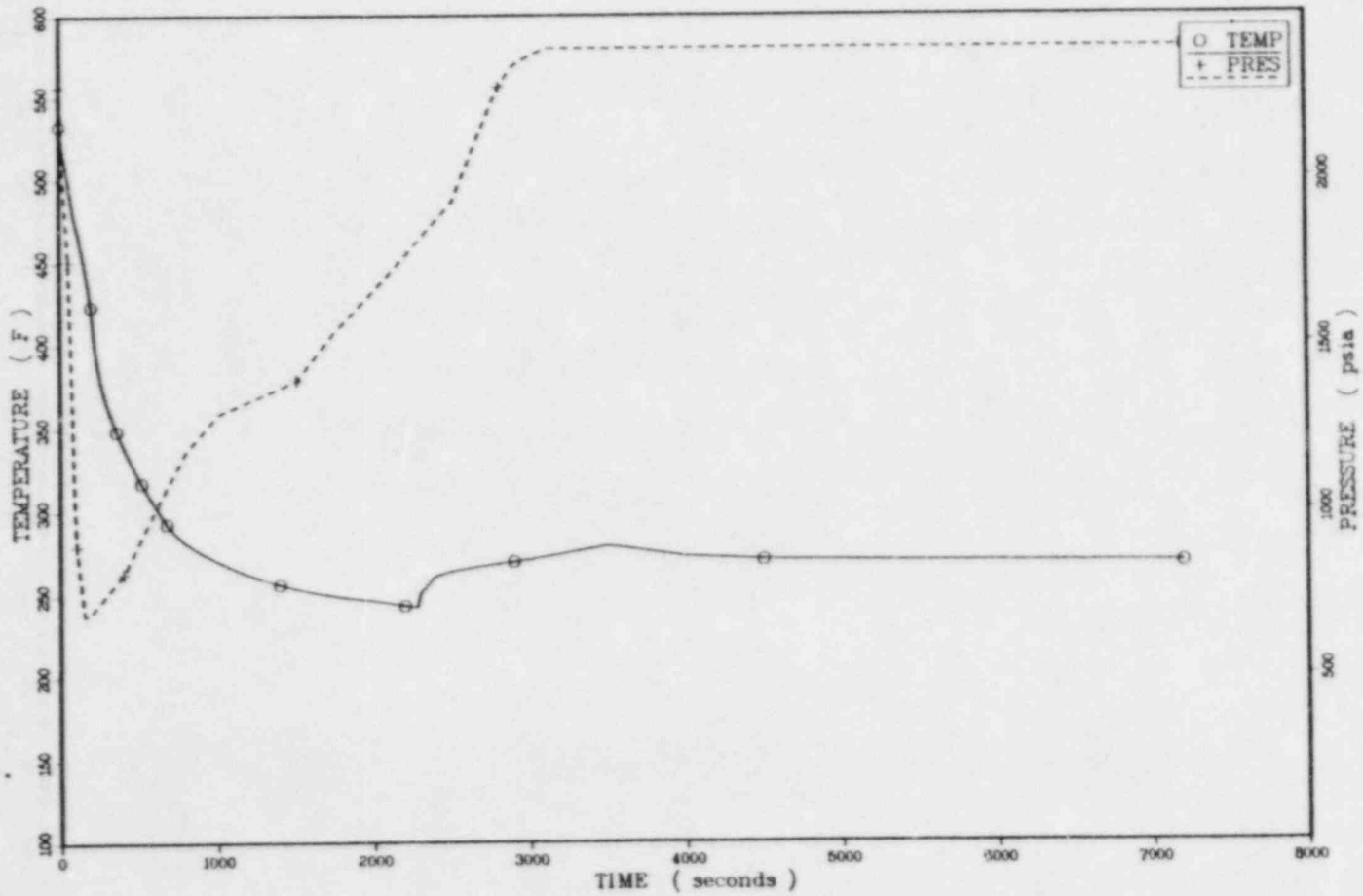

:T 1 00.33.11 WED 9 MAY, 1984 JOB-KTN030 , ISSCO DISSPLA VER 8.2

TEMPERATURES AND PRESSURES FOR SEQUENCE 25

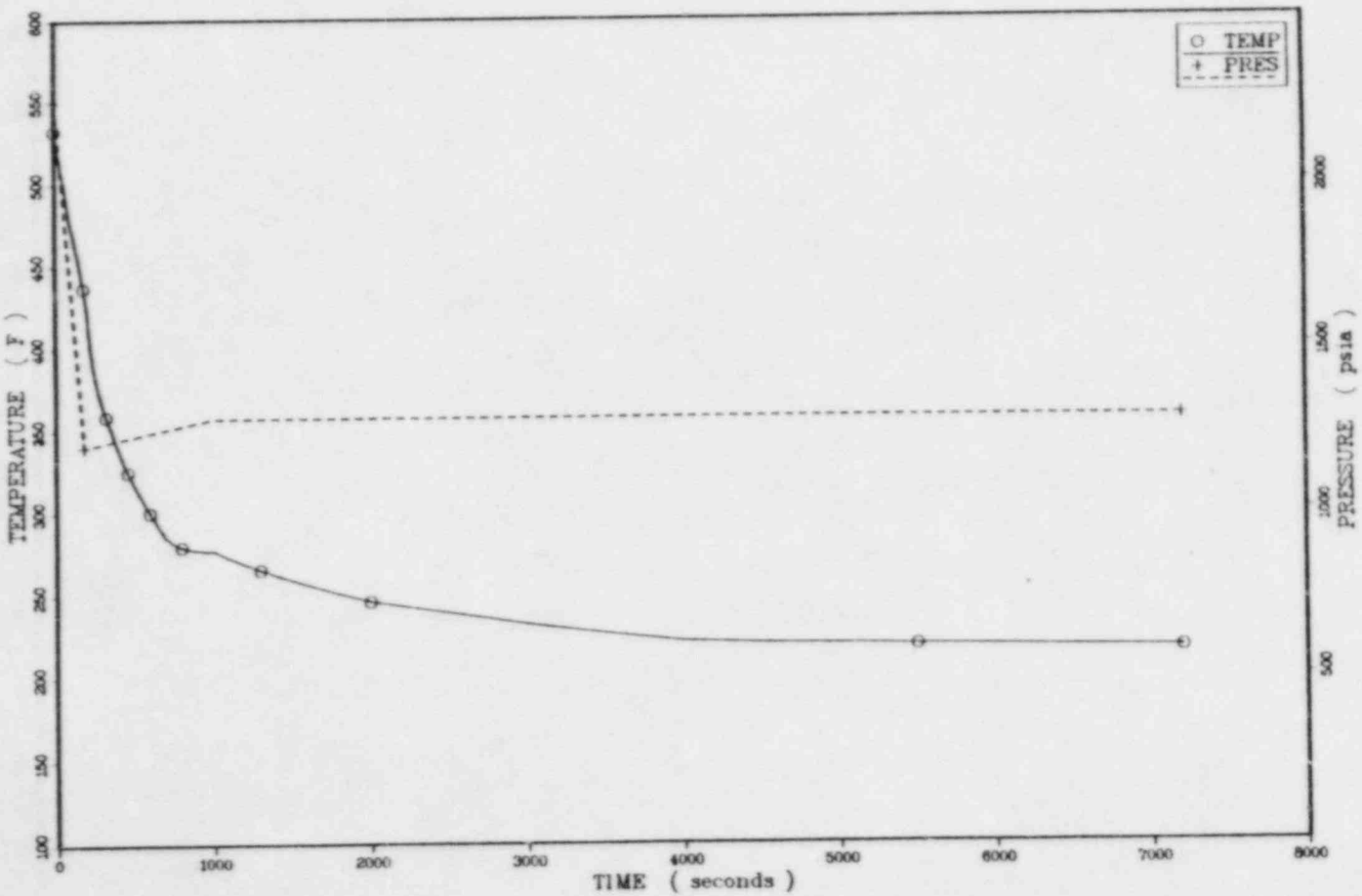

PLOT 1 00.35.06 WED 9 MAY, 1984 JOB-KIN031 , 15500 DISSPLA VER 8.2

TEMPERATURES AND PRESSURES FOR SEQUENCE 2.6

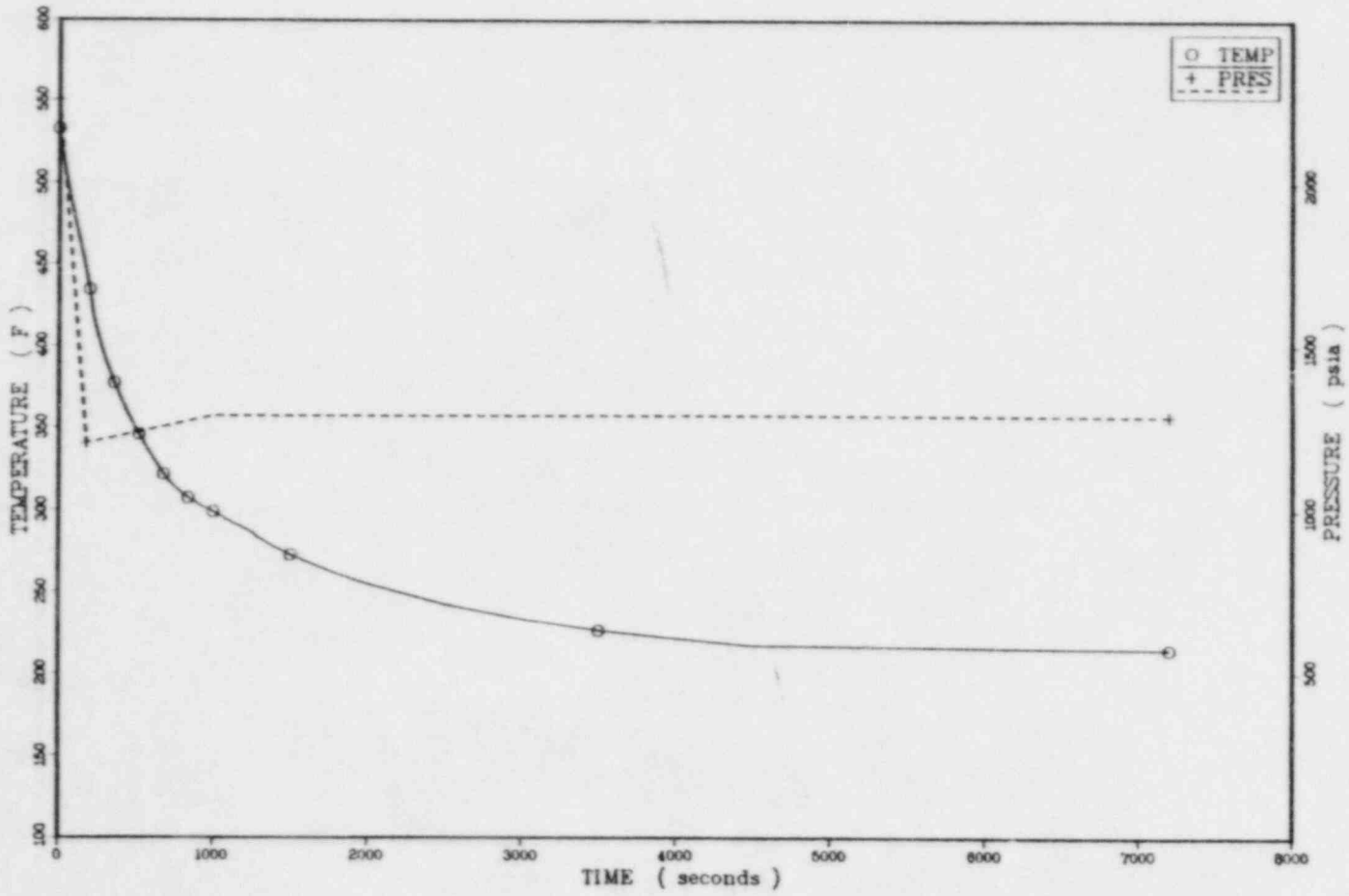

TEMPERATURES AND PRESSURES FOR SEQUENCE 27

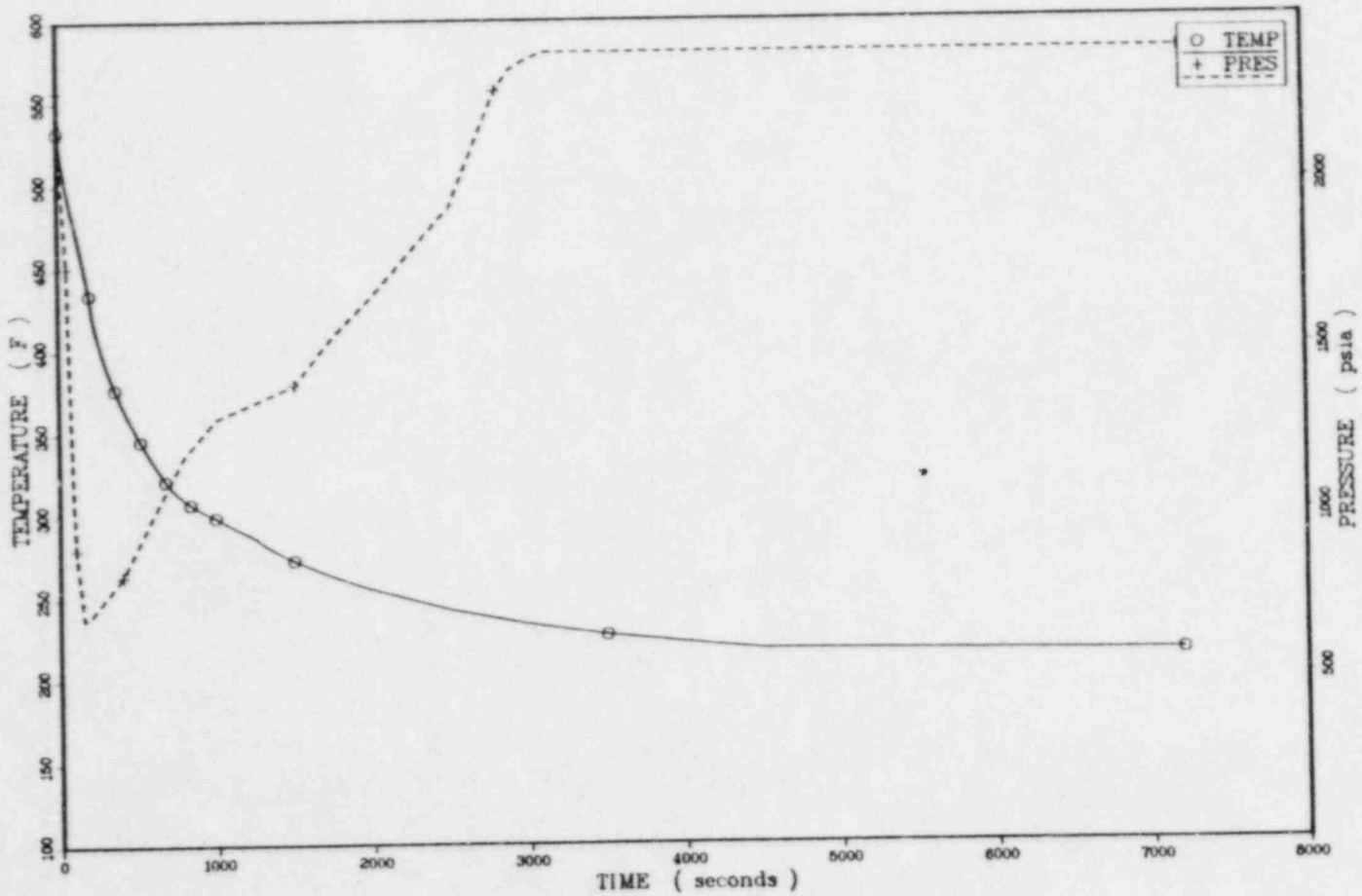

LOT 1 00.37.16 WED 9 MAY, 1984 JOB-KTN032 , ISSCO DISSPLA VER 8.2

TEMPERATURES AND PRESSURES FOR SEQUENCE 2.8

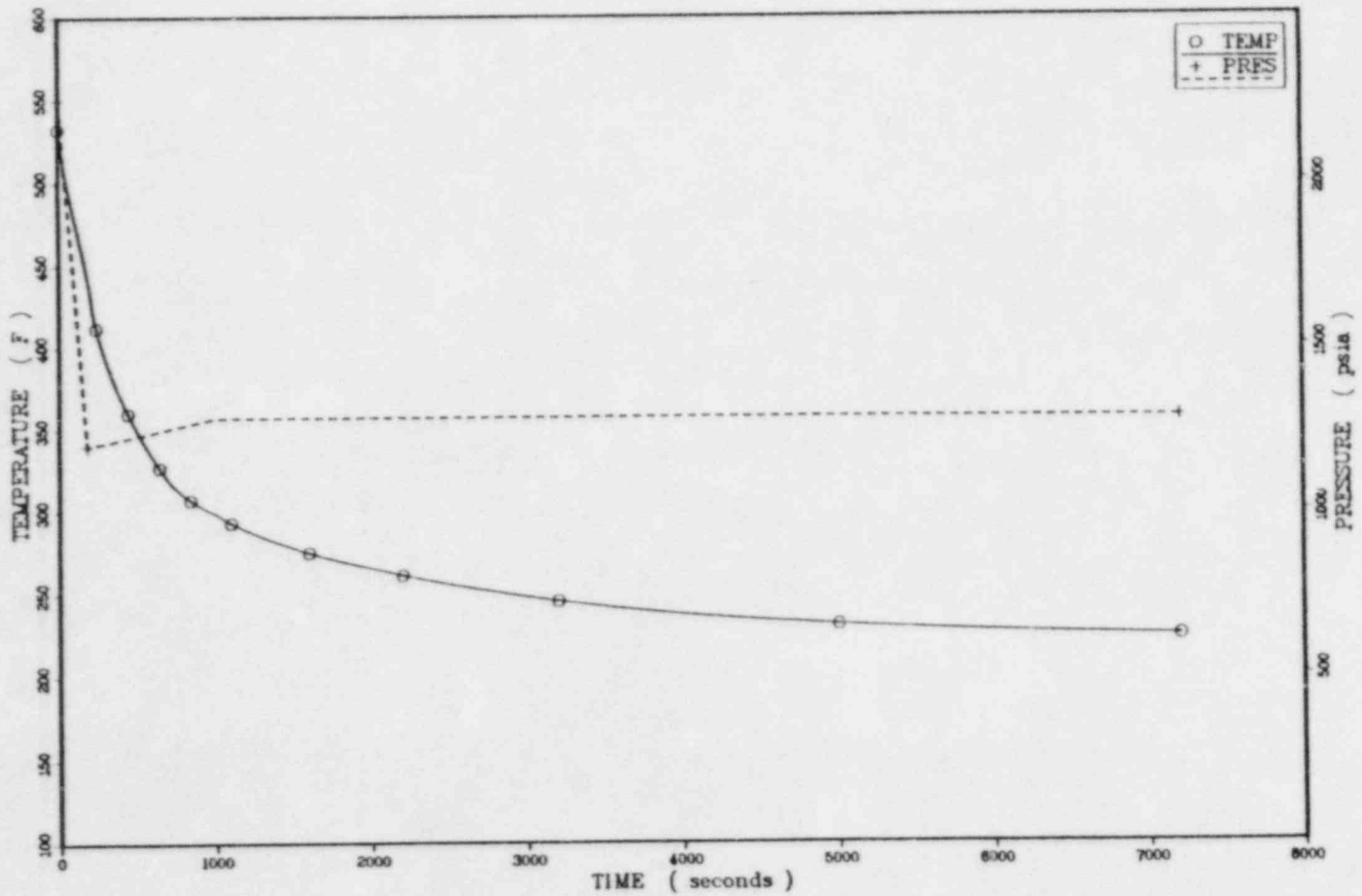

PLOT 1 00.41.26 WED 9 MAY, 1984 JOB-KIN039 , ISSCO DISSPLA VER 8.2

TEMPERATURES AND PRESSURES FOR SEQUENCE 3.5

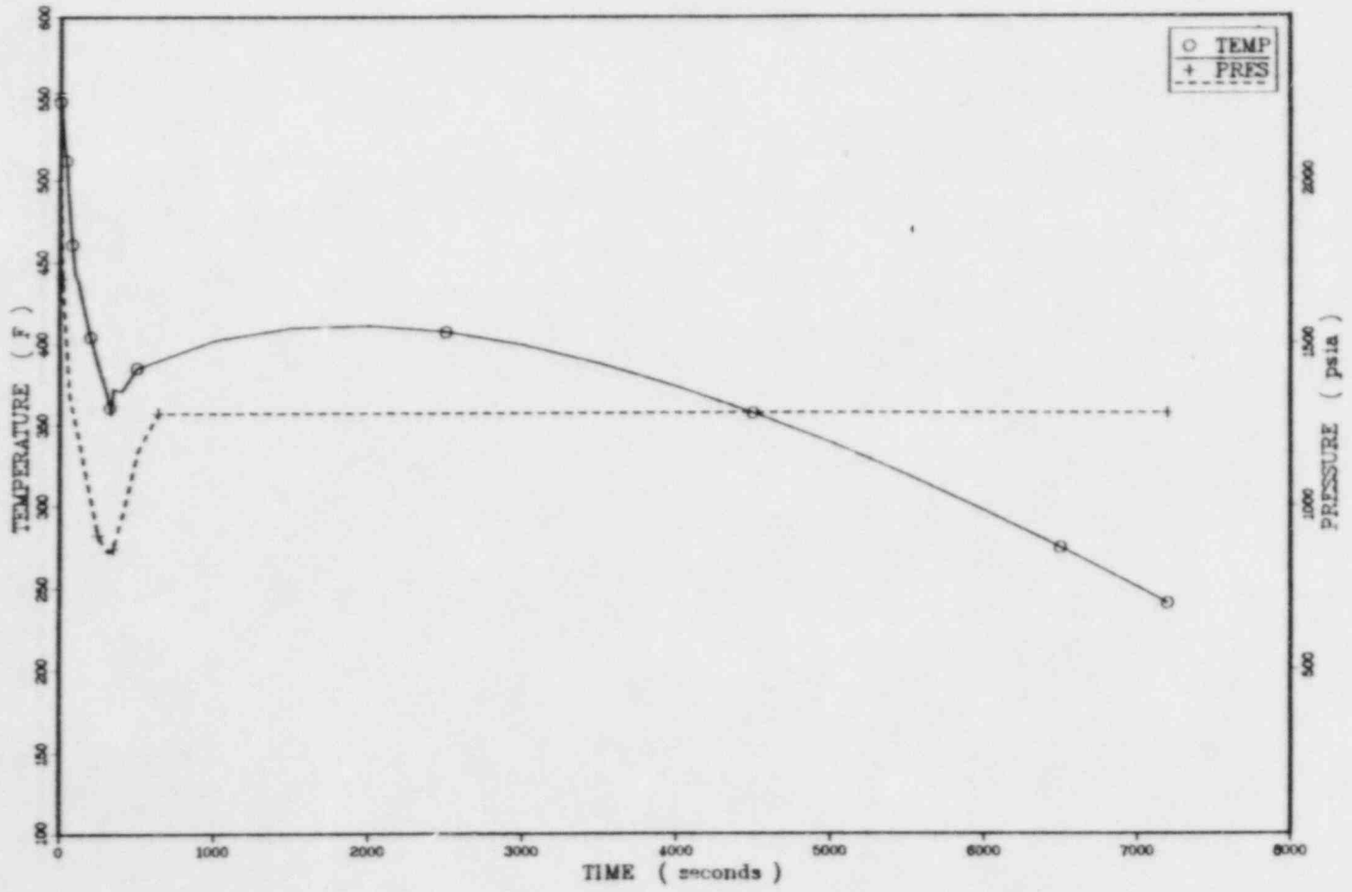

PLOT 1 00.58.16 WED 9 MAY, 1984 JOB-KIN006 , 1550 DISSPLA VER 8.2

TEMPERATURES AND PRESSURES FOR SEQUENCE 3.6

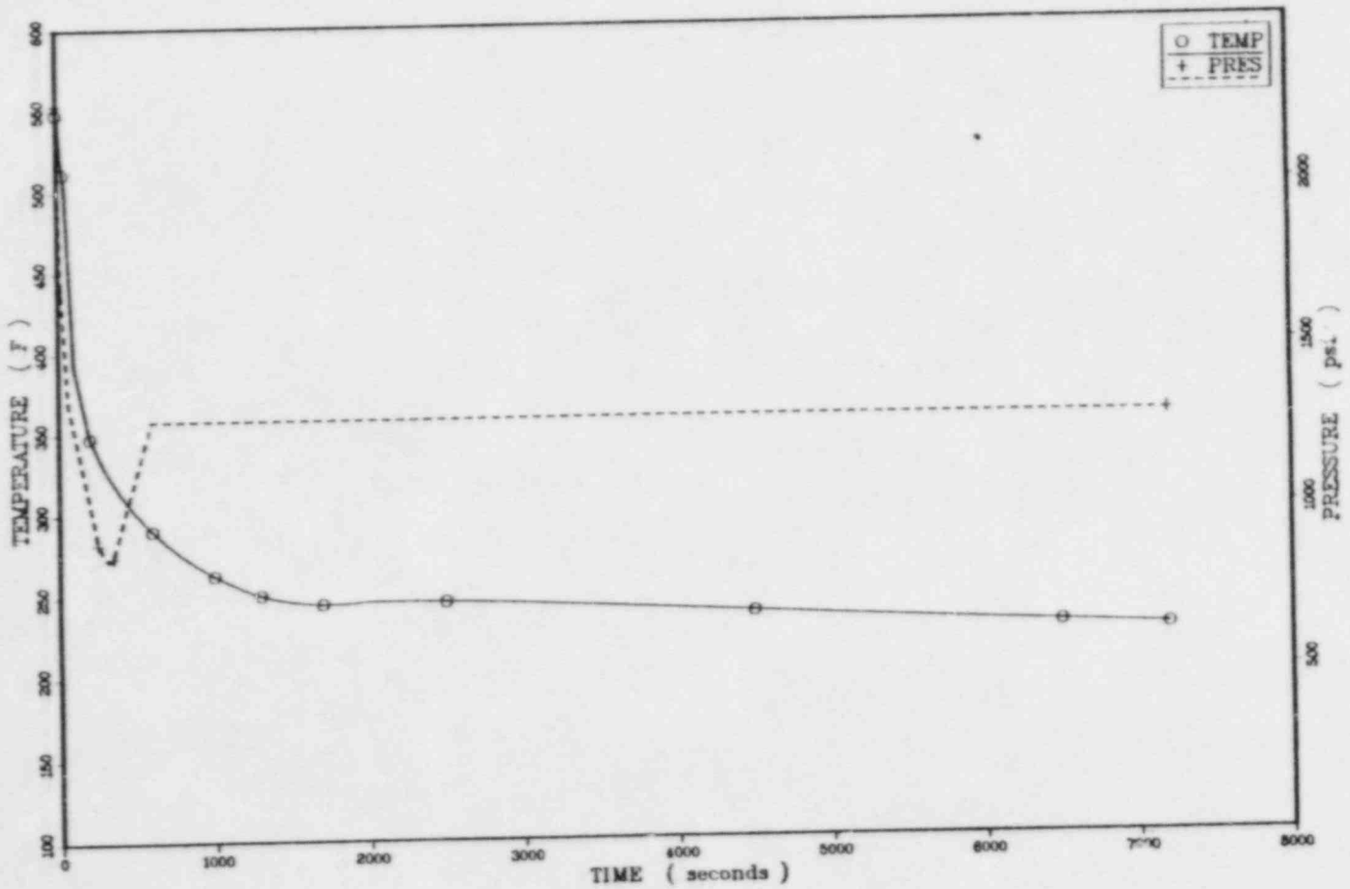

PLOT 1 00.50.15 WED 9 MAY, 1984 JOB-KTN007 , ISSCO DISSPLA VER 8.2

TEMPERATURES AND PRESSURES FOR SEQUENCE 3.7

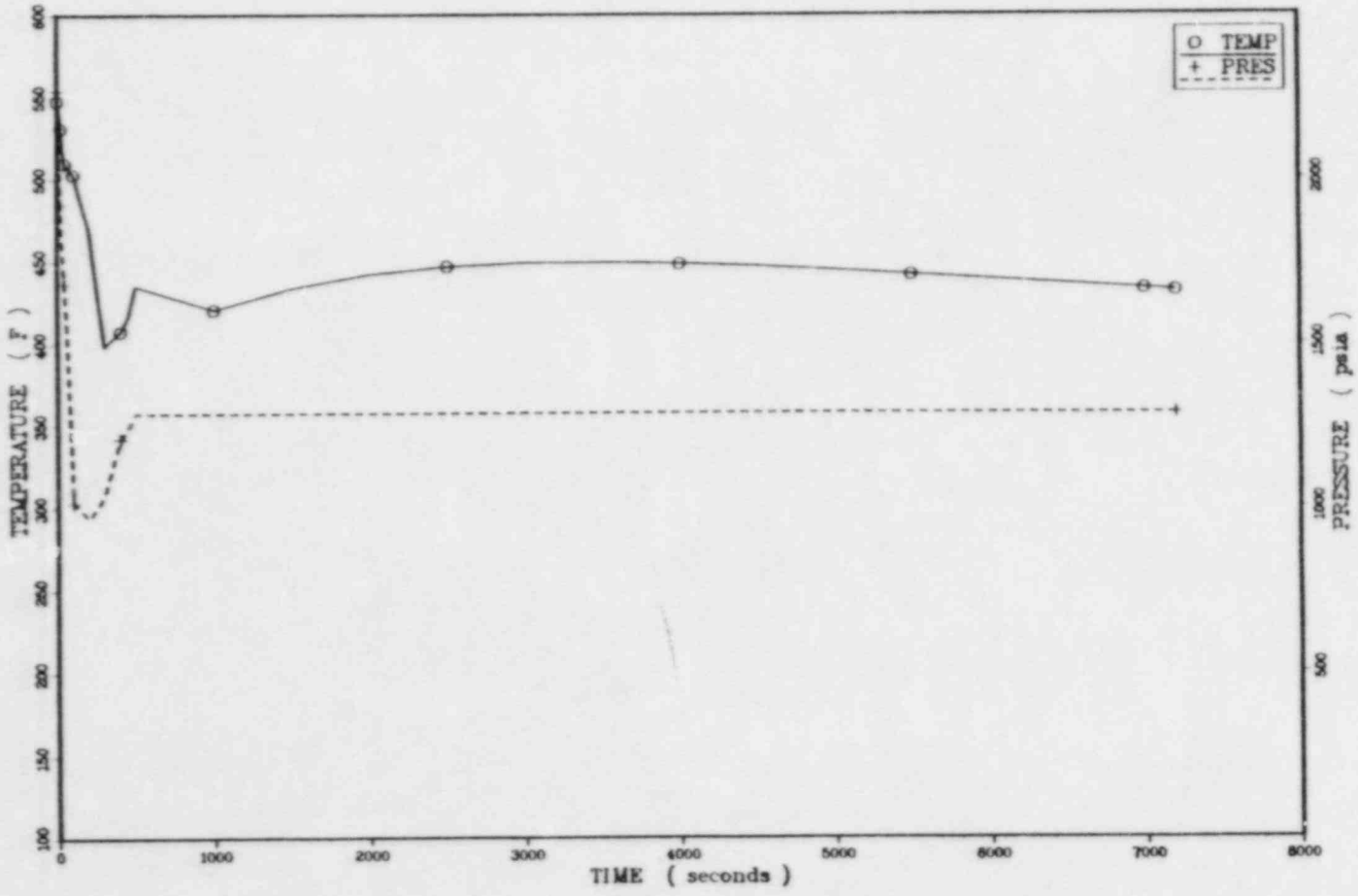

LOT 1 08.52.17 WED 9 MAY, 1984 XOB-XINOOB . ISSCO DISSPLA VER 8.2

TEMPERATURES AND PRESSURES FOR SEQUENCE 3.8

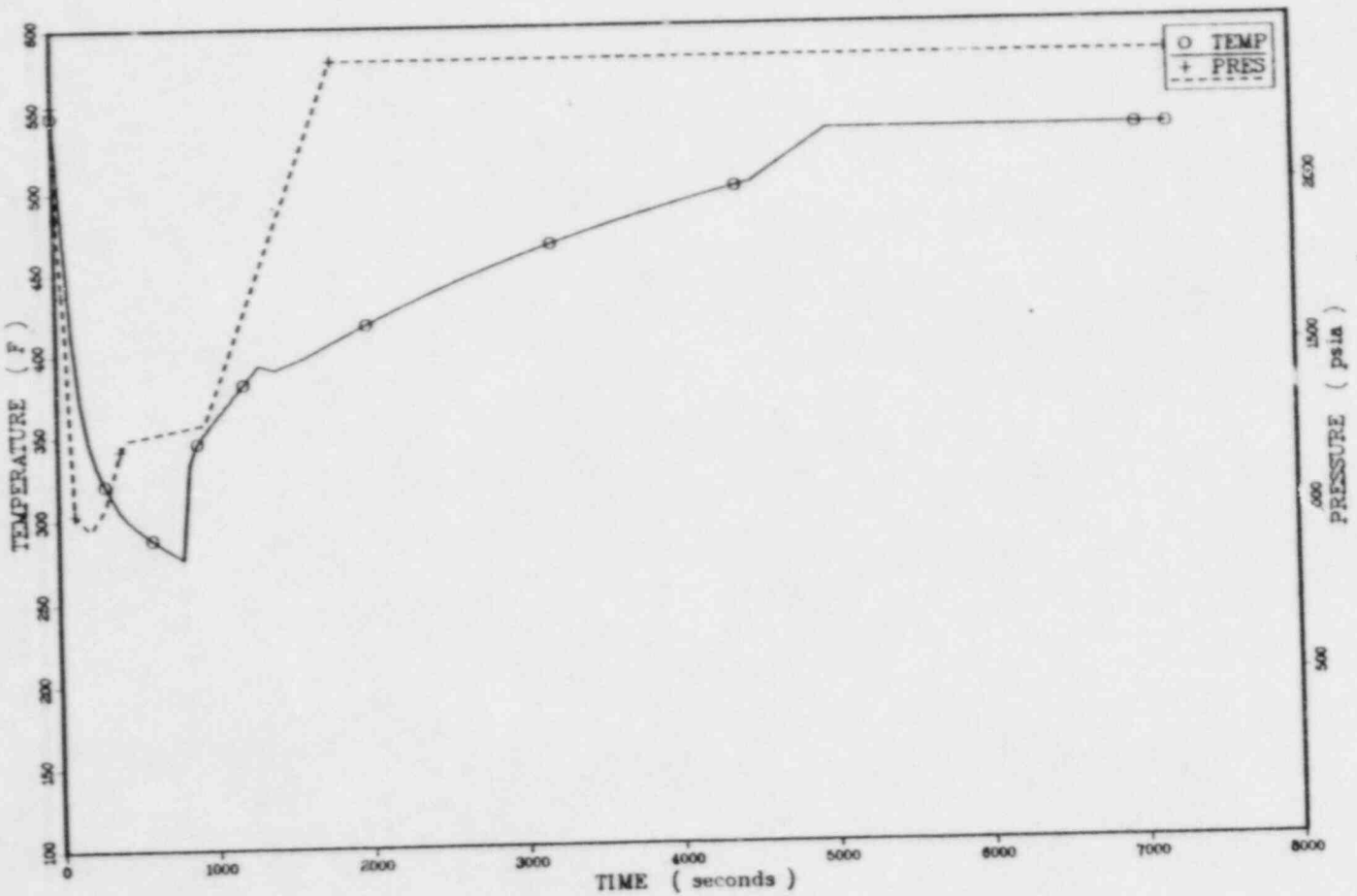

PLOT 1 08.54.24 WED 9 MAY, 1984 JOB-KIN026 , ISSCO DISSPLA VER 8.2

TEMPERATURES AND PRESSURES FOR SEQUENCE 4.2

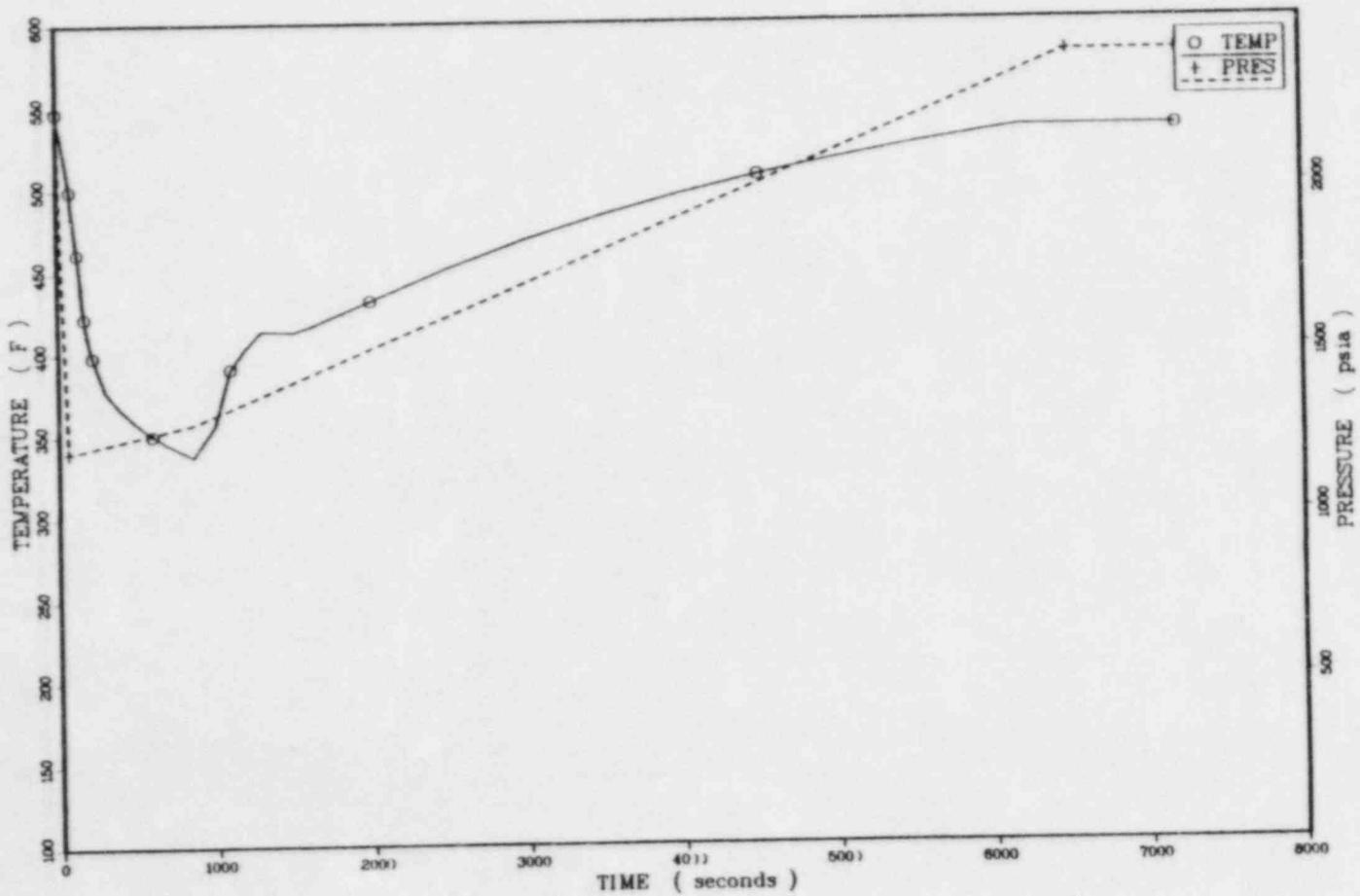

00.56.35 WED 9 MAY, 1984 JOB-KTH027 , 15500 DISSPLA VER 8.2

TEMPERATURES AND PRESSURES FOR SEQUENCE 4.4

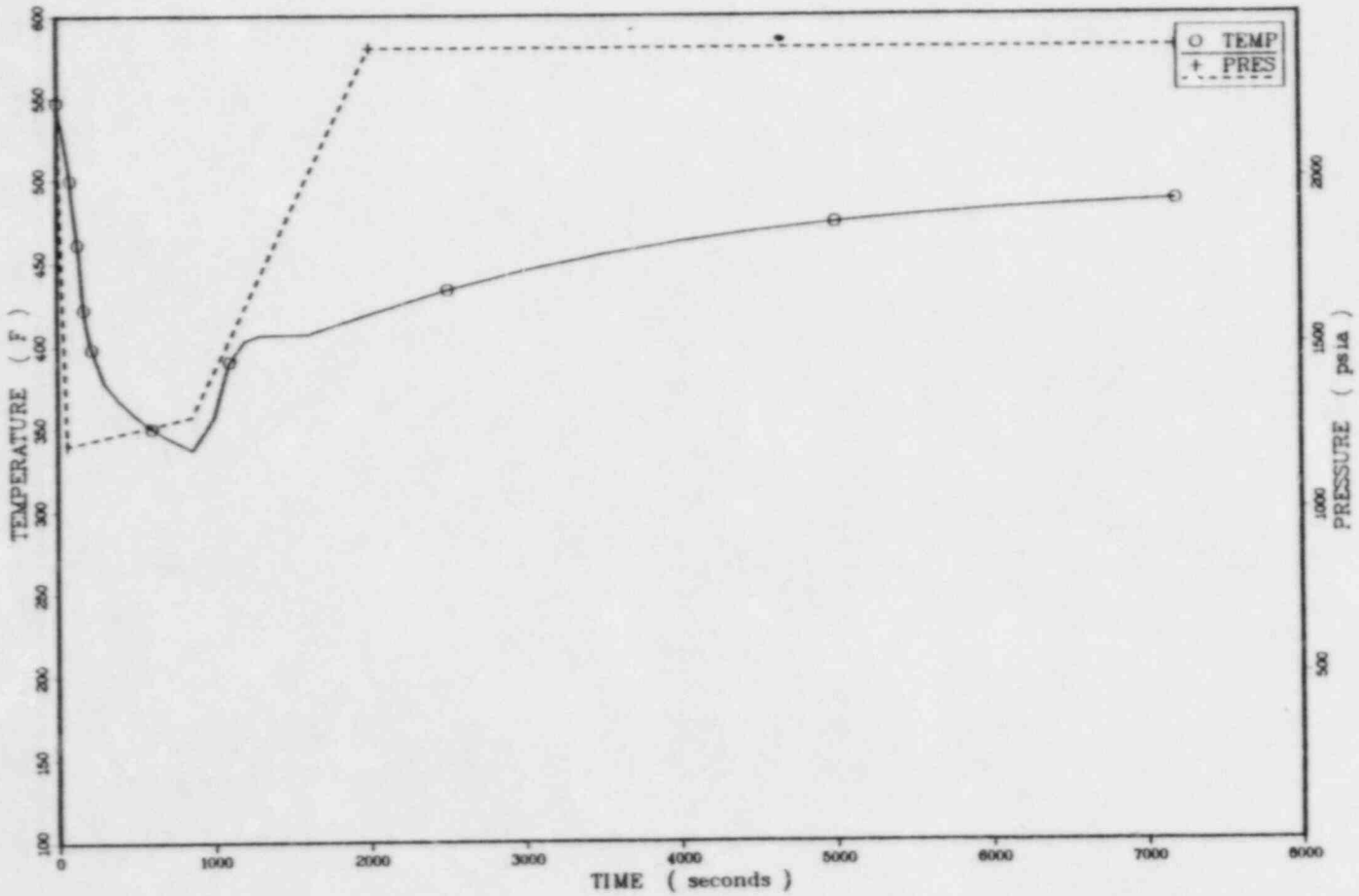

TEMPERATURES AND PRESSURES FOR SEQUENCE 4.5

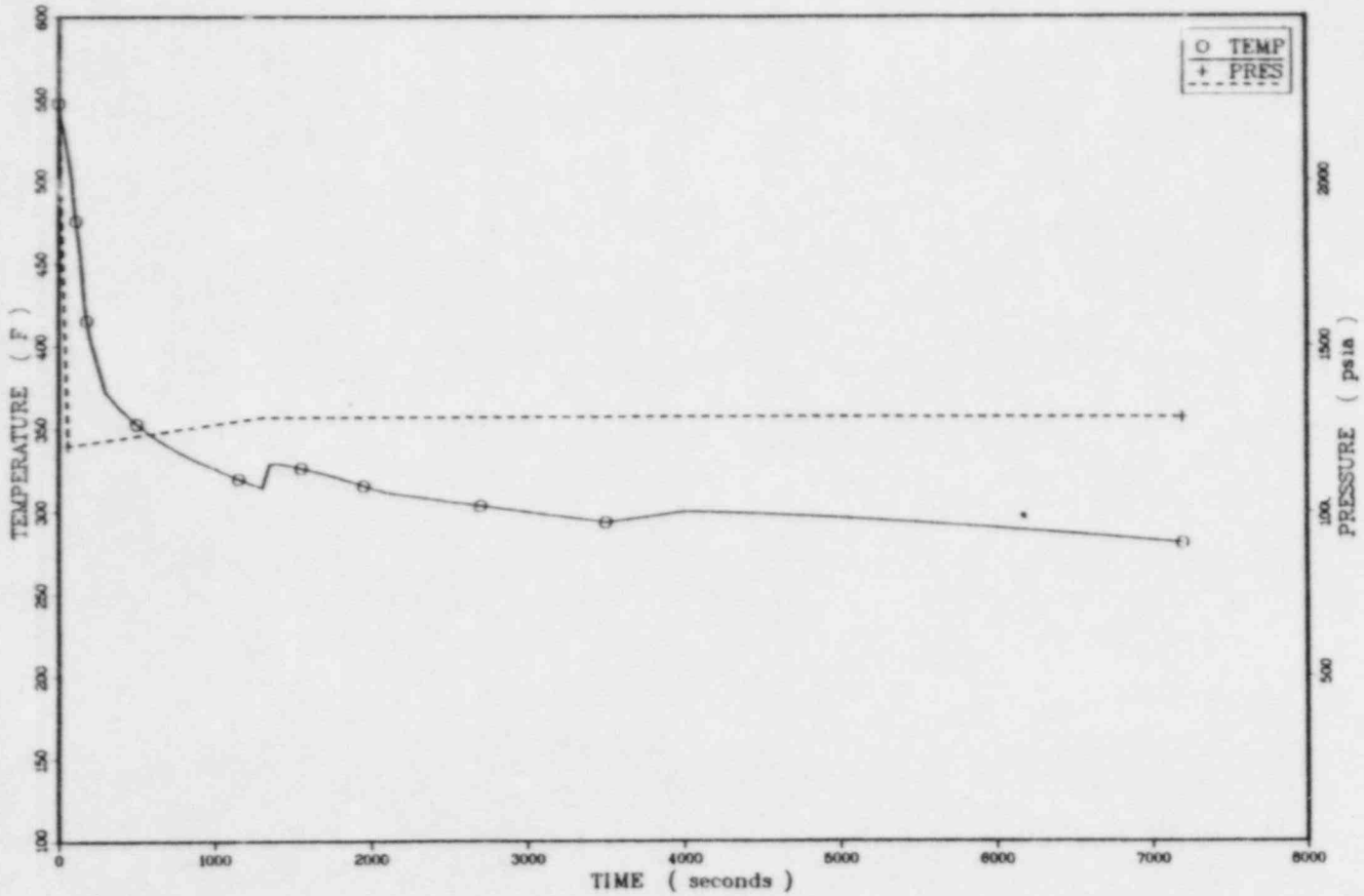

TEMPERATURES AND PRESSURES FOR SEQUENCE 4.6

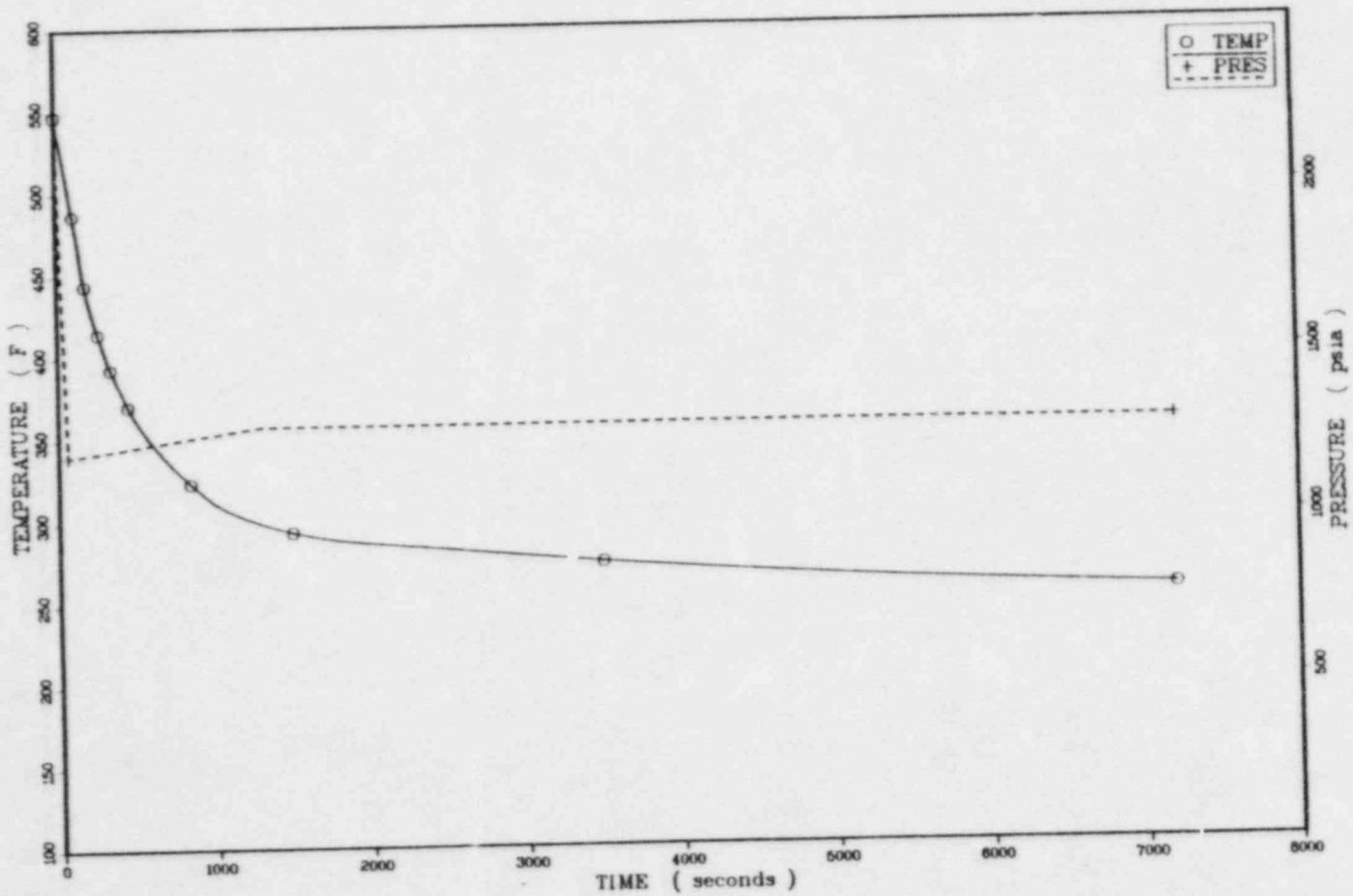

TEMPERATURES AND PRESSURES FOR SEQUENCE 4.7

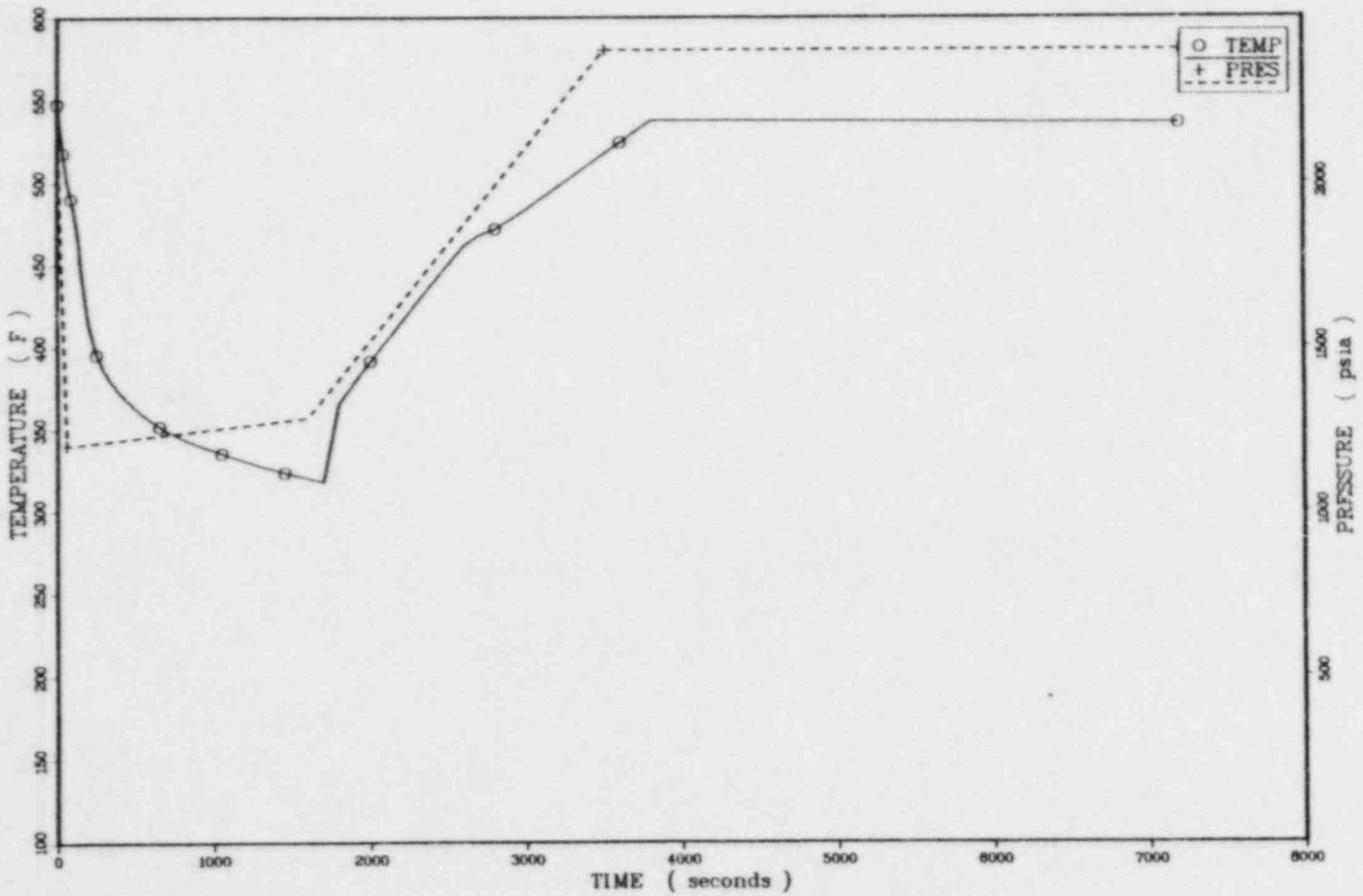

TEMPERATURES AND PRESSURES FOR SEQUENCE 4.8

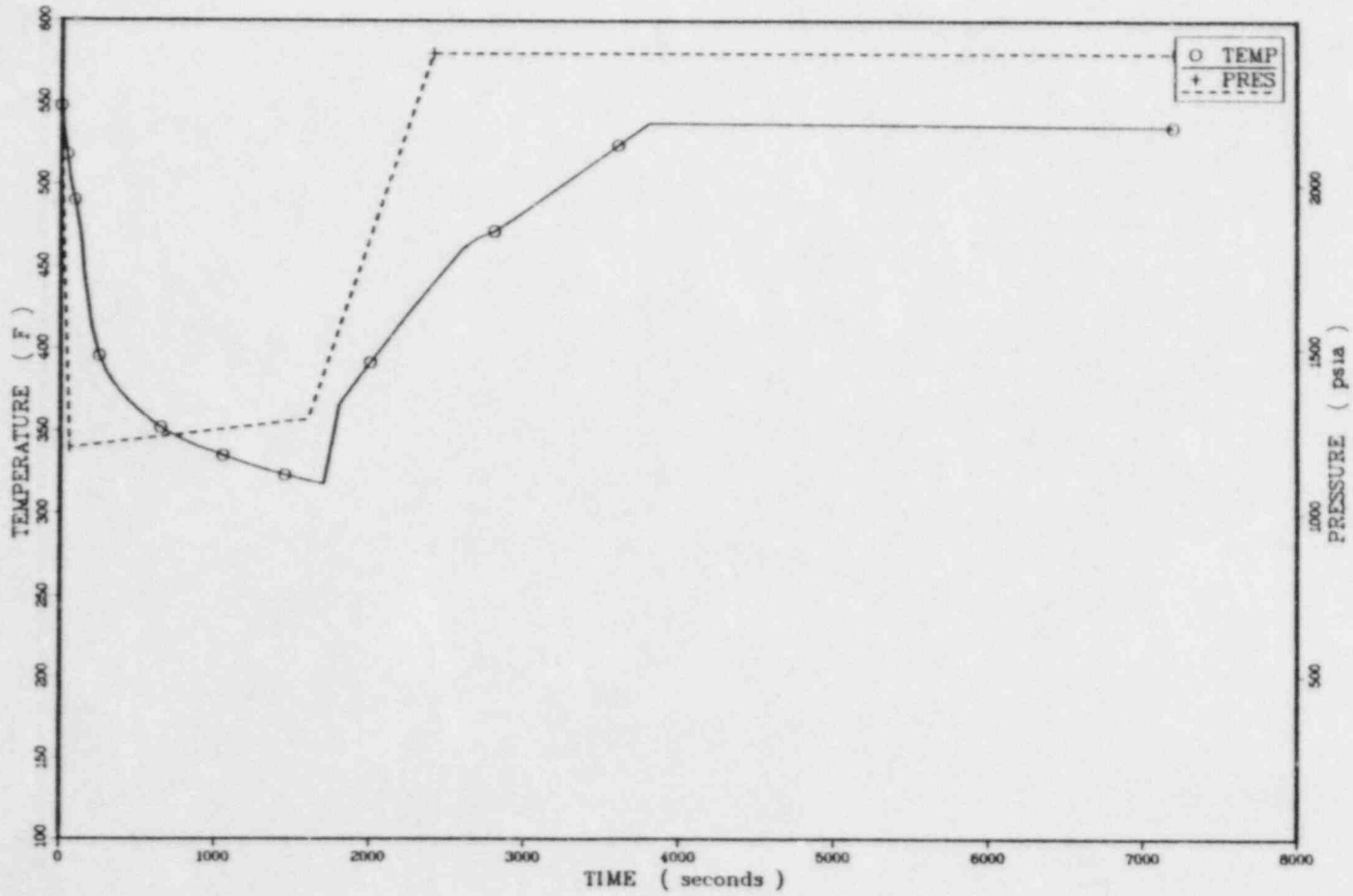

TEMPERATURES AND PRESSURES FOR SEQUENCE 4.11

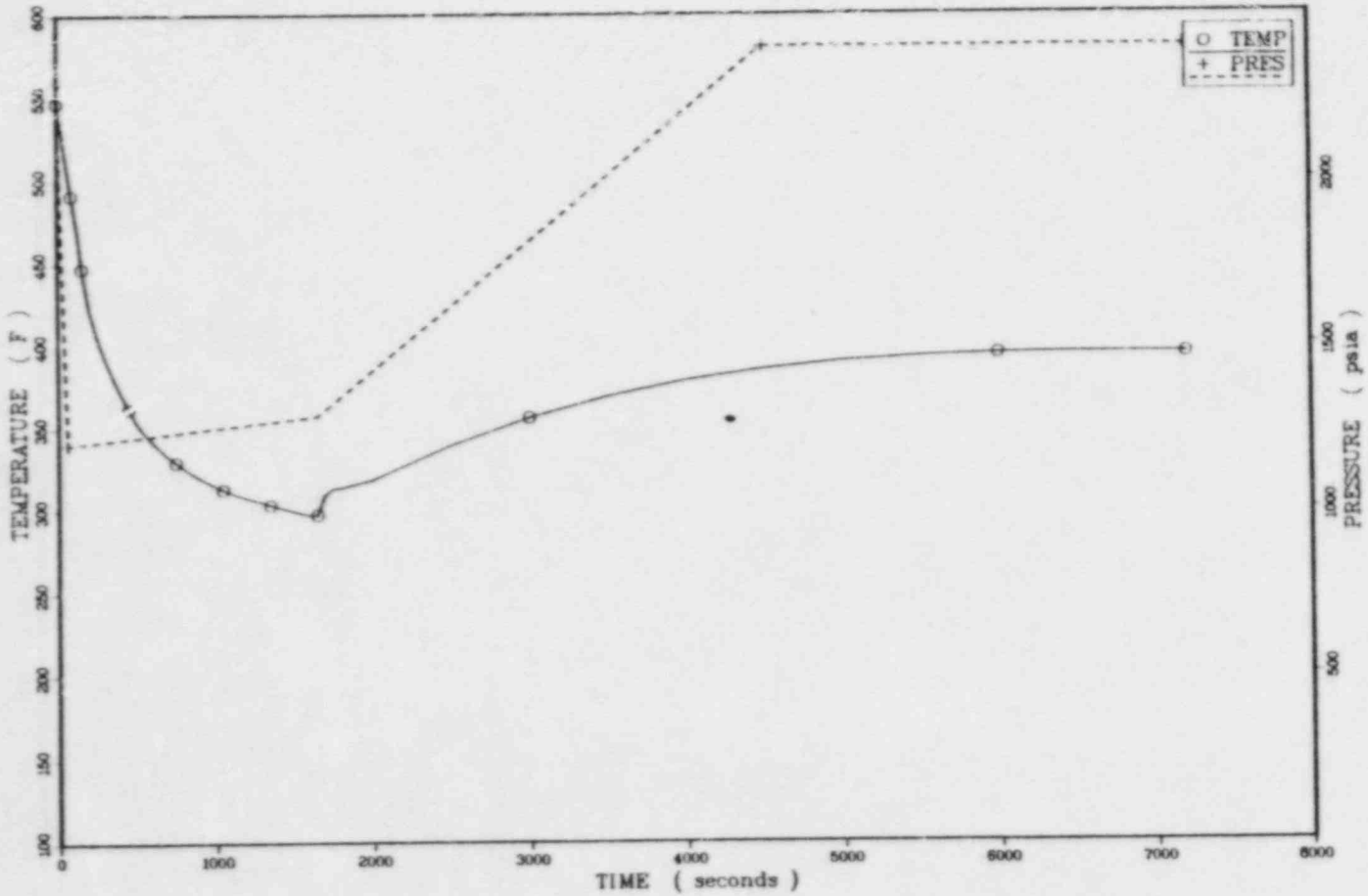

PLOT 1 01.27.58 WED 9 MAY, 1984 JOB-KING25 . ISSCO DISSPLA VER 8.2

TEMPERATURES AND PRESSURES FOR SEQUENCE 4.12

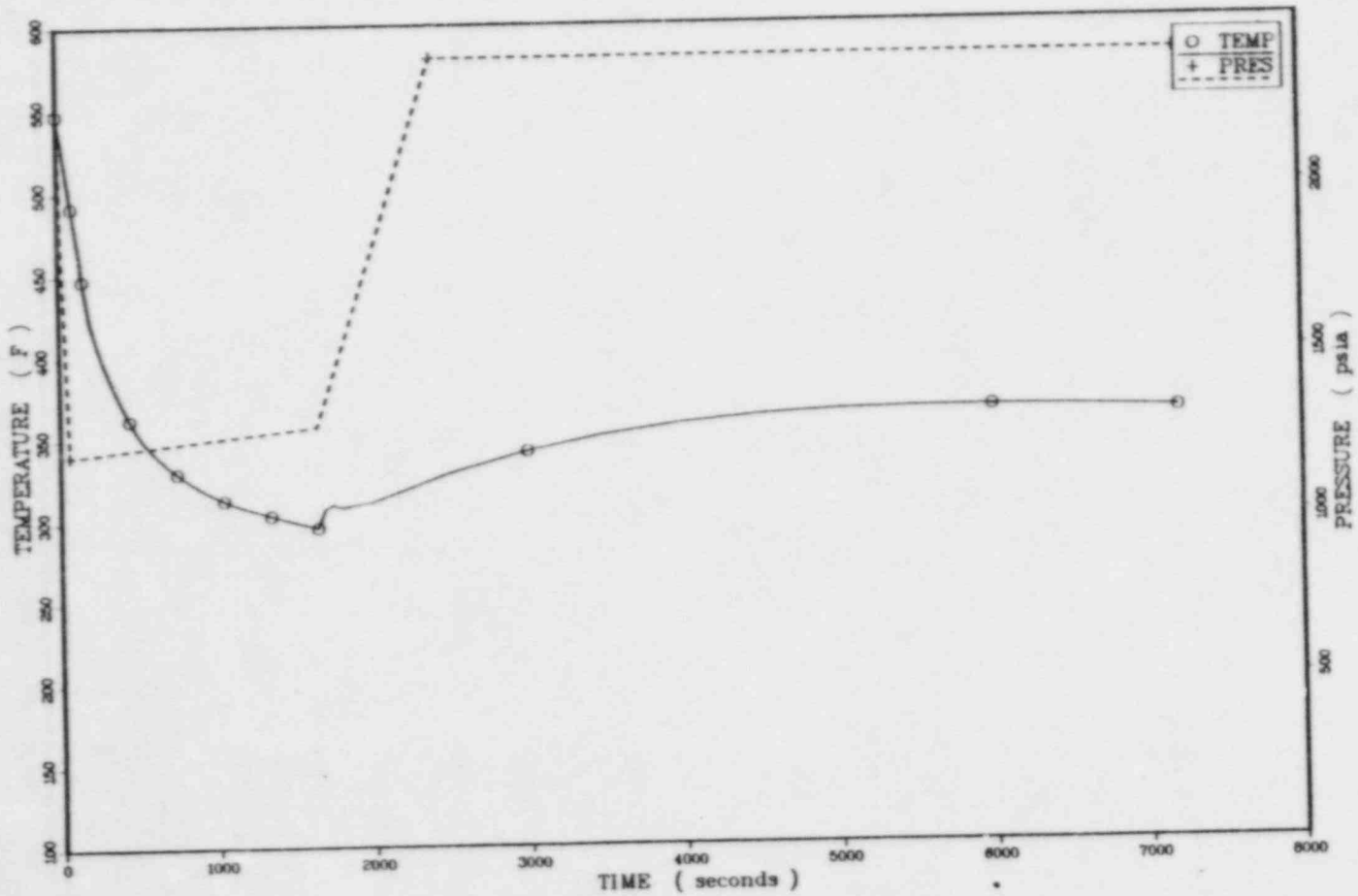

PLOT 1 01.29.42 WED 9 MAY, 1984 ROB-KINGS , ISSCO DISSPLA VER 8.2

TEMPERATURES AND PRESSURES FOR SEQUENCE 5.19

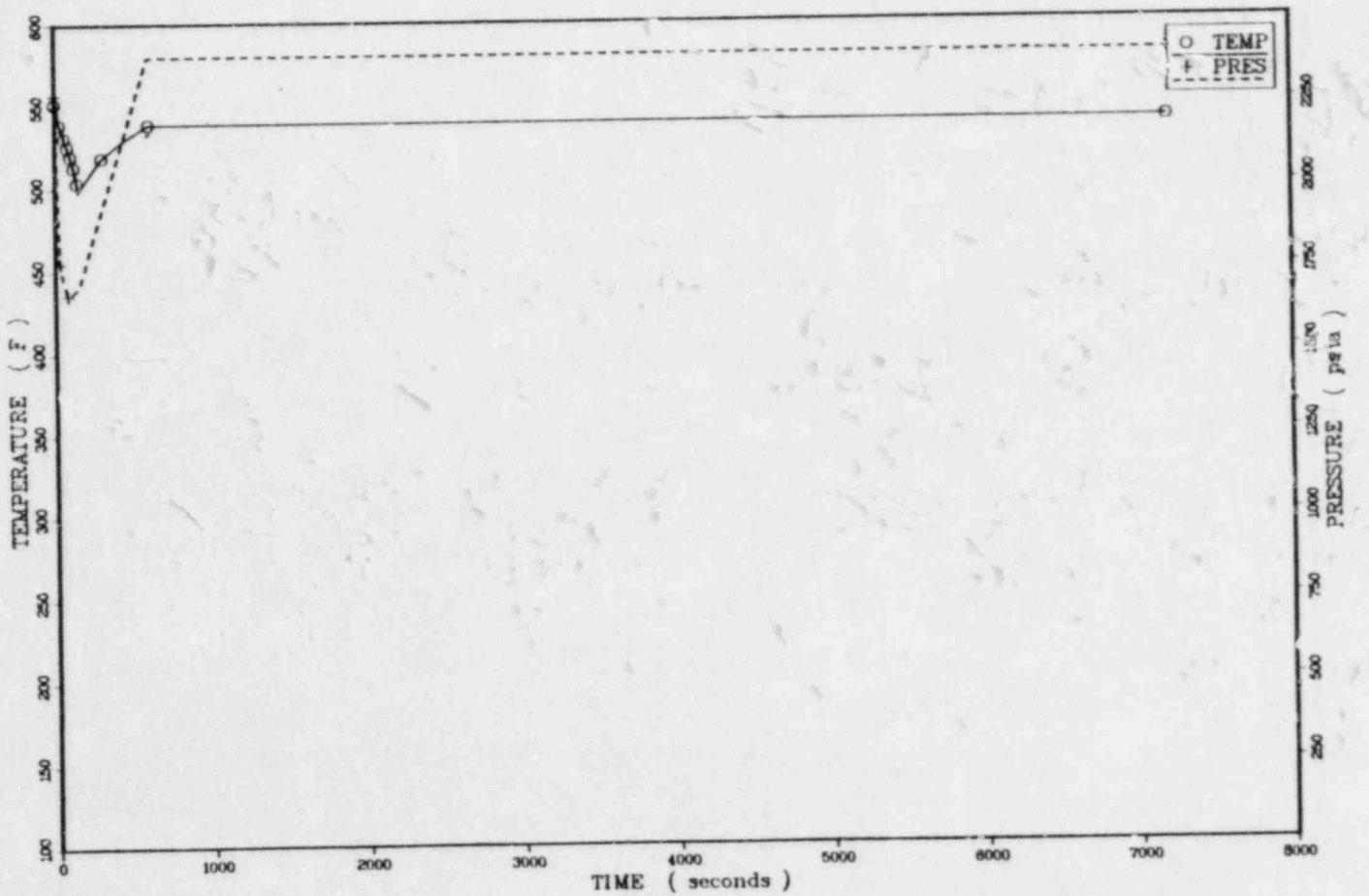

TEMPERATURES AND PRESSURES FOR SEQUENCE 5.20

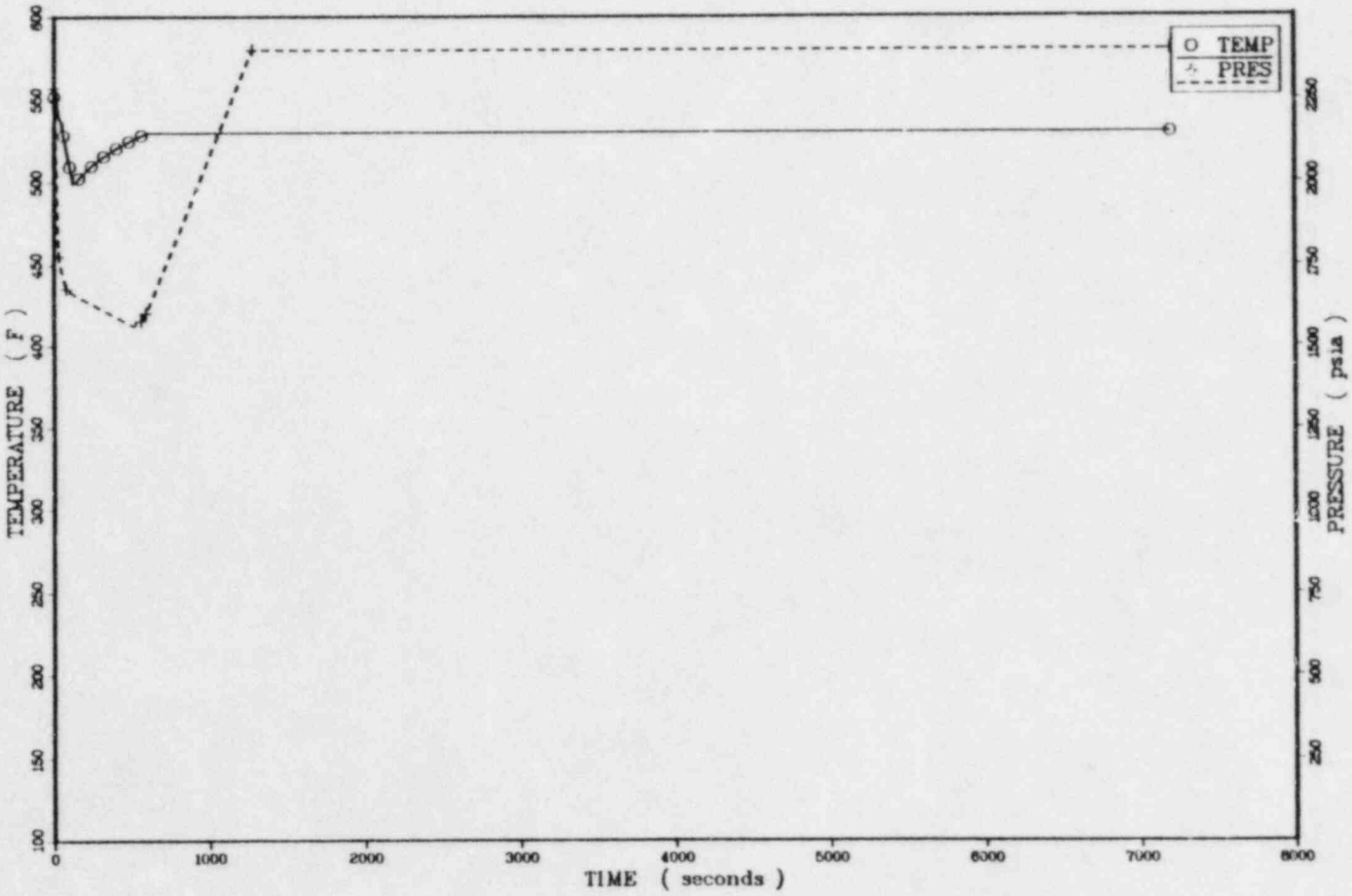

PLOT 1 01.33.14 WED 9 MAY, 1984 JOB-KTN011 , ISSCO DISSPLA VER 8.2

TEMPERATURES AND PRESSURES FOR SEQUENCE 5.21B

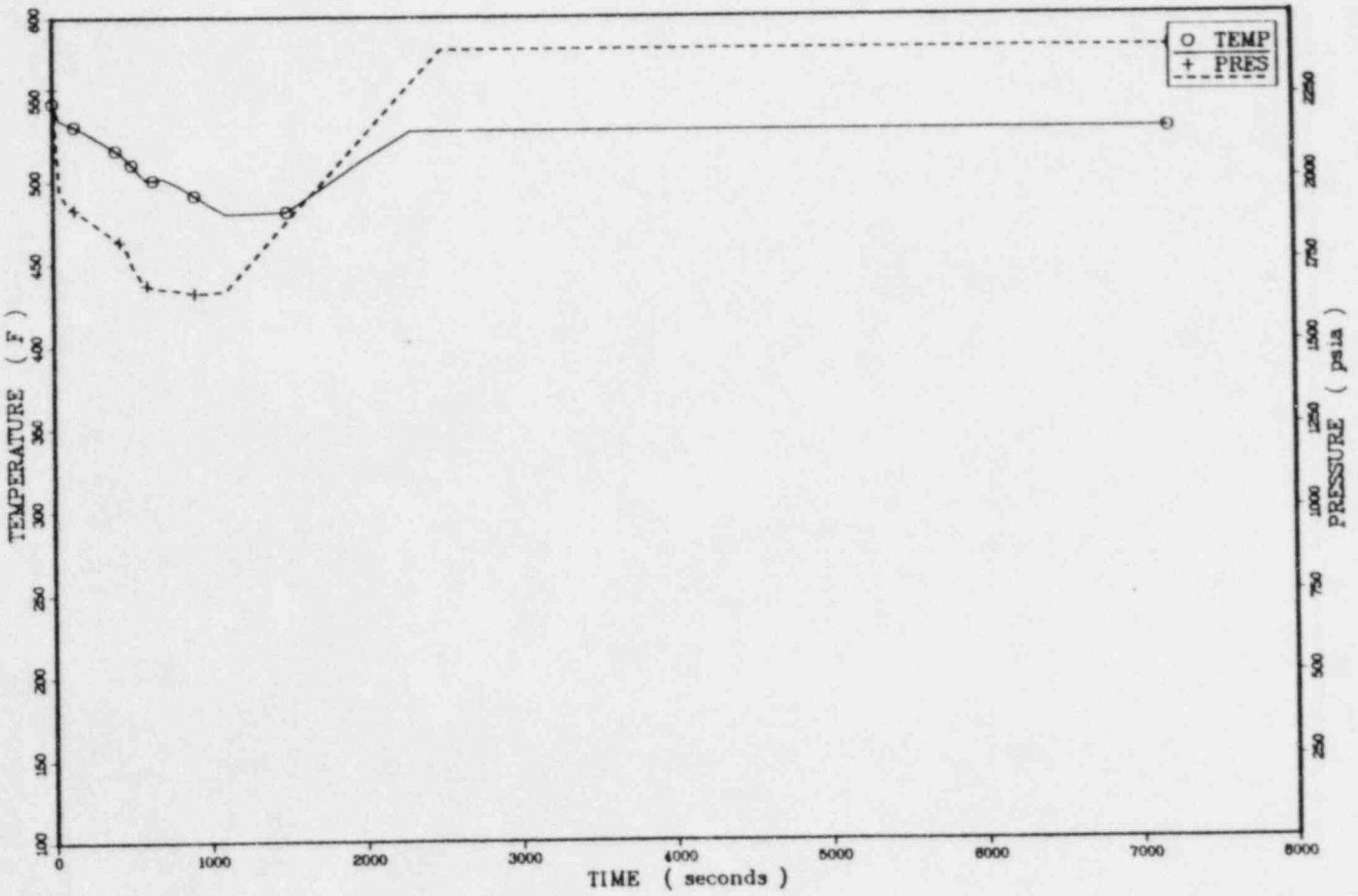

PLOT 1 01.35.14 WED 9 MAY, 1984 JOB-KIN012 , ISSCO DISSPLA VER 8.2

TEMPERATURES AND PRESSURES FOR SEQUENCE 5.22

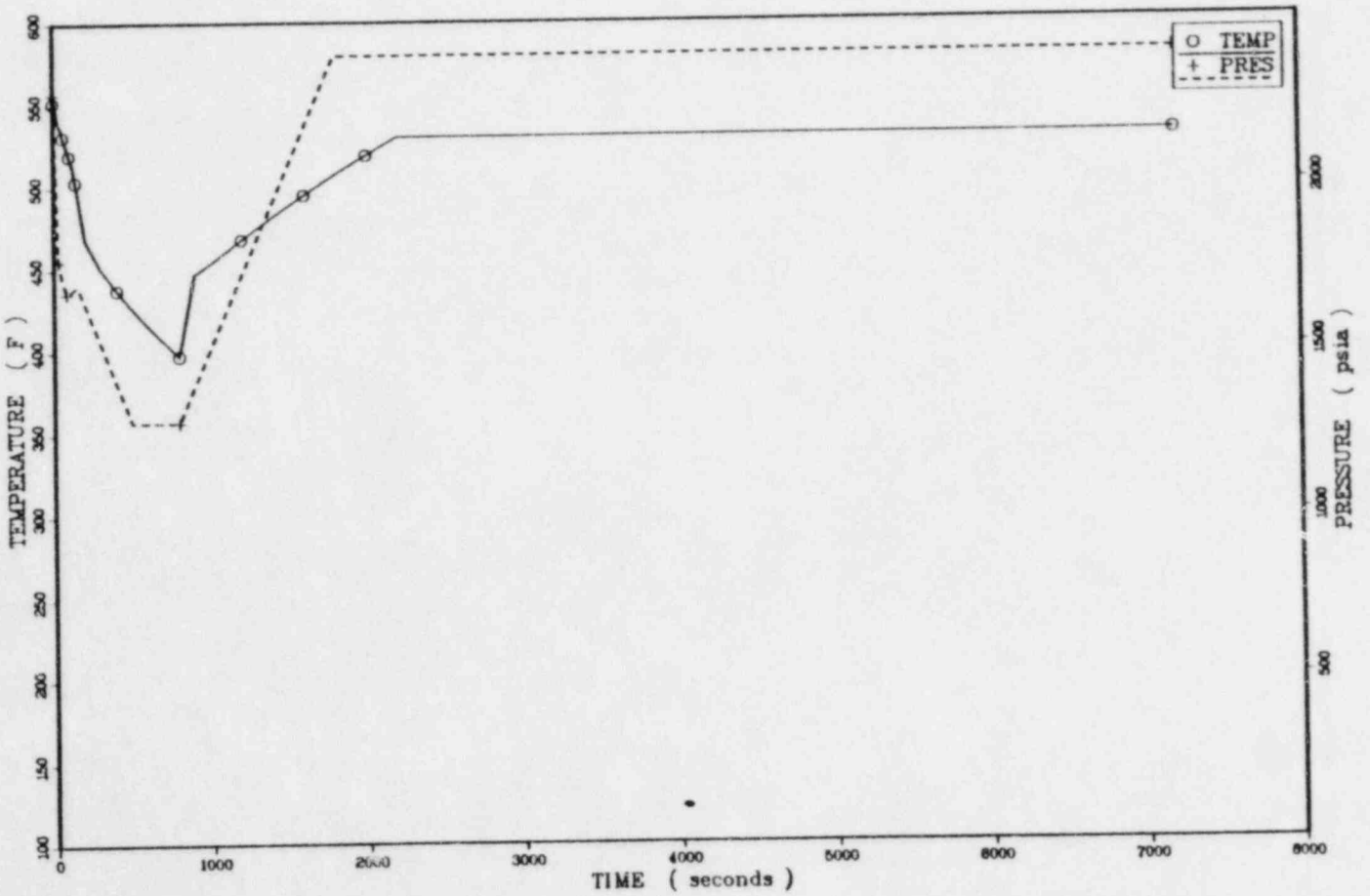

TEMPERATURES AND PRESSURES FOR SEQUENCE 5.25A

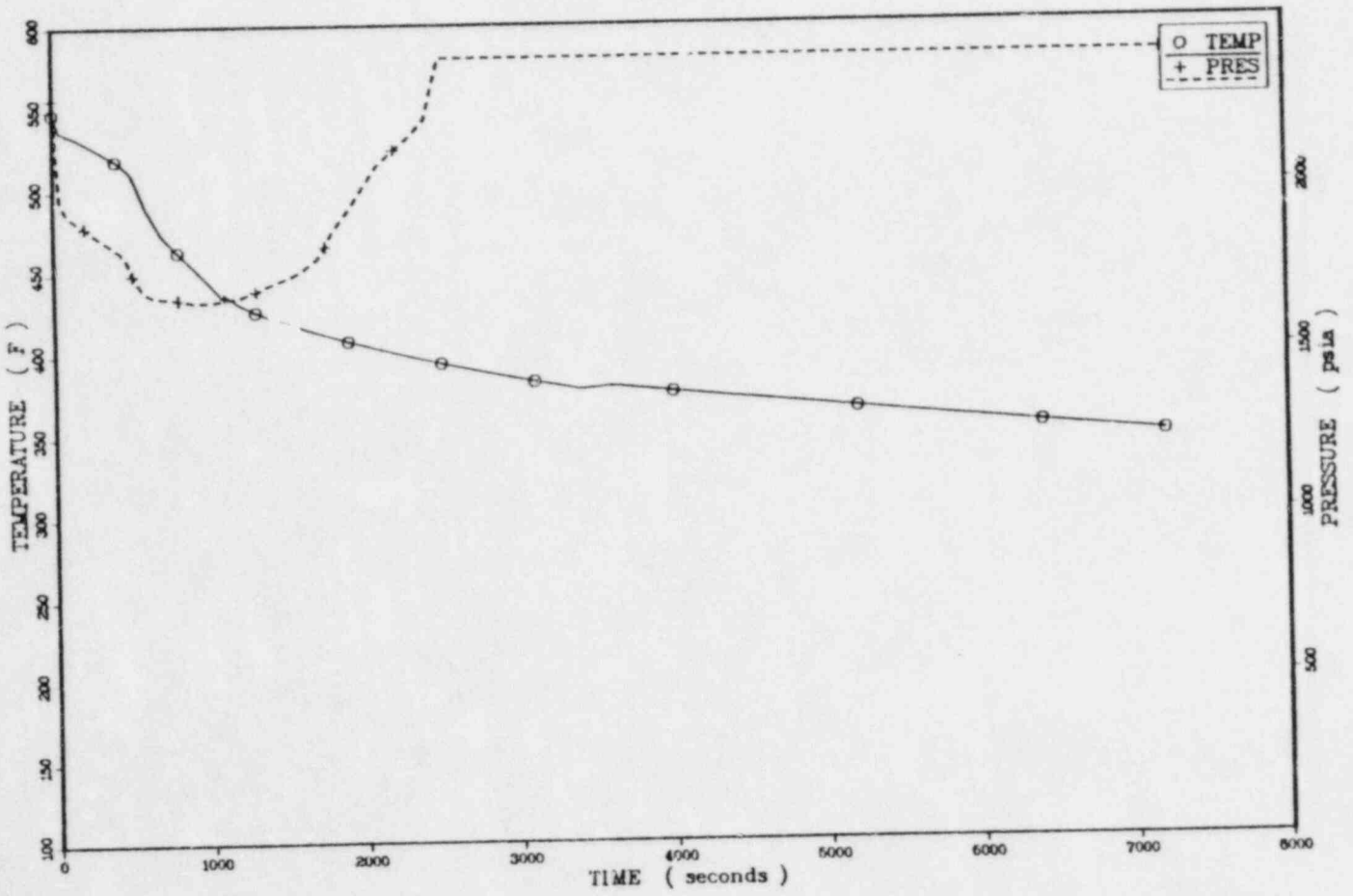

1 01.37.00 WED 9 MAY, 1984 JOB-KTN013 , ISSCO DISSPLA VER 8.2

TEMPERATURES AND PRESSURES FOR SEQUENCE 5.25B

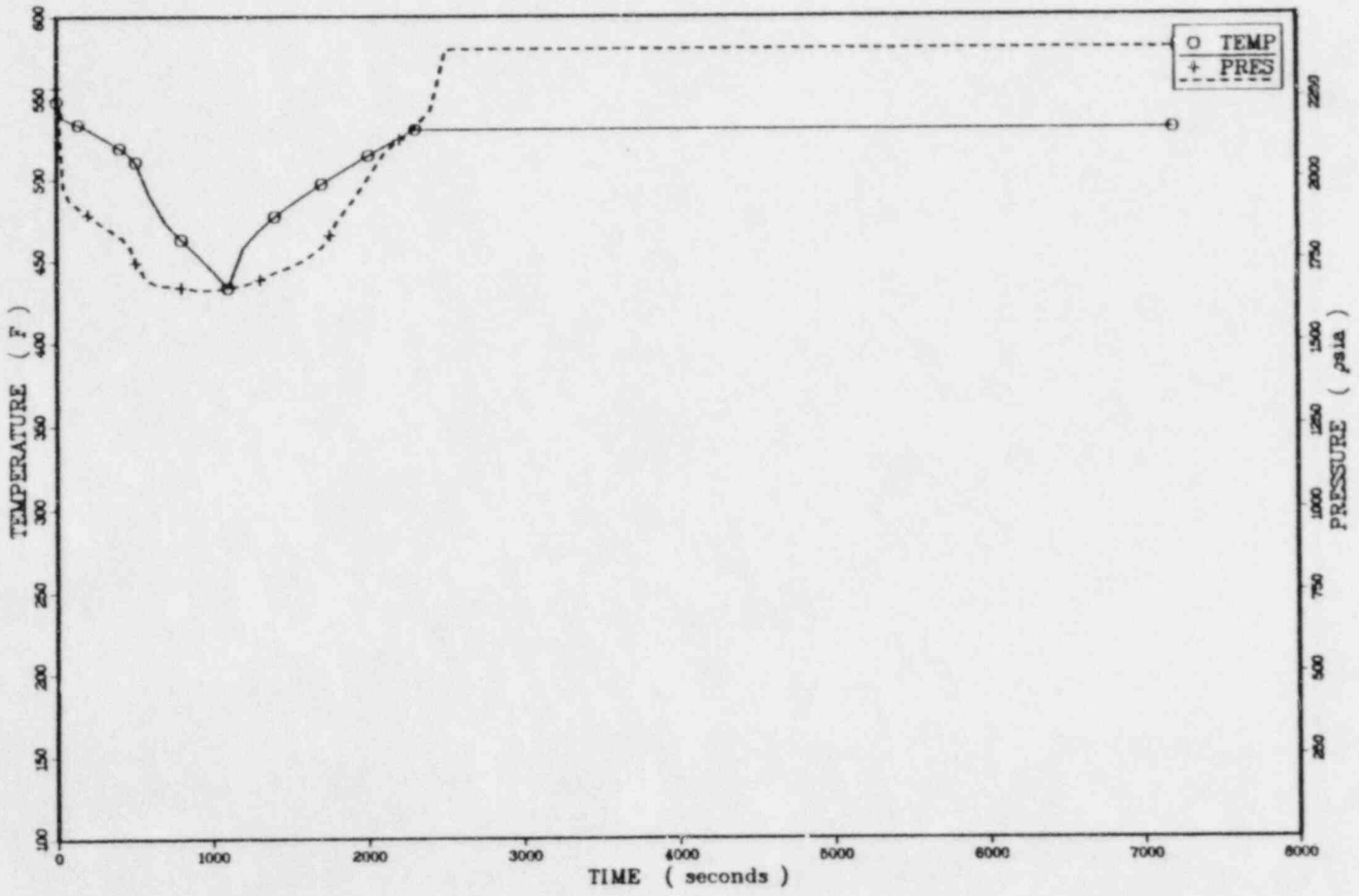

PLOT 1 01.38.46 WED 9 MAY, 1984 JOB-KIN040 , ISSCO DISSPLA VER 8.2

TEMPERATURES AND PRESSURES FOR SEQUENCE 5.26A

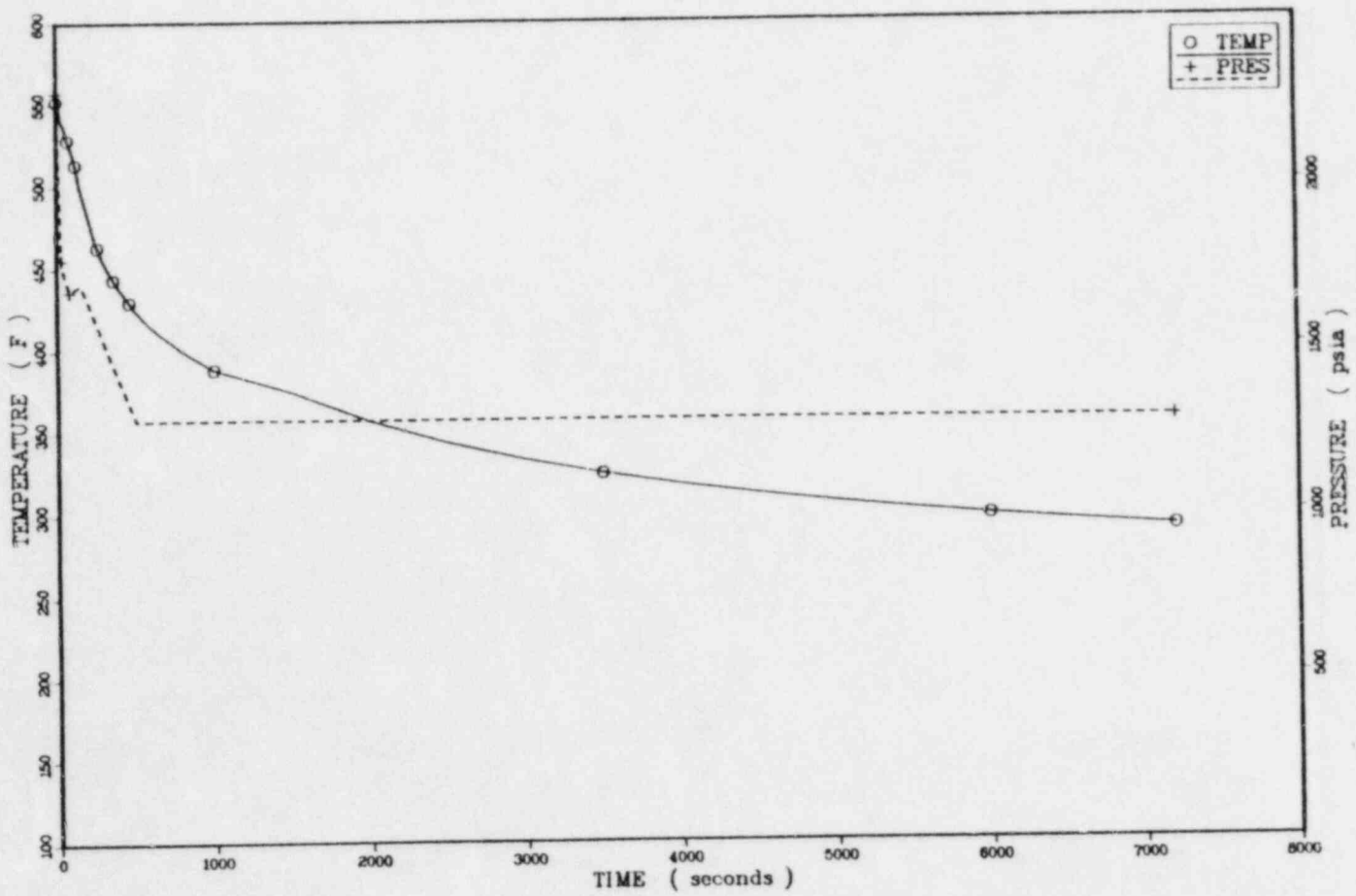

PLOT 1 01.40.31 WED 9 MAY, 1984 JOB-KIN015 , ISSCO DISSPLA VER 8.2

TEMPERATURES AND PRESSURES FOR SEQUENCE 5.26B

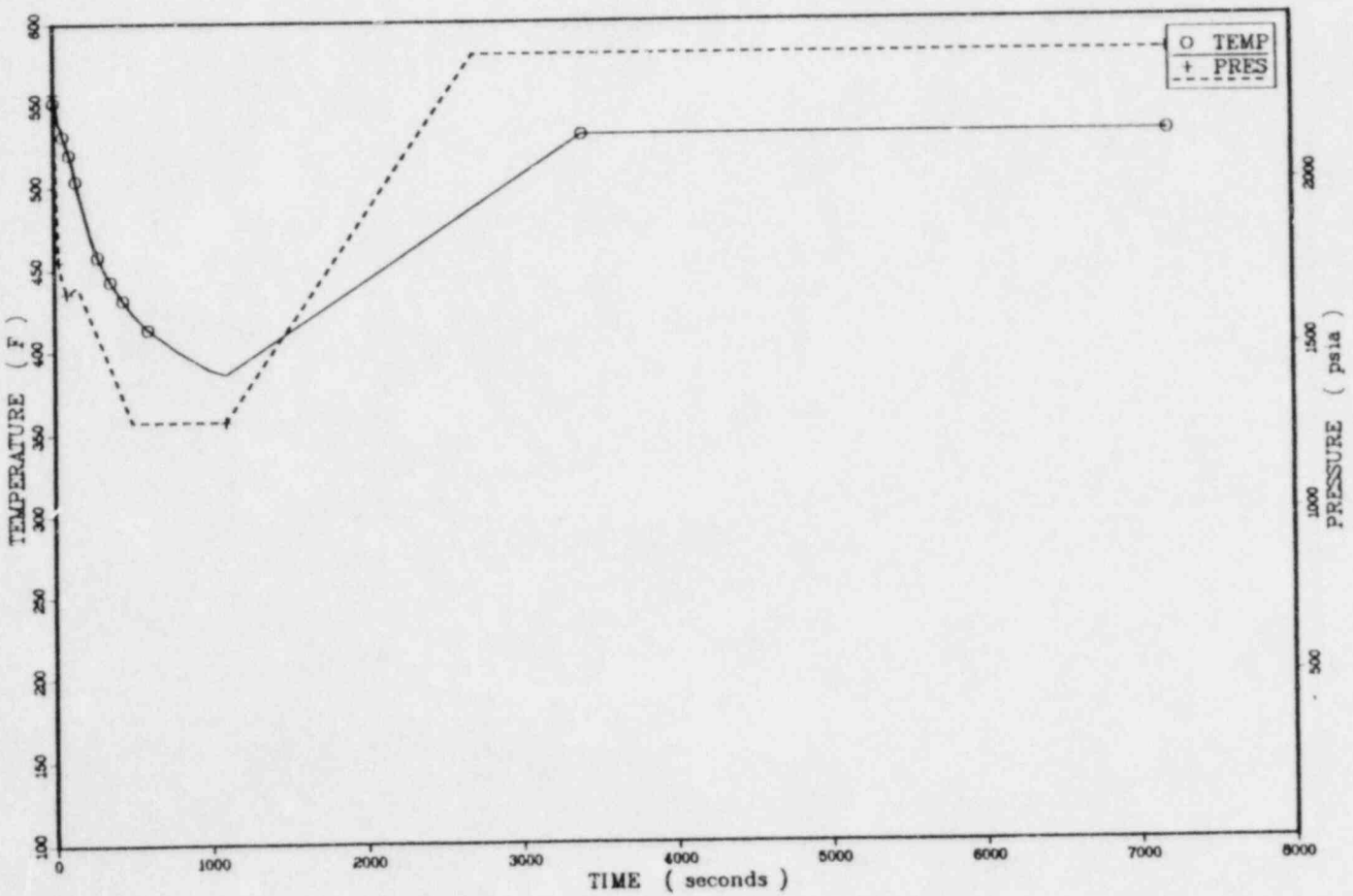

TEMPERATURES AND PRESSURES FOR SEQUENCE 5.27A

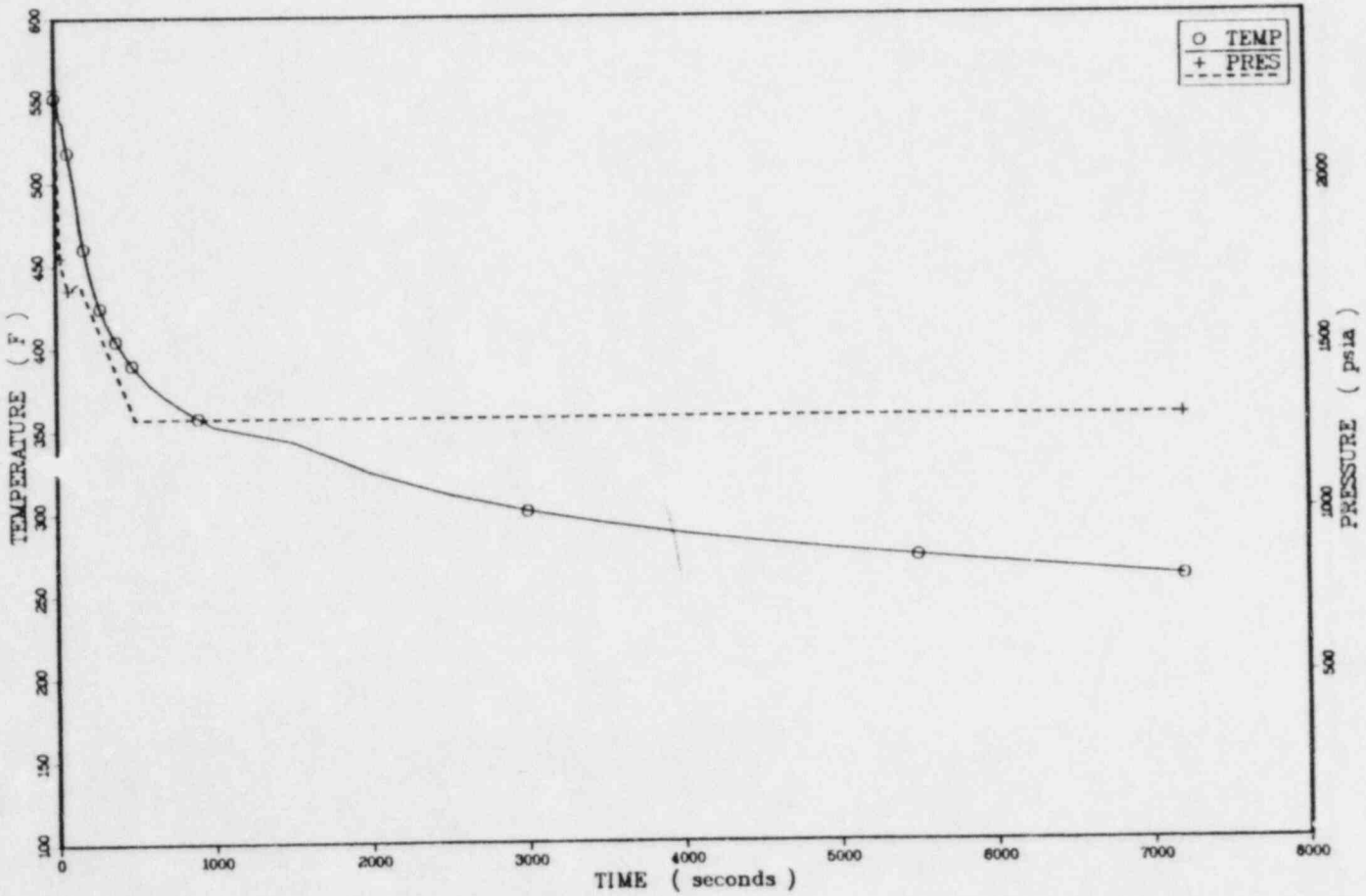

1 01.44.07 WED 9 MAY, 1984 JOB-KTN016 , ISSCO DISSPLA VER 8.2

TEMPERATURES AND PRESSURES FOR SEQUENCE 5.27B

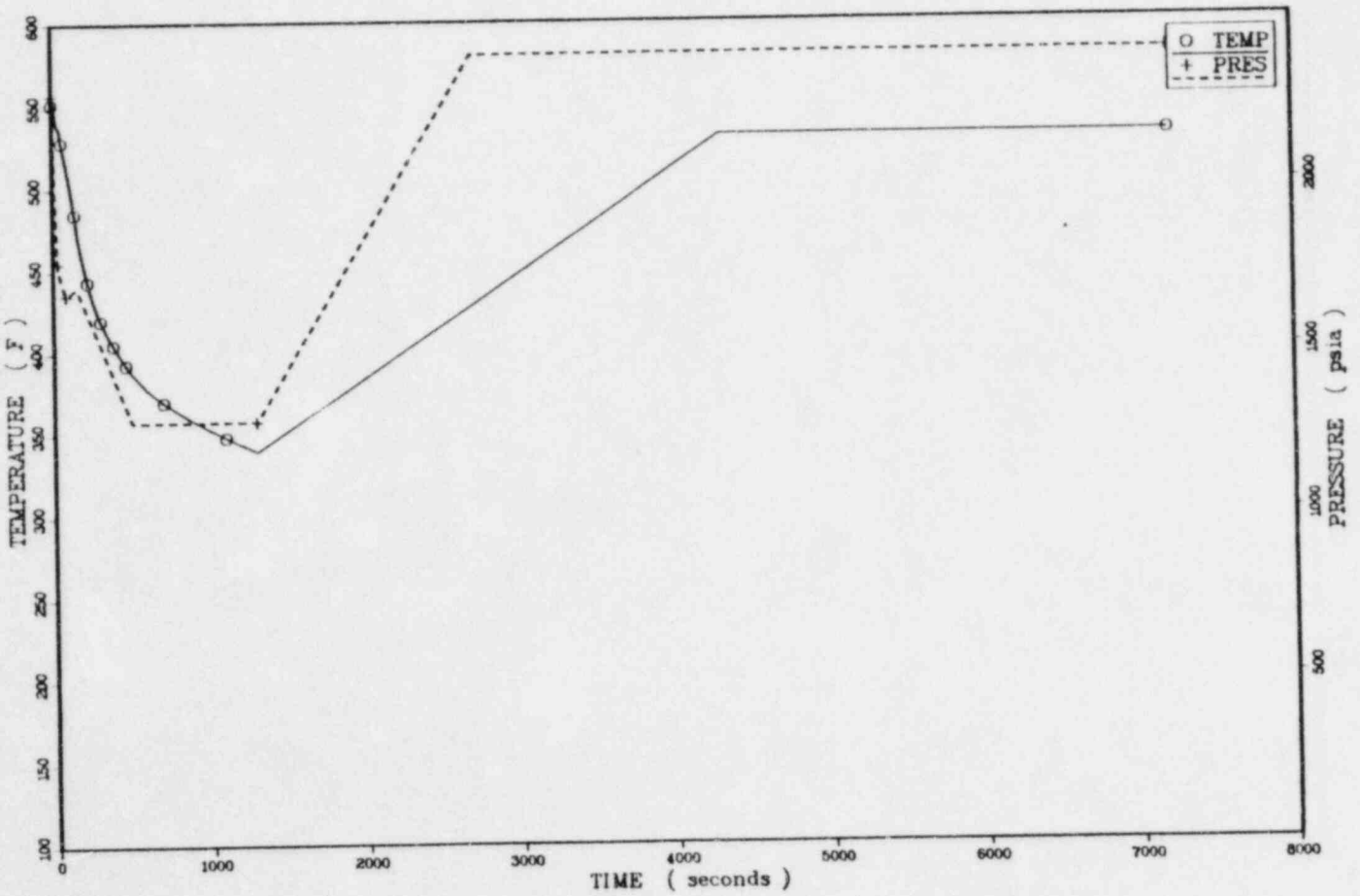

TEMPERATURES AND PRESSURES FOR SEQUENCE 5.35

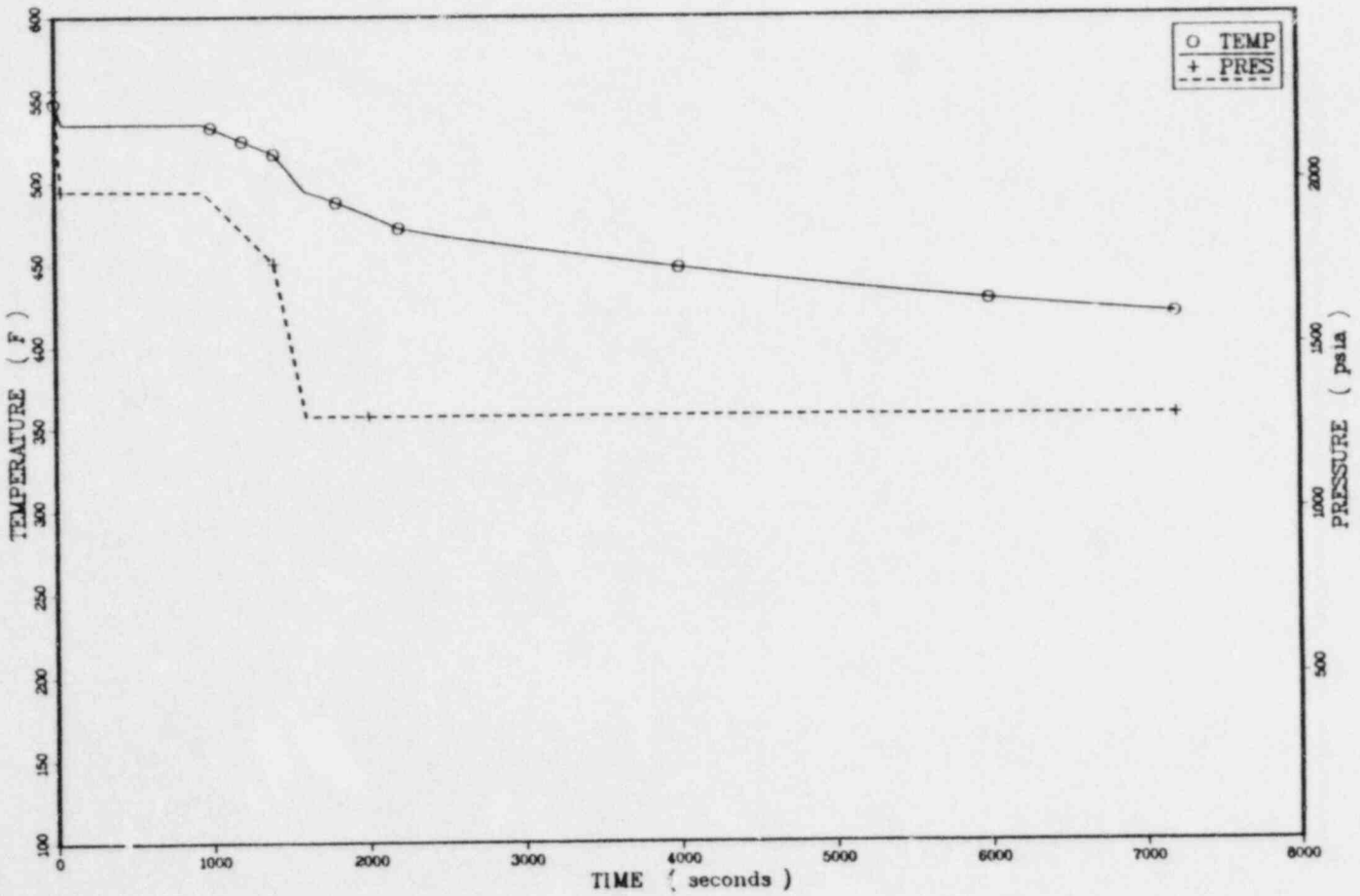

TEMPERATURES AND PRESSURES FOR SEQUENCE 5.36

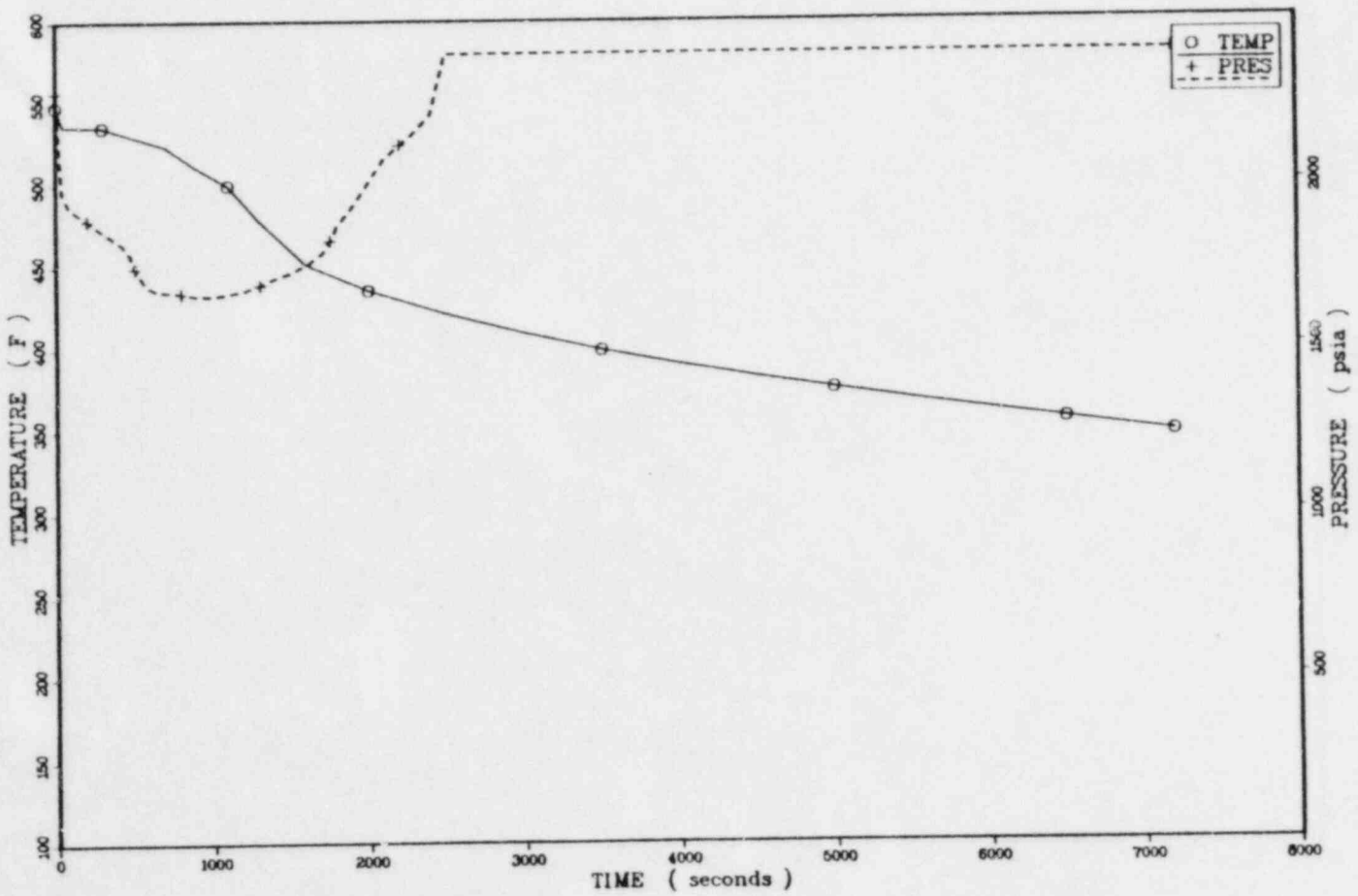

PLOT 1 01.51.16 WED 9 MAY, 1984 JOB-KIN045 , ISSCO DISSPLA VER 8.2

TEMPERATURES AND PRESSURES FOR SEQUENCE 6.1

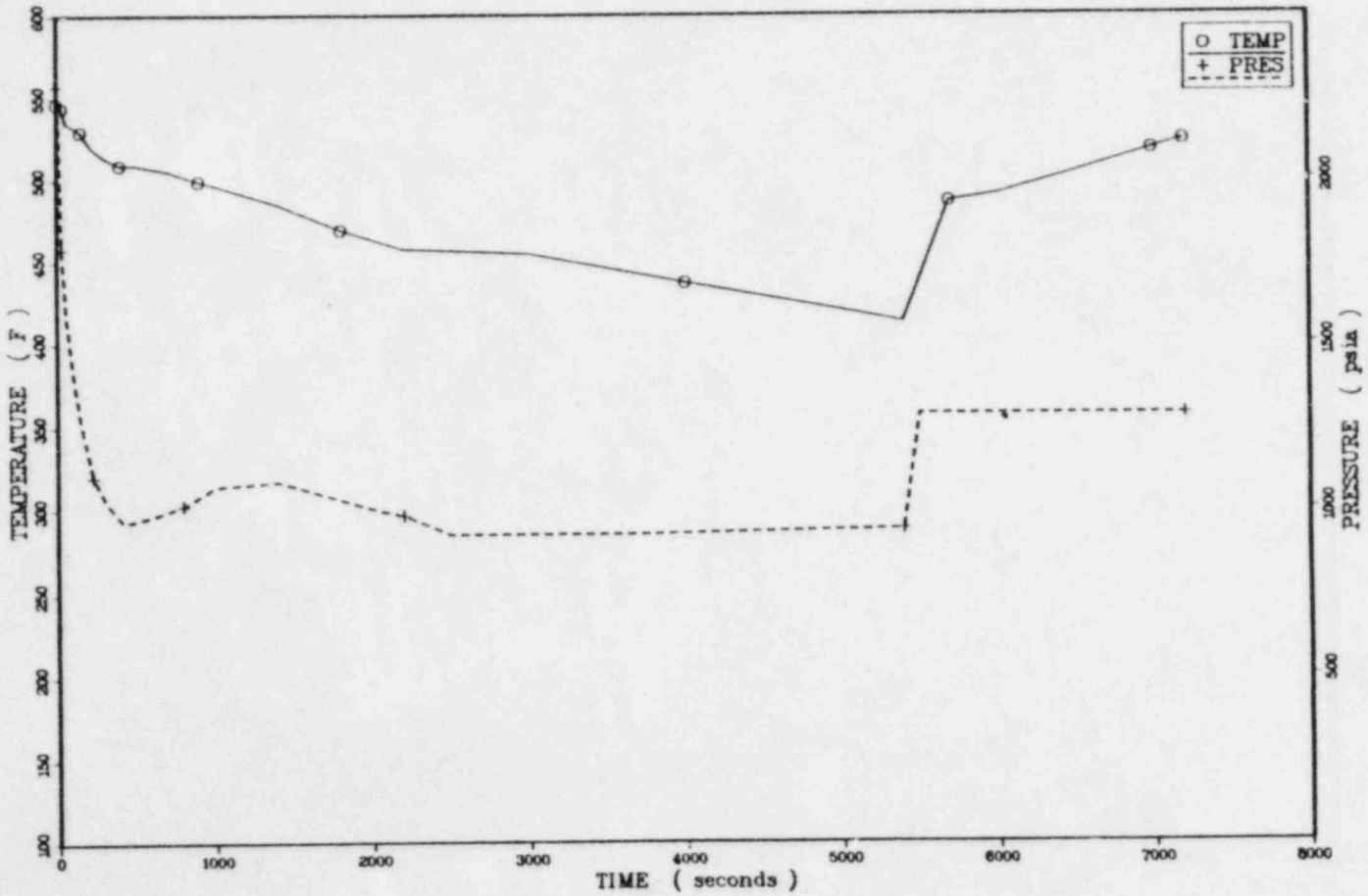

T 1 01.55.04 WED 9 MAY, 1984 JOB-KIN034 , ISSCO DISSPLA VER 8.2

TEMPERATURES AND PRESSURES FOR SEQUENCE 6.2

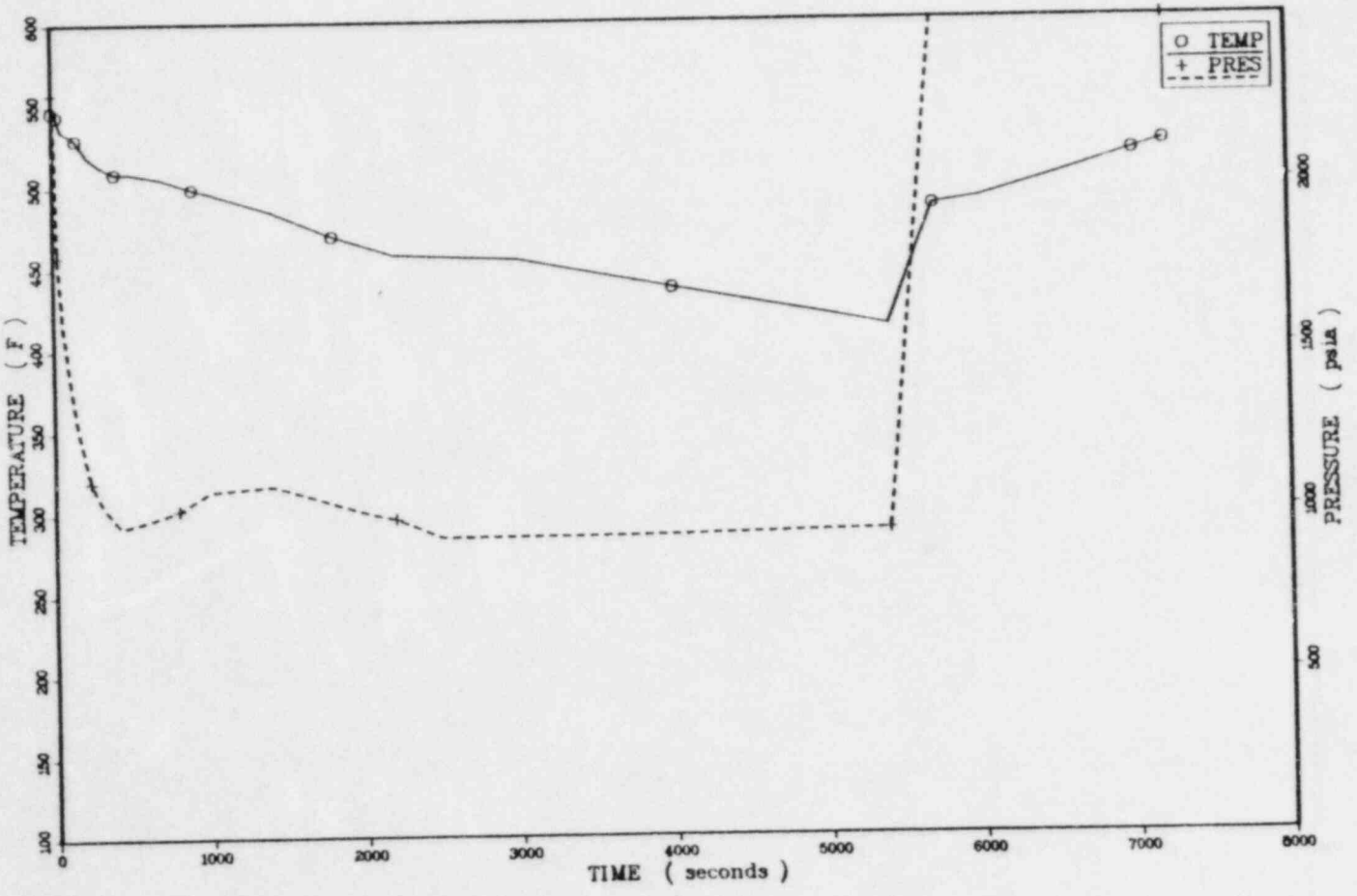

LOT 1 01.53.26 WED 9 MAY, 1984 JOB-KIN021 , ISSCO DISSPLA VER 8.2

TEMPERATURES AND PRESSURES FOR SEQUENCE 6.3

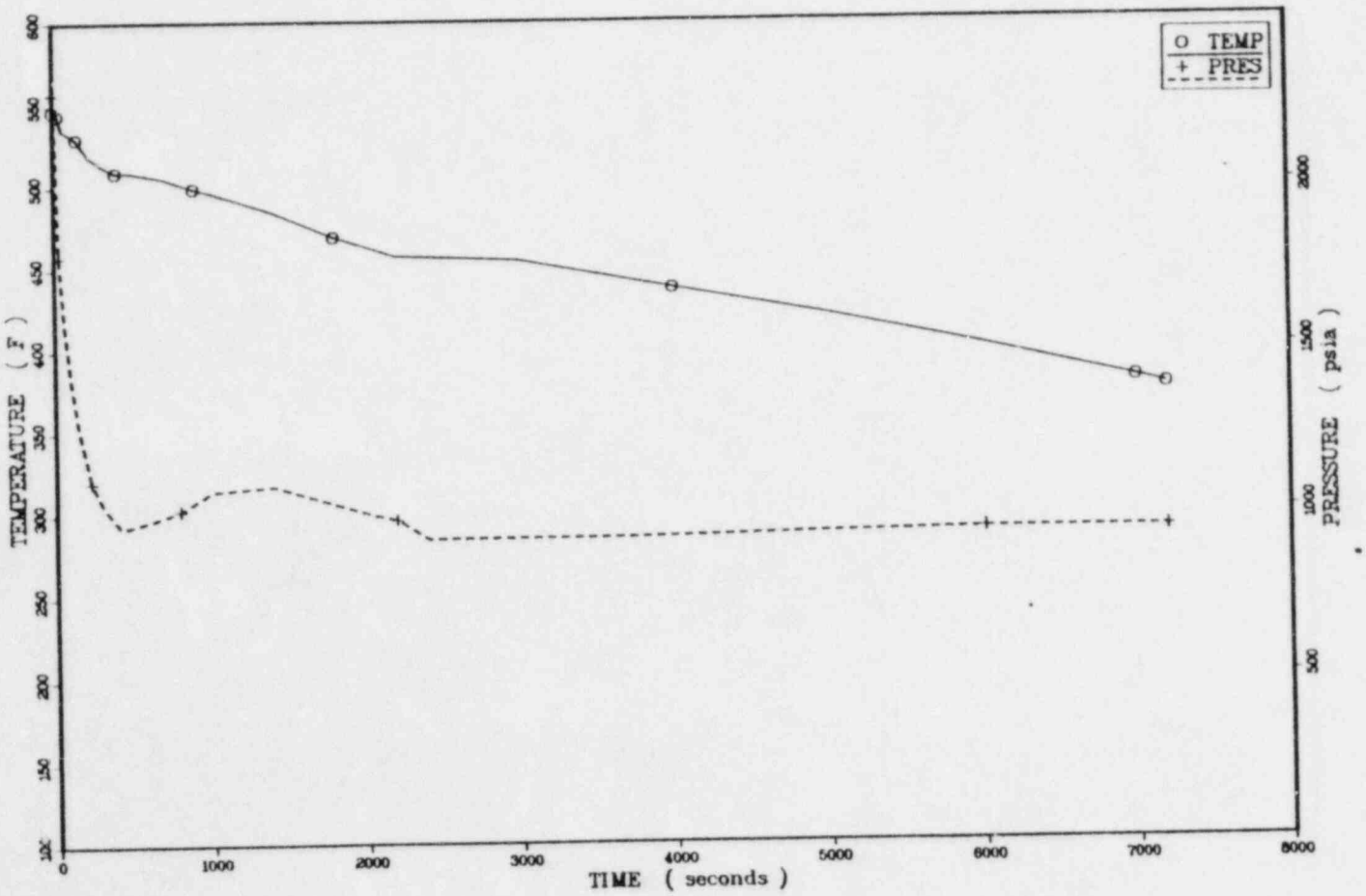

TEMPERATURES AND PRESSURES FOR SEQUENCE 6.8

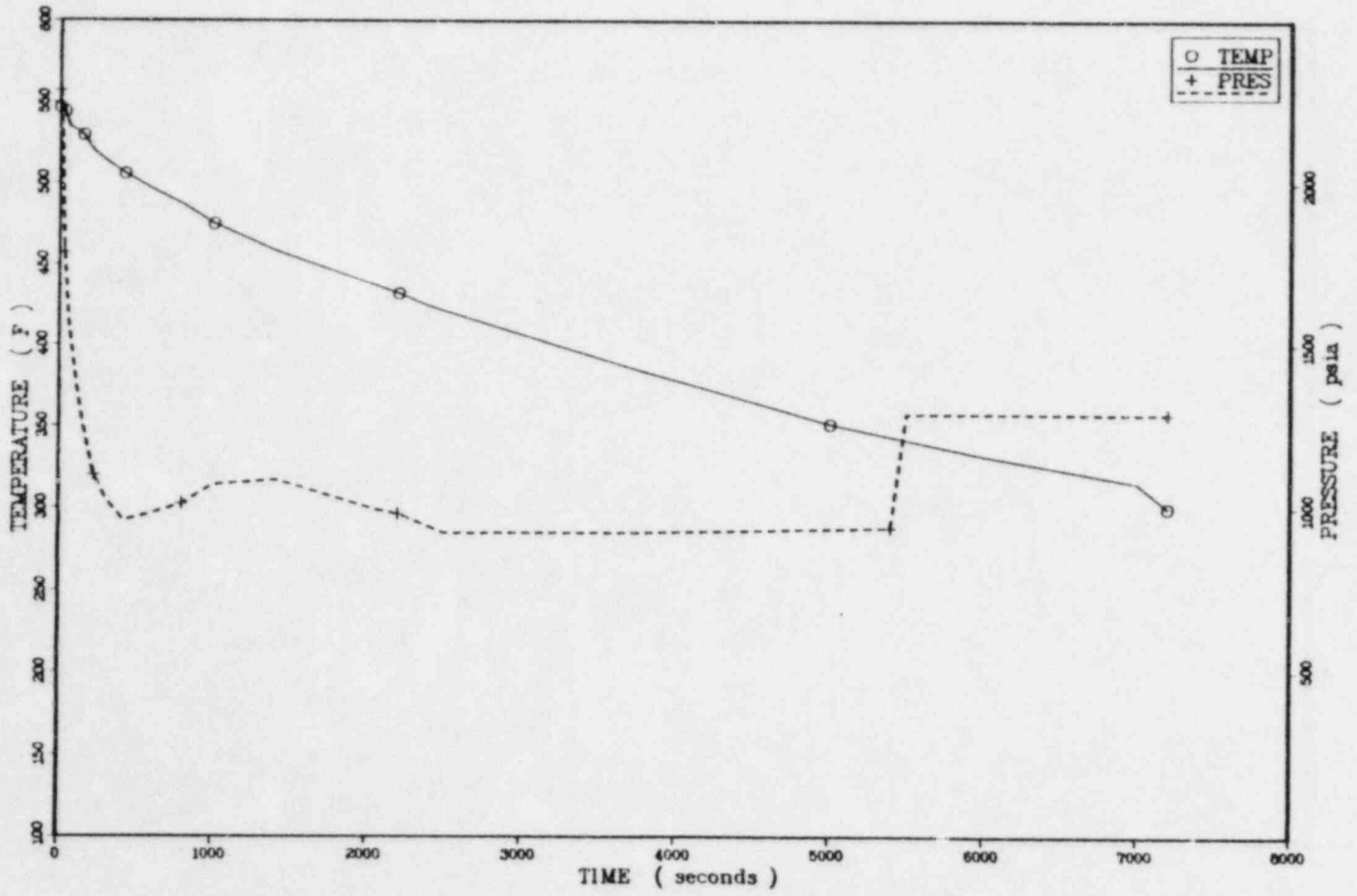

1 01.59.19 WED 9 MAY, 1984 JOB-KIN012 , ISSCO DISSPLA VER 8.2

TEMPERATURES AND PRESSURES FOR SEQUENCE 6.10

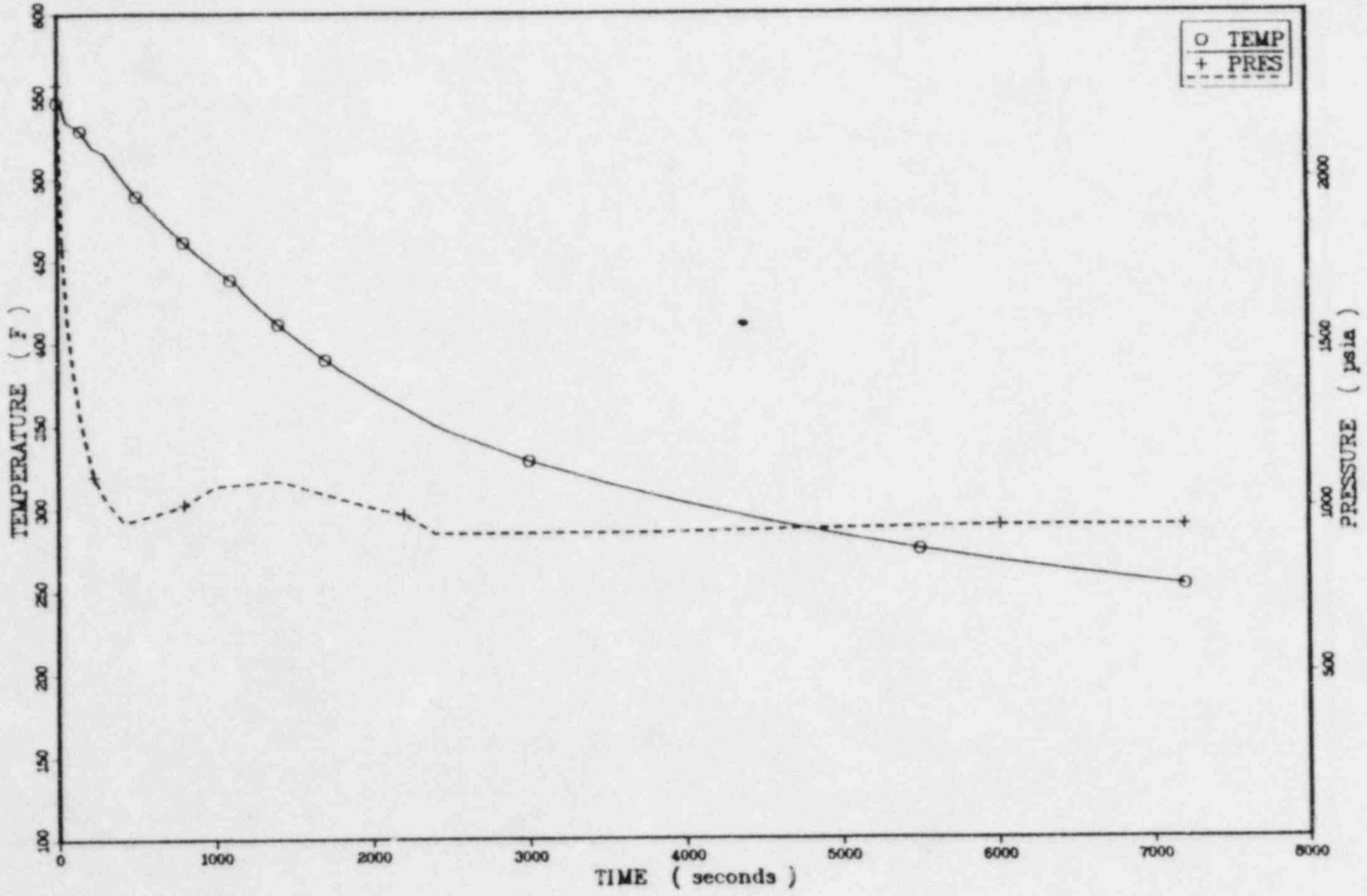

1 02.00.52 WED 9 MAY, 1984 JOB-KIN043 , ISSCO DISSPLA VER 8.2

TEMPERATURES AND PRESSURES FOR SEQUENCE 6.12

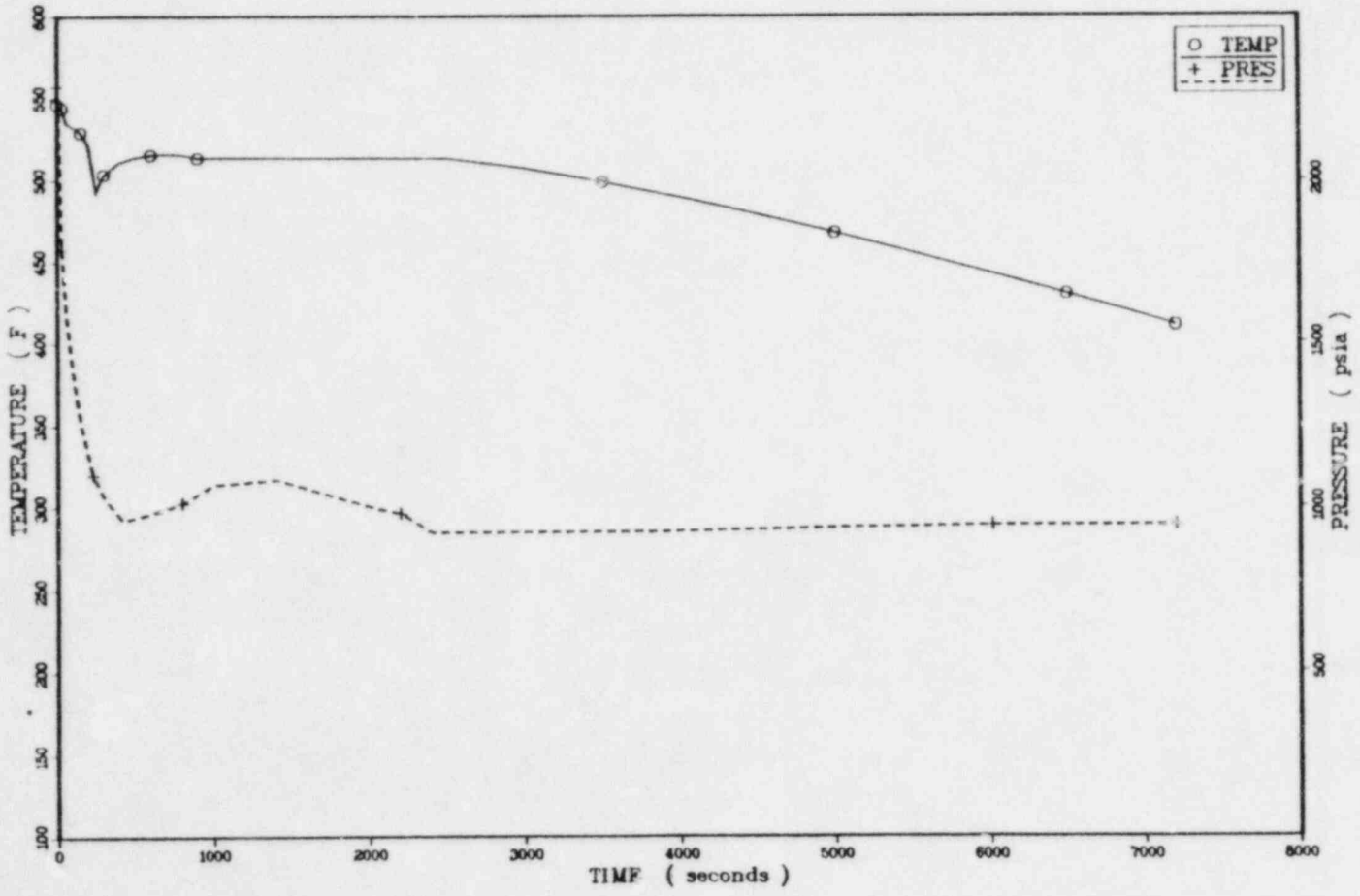

TEMPERATURES AND PRESSURES FOR SEQUENCE 71

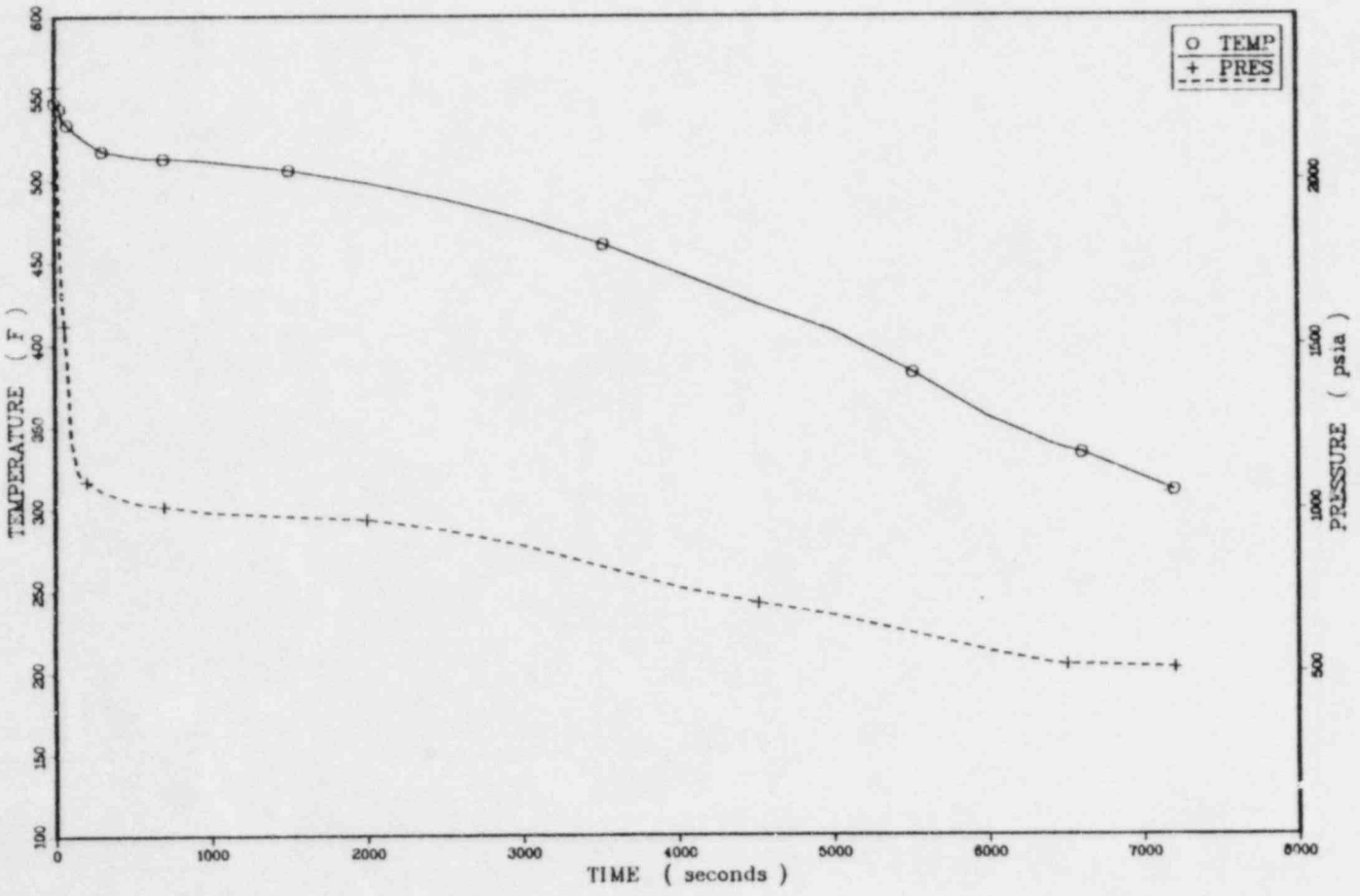

02.02.40 WED 9 MAY, 1984 JOB-KIN036 , ISSCO DISSPLA VER 8.2

TEMPERATURES AND PRESSURES FOR SEQUENCE 7.4

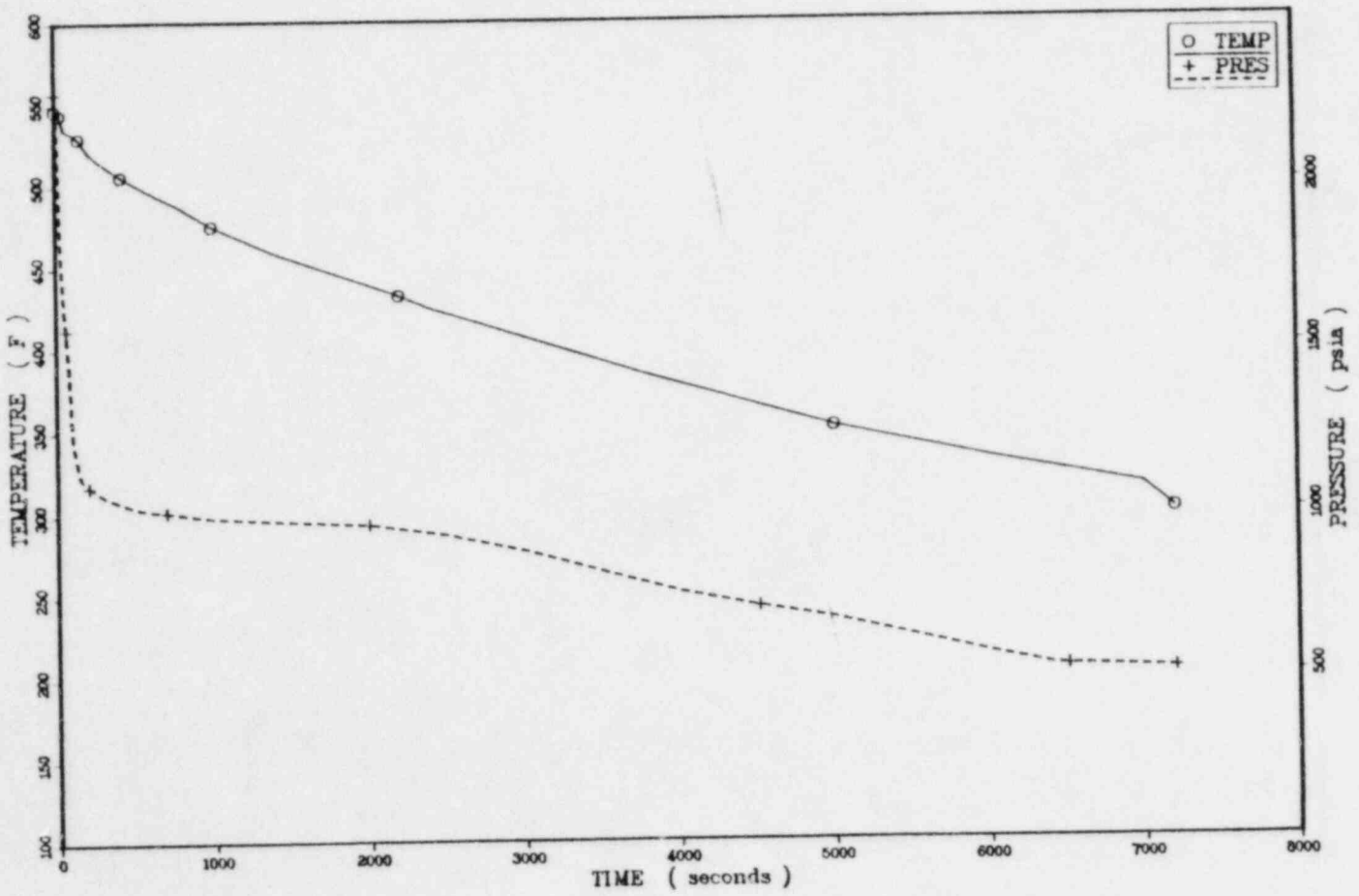

TEMPERATURES AND PRESSURES FOR SEQUENCE 7.6